The role of human CD23 in IgE homeostasis & allergic disease

Cooper, Alison Michelle

Awarding institution:
King's College London

Title: The role of CD23 in IgE homeostasis & allergic disease

Author: Ali Cooper

The role of human CD23 in

IgE homeostasis and allergic disease

Alison Cooper

A thesis submitted for the degree of

Doctor of Philosophy

MRC & Asthma UK Centre in Allergic Mechanisms of Asthma

& Randall Division of Cell & Molecular Biophysics

King's College London

July 2012

Abstract

CD23, the low affinity receptor for IgE on B cells, exists in membrane and soluble forms. CD23 also binds CD21 with a distinct binding site to IgE. Soluble CD23 (sCD23) fragments are released from trimeric membrane CD23 (mCD23) by the endogenous metalloprotease, ADAM10. It has been suggested that trimeric sCD23 fragments can co-ligate membrane IgE (mIgE) and membrane CD21 (mCD21) on the surface of human B cells, in a similar way to C3d-antigen complexes and mIgM, to up-regulate IgE synthesis and provoke allergic responses.

To test this hypothesis, purified tonsil B cells were stimulated with IL-4 and anti-CD40 to induce class switching to IgE *in vitro*. mCD23 was up-regulated and sCD23 accumulated in the medium prior to IgE synthesis. IL-10 and IL-21 were shown to enhance IgE synthesis by increasing cell division and plasma cell differentiation. siRNA inhibition of CD23 synthesis or inhibition of mCD23 cleavage by an ADAM10 inhibitor, GI254023X, were shown to suppress IgE synthesis. Addition of a recombinant trimeric sCD23, triCD23, enhanced IgE synthesis. This occurred even when endogenous mCD23 was protected from cleavage by GI254023X, indicating that IgE synthesis is positively controlled by sCD23. triCD23 was shown to bind to cells co-expressing mIgE and mCD21 and caused capping of these proteins on the B cell membrane. triCD23-mediated up-regulation of IgE secretion and capping of mCD21 was blocked in the presence of an anti-CD21 monoclonal antibody.

Up-regulation of IgE secretion by sCD23 occurred after class switch recombination and the effects were isotype-specific. Together, these results suggest that mIgE and mCD21 co-operate in the sCD23-mediated positive regulation of IgE synthesis by IgE-committed B cells.

These results have improved our understanding of the regulation of IgE in human B cells and provide evidence for sCD23 as a potential therapeutic target in allergy and asthma.

Table of Contents

Table of Figures

Table of Tables

Acknowledgements

Firstly, I would like to thank my supervisors, Professor Hannah Gould and Professor Brian Sutton, for giving me the opportunity to work in such an enjoyable and successful research group and for their continuous guidance throughout my PhD. I would particularly like to thank Hannah for the significant amount of time which she spent working with me on the Journal of Immunology manuscript.

I would also like to thank the MRC & Asthma UK Centre in Allergic Mechanisms of Asthma for providing the funding for my PhD. The centre also provided an excellent means of collaborating with other universities and the PhD student forum events were always useful and enjoyable.

Many thanks to the staff at the Evelina Children's Hospital and Guy's and St. Thomas' NHS Foundation Trust for their help with the collection of tonsils, without which the experiments in this thesis would not have been possible. Many thanks to Dave Fear for his guidance on setting up the siRNA and qPCR experiments and to Phil Hobson for helping me with all the confocal microscopy. Thanks also to Clare, Heather, Holly and Louisa for all their help in the lab. I am grateful to Becky, Michael, Daopeng, Bal and Marie for production of the CD23 proteins, Becky and Celine for production of the anti-CD40 monoclonal antibody and to Boris Schmidt and Binia Drung, from Technische Universität Darmstadt, for kindly providing the ADAM10 inhibitor. I would also like to thank Andrew and Becky for resolving every IT crisis I had, particularly when my hard drive gave up working one day! Thanks to the 'Lunch Club' (Clare, Heather, Holly, Katy, Nyssa and Saba) for providing a welcome break from experiments or writing. I have made some great friends during my PhD who I will always stay in contact with.

Finally, I would like to thank my family and boyfriend, Paul, for their endless support and encouragement throughout my PhD.

Abbreviations

aCD21	Anti-CD21
aCD40	Anti-CD40
ADAM	A Disintegrin and Metalloprotease
AET	2-aminoethylisothiouronium bromide
AHR	Airway hyperresponsiveness
AID	Activation induced cytidine deaminase
ANOVA	Analysis of variance
APC	Allophycocyanin
APC	Antigen presenting cell
ATCC	American Type Culture Collection
Bcl	B cell lymphoma
BCR	B cell receptor
BrdU	Bromodeoxyuridine
C3dg	Degradation product of the third component of Complement
CD	Cluster of differentiation
CD40L	CD40 ligand
cDNA	Complementary DNA
CFSE	Carboxyfluorescein diacetate succinimidyl ester
CLL	Chronic lymphocytic leukaemia
Ct	Threshold cycle
CR	Complement receptor
CSR	Class switch recombination

Da	Daltons
derCD23	16 kDa fragment of soluble CD23 resulting from cleavage by Der p I
Der p	Dermatophagoides pteronyssinus major mite allergen
εGLT	Epsilon germline transcript
ELISA	Enzyme-linked immunosorbent assay
FACS	Fluorescence-activated cell sorting
FAP	Facilitated antigen presentation
FcR	Fc receptor
FCS	Foetal calf serum
FITC	Fluorescein isothiocyanate
GAPDH	Glyceraldehyde 3-phosphate dehydrogenase
GI254023X	(*R*)-N-((*S*)-3,3-dimethyl-1-(methylamino)-1-oxobutan-2-yl)-2-((*S*)-1-(N-hydroxyformamido)ethyl)-5-phenylpentanamide
GWAS	Genome-wide association study
HCl	Hydrochloric acid
HEL	Hen egg lysozyme
HLA	Human leukocyte antigen
HPLC	High performance liquid chromatography
HRP	Horseradish peroxidise
IFN	Interferon
Ig	Immunoglobulin
IL-	Interleukin-
IU	International Units

JAK	Janus kinase
JNK	c-Jun N-terminal kinase
kDa	Kilo-Daltons
LT	Leukotriene
lzCD23	Leucine zipper CD23
mAb	Monoclonal antibody
mCD21	Membrane CD21
mCD23	Membrane CD23
mIgE	Membrane IgE
mIgM	Membrane IgM
MFI	Mean fluorescence intensity
mIgE	Membrane IgE
MMP	Matrix metalloprotease
mRNA	Messenger RNA
NGS	Normal goat serum
NK	Natural killer
ns	Non-significant
OPD	o-Phenylenediamine
PBMC	Peripheral blood mononuclear cell
PBS	Phosphate buffered saline solution
PBS-T	PBS with 0.05% Tween® 20
PE	Phycoerythrin
PG	Prostaglandin
qPCR	Quantitative real-time polymerase chain reaction

RNA	Ribonucleic acid
RPMI	Roswell Park Memorial Institute
S phase	Synthesis phase
SCID	Severe combined immunodeficiency
SCR	Short consensus repeat
sCD23	Soluble CD23
SEM	Standard error of the mean
sIgE	Secreted IgE
sIgG	Secreted IgG
SNP	Single nucleotide polymorphism
siRNA	Short interfering RNA
SPR	Surface plasmon resonance
STAT	Signal transducers and activators of transcription
Th	T helper cell
TMB	Tetramethyl benzidine
TNF	Tumour necrosis factor
triCD23	Recombinant trimeric CD23
WHO	World Health Organisation

Chapter 1. Introduction

1.1. Asthma & allergy

The prevalence of allergic disease has trebled in the last 20 years and now affects 44% of British adults. Of these 21 million sufferers, almost half say they suffer from more than one allergy. Asthma costs the NHS £1 billion per year and accounts for the loss of more than 18 million working days each year (Asthma-UK 2011).

Conditions which fall into the category of allergic disease include allergic rhinitis (hayfever), eczema, food allergies and asthma. Asthma can be defined as a complex inflammatory disease of the lung, characterised by 'reversible' bronchoconstriction, airway hyper responsiveness (AHR), infiltration of the bronchial mucosa with inflammatory cell types (mast cells, lymphocytes and eosinophils), as well as goblet cell hyperplasia and thickening of the submucosa. It is these cellular changes that cause the physiological changes associated with asthma; variable airflow obstruction and AHR (Wills-Karp 1999).

Asthma can be classified as atopic (extrinsic) or non-atopic (intrinsic) based on whether symptoms are precipitated by allergens or not. Beyond this, asthma is classified by severity from intermittent to severe persistent. The interactions between environmental and genetic factors, which cause asthma, are complex and not fully understood. Aside from atopy, other factors have been shown to increase the risk of developing asthma include obesity, exposure to air pollutants, viral respiratory infections and smoking. In 2007, results from the first genome-wide association study (GWAS) on asthma showed a strong association between the ORMDL3 locus and childhood asthma (Moffatt, Kabesch *et al.,* 2007). In 2010, the world-wide GABRIEL consortium reported the results of the largest study to date on the genetics of asthma.

The study replicated the ORMDL3 results and also discovered IL1RL1/IL18R1, HLA-DQ, IL33, SMAD3 and IL2RB loci to be significantly associated with asthma (Moffatt, Gut *et al.,* 2010).

1.2. Immunoglobulins

Immunoglobulin molecules consist of two functionally distinct parts: the variable region for antigen recognition and binding; and the constant region responsible for effector function (Figure 1.1). There are five classes of immunoglobulin molecules (IgM, IgD, IgG, IgA and IgE) determined by differences in the amino acid sequences in the constant region of the heavy chains. During B cell development in the bone marrow, the rearrangement of the variable region genes V (variable), D (diversity) and J (joining) and the nine different heavy chain constant (C) region genes takes place. B cells exiting into the periphery initially express IgM on their surface (Cμ heavy chain constant region) (Edry and Melamed 2004).

Upon antigen stimulation and T cell help, B cells proliferate and differentiate into cells producing other immunoglobulin classes in a process known as class switch recombination (CSR). In this process, an intervening DNA segment between the two recombining switch regions is deleted from the chromosome, termed a ‘switch circle’. ‘Switch circle’ production is controlled by the enzyme activation induced cytidine deaminase (AID), through the creation of DNA breaks (Kaminski and Stavnezer 2004; Yu, Chedin *et al.,* 2003).

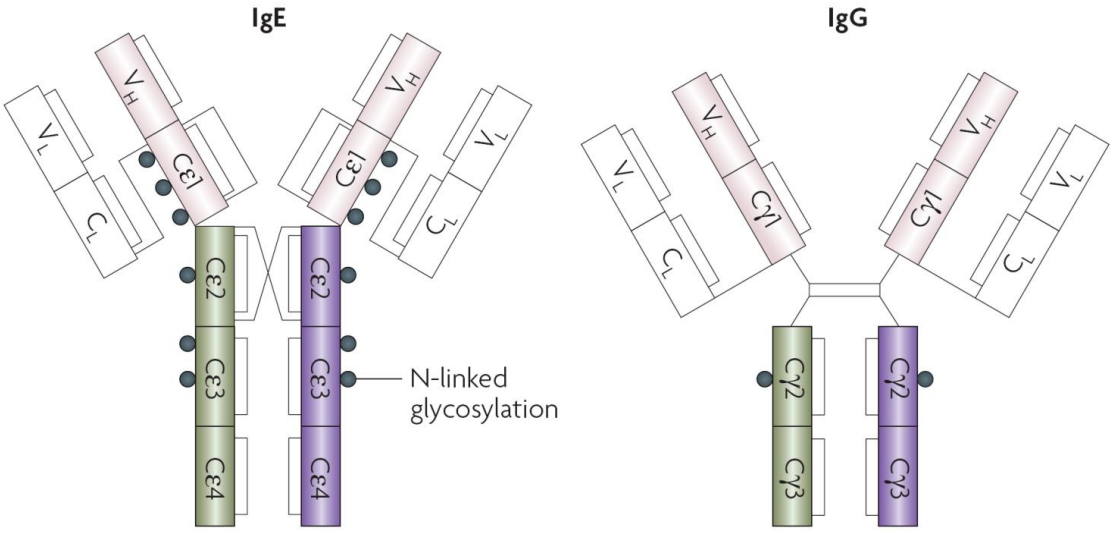

Figure 1.1. The domain structures of IgE and IgG.

Both IgE and IgG contain a variable (V) region, constant (C) region, two heavy (V_H and C) and two light (V_L and C_L) chains. IgE contains an extra immunoglobulin domain (Cε2) in place of the hinge region found in IgG.

From (Gould and Sutton 2008).

1.3. Class switch recombination to IgE

Allergic disease, such as asthma and allergic rhinitis, can be caused by the over-production of IgE antibodies to foreign antigens which are harmless to non-allergic individuals. Originally thought to only occur in germinal centres, local CSR and synthesis of IgE has been shown to take place at local sites of inflammation in the nasal mucosa of allergic rhinitis patients (Durham, Smurthwaite *et al.*, 2000; KleinJan, Vinke *et al.*, 2000; Takhar, Smurthwaite *et al.*, 2005) and the bronchial mucosa of asthmatics (Fiset, Cameron *et al.*, 2005; Takhar, Corrigan *et al.*, 2007; Ying, Humbert *et al.*, 2001).

CSR to IgE is induced by the Th2 cytokines, IL-4 and IL-13, and CD40L (ligand) expression (Figure 1.2). IL-4 and IL-13 induce the activation of JAK kinases

and the transcription factor STAT6 which binds to the ε germline gene promoter and activates transcription of the gene. CD40L expressed on activated T cells can ligate the B cell receptor CD40. This ligation event is required for JNK activation, which is important for AID activity required for CSR (Jabara and Geha 2005). These signalling events result in the transcription of ε germline gene transcripts (εGLT) and CSR to IgE. During recombination from IgM to IgE, the μ and ε switch regions, which contain potential DNA breakpoints, are broken and recombined to express ε chain mRNA and protein (Gould, Takhar *et al.*, 2006). IgE exerts it effects through the receptors FcεRI and FcεRII (CD23), which are discussed in further detail in the following sections.

1.4. The 'high affinity' IgE receptor (FcεRI)

FcεRI is expressed on a wide range of cells including monocytes, macrophages, basophils, mast cells, APCs, epithelial cells and smooth muscle cells. The Cε2 and Cε3 domains of IgE (Figure 1.2) bind FcεRI with a very high affinity ($K_a \sim 10^{10}$ M^{-1}), permanently coating cells with IgE. This "sensitisation" enables very rapid activation upon allergen re-exposure (Gould, Sutton *et al.*, 2003). When IgE binds to FcεRI on APCs, allergen cross-linking leads to presentation to allergen-specific Th2 cells (Figure 1.2). This induces IL-4 secretion and CD40 cross-linking, promoting further Th2 cell differentiation and CSR to IgE in neighbouring B cells, as described in Section 1.3 (Jabara, Fu *et al.*, 1990). Allergen can also cross-link IgE bound to FcεRI on the surface of mast cells to induce an immediate type I hypersensitivity reaction resulting in degranulation and release of pro-inflammatory mediators, including histamine (Figure 1.2). Repeated exposure to allergens leads to increased allergen-specific Th2 cells and

IgE antibodies which initiate a secondary immune response upon subsequent allergen exposure (Williams and Galli 2000).

Anti-IgE monoclonal antibodies (mAb) have been shown to down-regulate FcεRI expression on human basophils *in vivo* (MacGlashan, Bochner *et al.*, 1997) and *in vitro* (MacGlashan, McKenzie-White *et al.*, 1998). Omalizumab (Xolair, Novartis Pharmaceuticals Ltd) is an anti-IgE antibody therapy used in the treatment of refractory moderate to severe asthma (Figure 1.2). It binds to and neutralises free IgE to prevent binding to FcεRI on mast cells and APCs (Holgate, Bousquet *et al.*, 2001). However, omalizumab is very expensive to produce and, therefore, discovery of a small molecule inhibitor of the IgE-FcεRI interaction is in great demand as an alternative therapeutic approach with lower costs and a wider range of applications.

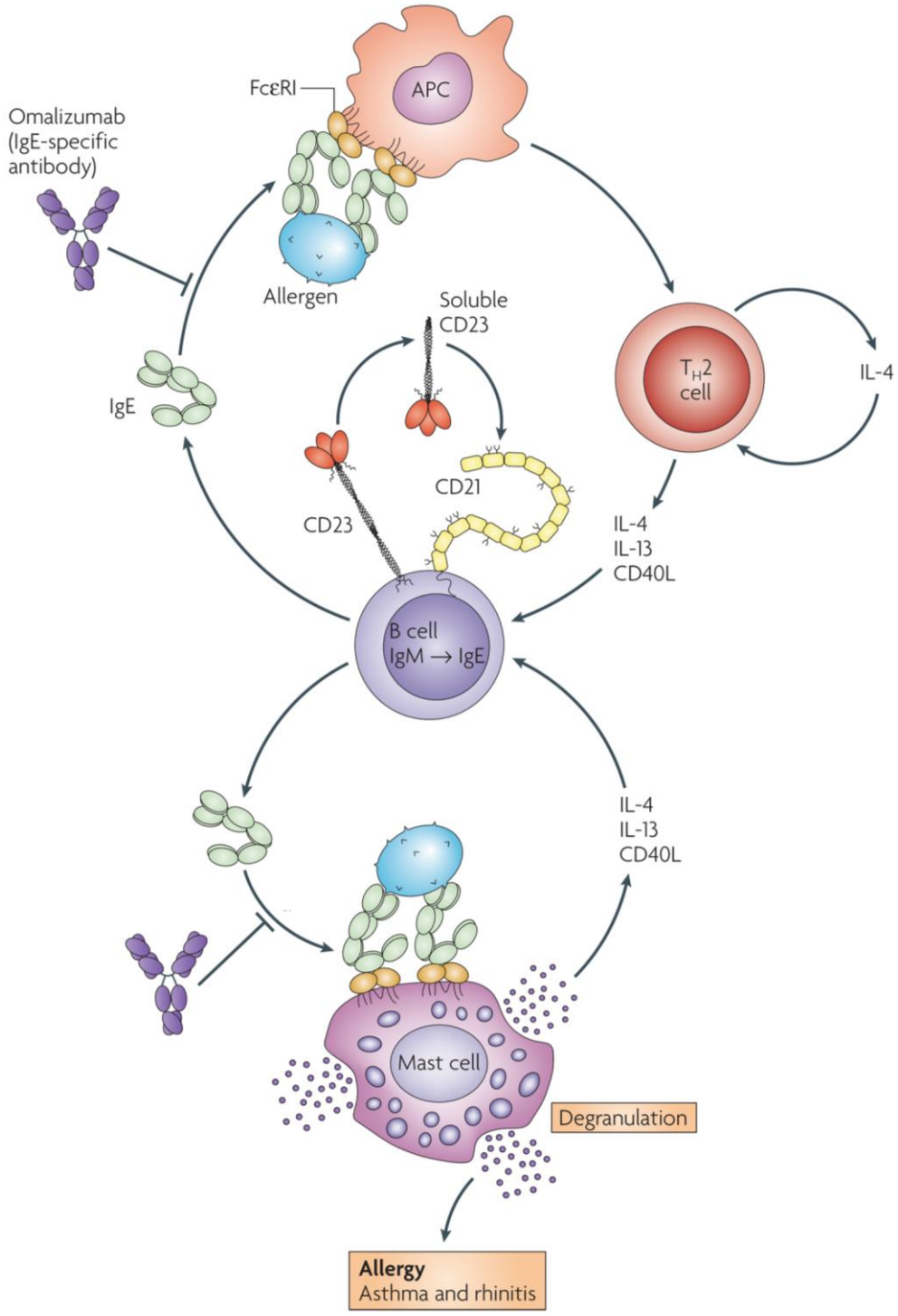

Figure 1.2. The role of IgE and IgE receptors (FcεRI and CD23) in the allergic response.

Following class switch recombination, IgE binds to FcεRI on APCs to sensitise cells to allergen. Upon allergen cross-linking of mIgE on APCs, recruited Th2 cells produce IL-4, IL-13 and CD40L, stimulating B cells to produce more IgE. Allergen also cross-links mIgE bound to FcεRI on mast cells, inducing degranulation and pro-inflammatory mediator release, initiating the allergic response. The B cell IgE receptor, CD23, is shown in the membrane and soluble form, with the co-receptor CD21.

From (Gould and Sutton 2008).

1.5. The 'low affinity' IgE receptor (FcεRII/CD23)

The focus of this thesis is an investigation into the IgE receptor FcεRII (CD23). The information provided below relates to human CD23, unless otherwise stated.

1.5.1. Distribution of CD23

Following the identification of CD23 as an IgE receptor on monocytes and B cells (Melewicz, Plummer *et al.,* 1982), many cell types have been subsequently found to express CD23. These include T cells, NK cells, eosinophils, platelets, macrophages, follicular dendritic cells (Delespesse, Suter *et al.,* 1991) and structural cells, such as airway smooth muscle cells (Belleau, Gandhi *et al.,* 2005).

1.5.2. Structure of CD23

Human CD23 is initially expressed as a 45 kDa type II integral membrane protein consisting of 321 amino acids. Unlike all other Fc receptors which belong to the Ig superfamily, CD23 is a member of the C-type (calcium-dependent) lectin family (Conrad 1990; Soilleux, Barten *et al.,* 2000). Membrane CD23 (mCD23) contains a C-type lectin 'head' domain, a triple-stranded coiled-coil stalk and a C-terminal 'tail' in the extracellular sequence (Figure 1.3A) (Gould and Sutton 2008; Spiegelberg 1991). The 'tail' is not present in murine CD23 (Dierks, Bartlett *et al.,* 1993).

CD23 is assembled into a trimer (Figure 1.3B) (Beavil, Graber *et al.,* 1995), the predominant form in the B cell membrane, by way of the α-helical coiled-coil stalk that links the three lectin 'head' and 'tail' domains to their transmembrane and cytoplasmic sequences (Beavil, Edmeades *et al.,* 1992). Structures of the CD23 lectin 'head' solved by NMR (Hibbert, Teriete *et al.,* 2005) and X-ray crystallography (Wurzburg, Tarchevskaya *et al.,* 2006), revealed binding sites for IgE and CD21. Following

observations in mice (Dierks, Bartlett *et al.*, 1993), it was discovered that although a monomer of human CD23 can only bind IgE with low affinity (K_a ~ 10^6-10^7 M^{-1}) (Shi, Ghirlando *et al.*, 1997), a trimer of human mCD23 is capable of binding IgE with high affinity (K_a ~ 10^9-10^{10} M^{-1}). This is due to an avidity effect when the three lectin 'heads' are brought together (Gould, Sutton *et al.*, 1991). Binding of CD23 to IgE and CD21 is discussed in more detail in Section 1.6.

.

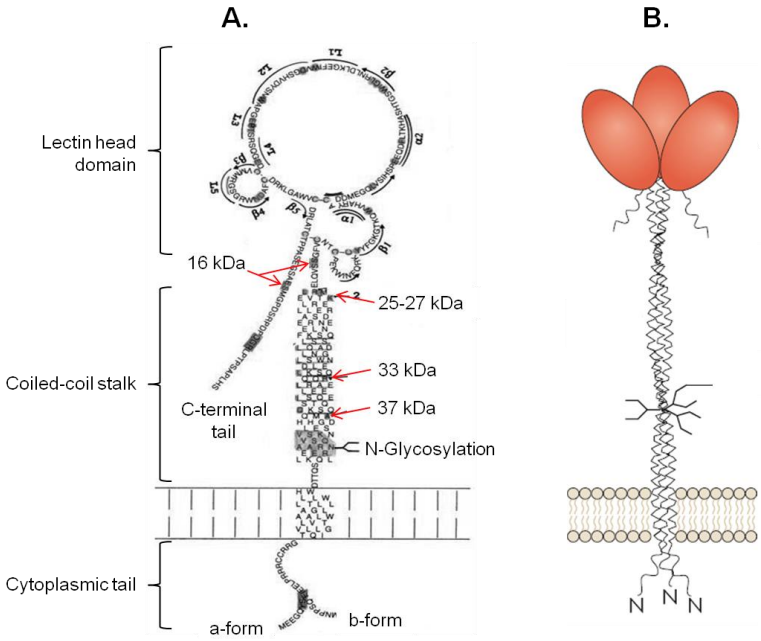

Figure 1.3. Structure of human membrane CD23.

(A) The structure of full length mCD23 is comprised of the lectin 'head' domain, coiled-coil stalk region and cytoplasmic tail region. The a-form and b-form are shown to differ by 6-7 amino acids in the cytoplasmic sequence. α helices (α), β sheets (β) and loops (L) are indicated. Red arrows indicate cleavage sites for production of sCD23 fragments with the corresponding molecular weights. **(B)** Model of three mCD23 molecules assembled into a trimer.

Adapted from (Kijimoto-Ochiai 2002) and (Gould and Sutton 2008).

Human CD23 is expressed as two isoforms, CD23a and CD23b, resulting from alternative transcription initiation sites and differing only by six or seven amino acids in the intracellular N-terminal cytoplasmic sequence (Figure 1.3A) (Yokota, Kikutani *et al.*, 1988). CD23a is expressed on antigen-activated B cells, while CD23b expression is up-regulated on a wide variety of cells, particularly by IL-4 (Ewart, Ozanne *et al.*, 2002).

1.5.3. Cleavage of CD23

The extracellular stalk region of mCD23 is susceptible to proteolysis, releasing a soluble form of CD23 (sCD23) (Sarfati, Nakajima *et al.*, 1987). sCD23 fragments can vary in molecular weight due to several potential cleavage sites (Table 1.1 and Figure 1.3A). All sCD23 fragments contain the lectin 'head' domain and, therefore, retain the ability to bind IgE, albeit at lower affinity (Beavil, Graber *et al.*, 1995). Larger sCD23 fragments still have the tendency to form trimers, depending on the length of the remaining stalk region (Schulz, Sutton *et al.*, 1997).

Members of the ADAM (A Disintegrin And Metalloprotease) family have been identified as the cleavage enzymes responsible for the production of 37 kDa and 33 kDa sCD23 (Table 1.1). ADAM10 is the principal sheddase of mCD23 both *in vitro* (Lemieux, Blumenkron *et al.*, 2007; Weskamp, Ford *et al.*, 2006) and *in vivo* (Gibb, El Shikh *et al.*, 2010; Mathews, Ford *et al.*, 2011; Weskamp, Ford *et al.*, 2006). In a B cell specific ADAM10 knock-out mouse model, sCD23 production was reduced by 70% (Gibb, El Shikh *et al.*, 2010). This same study, for the first time, showed ADAM10 to be essential for the initiation of Notch2 signalling (Gibb, El Shikh *et al.*, 2010). The Notch2 signalling pathway is known to regulate the development of the marginal zone

B cell lineage (Tanigaki and Honjo 2007) and plays a role in B cell activation by enhancing B cell receptor (BCR) and CD40 signalling (Thomas, Calamito *et al.*, 2007).

ADAM8 and ADAM33 have also been shown to produce sCD23 *in vitro* (Table 1.1). However, whether these enzymes contribute to sCD23 production *in vivo* is uncertain. ADAM8 and ADAM33 knock-out mice show no alteration in sCD23 production (Weskamp, Ford *et al.*, 2006) and human immune cells, including B cells, have been shown to express very low levels of ADAM8 and undetectable levels of ADAM33 (Richens, Fairclough *et al.*, 2007; Umland, Garlisi *et al.*, 2003).

sCD23 can subsequently degrade into smaller fragments with molecular weights of 25-27 kDa (Table 1.1 and Figure 1.3A). This has been observed in cell culture supernatants and human serum (Letellier, Sarfati *et al.*, 1989; Sarfati, Bron *et al.*, 1988). The smallest sCD23 fragment, termed derCD23, results from cleavage by the house dust mite allergen, *Der p* I, a cysteine protease (Figure 1.3A). The resulting 16 kDa monomer contains only the lectin 'head' domain and ten amino acids of the C-terminal 'tail' (Gough, Schulz *et al.*, 1999; Schulz, Sutton *et al.*, 1997).

In addition to extracellular processing, sCD23 can be produced by intracellular proteolytic processing of newly synthesised CD23. This results in the secretion of sCD23 fragments with molecular weights of 28-29 kDa (Table 1.1) (Lee, Simmons *et al.*, 1989). A recent study found mCD23 and ADAM10 inside endosomal compartments of murine and human B cells. This suggests a pathway of mCD23 internalisation and partial cleavage by ADAM10, prior to being secreted from the cell, as an alternative source of sCD23 (Mathews, Gibb *et al.*, 2010).

MW (kDa)	Origin	Enzyme
37	Extracellular shedding of membrane CD23 at position Ala^{80}	*in vivo*: ADAM10 and MMP9 *in vitro*: ADAM10, ADAM8 and ADAM 33
33	Extracellular shedding of membrane CD23 at position Arg^{101}	*in vivo*: ADAM10 and MMP9 *in vitro*: ADAM10, ADAM8 and ADAM 33
28-29	Intracellular processing of newly synthesised CD23 protein	Not defined
25-27	Proteolytic cleavage/degradation products of 33 kDa and 37 kDa sCD23	Not defined
16-17	Extracellular cleavage of membrane CD23 at Ser^{155} and Glu^{298}	Der p1

Table 1.1. The variety of soluble CD23 fragments

The locations of cleavage sites are shown on the structure of CD23 in Figure 1.3. From (Platzer, Ruiter *et al.*, 2011).

Shedding of mCD23 can be prevented by stabilisation through conformational changes which reduce the accessibility of the cleavage sites to ADAM10. This can occur upon binding to IgE or through the use of CD23 mAbs (Conrad, Ford *et al.*, 2007; Gould, Sutton *et al.*, 1991). The human anti-CD23 mAb lumiliximab (IDEC-152, Biogen Idec Ltd) is thought to inhibit production of sCD23 through stabilisation of mCD23 (Rosenwasser, Busse *et al.*, 2003). The resulting clinical impacts of lumiliximab treatment are discussed in Section 1.9.

1.6. The interactions of CD23

1.6.1. Interaction of CD23 with IgE

Upon binding to the high affinity receptor FcεRI, IgE undergoes a conformational change involving the Cε2 and Cε3 domains that is believed to be responsible for the high affinity interaction and slow dissociation rate as previously discussed in Section 1.4. This information was obtained from crystal structures of IgE Fc (Holdom, Davies *et al.*, 2011; Wan, Beavil *et al.*, 2002). No crystal structure has

been published of the CD23-IgE complex. NMR analysis of the interaction between derCD23 and IgE identified a number of residues in the Cε3 domain that are implicated in CD23 binding (Hibbert, Teriete *et al.,* 2005). Ultracentrifugation studies showed there to be two binding sites for CD23 on IgE, suggesting that one molecule of IgE may bind two lectin 'heads' of the same molecule of CD23 or that one molecule of IgE may bind to two lectin 'heads', each on separate CD23 molecules, leading to large cross-linked networks (Hibbert, Teriete *et al.,* 2005; Shi, Ghirlando *et al.,* 1997).

The kinetics and binding sites for IgE on CD23 were introduced in Section 1.5.2, however, the requirement of calcium for this interaction was not previously discussed. CD23 contains two calcium binding sites, a principal binding site conserved among C-type lectins and a non-conserved site (Weis, Drickamer *et al.,* 1992). NMR analysis following a calcium titration showed the second non-conserved calcium binding site to be occupied and that calcium is not required to stabilise the lectin 'head' for derCD23 to bind to IgE (Hibbert, Teriete *et al.,* 2005). In contrast, the crystal structure of the lectin 'head' in the presence of calcium revealed calcium binding at only the principal calcium binding site. In the crystal structure without calcium present, the principal calcium binding site is occupied by an arginine from a neighbouring loop (Wurzburg, Tarchevskaya *et al.,* 2006). The calcium-induced conformational change is in areas shown to be important in binding to IgE Fc (Bettler, Maier *et al.,* 1989).

1.6.2. Interaction of CD23 with CD21

CD21 is a type I membrane glycoprotein with a molecular mass of ~145 kDa. The protein consists of a large extracellular portion made up of 15-16 short consensus repeat (SCR) domains, a transmembrane region and a short cytoplasmic tail (Gilbert, Asokan *et al.,* 2006; Weis, Drickamer *et al.,* 1992). CD21 (also known as complement

receptor 2), associated with CD19, is the receptor for C3dg complement fragments, several copies of which covalently bind antigen. This lowers the threshold to initiate an immune response by two or three orders of magnitude. On antigen-specific B cells, C3dg co-ligates membrane IgM (mIgM) and the antigen receptor to form a 'signalling platform' to stimulate proliferation and antibody production. Downstream signalling events from mIgM and CD21 co-ligation lead to Bcl-x_L and Bcl-2 synthesis, reducing apoptosis and promoting B cell survival, proliferation and antibody production (Cherukuri, Cheng *et al.*, 2001; Fearon and Carter 1995; Pierce 2002; Roberts and Snow 1999).

Twenty years ago, Bonnefoy *et al* incorporated recombinant CD23 into fluorescent liposomes and used this as a probe to first identify CD21 as a co-receptor for CD23 (Aubry, Pochon *et al.*, 1994; Aubry, Pochon *et al.*, 1992). Of the sixteen possible extracellular SCR domains of CD21, they mapped CD23 binding to SCR1-2 and SCR 5-8. On CD23, structural studies have mapped the CD21 binding site to the C-terminal 'tail' (Figure 1.4) (Hibbert, Teriete *et al.*, 2005).

NMR studies by Hibbert *et al* showed the CD21 and IgE binding sites on CD23 to be distinct from each other and from the trimerisation interface (Figure 1.4). This study also showed the capability of the 16 kDa monomeric sCD23 fragment, derCD23, to simultaneously bind both IgE and CD21 to form a tri-molecular complex (Hibbert, Teriete *et al.*, 2005). The implications of an IgE-sCD23-CD21 complex are discussed in greater detail in Section 1.7.2.

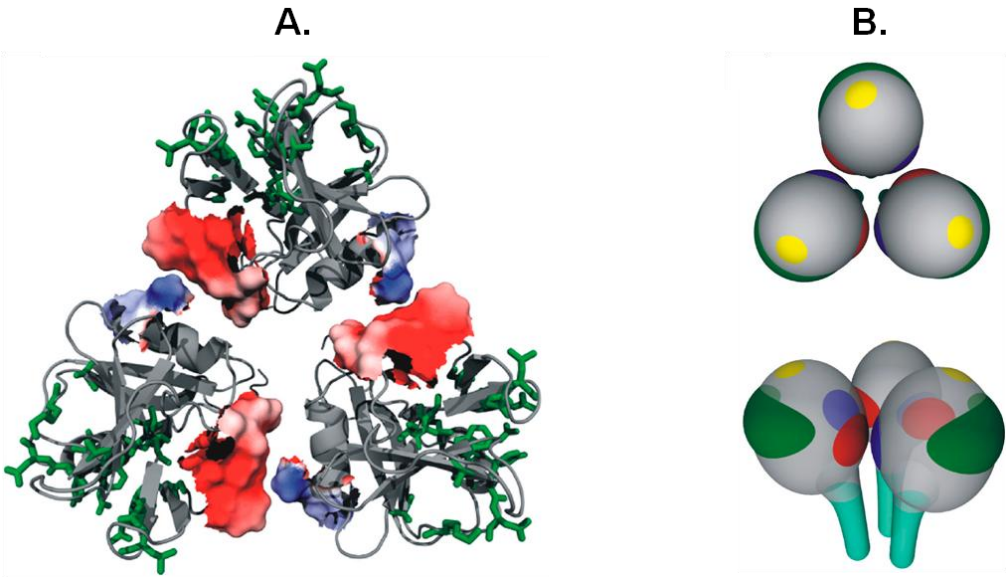

Figure 1.4: The structure of the CD23 trimer and its interactions with IgE and CD21.

(A) An overhead view of the proposed trimer of CD23, coloured according to electrostatic charge, with IgE interaction residues shown in green. **(B)** Ligand binding sites on the top and side of trimeric CD23. Oligomerisation sites are coloured blue and red, the IgE interaction sites green, the CD21 binding sites cyan and the calcium binding sites yellow.

From (Hibbert, Teriete *et al.*, 2005).

1.6.3. Other interactions of CD23

Human CD23 has also been shown to interact with the monocyte-expressed β_2 subfamily integrins CD11b and CD11c. These integrins pair with the β subunit CD18 to form the complement receptors $\alpha_M\beta_2$ (macrophage-1 antigen or CR3) and $\alpha_X\beta_2$ (CR4) (Bajorath and Aruffo 1996). CD23 binding activates nitric oxide synthase to induce the production of inflammatory cytokines such as IL-6, IL-8 and TNFα (Aubry, Dugas *et al.*, 1997; Lecoanet-Henchoz, Gauchat *et al.*, 1995). Human CD23 can also bind to the vitronectin receptor ($\alpha_v\beta_3$ integrin), associated with CD47, on monocytes to induce pro-inflammatory cytokine release (Hermann, Armant *et al.*, 1999).

1.7. The role of CD23 in IgE homeostasis

As only 0.0001% of all serum immunoglobulins are IgE in normal donors (at ~0.1µg/ml), 10^4 less than that of IgG (Waldmann, Iio *et al.,* 1976), the secretion of IgE must be a tightly regulated process. The interaction of CD23 with CD21, as described in Section 1.6.2, has been shown to be a key component in the regulation of IgE (Aubry, Pochon *et al.,* 1994). CD23 has been implicated in both the up- and down-regulation of IgE synthesis, depending on its structural form. The ability of CD23 to both increase and decrease IgE suggests different forms of CD23 may act as a two-way switch in IgE homeostasis (Figure 1.5).

1.7.1. The role of mCD23 in IgE homeostasis

It has long been known that CD23 negatively regulates the synthesis of IgE (Cho, Kilmon *et al.,* 1997; Yu, Kosco-Vilbois *et al.,* 1994). The most compelling evidence comes from CD23 knock-out mice, which exhibit greatly increased levels of antigen-specific IgE after immunisation (Cho, Kilmon *et al.,* 1997; Yu, Kosco-Vilbois *et al.,* 1994).

IgE synthesis is also inhibited in human B cells by anti-CD23 antibodies (McCloskey, Hunt *et al.,* 2007; Nakamura, Kloetzer *et al.,* 2000; Sherr, Macy *et al.,* 1989) and antigen-IgE complexes which bind to mCD23 (Figure 1.5) (Conrad, Ford *et al.,* 2007). This stabilises mCD23 and prevents the formation of sCD23 allowing a negative feedback pathway to dominate. Neither free IgE nor antibody Fab fragments have this inhibitory activity, suggesting that cross-linking of mCD23 is required for the inhibition (Sherr, Macy *et al.,* 1989). These observations suggest that mCD23 may act in a negative feedback mechanism on IgE synthesis to terminate allergen-specific IgE secretion (Figure 1.5).

1.7.2. The role of sCD23 fragments in IgE homeostasis

IL-4 and CD40L have been shown to synergistically promote CD23 expression and sCD23 production which, in turn, leads to an increase in IgE secretion from IgE-committed B cells. IL-4 and CD40L activate the transcription factors STAT6 and NFκB, respectively, to induce ε-germline gene expression and DNA recombination (Iciek, Delphin *et al.*, 1997; Jabara, Fu *et al.*, 1990; Linehan, Warren *et al.*, 1998). Although these studies showed a link between sCD23 and IgE up-regulation, the exact mechanisms still remain unclear.

In a similar mechanism to co-ligation of mIgM and CD21 by C3dg, as described in Section 1.6.2, it has been proposed that trimeric sCD23 can co-ligate mIgE and CD21 on the surface of IgE-committed B cells, stimulating proliferation of IgE-secreting plasma cells and increasing IgE secretion (Figure 1.5) (Gould, Beavil *et al.*, 1997). This hypothesis is based on experiments in which the hen egg lysozyme (HEL)-specific BCR and CD21 were cross-linked with a C3d-HEL fusion protein. This lowered the B cell activation threshold, resulting in cell proliferation and IgM secretion (Dempsey, Allison *et al.*, 1996; Dempsey and Fearon 1996). In human CD23, the binding site for CD21 resides in the C-terminal 'tail' (Hibbert, Teriete *et al.*, 2005). This 'tail' is not present in murine CD23 (Dierks, Bartlett *et al.*, 1993), which may explain why sCD23 expressed in transgenic mice does not up-regulate IgE during immunisation, leaving only down-regulation through mCD23 (Lamers and Yu 1995; Texido, Eibel *et al.*, 1994; Yu, Kosco-Vilbois *et al.*, 1994).

1.7.3. *In vitro* studies of the effect of sCD23 on IgE

A number of studies have shown recombinant sCD23 fragments to either up- or down-regulate IgE synthesis in primary human B cells. Addition of recombinant

oligomeric CD23 (lzCD23 or exCD23) has been shown to up-regulate IgE synthesis and derCD23 has been shown to down-regulate IgE synthesis (Aubry, Pochon *et al.*, 1992; Bowles, Jaeger *et al.*, 2011; Mayer, Bolognese *et al.*, 2000; McCloskey, Hunt *et al.*, 2007; Sarfati, Bettler *et al.*, 1992). These studies suggest the ability of sCD23 fragments to up-regulate IgE synthesis depends on their ability to form trimers. Despite the inability of derCD23 to oligomerise, distinct binding sites for CD21 and IgE have been identified (Hibbert, Teriete *et al.*, 2005). Dual binding to both mIgE and CD21 is not thought to be possible *in vivo* due to the relative sizes of the molecules and their positioning on the cell surface. This may explain the down-regulation of IgE following addition of monomeric derCD23 (Sarfati, Bettler *et al.*, 1992).

Several studies have utilised pharmacological inhibitors of ADAM10 (e.g. GI254023X) to inhibit mCD23 cleavage and, therefore, reduce sCD23 production (Lemieux, Blumenkron *et al.*, 2007; Mathews, Ford *et al.*, 2011; Mayer, Bolognese *et al.*, 2000; Weskamp, Ford *et al.*, 2006). Mayer *et al* showed inhibition of mCD23 cleavage to correlate with inhibition of IL-4-stimulated IgE production in human peripheral blood lymphocytes (PBL) and human PBL-reconstituted SCID mice. In this study, progressively later additions of the mCD23 processing inhibitor in the 14 day culture period resulted in less inhibition of both sCD23 production and IgE secretion (Mayer, Bolognese *et al.*, 2000). Mayer *et al* concluded that inhibition of mCD23 processing alone is sufficient to inhibit IL-4-stimulated IgE production both *in vitro* and *in vivo*.

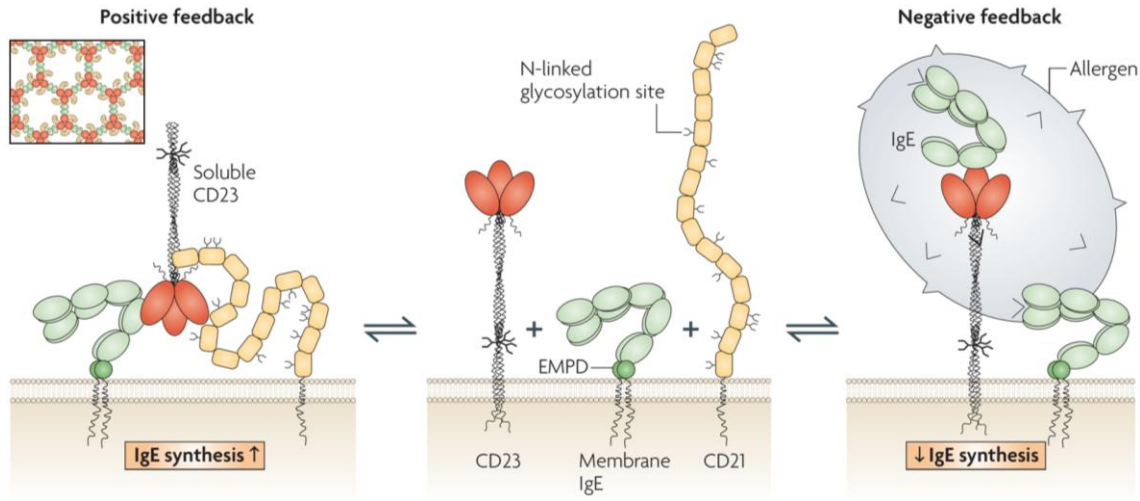

Figure 1.5. CD23-mediated regulation of IgE synthesis.

In this model, mCD23 is cleaved by ADAM10 to release trimeric sCD23 which co-ligates both mIgE and mCD21 on the surface of IgE-committed B cells to up-regulate IgE synthesis, triggering the onset of allergic symptoms. The inset shows the proposed formation of a large signalling network. Negative regulation occurs when the membrane form of CD23 is stabilised either through allergen-IgE complexes or certain anti-CD23 mAbs that bind the lectin 'head' domain (e.g. lumiliximab).

Adapted from (Gould and Sutton 2008).

1.8. Other functions of CD23

Allergen-IgE complexes can bind to CD23 on allergen-activated B cells, leading to antigen presentation to T cells in a process known as facilitated antigen presentation (FAP) (Carlsson, Hjelm *et al.*, 2007; Getahun, Hjelm *et al.*, 2005). Following internalisation of whole antigen, a range of peptides are displayed by HLA-DR molecules (Karagiannis, Warrack *et al.*, 2001) resulting in the generation of T cells with different epitope specificities, in a process known as 'epitope spreading' (Mudde, Bheekha *et al.*, 1995).

sCD23 can act as a B cell growth factor through the promotion of proliferation of IgE-specific plasmablasts. sCD23, together with IL-1, has been shown to rescue

germinal centre B cells from apoptosis through the up-regulation of Bcl-2 (Liu, Cairns *et al.,* 1991).

1.9. CD23 as a biomarker and clinical target

High sCD23 levels are observed in a wide variety of diseases such as haematopoietic cancers, auto-immune diseases and allergic disease. Chronic lymphocytic leukaemia (CLL) is currently the only disease in which sCD23 is used as a clinical biomarker. High plasma sCD23 concentrations correlate with CLL severity and progression (Meuleman, Stamatopoulos *et al.,* 2008; Reinisch, Willheim *et al.,* 1994; Sarfati, Chevret *et al.,* 1996; Schwarzmeier, Shehata *et al.,* 2002).

In the case of allergic disease, there is debate as to whether enhanced serum sCD23 is a predictive marker for diagnosing allergy or whether it is simply a consequence of the disease. Several studies have shown a correlation between elevated serum IgE and levels of both mCD23 and sCD23 in allergic patients (Aberle, Gagro *et al.,* 1997; Di Lorenzo, Drago *et al.,* 1999; Lorenzo, Mansueto *et al.,* 1996; Yanagihara, Sarfati *et al.,* 1990), whilst others have found no statistically significant correlation (Rogala and Rymarczyk 1999; Wilhelm, Klouche *et al.,* 1994).

The anti-CD23 mAb, lumiliximab, down-regulates IgE synthesis in human B cells *in vitro* (McCloskey, Hunt *et al.,* 2007). A phase I clinical trial of lumiliximab in patients with mild-to-moderate persistent allergic asthma reduced serum IgE levels (Rosenwasser, Busse *et al.,* 2003; Rosenwasser and Meng 2005). In 2004, lumiliximab in combination with chemotherapy drugs (fludarabine and cyclophosphamide) and rituximab (anti-CD20), entered a six year Phase I/II clinical trial for patients with relapsed $CD23^+$ B cell CLL (Byrd, Kipps *et al.,* 2010). Phase II randomised multi-

centre studies shortly followed, in patients with previously untreated CLL (clinical trial #NCT00801060) and relapsed CLL (clinical trial #NCT00391066). However, both of these trials were terminated in 2010.

sCD23, as well as mCD23, may be a promising target for therapy, as the work in this thesis shows. The use of selective ADAM10 inhibitors is considered a potential therapy for asthma, based on a recent pre-clinical trial in mice where intranasal administration of selective ADAM10 inhibitors led to reduced eosinophilia in the bronchoalveolar lavage fluid and reduced AHR (Mathews, Ford *et al.*, 2011). In support of this therapeutic potential, it is known that asthmatics express high levels of ADAM10 in the lung (Dijkstra, Postma *et al.*, 2009).

1.10. Hypothesis & Aims of the thesis

Due to the multiple forms of CD23, multiple ligands and various activities of the different complexes, the mechanisms involved in IgE regulation by CD23 are still poorly understood. The main aim of this thesis is to therefore investigate the role of different forms of CD23 in the regulation of IgE in primary human B cells.

The hypothesis that sCD23 can form a tri-molecular complex by binding to both mIgE and mCD21 to induce the up-regulation of IgE synthesis will be tested through the aims described below.

- Isolated human tonsil B cells will be cultured with IL-4 and anti-CD40 to induce CSR to IgE, expression of mCD23 and mCD21 and production of sCD23 and secretion of IgE. sCD23 levels will be reduced through siRNA-mediated inhibition of CD23 or ADAM10 inhibition using GI254023X.

- In contrast, sCD23 levels will be increased through addition of recombinant trimeric and monomeric sCD23 fragments.

- In all cases, the loss of mCD23 from the B cell surface, the appearance of sCD23 in the supernatant and the expression and secretion of IgE, as a function of time for up to 12 days, will be analysed by flow cytometry and ELISA.

- The expression patterns of mIgE and mCD21, during the incubation of tonsil B cells with recombinant monomeric or trimeric sCD23, will be visualised by confocal microscopy.

- An improved understanding of the regulation of IgE in human B cells may provide potential new therapeutic targets in the treatment of allergic disease.

Chapter 2. Materials & Methods

2.1. Materials

2.1.1. Buffers & Media

All chemicals were purchased from Sigma-Aldrich and diluted in deionised water unless otherwise stated.

BrdU Staining Buffer: 3% FCS (Invitrogen) + 0.09% sodium azide in PBS

Cell Culture Media: RPMI 1640, penicillin (100IU/ml), streptomycin (100µg/ml), glutamine (2mM) (Invitrogen), 10% FCS (Hyclone; Perbio Biosciences), transferrin (35µg/ml) and insulin (5µg/ml)

ELISA Carbonate Buffer: 0.2M $NaCO_3$ + 0.2M $NaHCO_3$ (pH 9.8)

FACS Buffer: 5% normal goat serum (Invitrogen) in PBS

FACS Fix Buffer: 4% paraformaldehyde (EMS Ltd) in PBS

FACS Permeabilisation Buffer: 0.05% Triton® X-100 + 0.5% saponin in PBS

Microscopy Fix Buffer: 4% paraformaldehyde in PBS

Microscopy Wash Buffer: 0.05% Triton® X-100 in PBS

PBS-T: 0.05% Tween® 20 in PBS

2.1.2. Antibodies

Application	Antibody	Manufacturer	Conjugated	Concentration used
Cell culture	Monoclonal mouse anti-human CD21 (HB-5)	Santa Cruz Biotechnology	-	0.1-10µg/ml
Confocal				1:100
Confocal	Goat anti-mouse (secondary)	Molecular Probes, Invitrogen	Alexa 594	1:500
FACS	Mouse anti-human ADAM10	R&D Systems	PE	1:50
FACS	Monoclonal mouse anti-human CD3	Dako	PE	1:50
FACS	Monoclonal mouse anti-human CD20	Dako	FITC	1:50
FACS	Monoclonal mouse anti-human CD21 (HB-5)	eBioscience	APC	1:50
FACS	Mouse anti-human CD23 (EBVCS-5)	BioLegend	APC	1:50
FACS	Mouse anti-human CD23 (MHM6)	Dako	FITC	1:50
FACS	Monoclonal mouse anti-human CD38	Dako	FITC	1:50
FACS	Monoclonal mouse anti-human CD38	Dako	PE	1:50
FACS	Monoclonal mouse anti-human CD138	AbD Serotec	PE	1:10
FACS	Polyclonal goat anti-human IgE	Vector Laboratories	FITC	1:500
Confocal				1:200
FACS	Monoclonal mouse anti-human IgG	Miltenyi Biotec	APC	1:50
FACS	Mouse anti-human BrdU	BD Biosciences	APC	1µl
ELISA	Polyclonal mouse anti-human IgE	Dako	-	1:7000

ELISA	Mouse anti-human IgE	Dako	HRP	1:1000
ELISA	Polyclonal goat anti-human IgG	AbD Serotec	-	1:1000
ELISA	Goat anti-human IgG	Sigma-Aldrich	HRP	1:1000
Luminex	Streptavidin	Millipore	PE	25µl/well

Table 2.1. Antibodies used

2.2. Isolation of human tonsil B cells

Following informed written consent, with ethical approval from Guy's Research Ethics Committee, human tonsils from donors undergoing routine tonsillectomies were obtained. The allergic status of the donor was determined by verbal communication with the parents at the time of consent. A list of tonsil donors, their allergic status and any medication the patients were taking is listed in Appendix 1. The tonsil donors used for each experiment is indicated in each figure legend. Mononuclear cells were separated by density on a Ficoll gradient (GE Healthcare) and B cells isolated using AET-treated sheep red blood cells (TCS Biosciences). The remaining cells were routinely >98% $CD20^+$ and <2% $CD3^+$, as determined by flow cytometry (Figure 2.1).

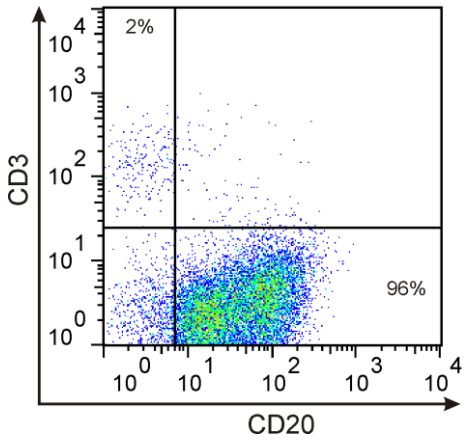

Figure 2.1. Purity of freshly isolated human tonsil B cells.

B cells were isolated from human tonsils by density centrifugation as described in Section 2.2. The expression of CD20 (B cell marker) and CD3 (T cell marker) were analysed by flow cytometry.

Data shown from 1 donor (tonsil number 2), representative of 35 (tonsil numbers 1-35).

2.3. Small interfering RNA (siRNA) transfection

Total B cells were transfected with the appropriate siRNA (3µg/960nM) (Thermo Scientific Dharmacon) as shown in Table 2.2 using the Amaxa™ Human B cell Nucleofector™ kit and Nucleofector™ II Device (Lonza), according to the manufacturer's instructions. Transfection efficiency, 30 minutes after transfection, was determined using a fluorescent non-functional siRNA (siGLO® Red) (Thermo Scientific Dharmacon). The efficiency of CD23 knockdown was quantified by qPCR (described in Section 2.8). Although siRNA is designed to be specific to the gene of interest, the small possibility of off-target effects cannot be excluded.

Target	siRNA details
Control (Non-targeting)	ON-TARGET*plus* Non-targeting siRNA Pool #1 (D-001206-13-05)
GAPDH	ON-TARGET*plus* GAPD Control siRNA (DZD11400120)
CD23	CD23 siGENOME SMARTpool®: GGAGGAAGGUCAAUAUUCA, CGGAACGUCUCUCAAGUUU, GAACAGCAGAGAUUGAAAU and CAUGGGACCUGAUUCAAGA (M-016242-00)
siGLO® Red	siGLO® Red Transfection Indicator DY-547 (D-001630-02-05)

Table 2.2. siRNA reagents

2.3.1. Post-transfection cell sorting

To separate positively and negatively transfected cells, human B cells were co-transfected with siGLO® Red and CD23 siRNA as described in Section 2.3. Live siGLO$^-$ and siGLO$^+$ cells were then separated using a FACS Aria™ Cell Sorter (BD Biosciences).

2.4. Cell Culture

B cells were cultured in 24-well plates (Nunc) at 0.5x10^6 cells/ml in Cell Culture Media. Cells were activated with IL-4 (200IU/ml) (R&D Systems) and anti-CD40 antibody (1µg/ml) (G28.5; ATCC) for up to 12 days.

2.4.1. ADAM10 inhibitor (GI254023X)

The ADAM10-specific hydroxamate-based small molecule inhibitor, GI254023X, was kindly provided by B Schmidt and B Drung from Technische

Universität Darmstadt, Germany. GI254023X ((*R*)-N-((*S*)-3,3-dimethyl-1-(methylamino)-1-oxobutan-2-yl)-2-((*S*)-1-(N-hydroxyformamido)ethyl)-5-phenylpentanamide)) was purified on a CombiFlash Rf® (Teledyne ISCO) system (column: RediSep Rf, 4 g silica; flow rate: 18ml/min; solvent: acetonitrile; t_R: 10 min). HPLC analysis at 220nm confirmed a purity ≥98% (Hoettecke, Ludwig *et al.,* 2010). Cells were grown for 5 days, to allow the up-regulation of CD23 and CSR to IgE, before addition of the inhibitor (0.25µM–15µM).

2.4.2. Recombinant CD23 proteins

Monomeric derCD23 (16145 Da) was made as previously described (Hibbert, Teriete *et al.,* 2005). lzCD23, made as previously described (McCloskey, Hunt *et al.,* 2007), was modified to produce the more stable trimer triCD23 (84414 Da), consisting of residues 131-321 of human CD23 prefixed by the trimerisation motif (IAAIESK)4 and expressed and refolded from inclusion bodies using the Escherichia coli vector pET151. This additionally provided N-terminal HIS_6 and V5 epitope tags and a TEV enzyme cleavage site that has been left uncleaved in the final product (designed by Rebecca Beavil and produced by Michael Wen-Pin Kao) (manuscript in preparation). Recombinant CD23 proteins were dialysed into PBS and sterile-filtered before addition to human B cell cultures. Concentrations were selected to be close to the calculated K_D value for trimeric CD23 binding to IgE (10^{-7}M) (Hibbert, Teriete *et al.,* 2005; McCloskey, Hunt *et al.,* 2007) and used at a weight ratio of 1:3 (triCD23:derCD23) to maintain the same number of mIgE/mCD21 binding sites in each condition.

2.4.3. Anti-CD21 mAb

Mouse anti-human CD21 mAb (HB-5) (Santa Cruz) was added to cells at 0.1, 1 or 10µg/ml. Epitope analysis has shown this clone to bind to SCRs 3-4 on CD21 and partially inhibit CD23 binding to CD21 (Aubry, Pochon *et al.*, 1994).

2.5. Flow cytometry

2.5.1. Analysis of cell viability

Cell viability was quantified using flow cytometry with the proportion of live cells determined by gating on forward versus side scatter.

2.5.2. Membrane and intracellular staining

At the appropriate timepoints, cells were collected into FACS tubes and washed in FACS Buffer. Antibodies to detect membrane-expressed markers (as shown in Table 2.1) were added and incubated on ice in the dark for 45 minutes. Cells were then washed in FACS Buffer, fixed with 500µl FACS Fix Buffer and incubated at room temperature for 15 minutes. Cells were then washed in FACS Buffer and resuspended in 200µl FACS Permeabilisation Buffer for 15 minutes. Intracellular antibodies were added (as shown in Table 2.1) and incubated on ice in the dark for 45 minutes. Collection of flow cytometry data was conducted using a FACS Calibur™ (BD Biosciences), with gating on live cells, and events analysed using FlowJo software (Treestar).

2.5.3. CFSE labelling for analysis of cell division

Cells were washed and resuspended at $1x10^6$ cells/ml in 2ml of RPMI (Invitrogen). CellTrace™ CFSE (5µM) (Invitrogen) in DMSO was added in 2ml of RPMI, for a final concentration of 2.5µM. Cells were incubated for 10 minutes at room temperature, washed twice in Cell Culture Media and counted. Cells were then cultured as described in Section 2.4 and CFSE content analysed by flow cytometry on day 7.

2.5.4. BrdU incorporation for proliferation analysis

Using the APC BrdU Flow kit (BD Pharmingen), cells were labelled with BrdU (1mM) by direct addition to a well containing 1ml of cells (final concentration of 10µM) and pulsed for 24 hours at 37°C. Cells were then washed in FACS tubes with 1 x Perm/Wash Buffer, resuspended in 100µl Cytofix/Cytoperm Buffer and incubated for 15-30 minutes at room temperature. Cells were then washed and resuspended in 100µl Cytoperm Plus Buffer and incubated for 10 minutes on ice. Cells were then washed, resuspended in 100µl Cytofix/Cytoperm Buffer and incubated for 5 minutes at room temperature. Next, cells were resuspended in 100µl of DNase solution (30µg) and incubated for 1 hour at 37°C. Cells were then washed and resuspended in 50µl Perm/Wash Buffer containing anti-human BrdU-APC. Finally, cells were resuspended in 1ml Staining Buffer and BrdU incorporation measured by flow cytometric analysis, at no more than 400 events/second.

2.6. ELISA

2.6.1. IgE

Maxisorp plates (Nunc) were coated with mouse anti-human IgE, in ELISA Carbonate Buffer, overnight at 4°C. Unbound sites were blocked with 2% milk powder in PBS-T for 1 hour at room temperature. Supernatant samples were then added at appropriate dilutions and plates incubated overnight at 4°C. Human serum IgE (NIBSC) was used to construct a standard curve. IgE binding was detected by mouse anti-human IgE-HRP in 1% milk in PBS-T for 2 hours at 37°C. The colour reaction was developed with OPD (Sigma-Aldrich) and analysed at 492nm using an automated plate reader (Titertek). Accumulated IgE concentrations were calculated from the standard curve using GraphPad Prism 5.03 software (San Diego, USA), with a minimum detectable concentration of 2ng/ml.

2.6.2. IgG

Maxisorp plates were coated with goat anti-human IgG, in ELISA Carbonate Buffer, overnight at 4°C. Unbound sites were blocked with 2% milk powder in PBS-T for 1 hour at room temperature. Supernatant samples were then added at appropriate dilutions and plates incubated overnight at 4°C. Human serum IgG (Sigma) was used to construct a standard curve. IgG binding was detected by goat anti-human IgG-HRP in 1% milk in PBS-T for 2 hours at 37°C. The colour reaction was developed with OPD and analysed at 492nm using an automated plate reader. Accumulated IgG concentrations were calculated from the standard curve using GraphPad Prism 5.03 software, with a minimum detectable concentration of 2ng/ml.

2.6.3. sCD23

Human sCD23 EASIA™ ELISA kits (BioSource International) were used according to the manufacturer's instructions. Briefly, supernatants were added to microtiter plates pre-coated with a mixture of monoclonal anti-CD23 antibodies and anti-CD23-HRP was added for 2 hours at room temperature. The colour reaction was developed with TMB and analysed at 450 nm using an automated plate reader. The kit recognises the 16, 25, 29 and 37 kDa fragments of sCD23. Accumulated sCD23 concentrations were calculated from the standard curve using GraphPad Prism 5.03 software, with a minimum detectable concentration of ~200pg/ml.

2.7. MILLIPLEX® MAP Human Cytokine Assay

A MILLIPLEX® MAP Human Cytokine 96-well Plate Assay (Millipore) was custom-made for the simultaneous quantification of human IL-2, IL-6, IL-10, IL-13 and IFNγ and used according to the manufacturer's instructions. Briefly, supernatants, controls and standards were added in duplicate to the 96-well filter plate with 25µl mixed antibody-immobilised beads per well and incubated on a plate shaker for 1 hour at room temperature. The fluid was removed by vacuum and the plate washed twice. 25µl biotinylated detection antibodies were added per well and incubated on a plate shaker for 30 minutes at room temperature. Next, 25µl streptavidin-PE was added per well and incubated on a plate shaker for 30 minutes at room temperature. The fluid was removed by vacuum and the plate washed twice. 150µl of PBS was added per well and the beads resuspended on a plate shaker for 5 minutes. The plate was run on a FLEXMAP 3D® machine (Luminex Corporation, Texas, USA) and the cytokine

concentrations were calculated from analysis of MFI values. The minimum detection level for all cytokines was 0.4pg/ml.

2.8. Quantitative PCR (qPCR)

Total RNA was isolated from cells using RNeasy Mini kits (Qiagen), primed with oligo(dT) and random hexamers and reverse transcribed using Superscript II (Invitrogen). qPCR was performed using TaqMan® MGB gene expression assays (Table 2.3) and TaqMan® Universal PCR Master Mix on a 7900HT Real-Time PCR machine (Applied Biosystems). Gene expression was normalised to an endogenous reference gene (β2-microglobulin) and quantified by ΔΔ threshold cycle (C_t) analysis (SDS 2.1 software). All reactions were carried out in triplicate.

Target gene	Assay details/oligo sequence
β2-microglobulin	4310886E
CD23	Hs00233627_m1
εGLT	F: 5' CTGTCCAGGAACCCGACAGA 3' R: 5' TGCAGCAGCGGGTCAAG 3' Probe: 6FAM-AGGCACCAAATG-MGB
GAPDH	Hs02786624_g1

Table 2.3. qPCR reagents.

2.9. PyroGene™ Recombinant Factor C assay for endotoxin detection

The Pyrogene™ Recombinant Factor C (rFC) Endpoint Fluorescent Assay (Lonza) was used according to the manufacturer's instructions. Briefly, 100µl of samples and endotoxin standards were added in triplicate to the 96-well plate and incubated at 37ºC for 10 minutes. rFC enzyme solution, assay buffer and fluorogenic substrate were mixed at a ratio of 1:4:5 and 100µl was added per well. The fluorescence at time zero and at 1 hour was analysed at 380nm using an automated plate reader. Endotoxin concentration was calculated from the standard curve using GraphPad Prism 5.03 software.

2.10. Confocal microscopy

Human tonsillar B cells were stimulated for 8 days with IL-4 and anti-CD40, harvested and dead cells removed by density on a Ficoll gradient. $3x10^5$ cells were stimulated with either media alone, derCD23 (3µM/48µg/ml), triCD23 (1µM/84µg/ml) or anti-CD21 mAb (10µg/ml) at 37ºC for 30 minutes. Cells were fixed with Microscopy Fix Buffer, washed with Microscopy Wash Buffer, mounted onto poly-$_L$-lysine-coated coverslips and fixed again. Coverslip-mounted cells were stained with goat anti-human IgE-FITC and mouse anti-human CD21 for 1 hour, washed, and secondary goat anti-mouse-Alexa 594 was added for 45 minutes. The nuclear stain Hoescht 33258 (1:20,000) (Molecular Probes, Invitrogen) was added for 10 minutes, cells were washed 3 times and immunofluorescence visualised with an SP2 confocal microscope (Leica Microsystems). Multi-colour overlay images were created using ImageJ software (National Institutes of Health, USA).

2.11. Statistical analysis

Flow cytometry and ELISA data are shown relative to control-treated cells (either transfected with control siRNA or stimulated with IL-4 and anti-CD40 alone, depending on the experiment), to compensate for inter-donor variation. Data from the 7 out of 32 donors that failed to respond to IL-4 and anti-CD40, with undetectable levels of IgE expression and secretion by day 12, were excluded from selected figures.

Data are summarised as mean ± SEM. For comparisons between two non-paired groups, statistical analysis was performed using the Mann-Whitney *U* test. For comparisons between two paired groups, statistical analysis was performed using the Wilcoxon matched-pairs signed rank test. For comparisons between multiple groups, statistical analysis was performed using ANOVA with Bonferroni correction. The post-test for linear trend was used to analyse dose-dependent trends. In all cases, a p-value of <0.05 was considered significant (ns = non-significant, * = <0.05, ** = <0.01, *** = <0.001). Significance to control conditions is indicated above data and significance between two conditions is shown between data. Correlation analysis was performed using Spearman's rank correlation coefficient.

Chapter 3. Improving *in vitro* CSR to IgE in human B cells

3.1. Introduction

Isotype class-switching to IgE in human B cells is induced by the interaction with Th2 cells. In the lymph nodes, Th2 cells secrete IL-4 and IL-13 and express CD40L which can co-ligate CD40 on B cells. Together, this promotes further Th2 cell differentiation and CSR to IgE (Jabara, Fu *et al.*, 1990). To re-create this scenario *in vitro*, primary human tonsillar B cells were stimulated with recombinant human IL-4 and an anti-CD40 mAb (aCD40). This chapter describes the *in vitro* model for induction of IgE expression and secretion from primary human B cells and how this can be enhanced by the inclusion of the additional cytokines IL-10 and IL-21.

3.2. CSR to IgE *in vitro* requires IL-4 and anti-CD40

In order to initially determine the correct functioning of this system, primary human B cells were cultured for up to 12 days, in culture media alone or in the presence of IL-4 and anti-CD40. Surface and intracellular expression of IgE was assessed by flow cytometry (as described in Section 2.5.1) and secreted IgE (sIgE) levels assessed by ELISA (as described in Section 2.6.1). Figure 3.1 shows one example, from 32 donors, of how IgE expression and secretion were modulated by the addition of IL-4 and anti-CD40. As expected, the presence of both IL-4 and anti-CD40 were essential for cell survival and up-regulation of IgE from human B cells, levels of which could be detected from day 4 onwards (Figure 3.1).

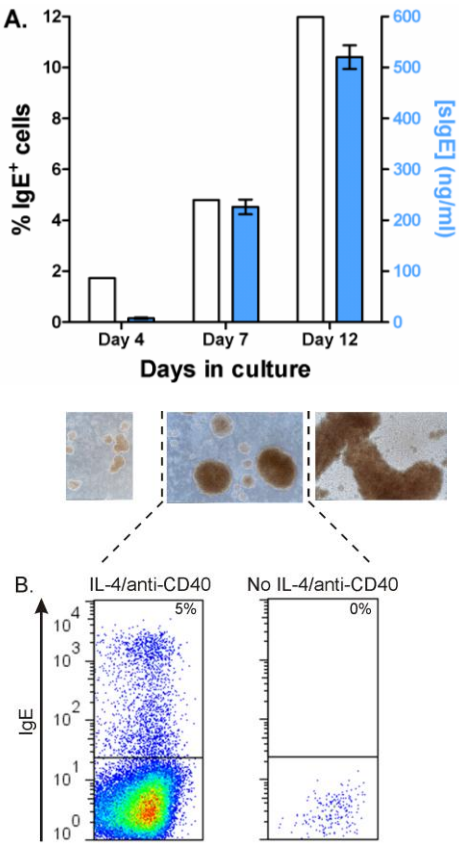

Figure 3.1. Human B cells require IL-4 and anti-CD40 for IgE expression and secretion.

Total B cells were cultured for 12 days in the presence or absence of IL-4 (200IU/ml) and anti-CD40 (1µg/ml) and monitored for the expression of membrane and intracellular IgE by flow cytometry and sIgE by ELISA. **(A)** % of live IgE^+ cells measured by flow cytometry (white bars, left y-axis) and sIgE production by ELISA (blue bars, right y-axis), on days 4, 7 and 12, from cells stimulated with IL-4 and anti-CD40. Error bars represent SEM from experimental triplicates. Photographs show the proliferation and clumping of B cells over the culture period. **(B)** IgE expression 7 days after stimulation with or without IL-4 and anti-CD40, where % values shown represent the % of live IgE^+ cells.

Data shown from 1 (tonsil number 5) of 32 donors.

A titration of IL-4 and anti-CD40 was carried out to dissect the individual roles of each stimulation on human B cells. Cells were stimulated with either 100%, 50% or 25% of the normal IL-4 and anti-CD40 concentrations (as described in Section 2.4) and cultured for 12 days before analysis of viability, IgE expression and IgE secretion. Figure 3.2A and Figure 3.2B show that the addition of IL-4 was more important for maintaining cell viability than the addition of anti-CD40. IgE expression was vastly

reduced with decreasing concentrations of IL-4 (Figure 3.2C) and IgE secretion was reduced with decreasing concentrations of either IL-4 or anti-CD40 (Figure 3.2D).

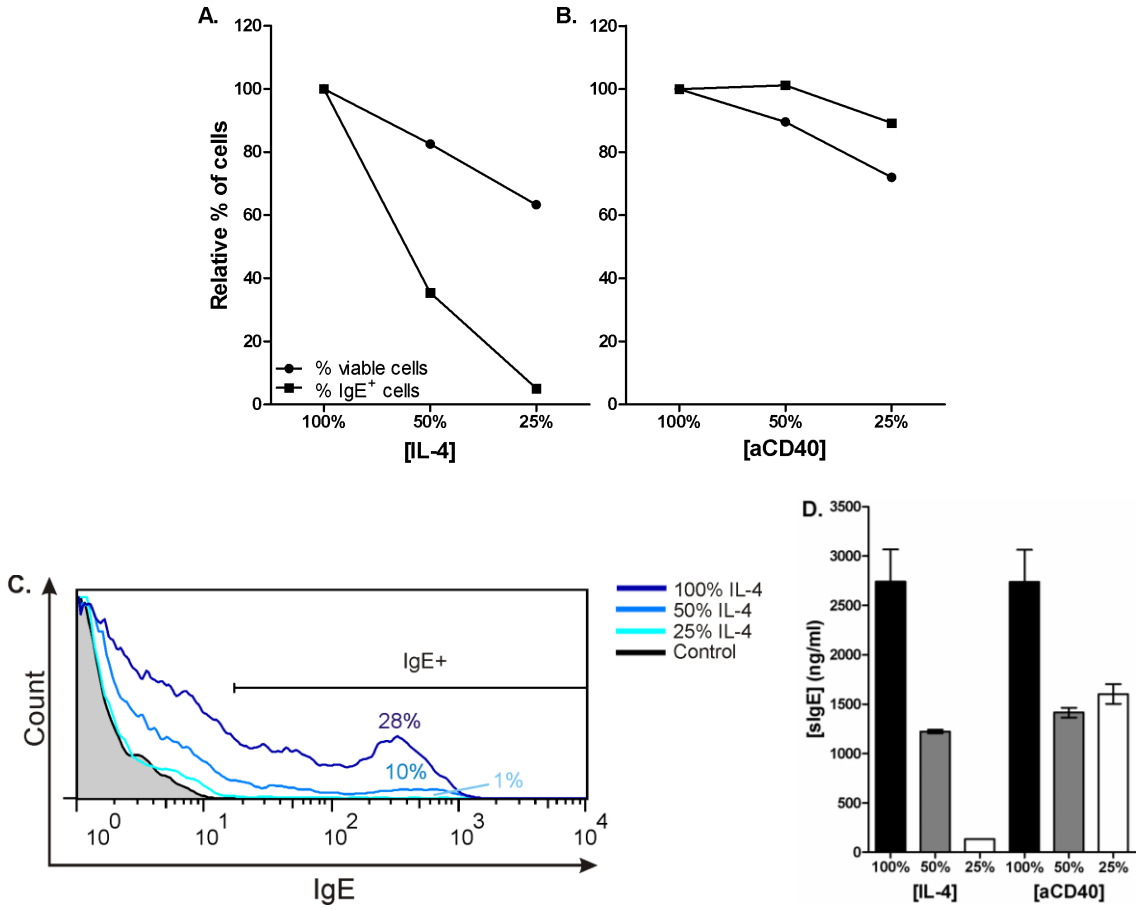

Figure 3.2. IgE expression and secretion are dependent on both IL-4 and anti-CD40.

Total B cells were cultured for 12 days in the presence of reducing concentrations of either IL-4 or anti-CD40 and monitored for the expression of membrane and intracellular IgE by flow cytometry and sIgE by ELISA. **(A)** Day 12 cell viability and IgE expression of cells cultured with IL-4 at 100% (200IU/ml), 50% (100IU/ml) or 25% (50IU/ml) and 100% anti-CD40 (1µg/ml), relative to cells cultured with 100% IL-4 and anti-CD40. **(B)** Day 12 cell viability and IgE expression of cells cultured with anti-CD40 at 100% (1µg/ml), 50% (500ng/ml) or 25% (250ng/ml) and 100% IL-4 (200IU/ml), relative to cells cultured with 100% IL-4 and anti-CD40. **(C)** Day 12 IgE expression in cells cultured with sub-optimal IL-4 concentrations and 100% anti-CD40. **(D)** IgE secretion by day 12 from cells cultured with sub-optimal IL-4 or anti-CD40 concentrations. Error bars represent SEM from experimental triplicates.

n=1 (tonsil number 16).

3.2.1. IgE secretion from non-allergic versus allergic donors

Since May 2009 it became possible to question the parents of tonsil donors on the allergic status of their child. Before this date, due to ethical restrictions, the allergic status of tonsil donors was unknown and, therefore, it was not possible to correlate *in vitro* IgE expression and secretion with allergic status. Figure 3.3A shows the range of IgE secretion from human B cells cultured for 12 days with IL-4 and anti-CD40 (n=29). Excluding the 5 donors which did not produce any detectable sIgE by day 12, sIgE levels varied from 2 – 2742ng/ml (mean = 573 ± 151ng/ml, n=24). There was no significant difference between the levels of IgE secretion from non-allergic donors versus allergic donors. Figure 3.3B shows the range of IgG secretion from human B cells cultured for 12 days with IL-4 and anti-CD40 (n=21). Less donors are shown in Figure 3.3B compared to Figure 3.3A due to not enough supernatants available to test for both IgE and IgG. The difference of 8 donors is, therefore, not due to the fact that no IgG was detected in these particular donors. There was no significant difference between the levels of IgG secretion from non-allergic donors versus allergic donors.

It is of interest that the level of *in vitro* IL-4 and anti-CD40-stimulated IgE secretion does not appear to correlate with allergic severity. Specific allergies or allergic conditions are annotated on Figure 3.3, with the most atopic patient (allergic rhinitis, eczema, egg and nut allergy) producing the least sIgE of all the allergic patients (only 15ng/ml by day 12). This indicates that any differences seen in IgE secretion in future experiments cannot be attributed to the allergic status of the patient from which the tonsil and B cells were isolated.

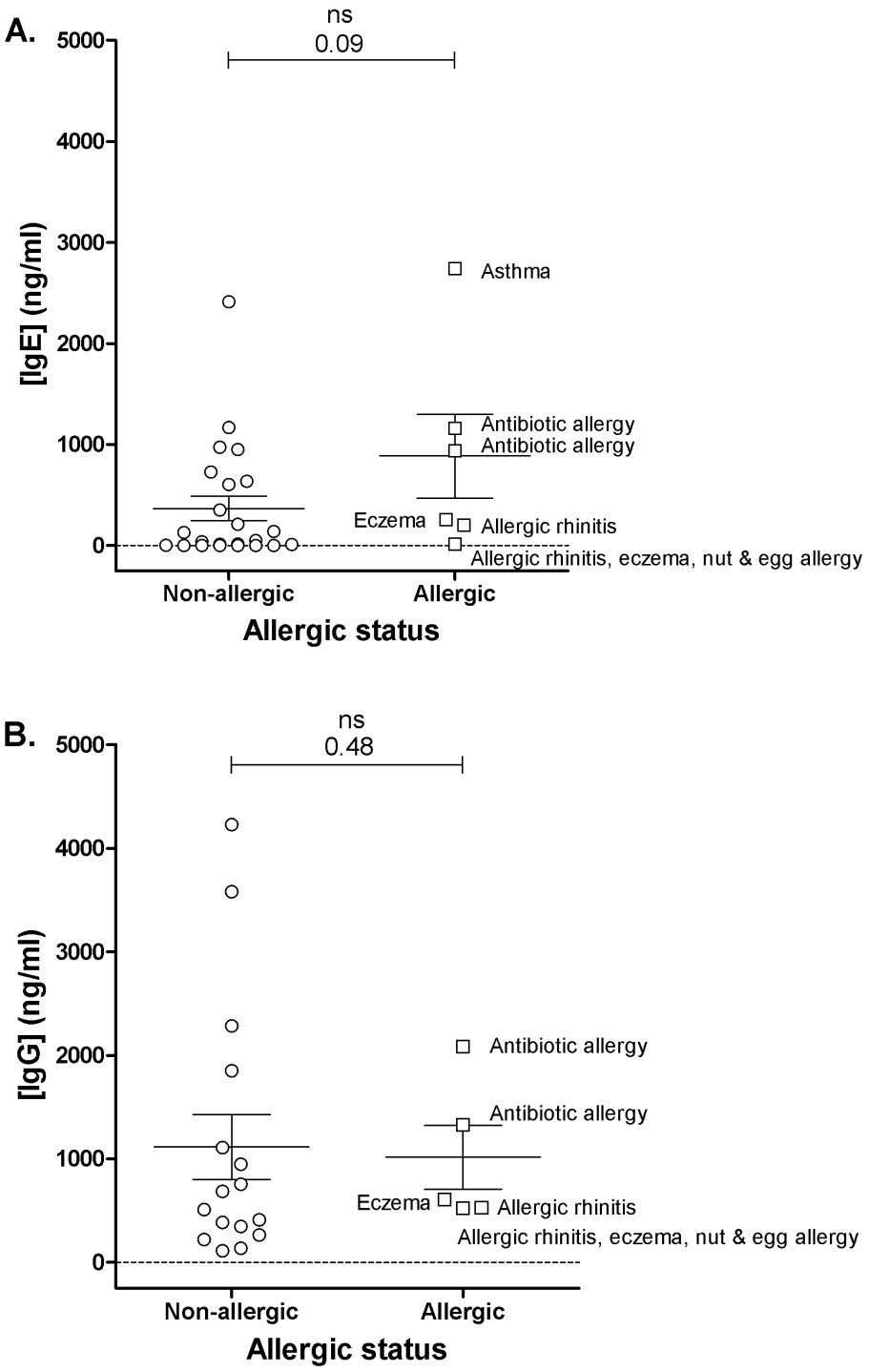

Figure 3.3. Levels of in vitro IgE and IgG secretion are not associated with allergic status.

Total B cells, from either non-allergic (○) (n=23) or allergic donors (□) (n=6), were cultured with IL-4 (200IU/ml) and anti-CD40 (1µg/ml) and **(A)** IgE secretion (n=29, tonsil numbers 4-32) and **(B)** IgG secretion (n=21, tonsil numbers 8, 11-15, 17-25 & 27-32) were analysed by ELISA on day 12. Specific allergies or allergic conditions are annotated by each allergic donor.

Error bars represent SEM and statistical analysis was performed using the Mann-Whitney *U* test.

3.3. Increasing IgE production with the addition of IL-10 and IL-21

The induction of class switching to IgE in human B cells *in vitro* was already a well established protocol within the group. However, IgE levels often varied hugely between donors and it was a regular occurrence to detect no IgE expression or secretion after 12 days in culture, as demonstrated in Figure 3.3. Designing a reliable system which would consistently result in high IgE expression and secretion would greatly benefit my own studies and others working within the group, especially for future assays which aim to decrease IgE levels. In view of this, the addition of IL-10 and IL-21 into the culture media was investigated.

IL-10 is considered a suppressive agent in the immune response and, therefore, it would seem important to investigate its effect on the regulation of IgE. It is well documented that IL-10 increases cell division in the murine system (Hasbold, Lyons *et al.,* 1998; Hodgkin, Lee *et al.,* 1996) and, more recently, an IL-10-mediated association between CSR to IgG and cell division was shown in the human *in vitro* (Tangye, Avery *et al.,* 2003; Tangye, Ferguson *et al.,* 2002). However, similar studies on human IgE have been restricted due to low IgE production from primary human B cells *in vitro*. Conflicting reports surround this field, with some reports stating that IL-10 inhibits IL-4 and anti-CD40-stimulated IgE production from PBMCs (Milovanovic, Heine *et al.,* 2009; Punnonen, de Waal Malefyt *et al.,* 1993) and purified B cells (Akdis, Blesken *et al.,* 1998), whilst other reports show an increase in IgE due to increased proliferation and plasma cell differentiation (Kobayashi, Nagumo *et al.,* 2002; Rousset, Peyrol *et al.,* 1995). Differences appear to be most likely due to the source of B cells and the chosen method to stimulate CD40 signalling.

IL-21, a recently identified type I cytokine produced by $CD4^+$ T cells and NKT cells, is known to enhance B cell proliferation (Parrish-Novak, Dillon *et al.*, 2000). Like IL-10, conflicting reports exist on whether IL-21 up-regulates (Caven, Shelburne *et al.*, 2005; Caven, Sturgill *et al.*, 2007) or down-regulates (Pene, Guglielmi *et al.*, 2006; Wood, Bourque *et al.*, 2004) IgE production from human B cells *in vitro*. These differences are most likely due to the concentration of IL-21 and B cell density. It has been reported that IL-21 up-regulates IgE production from human B cells through the promotion of plasma cell differentiation (increase in BLIMP-1, XBP-1 and $CD38^{hi}$ cells) and enhancement of AID expression, working in synergy with IL-10 (Caven, Shelburne *et al.*, 2005; Caven, Sturgill *et al.*, 2007; Kobayashi, Nagumo *et al.*, 2002; Kobayashi, Haruo *et al.*, 2009). This signalling pathway has been shown to involve STAT3 (Avery, Ma *et al.*, 2008) and Bcl-6 (Kitayama, Sakamoto *et al.*, 2008).

3.3.1. IL-10 and IL-21 increase IgE and IgG expression

Initially, the effect of IL-10 and IL-21 on the expression of IgE and IgG was investigated in human B cells. Cells were isolated and stimulated with IL-4 and anti-CD40 alone, plus the addition of IL-10, IL-21 or a combination of IL-10 & IL-21, and cultured for up to 12 days. The population size (% positive cells) and mean fluorescence intensity (MFI) of IgE^+ and IgG^+ cells were analysed by flow cytometry (as described in Section 2.5.1) on days 5, 7 and 12 and compared to cells cultured with IL-4 and anti-CD40 alone.

Under the normal culture conditions of IL-4 and anti-CD40 alone, the population size of IgE^+ cells increased over the 12 day culture period. The majority of this expansion took place between days 7 and 12 (Figure 3.4A). The addition of IL-10 ± IL-21 caused an increase in the percentage and MFI of IgE^+ cells on days 5 and 7. By day

12, the presence of the additional cytokines no longer resulted in a larger proportion of IgE^+ cells or higher MFI, compared to cells cultured with IL-4 and anti-CD40 alone. However, none of these differences reached statistical significance (Figure 3.4).

Figure 3.5 shows flow cytometric analysis of IgG expression following stimulation with IL-4 and anti-CD40 alone, plus the addition of IL-10, IL-21 or IL-10 & IL-21. Unlike the IgE^+ population, the IgG^+ population size decreased over the 12 day culture period, in cells cultured with IL-4 and anti-CD40 alone, presumably as CSR to other isotypes was taking place (Figure 3.5A). By days 5 and 7, the addition of either IL-10, IL-21 or IL-10 & IL-21 all caused an increase in the size of the IgG^+ population and MFI of IgG^+ cells. The addition of both IL-10 & IL-21 resulted in a statistically larger IgG^+ population by day 7 ($p=0.006$, $n=6$) (Figure 3.5A). With similarity to the effects on IgE expression, IgG expression was no longer elevated by day 12 in cells stimulated with IL-21 or IL-10 & IL-21.

It appears that the stronger the stimulus to increase IgE and IgG expression at the early timepoints, the larger the decrease in expression by day 12. The mechanisms by which this may occur will be discussed later in this chapter.

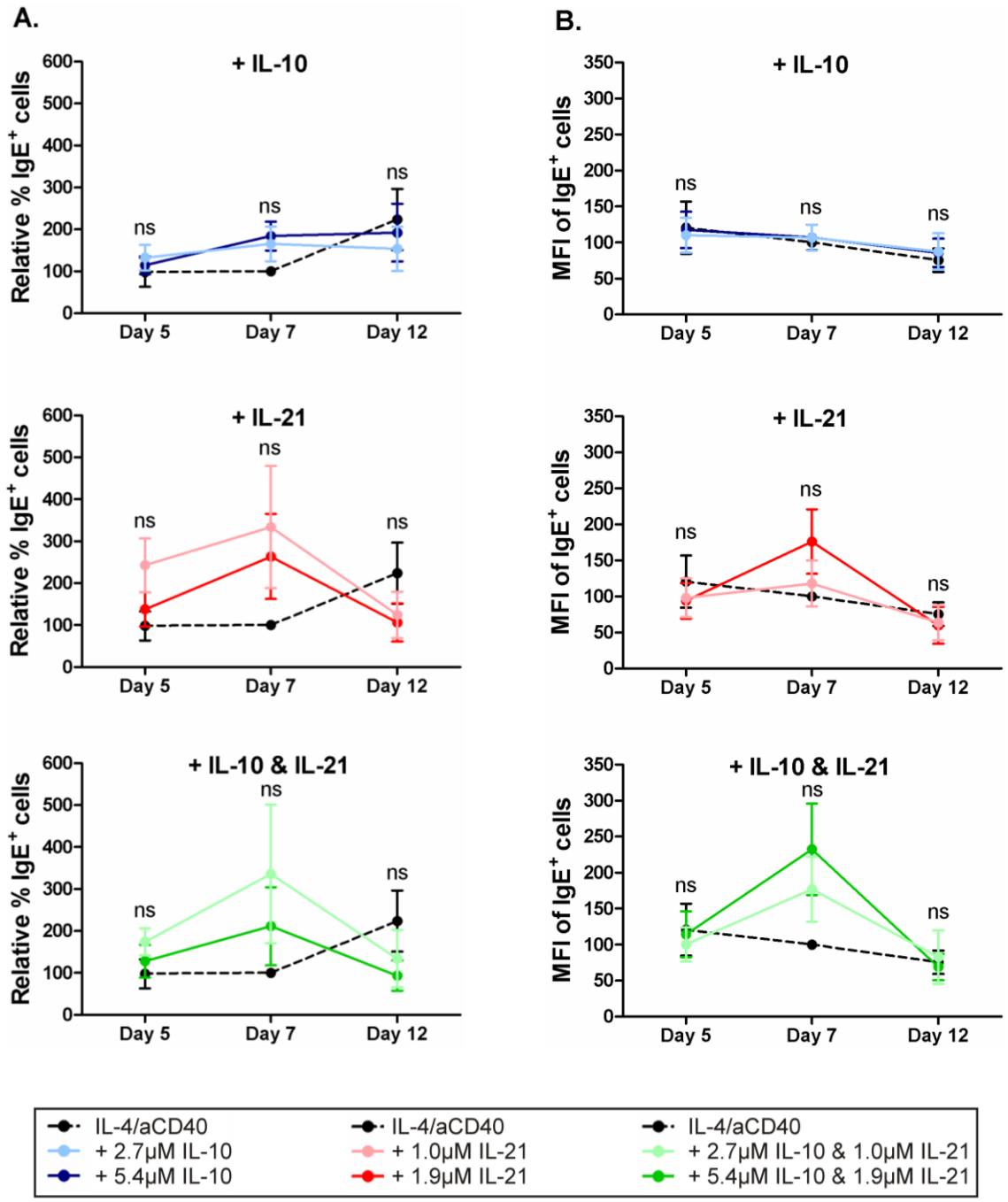

Figure 3.4. The addition of IL-10 or IL-21 increases early IgE expression.

Total B cells were cultured for up to 12 days in the presence of IL-4 (200IU/ml) and anti-CD40 (1μg/ml), with the addition of IL-10 (2.7μM/50ng/ml or 5.4μM/100ng/ml), IL-21 (1.0μM/30ng/ml or 1.9μM/60ng/ml) or combinations of IL-10 & IL-21. The expression of membrane and intracellular IgE was analysed on days 5, 7 and 12 by flow cytometry. **(A)** The % of live IgE^+ cells, relative to cells cultured with IL-4 and anti-CD40 alone at day 7 (100%). **(B)** The MFI of live IgE^+ cells, relative to cells cultured with IL-4 and anti-CD40 alone at day 7 (100%).

Error bars represent SEM and statistical analysis was performed using ANOVA with Bonferroni correction (n=9, tonsil numbers 4-7, 9, 10, 12, 15 & 17).

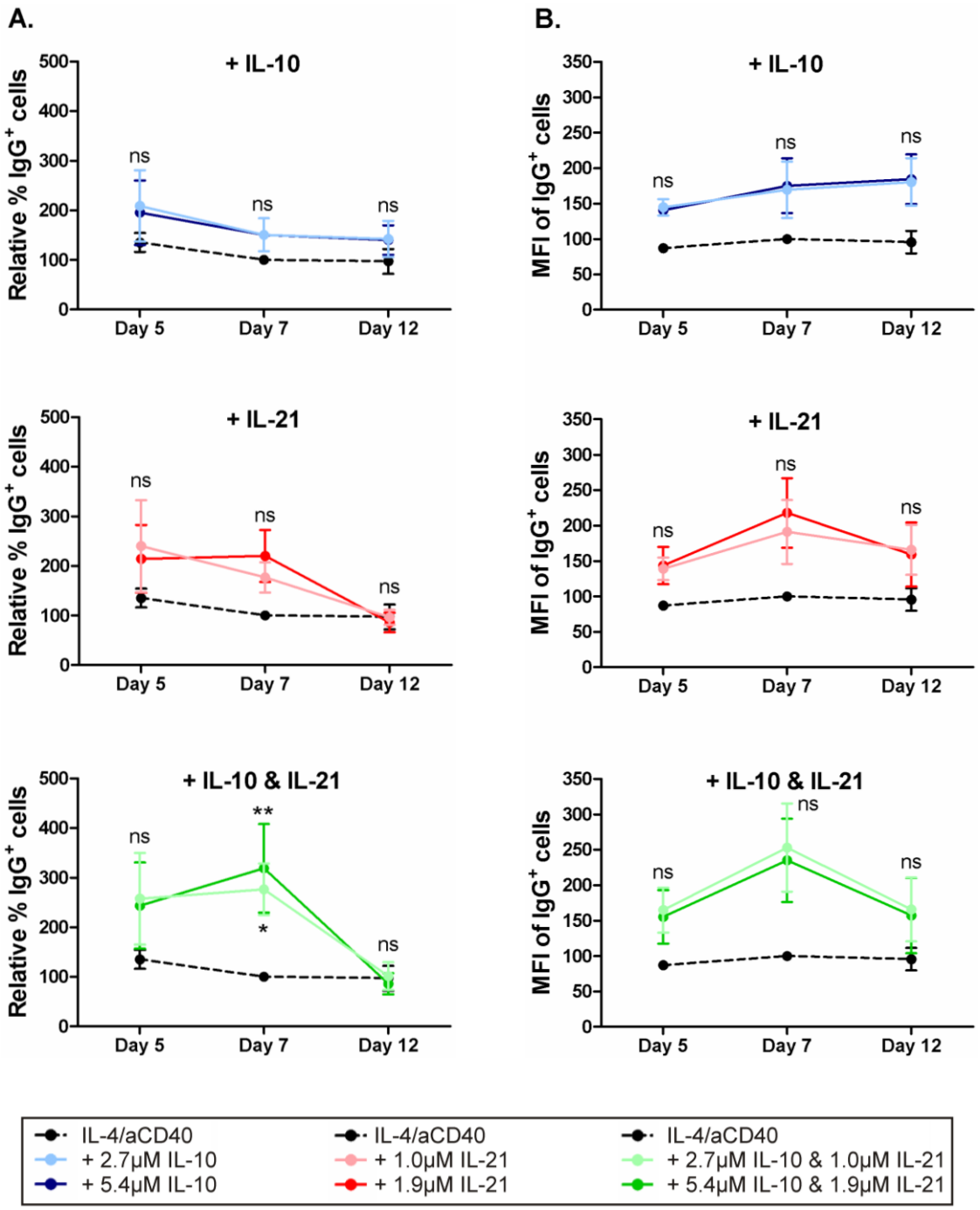

Figure 3.5. The addition of IL-10 or IL-21 increases early IgG expression.

Total B cells were cultured for up to 12 days in the presence of IL-4 (200IU/ml) and anti-CD40 (1μg/ml), with the addition of IL-10 (2.7μM/50ng/ml or 5.4μM/100ng/ml), IL-21 (1.0μM/30ng/ml or 1.9μM/60ng/ml) or combinations of IL-10 & IL-21. The expression of membrane and intracellular IgG was analysed on days 5, 7 and 12 by flow cytometry. **(A)** The % of live IgG^+ cells, relative to cells cultured with IL-4 and anti-CD40 alone at day 7 (100%). **(B)** The MFI of live IgG^+ cells, relative to cells cultured with IL-4 and anti-CD40 alone at day 7 (100%).

Error bars represent SEM and statistical analysis was performed using ANOVA with Bonferroni correction (n=6, tonsil numbers 7, 9, 12, 15 & 17). * $p<0.05$, ** $p<0.01$

3.3.2. IL-21 generates an IgE^{hi} population

The increase in the MFI of IgE^{+} and IgG^{+} cells due to the addition of IL-10 and/or IL-21 (Figure 3.4B and Figure 3.5B) required further investigation. Figure 3.6A shows raw flow cytometry data of this phenomenon, also shown as a histogram in Figure 3.6B. By day 7, in this particular donor, 0.37% of live cells were positive for IgE. This increased to 0.51% with IL-10, 2.75% with IL-21 and 2.36% with IL-10 & IL-21. IL-21 was particularly potent at causing the expansion of an IgE^{hi} population in this donor (Figure 3.6A and Figure 3.6B). The behaviour and properties of this IgE^{hi} population are discussed later in this chapter.

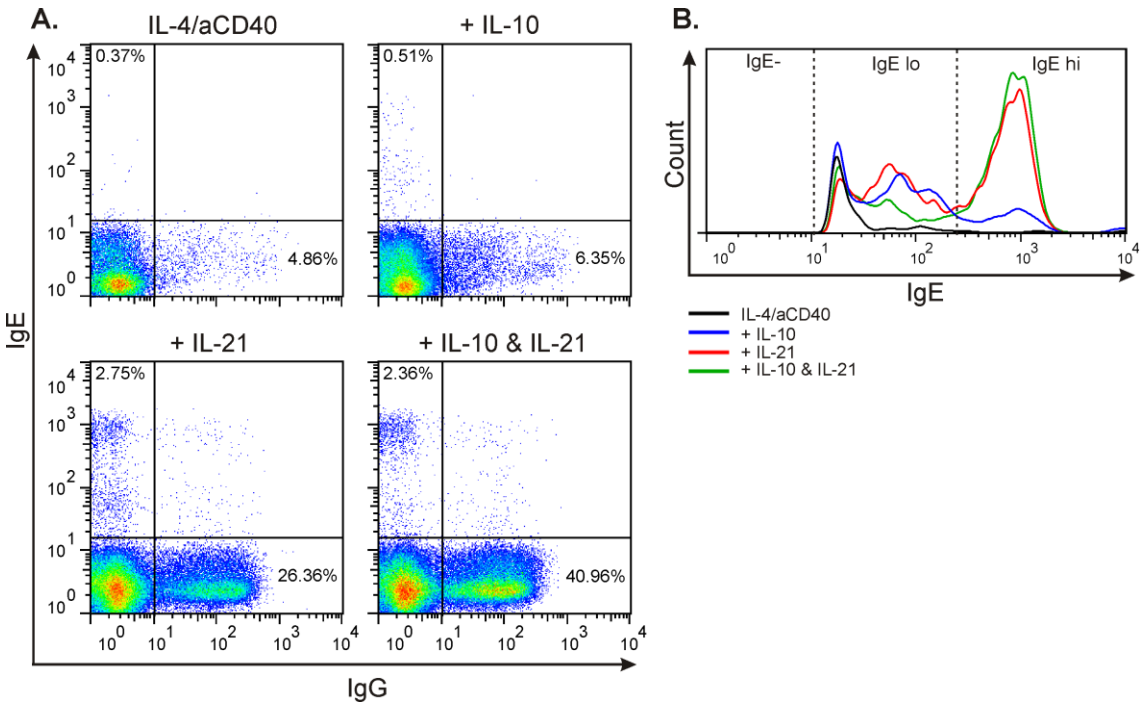

Figure 3.6. IL-10 and IL-21 generate an IgE^{hi} population.

Total B cells were cultured for 7 days in the presence of IL-4 (200IU/ml) and anti-CD40 (1µg/ml), with the addition of IL-10 (5.4µM/100ng/ml), IL-21 (1.9µM/60ng/ml) or a combination of IL-10 & IL-21. The expression of membrane and intracellular IgE and IgG were analysed on day 7 by flow cytometry. **(A)** IgE and IgG expression on day 7, represented as dot plots, where % values shown represent the % of live IgE^{+} (y-axis) or IgG^{+} (x-axis) cells. **(B)** IgE expression on day 7, represented as a histogram, with IgE^{lo} and IgE^{hi} cells separated by dotted lines. The IgE^{-} (negative) cells are excluded from this histogram for clarity.

Data shown from 1 (tonsil number 9) of 9 donors.

3.3.3. IL-10 and IL-21 increase early IgE secretion

Following on from the increase seen in IgE expression shown in Figure 3.4, sIgE levels were analysed by ELISA (as described in Section 2.6.1) on days 5, 7 and 12 following stimulation with IL-4 and anti-CD40 alone, plus the addition of IL-10, IL-21 or IL-10 & IL-21 (Figure 3.7).

By day 5, the addition of IL-10 or IL-21 led to a small increase in IgE secretion, compared to cells cultured with IL-4 and anti-CD40 alone. The combination of IL-10 & IL-21 resulted in a synergistic 2-fold increase in IgE secretion (Figure 3.7A). In cells cultured with IL-4 and anti-CD40 alone, the majority of IgE secretion (59 ± 14%, n=9) took place during days 8 to 12 in the culture period (Figure 3.7A and Figure 3.7B). The addition of IL-10 or IL-21 caused IgE secretion to begin earlier and in larger volumes.

By day 7, IgE secretion from cells cultured with IL-10 was 7-fold higher than from cells cultured with IL-4 and anti-CD40 alone. Addition of IL-21 increased IgE secretion by only 2.5-fold and addition of the combination of IL-10 & IL-21 increased IgE secretion by 4-fold (Figure 3.7A). In cells cultured with IL-21 present, a larger proportion of IgE secretion took place between days 0-7, compared to cells stimulated with IL-4 and anti-CD40 alone (Figure 3.7B).

By day 12, only cells cultured with the addition of IL-10 continued to secrete more IgE (2.7-fold higher) than cells cultured with IL-4 and anti-CD40 alone. Whilst cells stimulated with IL-21 or IL-10 & IL-21 did still continue to secrete IgE between days 8 and 12, the level of secretion was lower than from cells stimulated with IL-4 and anti-CD40 alone by day 12 (Figure 3.7A). In similarity to the pattern of IgE expression shown in Figure 3.4, it appears that the stronger the stimulus to increase IgE secretion at

the early timepoints, the smaller the increase in IgE secretion by day 12. The mechanisms by which this occurs will be discussed later in this chapter.

It is important to remember that the data in Figure 3.7A is shown as fold change in IgE secretion, relative to the level of IgE secreted from cells cultured with IL-4 and anti-CD40 alone by day 7. The data is not shown as sIgE (in ng/ml) due to the large inter-donor variation in the levels of IgE secretion. However, the *fold-changes* in IgE secretion were of similar magnitudes between donors (Figure 3.7A). The method of data presentation in Figure 3.7A does not provide any information on the raw accumulated levels of IgE secreted into the supernatant (in ng/ml). By looking at the raw data, donors appeared to fall into three categories of IgE secretion: undetectable levels of IgE; medium levels of IgE (up to 500ng/ml); or high levels of IgE (above 500ng/ml). The addition of IL-10 and/or IL-21 was capable of increasing IgE secretion from the first two groups. However, in cells which went onto secrete already high levels of IgE with IL-4 and anti-CD40 alone, the addition of IL-10 or IL-21 did not further enhance the level of IgE secretion by day 12 (Figure 3.8).

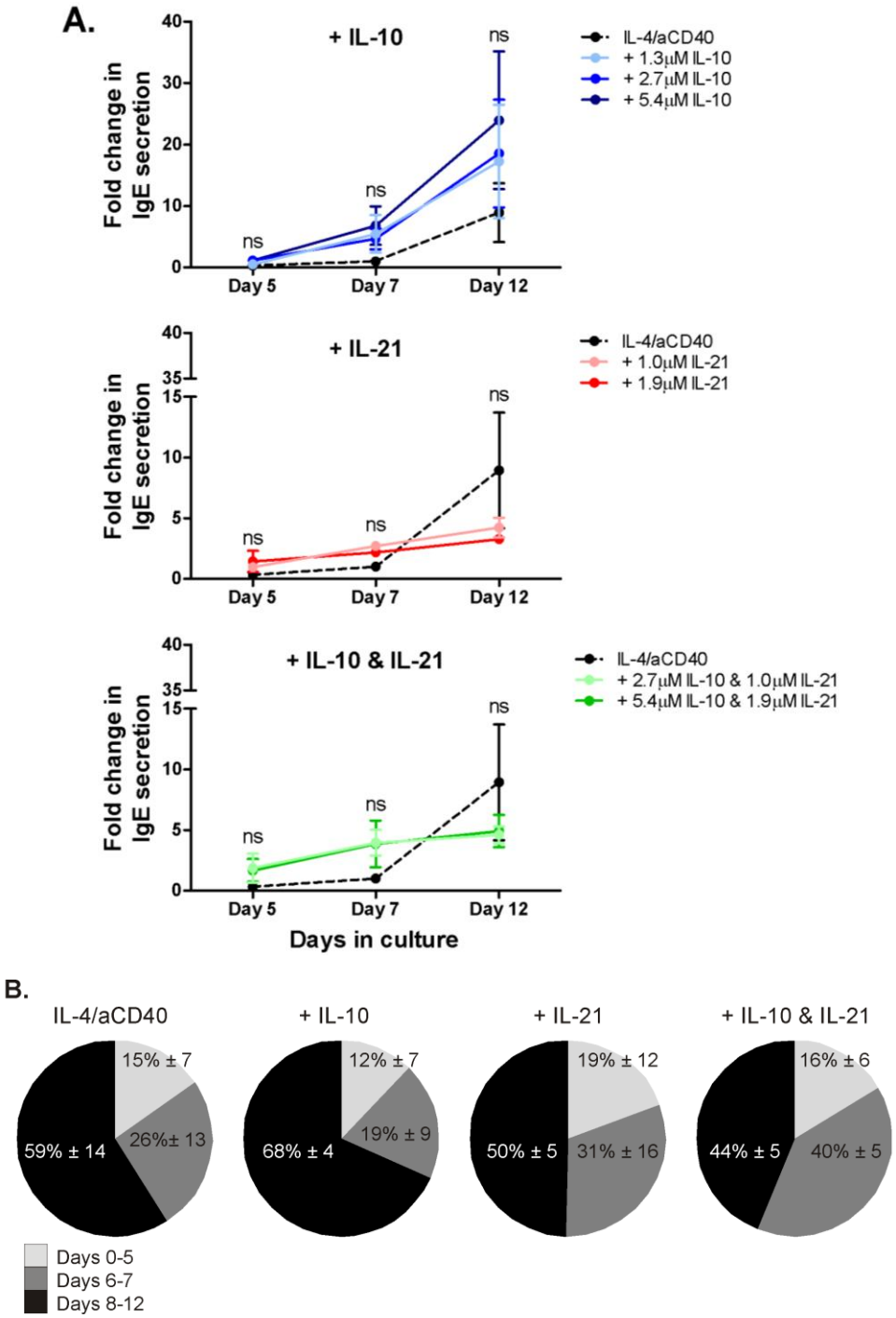

Figure 3.7. IL-10 and IL-21 increase the level and rate of IgE secretion.

Total B cells were cultured for up to 12 days in the presence of IL-4 (200IU/ml) and anti-CD40 (1μg/ml), with the addition of IL-10, IL-21 or a combination of IL-10 & IL-21. IgE secretion was analysed by ELISA on days 5, 7 and 12. **(A)** Fold change in accumulated IgE secretion, relative to cells cultured with IL-4 and anti-CD40 alone at day 7, with the addition of IL-10 (2.7μM/50ng/ml or 5.4μM/100ng/ml), IL-21 (1.0μM/30ng/ml or 1.9μM/60ng/ml) or combinations of IL-10 & IL-21. Error bars represent SEM and statistical analysis was performed using ANOVA with Bonferroni correction. **(B)** Accumulated IgE secretion was separated into days 0-5, 6-7 and 8-12 for cells cultured with IL-4 and anti-CD40 alone, with the addition of IL-10 (5.4μM/100ng/ml), IL-21 (1.9μM/60ng/ml) or a combination of IL-10 & IL-21. The % values shown represent the proportion of IgE secretion which took place during each time period. % values are expressed as mean ± SEM.

n=9 (tonsil numbers 4-7, 9, 10, 12, 15 & 17).

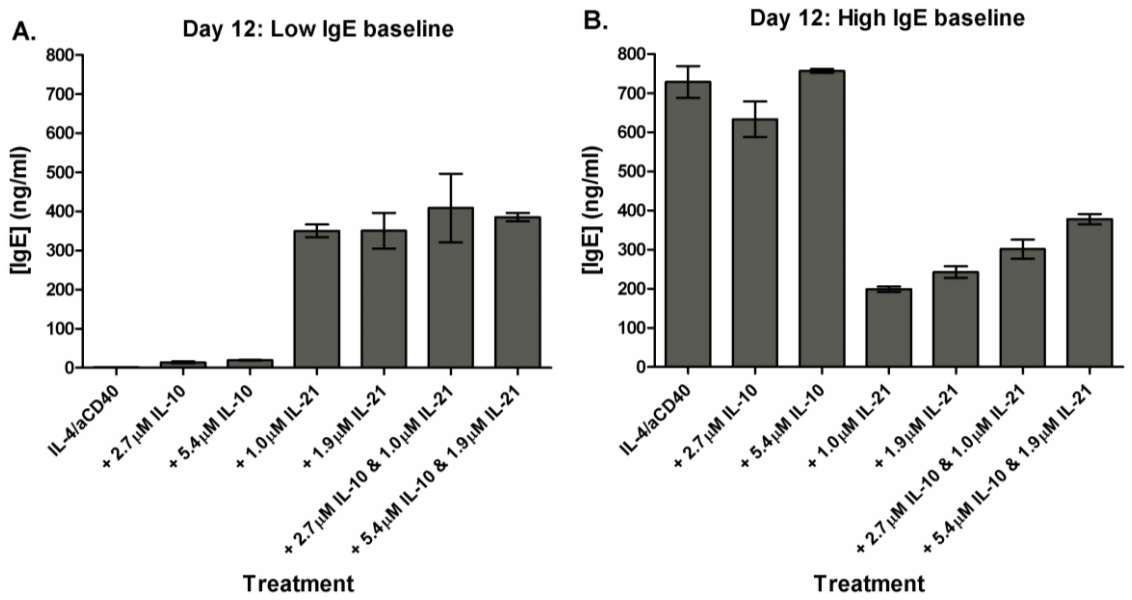

Figure 3.8. IL-10 and IL-21 cannot increase IgE secretion from cells already secreting high levels of IgE.

Total B cells were cultured for 12 days in the presence of IL-4 (200IU/ml) and anti-CD40 (1μg/ml), with the addition of IL-10 (2.7μM/50ng/ml or 5.4μM/100ng/ml), IL-21 (1.0μM/30ng/ml or 1.9μM/60ng/ml) or combinations of IL-10 & IL-21. IgE secretion was analysed by ELISA on day 12. **(A)** IgE secretion from a donor (tonsil number 7) with a low IgE secretion baseline (IL-4 and anti-CD40 alone) and **(B)** a high IgE secretion baseline (tonsil number 12).

Error bars represent SEM from experimental triplicates. Data shown from 2 of 9 donors.

3.3.4. IL-10 and IL-21 support early cell growth

Having established that IL-10 and IL-21 are capable of rapidly up-regulating IgE and IgG expression and IgE secretion from human B cells, the mechanism by which this may occur was then investigated.

Cell viability was assessed by flow cytometry with live cell gating determined by forward versus side scatter. Figure 3.9 shows cell viability on days 5, 7 and 12 following stimulation with IL-4 and anti-CD40 alone or with the addition of combinations of IL-10 and IL-21. Figure 3.9A shows the raw flow cytometry data of the percentage of viable cells and Figure 3.9B shows this same data expressed relative to

cells cultured with IL-4 and anti-CD40 alone at each timepoint (100%). In cells cultured with IL-4 and anti-CD40 alone, cell viability was 35 ± 3% by day 5, 30 ± 4% by day 7 and 20 ± 4% by day 12 (n=9) (Figure 3.9A). By day 5, the addition of IL-10, IL-21 or IL-10 & IL-21 improved cell viability by up to 20% with IL-21 or a combination of both IL-10 & IL-21.

By day 7, only the addition of IL-10 alone continued to improve cell viability from that of cells cultured with IL-4 and anti-CD40 alone. Cells cultured with IL-21 began to rapidly die between days 5 and 7, with cell viability halved to only 15 ± 5% (n=9) in cells cultured with the top concentration of IL-10 & IL-21, compared to cells cultured with IL-4 and anti-CD40 alone (Figure 3.9A).

By day 12, this effect was even more prominent, with relative cell viability significantly lower in cells cultured with IL-21 or IL-10 & IL-21 ($p=0.0004$, n=9), compared to IL-4 and anti-CD40 alone (Figure 3.9B).

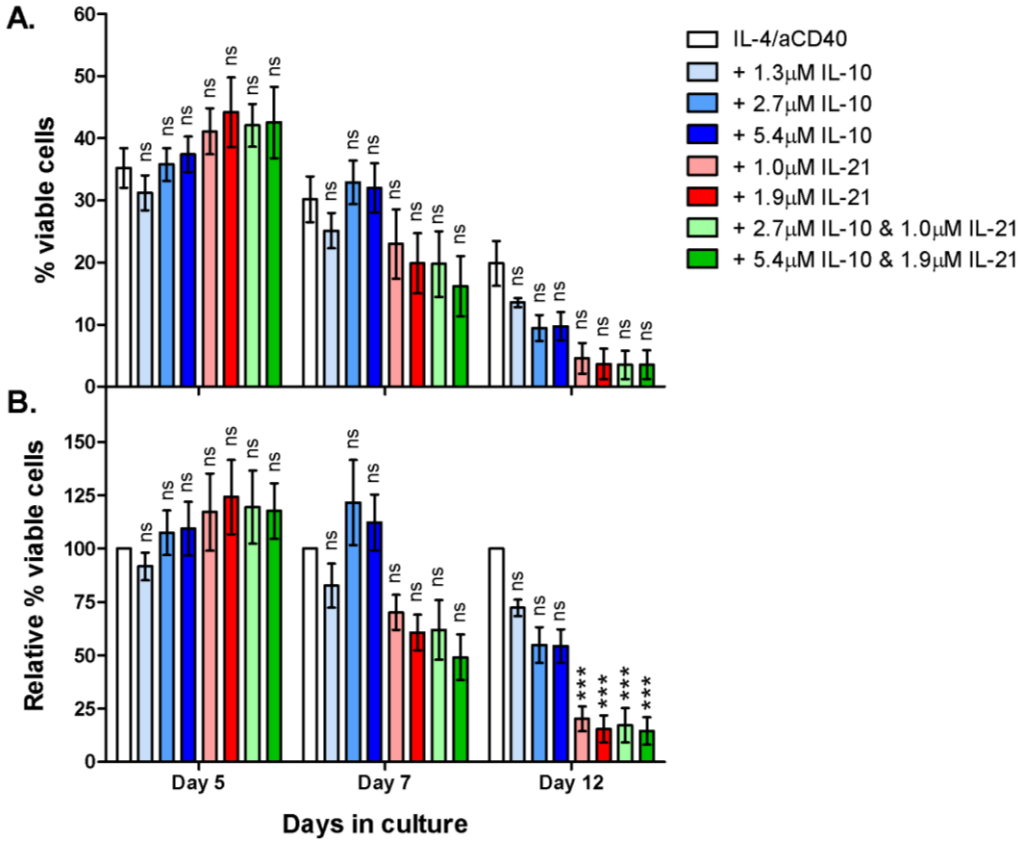

Figure 3.9. IL-10 and IL-21 promote early cell survival followed by rapid cell death.

Total B cells were cultured for up to 12 days in the presence of IL-4 (200IU/ml) and anti-CD40 (1μg/ml), with the addition of IL-10 (1.3μM/25ng/ml, 2.7μM/50ng/ml or 5.4μM/100ng/ml), IL-21 (1.0μM/30ng/ml or 1.9μM/60ng/ml) or combinations of IL-10 & IL-21. The % of viable cells was analysed by flow cytometry with live cell gating determined by forward versus side scatter. Cell viability is displayed as **(A)** the % of viable cells and **(B)** the % of viable cells relative to cells cultured with IL-4 and anti-CD40 alone at each timepoint (100%).

Error bars represent SEM and statistical analysis was performed using ANOVA with Bonferroni correction (n=9, tonsil numbers 4-7, 9, 10, 12, 15 & 17). *** $p<0.001$

3.3.5. IL-10 and IL-21 increase cell proliferation

The effect of IL-10 and IL-21 on the proliferation of total human B cells was next investigated. BrdU is a synthetic analogue of thymidine, which can incorporate into newly synthesised DNA during the S (synthesis) phase of the cell cycle. Following DNase treatment to expose the labelled epitopes, a fluorescent anti-BrdU antibody was then used to detect the incorporated BrdU as a measure of proliferating cells (as

described in Section 2.5.4). Total B cells were cultured for 7 days with IL-4 and anti-CD40, with or without the addition of IL-10 and IL-21, and then pulsed for 24 hours with BrdU. Cells were stained with anti-BrdU-APC and incorporation detected by flow cytometry. Figure 3.10 shows the percentage of $BrdU^+$ cells, relative to cells cultured with IL-4 and anti-CD40 alone, in 3 different donors. The level of BrdU incorporation varied between the three donors. In two of the three donors, addition of IL-10 and/or IL-21 resulted in increased proliferation (Figure 3.10). The increased proliferation rate in these two donors was associated with a large increase in IgE expression and secretion (data not shown).

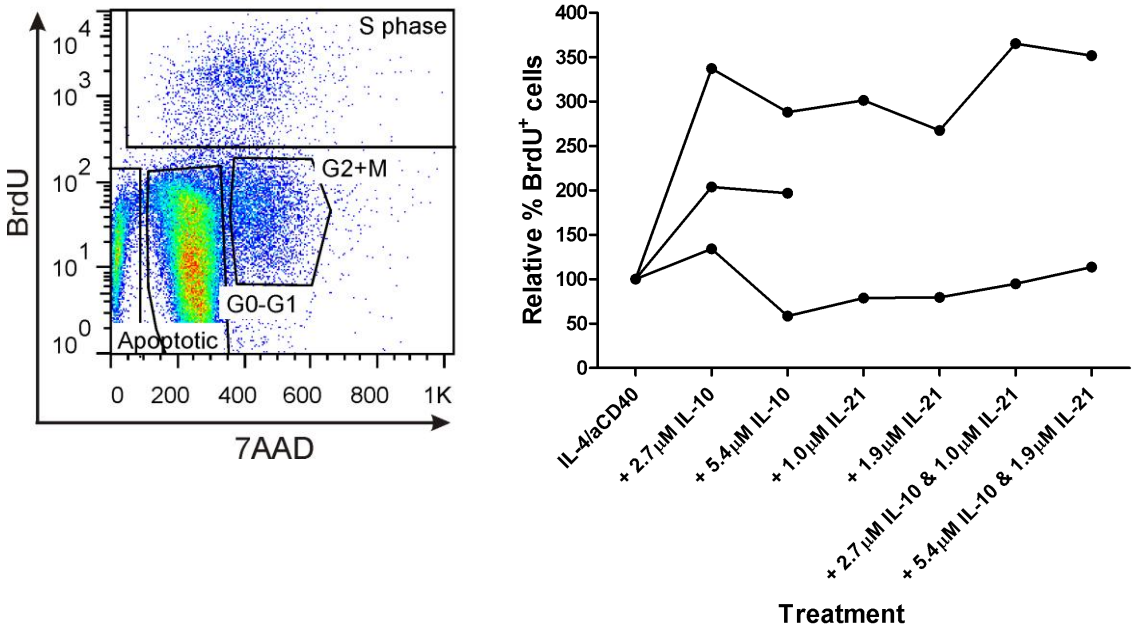

Figure 3.10. IL-10 and IL-21 increase human B cell proliferation.

Total B cells were cultured for 7 days in the presence of IL-4 (200IU/ml) and anti-CD40 (1µg/ml), with the addition of IL-10 (2.7µM/50ng/ml or 5.4µM/100ng/ml), IL-21 (1.0µM/30ng/ml or 1.9µM/60ng/ml) or combinations of IL-10 & IL-21. Cells were pulsed for 24 hours with BrdU then stained with anti-BrdU-APC (S phase) and 7-AAD for cell cycle analysis by flow cytometry. **(A)** An example of cell cycle analysis in cells cultured with IL-4 and anti-CD40 only (tonsil number 7). A: apoptotic/sub G_0 phase; M: mitosis (cell division); S: synthesis. **(B)** % of cells in S phase ($BrdU^+$), relative to cells cultured with IL-4 and anti-CD40 alone (100%), in three separate donors (n=3, tonsil numbers 4, 7 & 10).

3.3.6. IL-10 and IL-21 increase cell division

In the late 1990s, Hodgkin *et al* showed that multiple rounds of cell division are required for isotype switching to IgG (3 divisions) and IgE (5 divisions) in IL-4 and anti-CD40-stimulated human B cells *in vitro*. Cell division is also associated with a loss of surface IgM and IgD (Hasbold, Lyons *et al.,* 1998; Hodgkin, Lee *et al.,* 1996). Following on from this work, they showed addition of IL-10 increases the number of cell divisions and, therefore, isotype switching to IgG (Tangye, Ferguson *et al.,* 2002). The combination of IL-10 and IL-21 has also been reported to synergistically increase isotype switching to IgE through increasing cell division (Caven, Shelburne *et al.,* 2005).

The effect of IL-10, IL-21 or IL-10 & IL-21 on cell division-associated isotype switching to IgE was investigated in primary human tonsil B cells. Total B cells were isolated and stained with CFSE, a fluorescent marker which reduces in concentration upon cell division (as described in Section 2.5.3), before stimulation for 7 days with either IL-4 and anti-CD40 alone or with the addition of combinations of IL-10 and IL-21. Figure 3.11 shows flow cytometric analysis on day 7, from one donor, with the lower histograms showing individual CFSE peaks and the upper dot plots showing co-staining of CFSE with IgE. In cells cultured with IL-4 and anti-CD40 alone, 47% of live cells remained undivided by day 7, represented by the brightest CFSE peak on the far right. 0.25% of live cells were positive for IgE, and it was clear that the IgE^+ cells were the cells which had undergone the most rounds of cell division (~4 or 5 divisions) (Figure 3.11). When IL-10 was included in the cell culture, only 16% of live cells remained undivided by day 7. As previously discussed in Section 3.3.1 and shown in Figure 3.4, the addition of IL-10 increased IgE expression. Building on this observation, Figure 3.11 shows that the expansion of IgE^+ cells takes place following 5 or more

rounds of cell division (60% of divided cells). In cells stimulated with IL-21 present, even less cells remained undivided (8-11%). However, a smaller proportion of cells reached the stage of 5 or more cell divisions with two thirds of the divided cells having only divided 1-4 times (Figure 3.11). This correlates with less IgE expression as, in this donor, cells stimulated with IL-21 led to very poor cell viability by day 7 (also see Figure 3.9).

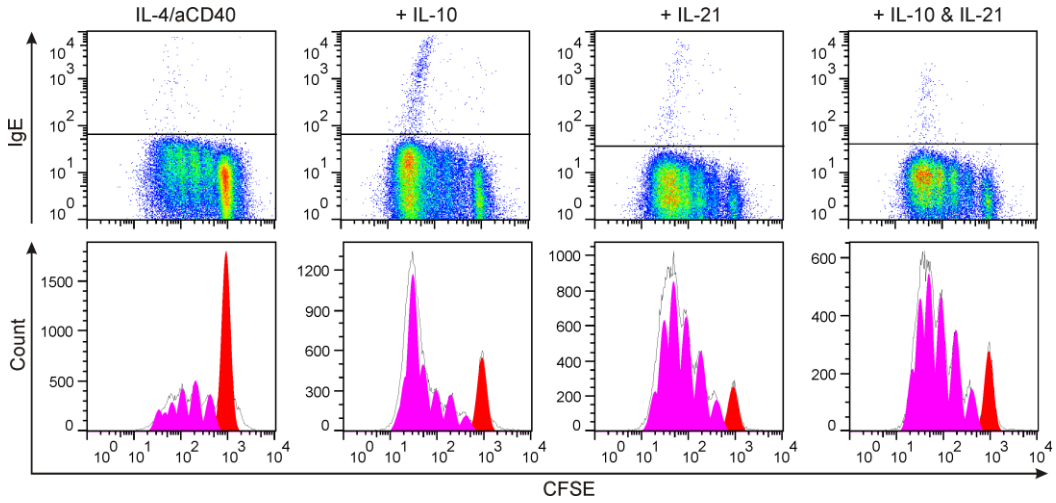

	IL-4/aCD40	+ IL-10	+ IL-21	+ IL-10 & IL-21
% undivided	47	16	8	11
% divided 5 or more times	20	60	31	31
% IgE$^+$	0.25	1.41	0.51	0.53

Figure 3.11. Increased IgE expression with IL-10 and IL-21 is associated with increased rounds of cell division.

Total B cells were stained with CFSE and cultured for 7 days in the presence of IL-4 (200IU/ml) and anti-CD40 (1µg/ml), with the addition of IL-10 (5.4µM/100ng/ml), IL-21 (1.9µM/60ng/ml) or a combination of IL-10 & IL-21. Cell division and IgE expression were analysed by flow cytometry on day 7, with each peak of decreased fluorescence representing a round of cell division. The table summarises the relationship between the proportion of undivided, highly divided (5 or more divisions) and IgE$^+$ cells.

n=1 (tonsil number 9).

3.3.7. IL-10 and IL-21 drive rapid plasma cell differentiation

The phenotype of cells stimulated with or without the addition of IL-10 and IL-21 was next investigated. Flow cytometric analysis of CD38, highly expressed on the surface of plasma cells, was carried out on days 5, 7 and 12 and is summarised in Figure 3.12. Cells cultured with IL-4 and anti-CD40 alone expressed low levels of CD38, even by day 12 (17 ± 7%, n=4).

By day 5, the proportion of $CD38^+$ cells increased 5-fold with the addition of IL-10, 6-fold with the addition of IL-21 and up to 7.5-fold with IL-10 & IL-21 in combination (Figure 3.12A). By day 7, there was no further increase in the proportion of $CD38^+$ cells with the addition of IL-10, compared to day 5. With the stronger stimulations of IL-21 or IL-10 & IL-21, CD38 expression continued to rise, with the highest concentrations of IL-10 & IL-21 leading to significantly higher levels of CD38 compared to IL-4 and anti-CD40 alone ($p=0.037$, n=4) (Figure 3.12A). By day 12, CD38 expression had continued to increase in cells cultured with IL-10. However, cells cultured in the presence of IL-21 expressed lower levels of CD38, compared to day 7.

In addition to a larger proportion of cells expressing CD38, the MFI of $CD38^+$ cells also increased with the addition of IL-10 or IL-21. Figure 3.12B shows the MFI of $CD38^+$ cells on days 5, 7 and 12. In cells cultured with IL-4 and anti-CD40 alone, the MFI remained constant over the 12 day period.

With increasing strengths of cytokine addition, from IL-10 alone up to IL-10 & IL-21 in combination, the MFI increased accordingly. This increase was most prominent at day 7 (Figure 3.12C). By day 12, the MFI of $CD38^+$ cells cultured with IL-10 or IL-21 had reduced to the level on cells cultured with IL-4 and anti-CD40 alone.

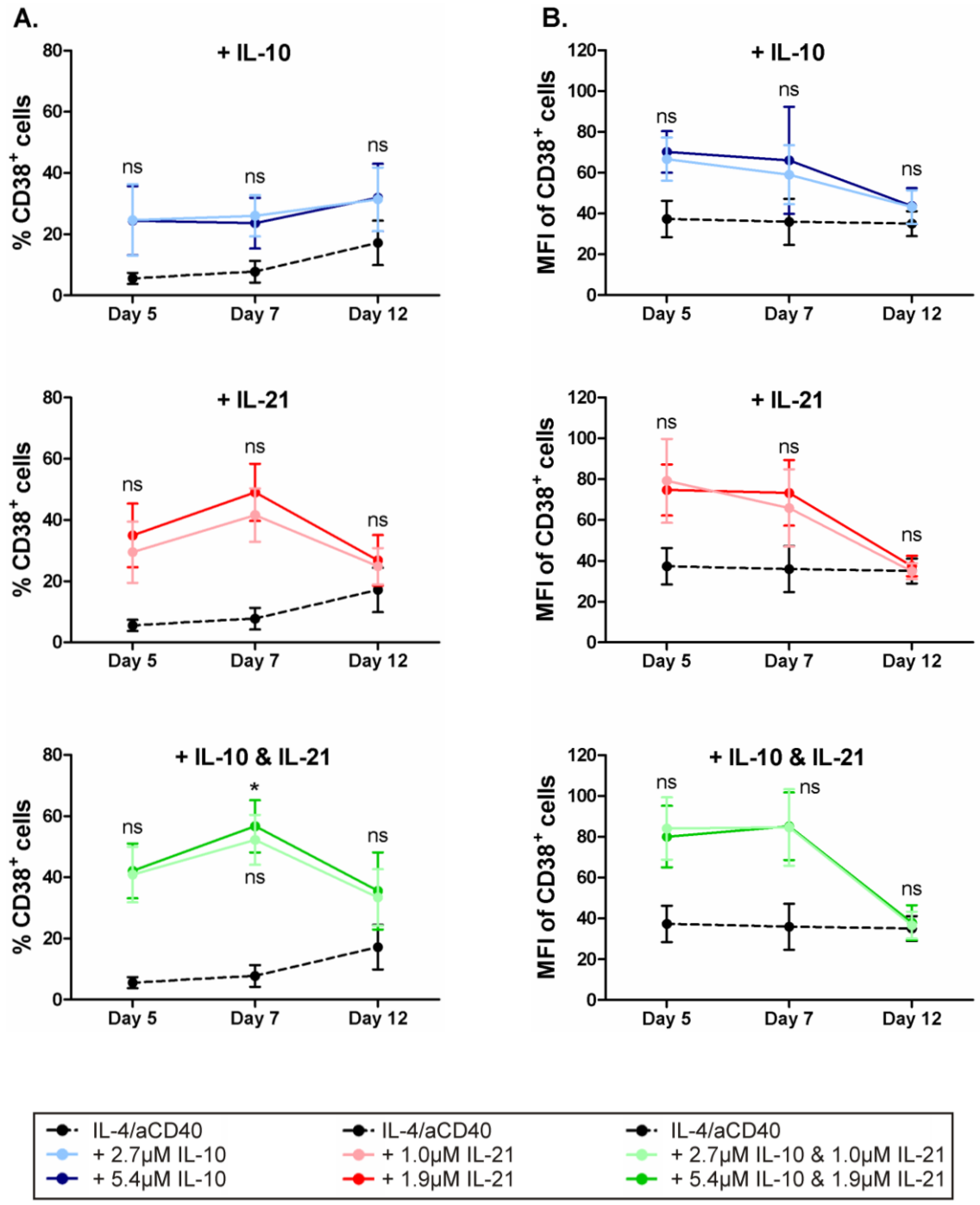

Figure 3.12 is continued on the following page.

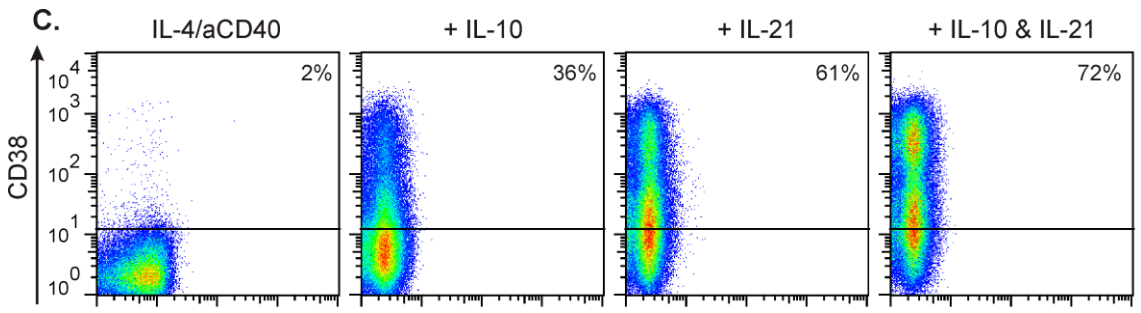

Figure 3.12. The addition of IL-10 and IL-21 induces B cell differentiation into CD38^{hi} plasmablasts.

Total B cells were cultured for 12 days in the presence of IL-4 (200IU/ml) and anti-CD40 (1µg/ml), with the addition of IL-10 (2.7µM/50ng/ml or 5.4µM/100ng/ml), IL-21 (1.0µM/30ng/ml or 1.9µM/60ng/ml) or combinations of IL-10 & IL-21. The expression of surface CD38 was analysed on days 5, 7 and 12 by flow cytometry. Data is shown as **(A)** the % of live CD38^{+} cells and **(B)** the MFI of live CD38^{+} cells. Error bars represent SEM and statistical analysis was performed using ANOVA with Bonferroni correction (n=4, tonsil numbers 7, 9, 10 & 12). * $p<0.05$ **(C)** CD38 expression on day 7, represented as dot plots, where % values shown represent the % of live CD38^{+} cells in cells cultured with IL-4 and anti-CD40 alone, with the addition of IL-10 (5.4µM/100ng/ml), IL-21 (1.9µM/60ng/ml) or a combination of IL-10 & IL-21. Data shown from 1 (tonsil number 12) of 4 donors.

CD138 (syndecan-1) is an integral membrane protein, encoded by the SDC1 gene, which plays a role in cell proliferation, migration and apoptosis. Expression of CD138 is also a useful marker for the detection of mature plasma cells as it is not expressed on plasmablasts (Ala-Kapee, Nevanlinna *et al.*, 1990; Mali, Jaakkola *et al.*, 1990; van Zaanen, Vet *et al.*, 1995). Figure 3.13 shows flow cytometric analysis of CD38 and CD138 expression on cells cultured either with IL-4 and anti-CD40 alone, or with the addition of IL-10, for 12 days. In the absence of IL-10, a very small proportion of CD138^{+} plasma cells were detected. However, a distinct population of CD38^{hi}CD138^{+} plasma cells (2.9%) were present in cells cultured with the addition of IL-10 (Figure 3.13).

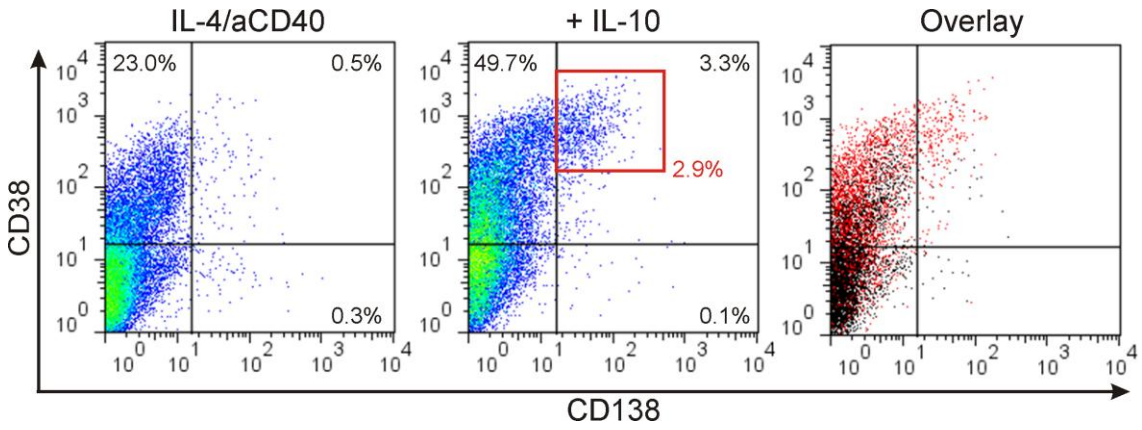

Figure 3.13. IL-10 induces a CD38^{hi}CD138^{+} plasma cell population.

Total B cells were cultured for 12 days in the presence of IL-4 (200IU/ml) and anti-CD40 (1µg/ml) alone or with the addition of IL-10 (5.4µM/100ng/ml). Cells were stained with antibodies against CD38 (y-axis) and CD138 (x-axis) on day 12 and analysed by flow cytometry. The % of live CD38^{+}CD138^{-} cells is shown in the upper-left quadrant, CD38^{-} CD138^{+} in the lower-right quadrant and double positive CD38^{+}CD138^{+} in the upper-right quadrant. CD38^{hi}CD138^{+} plasma cells are highlighted in the red box. The far right dot plot shows an overlay of cells stimulated with IL-4/anti-CD40 alone (black) or with the addition of IL-10 (red).

n=1 (tonsil number 12).

3.4. Summary

The key objectives of this chapter were to firstly establish the *in vitro* assay for inducing CSR to IgE in primary human tonsillar B cells. Expression and secretion of IgE was shown to be dependent upon the addition of anti-CD40 mAb and IL-4, which were also important for cell viability (Figure 3.1 and Figure 3.2). Under the normal cell culture conditions cell viability was shown to reduce rapidly over the 12 day period (Figure 3.9). It is, therefore, important to consider the possible effects of this when analysing data throughout the culture period. It became apparent that the level of IgE secretion would vary widely between donors, although this did not correlate with the allergic status of the donor (Figure 3.3). This confirmed that any changes seen in sIgE levels in future chapters, which will aim to modify the secretion of IgE, cannot be attributed to the donor's allergic status.

As cells from some donors did not express or secrete any IgE by day 12, the addition of extra cytokines was investigated as a means to overcome this. As explained in Section 3.1, there are many conflicting reports as to whether the addition of IL-10 and IL-21 can increase IgE synthesis in human B cells *in vitro*. In our hands, the addition of these cytokines led to an early increase in the expression of IgE and IgG, indicating an overall increase in the level of CSR. By day 12, the latest timepoint examined, the presence of these additional cytokines resulted in *less* IgE and IgG expression, compared to cells cultured with IL-4 and anti-CD40 alone (Figure 3.4 and Figure 3.5). In accordance with this, the additional cytokines were capable of rapidly increasing IgE secretion at early timepoints. However, this effect had worn off by day 12 (Figure 3.7). It was subsequently shown that the presence of the additional cytokines, for long periods of time, led to very poor cell viability, particularly the combination of both IL-10 & IL-21 (Figure 3.9).

It was shown that addition of IL-10 ± IL-21 could not further enhance IgE secretion from donors which secreted a high level of IgE with IL-4 and anti-CD40 alone (Figure 3.8). This may explain why B cells isolated from the highly atopic tonsil donor shown in Figure 3.3 (tonsil number 23) were only capable of secreting very low levels of IgE. *In vivo,* B cells from this donor would be secreting high levels of IgE. Perhaps this means that they could not be stimulated by IL-4 and anti-CD40 to continue to secrete more IgE when *in vitro.*

The mechanisms by which IL-10 and IL-21 were capable of increasing CSR were next investigated. These cytokines were shown to increase cell proliferation and division, increasing rounds of which were shown to correlate with increased IgE expression (Figure 3.10 and Figure 3.11). Increasing strength of cytokine stimulation (from IL-10 alone, to IL-21 alone and then the combination of both) was shown to induce rapid B cell differentiation, as measured by the B cell differentiation marker CD38 (Figure 3.12), and high IgE expression (Figure 3.6). The presence of $CD38^{hi}CD138^{+}$ plasma cells were detected following stimulation with IL-10 (Figure 3.13).

In summary, the addition of IL-10 and IL-21 served as a useful experimental tool to reliably stimulate IgE secretion from human B cells, including those which would have otherwise not secreted any IgE by day 12. For short *in vitro* cultures of human B cells (up to 7 days), the combination of both IL-10 & IL-21 can be added to greatly increase the expression and secretion of IgE, cell division and CD38 expression. This would be particularly useful for subsequent isolation of IgE^{+} cells for a variety of purposes. However, for longer cultures up to 12 days, the presence of IL-21 leads to very poor cell viability. In this case, addition of IL-10 alone, or a lower concentration of IL-21, may be a more appropriate stimulation.

3.4.1. Further experiments

It would be of interest to conduct more experiments to investigate whether the population of IgE^{hi} cells also co-express CD138. qPCR could be utilised to detect plasma cell differentiation markers such as BLIMP-1 and XBP-1. To definitively confirm that IL-10 and IL-21 are increasing CSR in human B cells, switch circles could be measured by PCR and AID and εGLT levels by qPCR (Takhar, Corrigan *et al.*, 2007).

Chapter 4. siRNA-mediated inhibition of CD23

4.1. Introduction

Discovery of an ancient endogenous defence mechanism of plants against viruses (Napoli, Lemieux et al., 1990; van der Krol, Mur et al., 1990) led to the development of a novel gene silencing technique using small interfering RNA (siRNA). In this chapter, this technique was utilised to target CD23 in primary human B cells.

4.2. Optimisation of siRNA conditions

4.2.1. Transfection efficiency

Since the procedure of human B cell transfection with siRNA (as described in Section 2.3) had not been attempted before within the research group, it was first necessary to optimise the assay conditions. To assess whether it was possible to transfect human B cells by nucleofection, the transfection indicator siGLO® Red was utilised. This reagent contains fluorescent oligonucleotides that localise to the nucleus to allow flow cytometric analysis of transfection uptake into cells. Figure 4.1 shows that at 30 minutes following transfection a very high proportion of cells were positive for siGLO® Red (97%), indicating a high transfection efficiency.

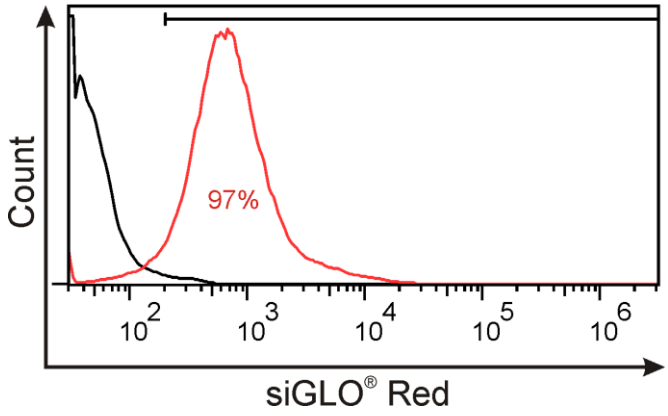

Figure 4.1. siGLO® Red enters B cells following electroporation.

Total B cells were transfected with either siGLO® Red (3µg/960nM) (red) or cell culture media alone (black) by electroporation. Transfection efficiency was analysed by flow cytometry 30 minutes following transfection. The % of live cells positive for siGLO® Red is indicated on the histogram.

Data shown from 1 donor (tonsil number 17), representative of 11 (tonsil numbers 4, 8, 11-15, 17, 19, 21 & 22).

4.2.1. siGLO® Red cell sorting

To avoid any untransfected cells, albeit only a small percentage, from contaminating the cell cultures and possibly skewing results, cell sorting using a FACS Aria™ was utilised to separate siGLO$^-$ and siGLO$^+$ cells (as described in Section 2.3.1). Figure 4.2A shows the purity of the cell sorting procedure. Once sorted, the siGLO$^-$ and siGLO$^+$ cell populations were placed into culture with IL-4 and anti-CD40 (as described in Section 2.4). The sorting procedure resulted in very poor cell viability with only 5% of siGLO$^+$ and 11% of siGLO$^-$ cells remaining live 24 hours after sorting (Figure 4.2B). The average viability of un-sorted transfected cells, 24 hours after transfection, was 31% (n=13) as shown in Figure 4.3. By day 9, in the sorted cell cultures, no live cells could be detected by flow cytometry (data not shown).

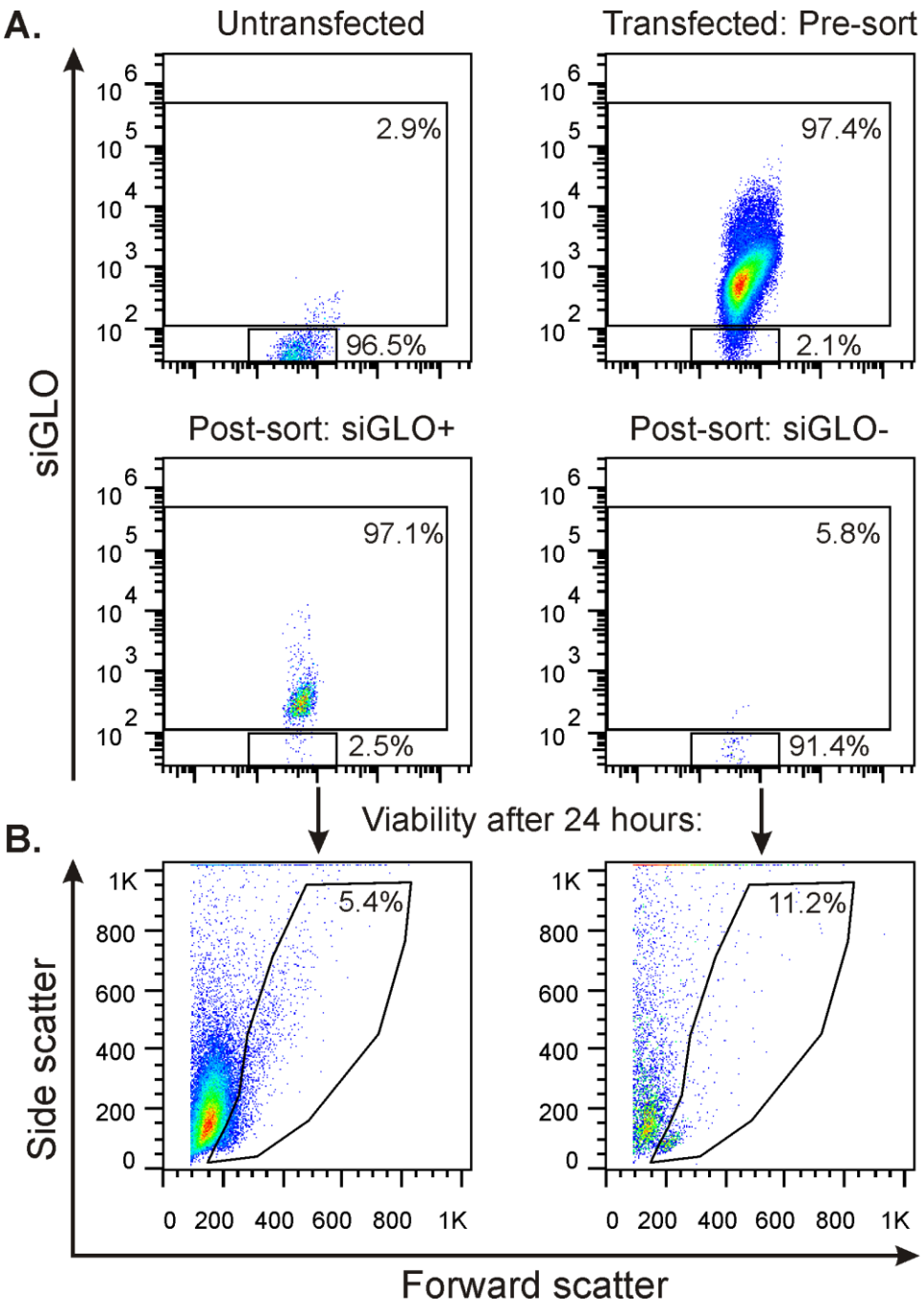

Figure 4.2. siGLO cell sorting results in very poor cell viability.

Total B cells were transfected with siGLO® Red (3µg/960nM) by electroporation. 30 minutes following transfection, cells were sorted with a FACS Aria™ into tubes containing siGLO+ and siGLO- cells, according to gates set using untransfected cells as a guide. **(A)** The % of live siGLO+ and siGLO- cells are indicated on the dot plots. **(B)** Cells were subsequently cultured in the presence of IL-4 (200IU/ml) and anti-CD40 (1µg/ml) and the cell viability after 24 hours is indicated on the dot plots.

n=1 (tonsil number 17).

4.2.2. Effect of siRNA transfection on cell viability

In the process of electroporation approximately 50% of the cells were killed (data not shown). It was therefore necessary to make sure that the viability of the electroporated cells, and also those transfected with siRNA, would be high enough to survive the necessary 12 day culture period. To test this, cells were transfected with control siRNA (scrambled), GAPDH siRNA or CD23 siRNA (as described in Section 2.3). Cells which had been electroporated without siRNA (EP only) and cells which had not been electroporated (untreated) were included as control conditions.

Figure 4.3 shows cell viability measured by flow cytometry at 24 hours, 48 hours, 5 days, 7 days and 12 days after transfection. It is clear to see that the process of electroporation caused a reduction in cell viability. This reduction was most significant at 24 hours following transfection when cells electroporated and transfected with control siRNA were 44% less viable than untreated cells ($p=<0.0001$, $n=12$) (Figure 4.3). Over the 12 day period, cell viability declined at a faster rate in untreated cells, compared with electroporated cells, until there was no significant difference in cell viability between untreated and control siRNA-transfected cells by day 12 (Figure 4.3).

Importantly, there was no additional reduction in viability when cells were electroporated with siRNA, compared to electroporation alone (EP only). This indicates the reduction in cell viability was due to the procedure of electroporation and not the presence of siRNA. In addition, there were no differences in cell viability between cells transfected with control, GAPDH or CD23 siRNA (Figure 4.3).

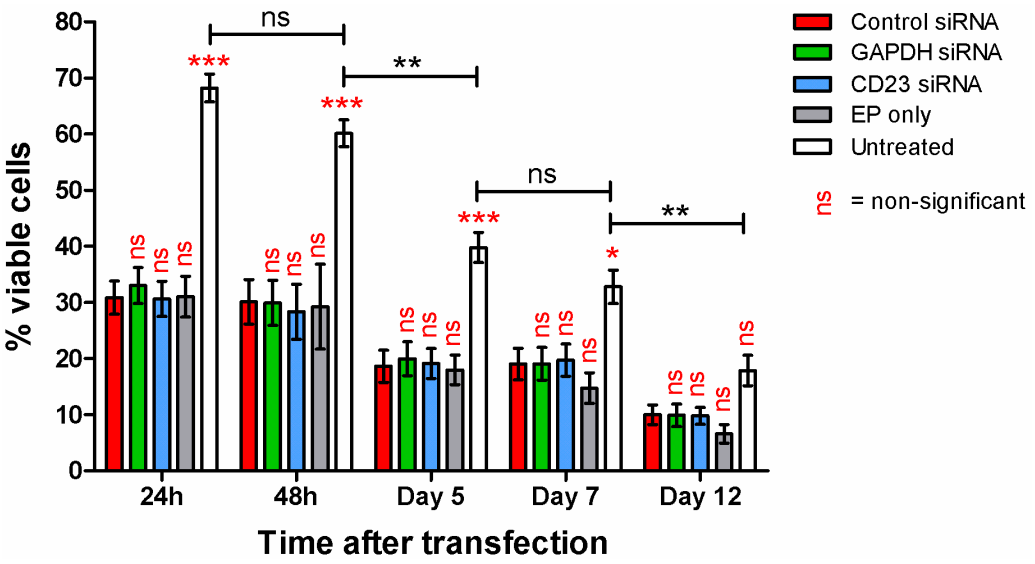

Figure 4.3. Electroporation, but not the addition of siRNA, reduces cell viability.

Total B cells were transfected with either control siRNA (red), GAPDH siRNA (green) or CD23 siRNA (blue) by electroporation and cultured for up to 12 days in the presence of IL-4 (200IU/ml) and anti-CD40 (1µg/ml). For comparison, cells which had been electroporated with no siRNA (EP only) (grey) and cells which had not been electroporated (untreated) (white) are also shown. The % of viable cells was analysed by flow cytometry with live cell gating determined by forward versus side scatter.

Error bars represent SEM and statistical analysis was performed using ANOVA with Bonferroni correction (n=13, tonsil numbers 1, 2, 4, 8, 11-15, 17, 19, 21 & 22). Statistics in red indicate significance compared to control siRNA-transfected cells at each timepoint and statistics in black indicate significance between untreated cells at different timepoints. * $p<0.05$, ** $p<0.01$, *** $p<0.001$

4.3. Validation of siRNA knockdowns

4.3.1. CD23 siRNA reduces mRNA levels

Before investigating the ability of siRNA to inhibit the mRNA levels of target genes, it was important to check that electroporation alone did not cause a reduction in the mRNA levels of GAPDH and CD23, given the reduction observed in cell viability (Figure 4.3). Cells were electroporated, cultured with IL-4 and anti-CD40 and qPCR performed (as described in Section 2.8) to quantify GAPDH and CD23 mRNA levels.

Figure 4.4 shows that the procedure of electroporation did not significantly alter GAPDH or CD23 mRNA levels.

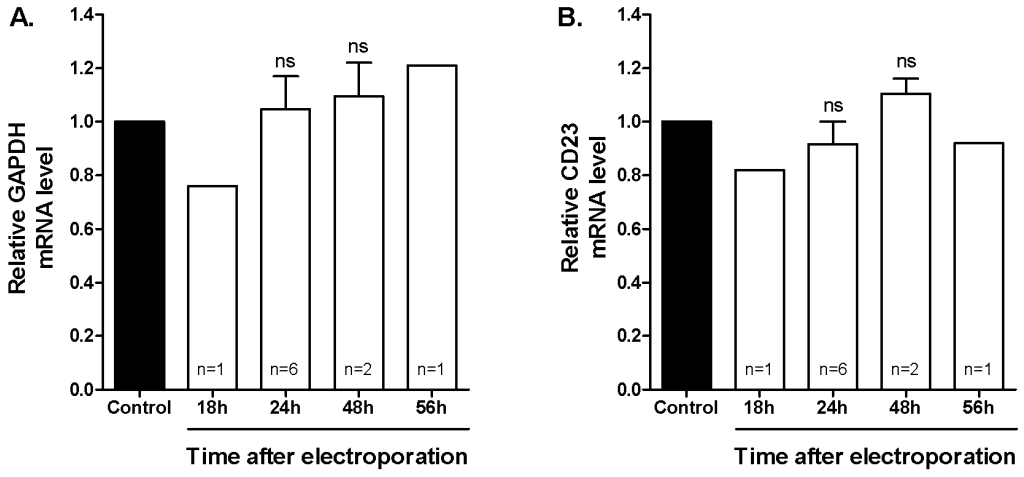

Figure 4.4. Electroporation alone does not decrease GAPDH or CD23 mRNA levels.

Total B cells were either transfected with control siRNA (black) by electroporation or electroporated alone (white) and cultured for up to 56 hours in the presence of IL-4 (200IU/ml) and anti-CD40 (1µg/ml). Cell samples were harvested at the times indicated and qPCR was performed to quantify **(A)** GAPDH mRNA levels and **(B)** CD23 mRNA levels. Expression levels were calculated by ΔΔCt analysis, normalised against the endogenous reference gene β2-microglobulin and expressed relative to control siRNA-transfected cells at each timepoint.

Error bars represent SEM and statistical analysis was performed using ANOVA with Bonferroni correction (n as indicated, max n=6, tonsil numbers 1, 4 & 11-14).

Following this, human tonsillar B cells were transfected with siRNA to specifically target GAPDH or CD23. The level of knockdown was quantified by qPCR, relative to cells transfected with control siRNA, from 5 hours to 5 days following transfection. Figure 4.5A and Figure 4.5B show there was a significant decrease in GAPDH mRNA levels in cells transfected with GAPDH siRNA, with no significant effect on CD23 mRNA. The largest decrease in GAPDH mRNA was observed at 18 hours (75 ± 10%, n=2) and 24 hours (69 ± 4%, n=8) following transfection.

Figure 4.5C and Figure 4.5D show there was a significant knockdown of CD23 mRNA levels in cells transfected with CD23 siRNA, with no significant effect on GAPDH mRNA. The maximum knockdown of CD23 (70 ± 0.1%, n=11) occurred between 18 and 24 hours following transfection. From 24 hours onwards, in both GAPDH- and CD23 siRNA-transfected cells, mRNA levels began to recover to that of control siRNA-transfected cells highlighting the transient nature of this knockdown technique.

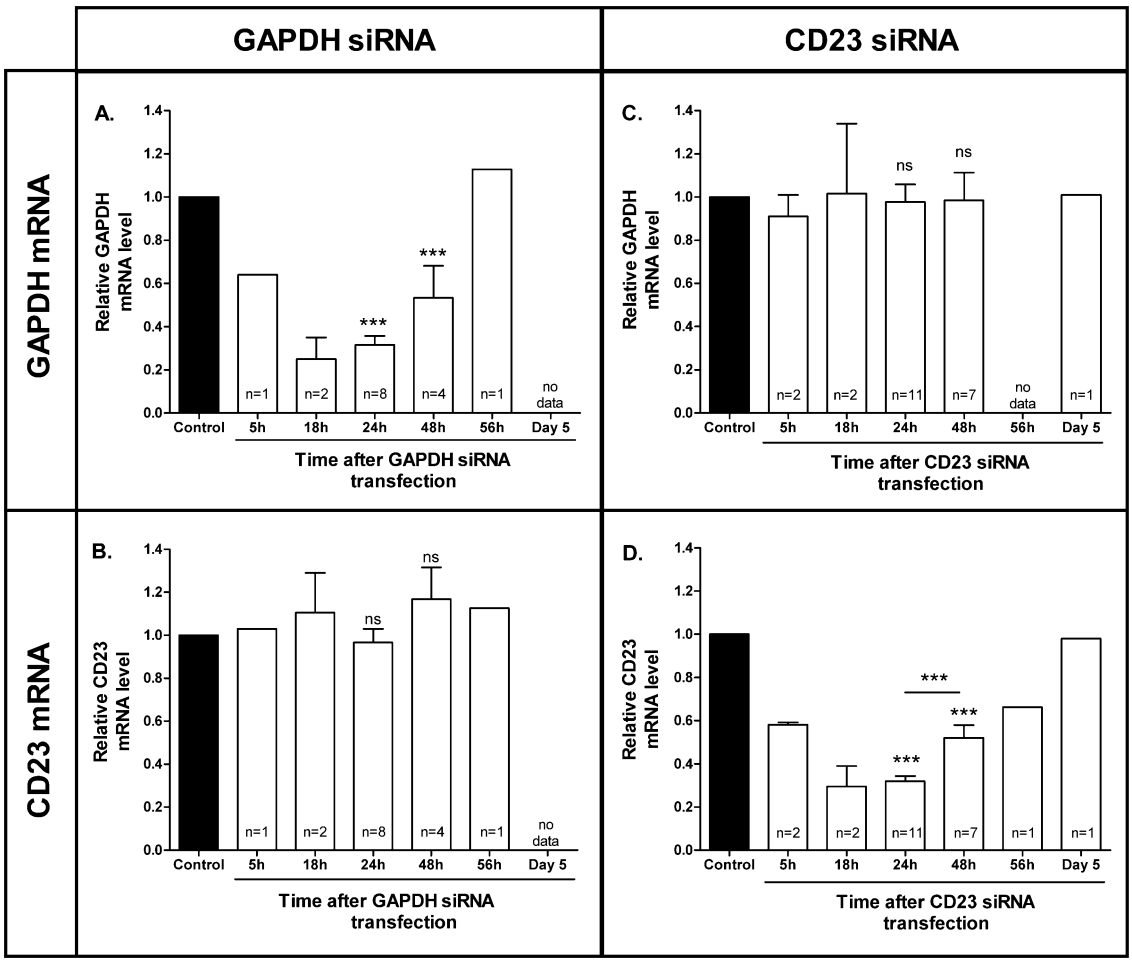

Figure 4.5. GAPDH siRNA specifically reduces GAPDH mRNA levels and CD23 siRNA specifically reduces CD23 mRNA levels.

Total B cells were transfected with either control siRNA, GAPDH siRNA or CD23 siRNA by electroporation and cultured for up to 5 days in the presence of IL-4 (200IU/ml) and anti-CD40 (1µg/ml). Cell samples were harvested at the times indicated and qPCR was performed to quantify **(A)** GAPDH mRNA levels in cells transfected with GAPDH siRNA, **(B)** CD23 mRNA levels in cells transfected with GAPDH siRNA, **(C)** GAPDH mRNA levels in cells transfected with CD23 siRNA and **(D)** CD23 mRNA levels in cells transfected with CD23 siRNA. Expression levels were calculated by ΔΔCt analysis, normalised against the endogenous reference gene β2-microglobulin and expressed relative to control siRNA-transfected cells at each timepoint (black bars).

Error bars represent SEM and statistical analysis was performed using ANOVA with Bonferroni correction (n as indicated, max n=11, tonsil numbers 1, 4, 8, 11-15, 17, 19 & 21). *** $p<0.001$

4.3.2. CD23 siRNA reduces mCD23 expression

After having confirmed that CD23 siRNA could successfully reduce CD23 mRNA levels, the knock-on effect of this on mCD23 expression was next investigated. Human tonsil B cells were transfected and cultured, as previously described, for up to 12 days. Cell samples were taken after 18 hours, 24 hours, 48 hours, 5 days, 7 days and 12 days, stained for mCD23 expression and analysed by flow cytometry (as described in Section 2.5.1). Figure 4.6A shows an example of flow cytometric analysis of mCD23 levels from 18 hours to 12 days following transfection with either control siRNA or CD23 siRNA. In control siRNA-transfected cells, mCD23 expression increased gradually over the first 48 hours and reached a peak on day 5 (88 ± 2.8%, n=8, data not shown graphically). mCD23 expression was dramatically decreased in CD23 siRNA-transfected cells.

Figure 4.6B shows pooled data from multiple donors, expressed relative to mCD23 expression on control siRNA-transfected cells. The percentage of $mCD23^+$ cells was reduced following transfection with CD23 siRNA. The maximum inhibition was observed at 18 hours after transfection (69%), although this timepoint was only recorded in one donor. The reduction remained statistically significant until day 7, although was largely recovered by 48 hours (19 ± 2%, n=6). Figure 4.6C shows the level of mCD23 expression on cells, as measured by the MFI, was significantly lower on cells transfected with CD23 siRNA, compared to control siRNA. This reduction also remained statistically significant until day 7 but the MFI was suppressed to a greater degree (66 ± 6% inhibition after 48 hours, n=6) than the percentage of $mCD23^+$ cells and took longer to recover. In summary, despite the short-term inhibition of CD23 mRNA shown in Figure 4.5, the inhibition of mCD23 expression by CD23 siRNA remained significant until day 7.

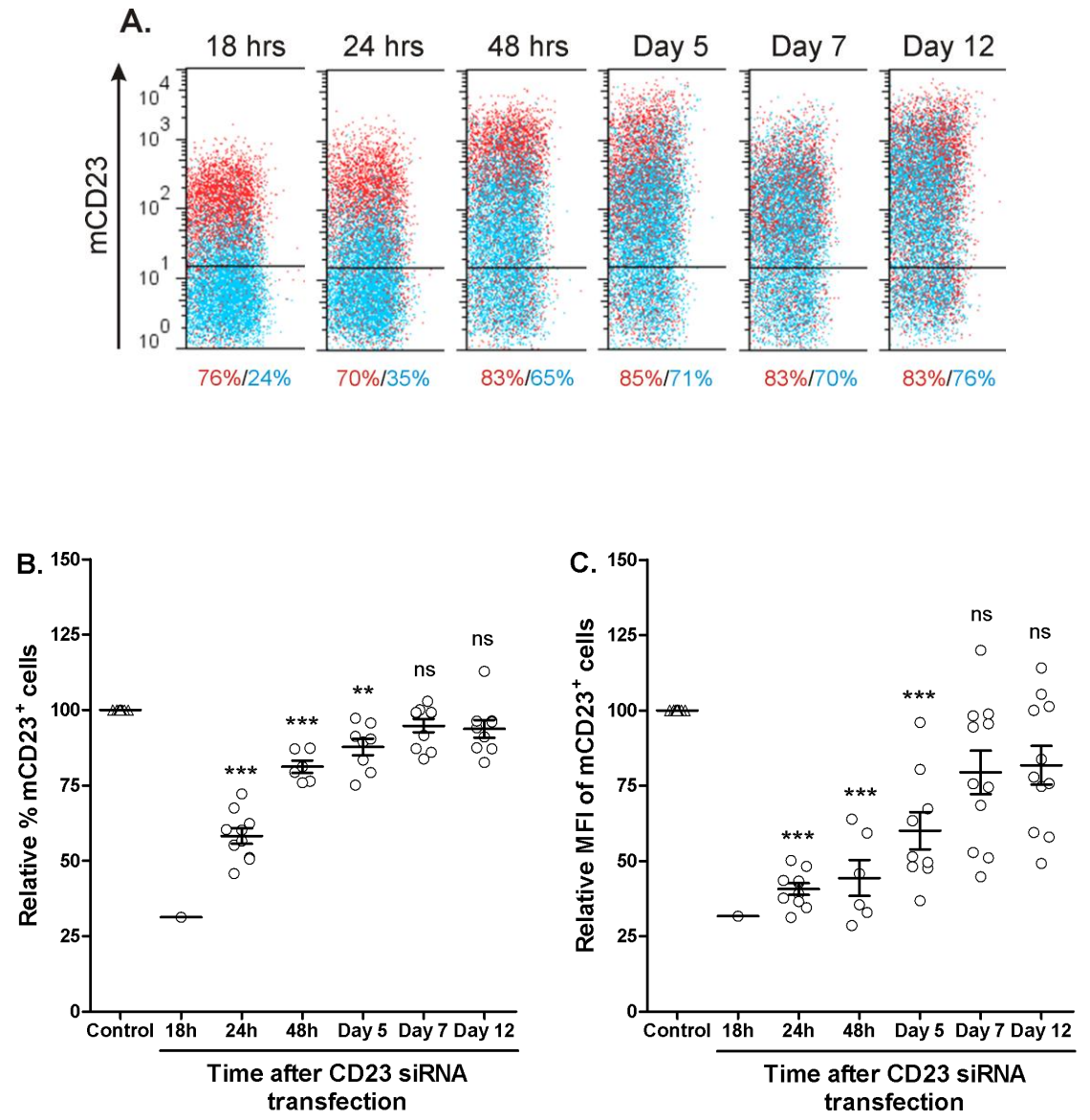

Figure 4.6. CD23 siRNA significantly reduces mCD23 expression for up to 7 days following transfection.

Total B cells were transfected with either control siRNA or CD23 siRNA by electroporation and cultured for up to 12 days in the presence of IL-4 (200IU/ml) and anti-CD40 (1µg/ml). The expression of mCD23 was analysed at the times indicated by flow cytometry. **(A)** Overlay of mCD23 expression on cells transfected with control siRNA (red) or CD23 siRNA (blue). % of $mCD23^+$ cells are indicated below each dot plot. Data shown from 1 (tonsil number 8) of 11 donors. Pooled multiple donor data for cells transfected with CD23 siRNA (○), relative to control siRNA (Δ) at each timepoint, is shown for **(B)** % of $mCD23^+$ cells and **(C)** $CD23^+$ MFI. Error bars represent SEM and statistical analysis was performed using ANOVA with Bonferroni correction (n=11, tonsil numbers 4, 8, 11-15, 17, 19, 21 & 22). ** $p<0.01$, *** $p<0.001$

4.3.3. CD23 siRNA reduces sCD23 production

sCD23 is produced by cleavage of mCD23, initially by the membrane-bound metalloprotease ADAM10 (Weskamp, Ford *et al.*, 2006). In the same experiments as described in the previous section, supernatants were harvested at 18 hours, 24 hours, 48 hours, 5 days, 7 days and 12 days after transfection and the sCD23 content was analysed by ELISA (as described in Section 2.6.3). sCD23 was first detectable in the supernatant 4 days after transfection with control siRNA (data not shown) and reached levels of 13 – 102ng/ml (mean = 58 ± 4ng/ml, n=32) by day 12 (Figure 4.8). In accordance with the reduced mCD23 levels shown in Figure 4.6, sCD23 production decreased significantly following CD23 siRNA transfection (Figure 4.7). By day 12, sCD23 levels were, on average, 17.4 ± 5.7% ($p=0.13$, n=6) lower in supernatants from cells transfected with CD23 siRNA, compared to control siRNA. No significant reduction was seen at the earlier timepoints of day 5 or day 7.

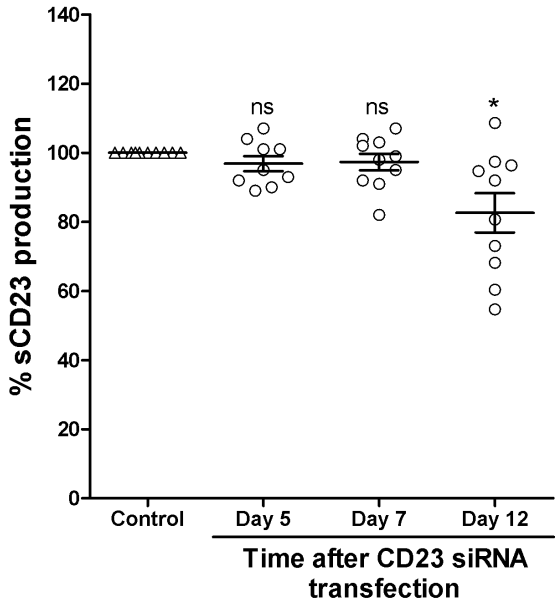

Figure 4.7. CD23 siRNA reduces sCD23 production by day 12.

Total B cells were transfected with either control siRNA (Δ) or CD23 siRNA (○) by electroporation and cultured for up to 12 days in the presence of IL-4 (200IU/ml) and anti-CD40 (1μg/ml). Supernatants were analysed for sCD23 content by ELISA on the days indicated, relative to control siRNA-transfected cells (100%). Error bars represent SEM and statistical analysis was performed using ANOVA with Bonferroni correction (n=10, tonsil numbers 1, 8, 11, 13-15, 17, 19, 21 & 22). * $p<0.05$

4.4. CD23 siRNA-mediated effects on IgE and IgG

Having shown that the transfection of human B cells with CD23 siRNA resulted in a reduction in the levels of CD23 mRNA, mCD23 expression and sCD23 production, the effect of these reductions on switching to, and expression of, IgE was next investigated. As introduced in Section 1.9, there are conflicting opinions as to whether there is a clinical relationship between elevated sCD23 levels, IgE levels and severity of allergic symptoms (Aberle, Gagro *et al.*, 1997; Di Lorenzo, Drago *et al.*, 1999; Lorenzo, Mansueto *et al.*, 1996; Rogala and Rymarczyk 1999; Wilhelm, Klouche *et al.*, 1994; Yanagihara, Sarfati *et al.*, 1990).

4.4.1. Correlation between sCD23 and sIgE

It was first necessary to show whether there was a correlation between sCD23 production and IgE secretion in the *in vitro* human tonsillar B cell cultures. Figure 4.8 shows the relationship between sCD23 and sIgE levels measured in the supernatant following 12 days stimulation with IL-4 and anti-CD40. In Figure 4.8A, the sCD23 concentrations are indicated in both ng/ml and μM to facilitate comparisons with the known K_D values of interaction with IgE and CD21 (discussed in Sections 1.5.2 and 2.4.2). Figure 4.8A shows a significant positive correlation between sCD23 and sIgE levels (r=0.79) as determined by Spearman's rank correlation coefficient (p=<0.0001, n=32). There appears to be two phases in the relationship. Only a slight increase in sIgE was observed at low sCD23 concentrations, up to 60ng/ml (concentrations calculated for the 37 kDa fragment). However, above this threshold in the range of 60-100ng/ml of sCD23, there was a steep rise in sIgE with increasing concentrations of sCD23 (Figure 4.8).

Figure 4.8B shows the same data as Figure 4.8A. However, the concentration of sCD23 is plotted against the log concentration of sIgE (in ng/ml). This form of data analysis clearly shows the positive correlation between sIgE and sCD23 (r=0.75, n=28). Four donors did not secrete any IgE by day 12 (tonsil numbers 1, 8, 13 & 14) and are, therefore, excluded from Figure 4.8B as it is not possible to log a value of zero.

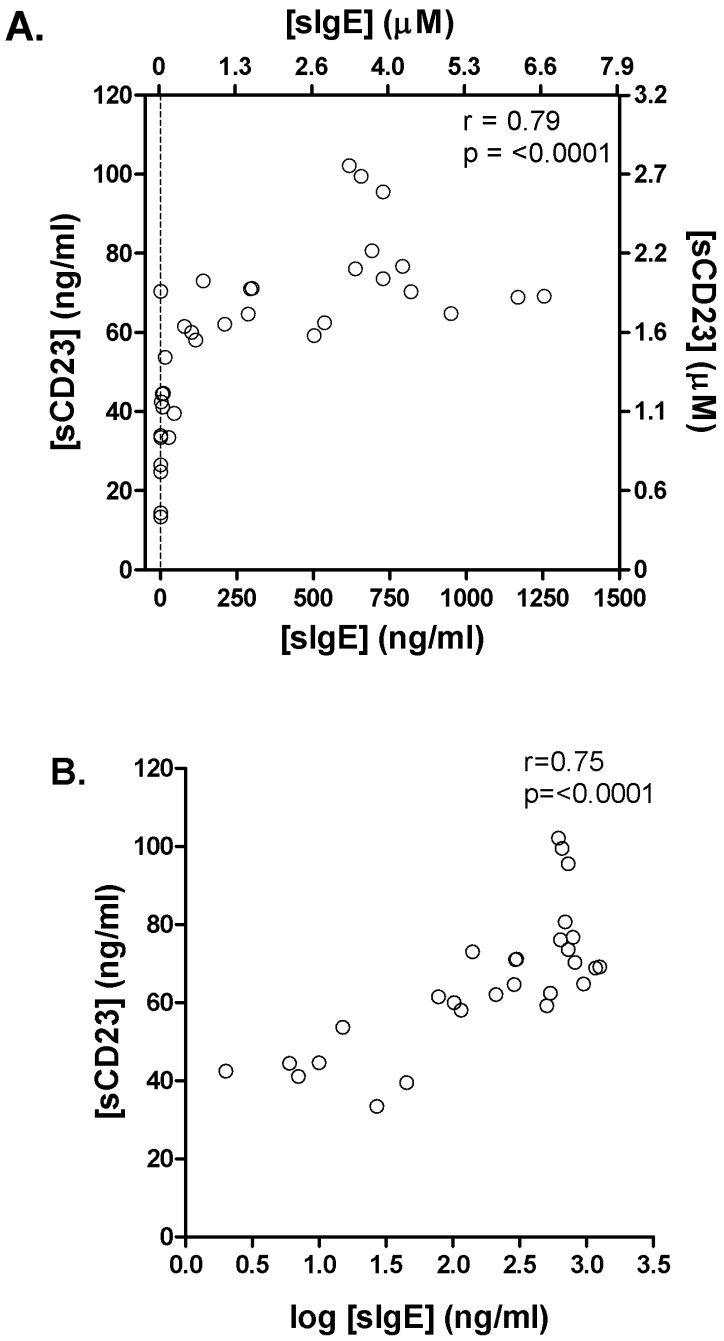

Figure 4.8. sCD23 production positively correlates with IgE secretion.

Total B cells were cultured for 12 days in the presence of IL-4 (200IU/ml) and anti-CD40 (1μg/ml). sCD23 production and IgE secretion were analysed by ELISA on day 12. **(A)** Values are shown in ng/ml on the bottom x-axis and left y-axis and in μM on the top x-axis and right y-axis (1μM 190kDa sIgE = 190ng/ml and 1μM 37kDa sCD23 = 37ng/ml) (n=32, tonsil numbers 1-32). **(B)** Re-analysis of the data shown in (A) with the sIgE concentration shown in log ng/ml (n=28, tonsil numbers 2-7, 9-12 & 15-32).

Correlation analysis was performed using Spearman's rank correlation coefficient (r values indicated on graphs).

4.4.1. CD23 siRNA reduces IgE secretion

Having shown a positive correlation between the levels of sCD23 production and IgE secretion, the effect of reduced sCD23 production, due to CD23 siRNA transfection, on IgE secretion was analysed. Initially it was important to check the impact of electroporation and transfection with control siRNA on IgE secretion. Figure 4.9 shows that cells which were left untreated (no electroporation or transfection with control siRNA) secreted significantly higher levels of IgE (p=0.031, n=6) after 12 days in culture with IL-4 and anti-CD40 (ranged from 38 – 1160ng/ml), compared to control siRNA-transfected cells (ranged from 36 – 729ng/ml). Despite this, control siRNA-transfected cells were still able to secrete detectable levels of IgE by day 12.

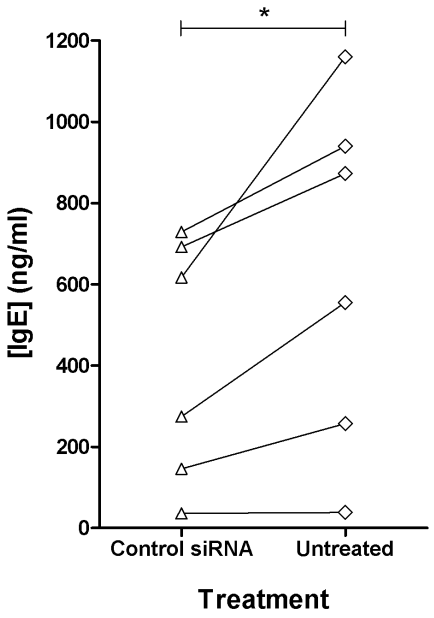

Figure 4.9. Electroporation reduces IgE secretion.

Total B cells were either transfected with control siRNA (Δ) or left untreated (no electroporation) (◊) and cultured for 12 days in the presence of IL-4 (200IU/ml) and anti-CD40 (1μg/ml). IgE secretion was analysed by ELISA on day 12.

Statistical analysis was performed using the Wilcoxon matched-pairs signed rank test (n=6, tonsil numbers 11, 15, 17, 19, 21 & 22). * $p<0.05$

Next, the levels of sIgE in the supernatants of cells transfected with control siRNA or CD23 siRNA were analysed and compared by ELISA. Low levels of sIgE were first detectable in the supernatant 5 days after stimulation with IL-4 and anti-CD40 (data not shown). Figure 4.10 shows the relative levels of sIgE on days 5, 7 and 12 after transfection with control siRNA or CD23 siRNA. Of the ten donors analysed for sCD23 production in Figure 4.7, four donors (tonsil numbers 1, 8, 13 & 14) did not produce any detectable sIgE by day 12 and so were excluded from the analysis shown in Figure 4.10. By day 12, CD23 siRNA-transfected cells had secreted 47% (± 9.5%) less IgE than control siRNA-transfected cells. For comparison, the average IgE secretion from GAPDH siRNA-transfected cells was only 2.8% less than that of control siRNA-transfected cells by day 12 (n=10, data not shown). Figure 4.11 shows there was no significant difference in the level of IgG secretion by day 12, between control siRNA- and CD23 siRNA-transfected cells.

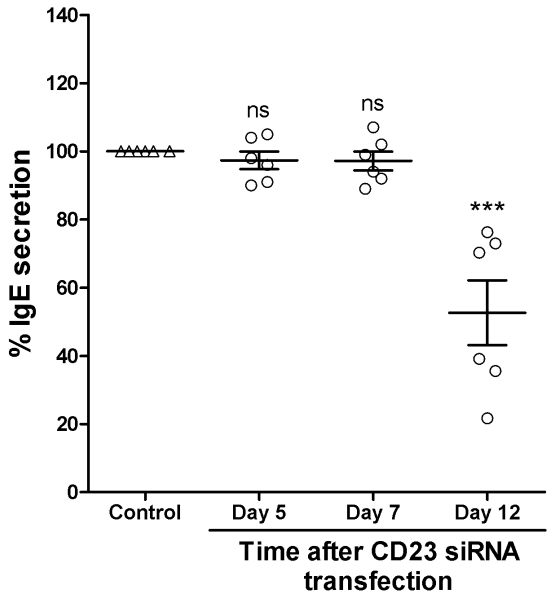

Figure 4.10. CD23 siRNA reduces IgE secretion by day 12.

Total B cells were transfected with either control siRNA (Δ) or CD23 siRNA (○) by electroporation and cultured for up to 12 days in the presence of IL-4 (200IU/ml) and anti-CD40 (1µg/ml). Supernatants were analysed for sIgE content by ELISA on the days indicated, relative to control siRNA-transfected cells (100%).

Error bars represent SEM and statistical analysis was performed using ANOVA with Bonferroni correction (n=6, tonsil numbers 11, 15, 17, 19, 21 & 22). *** $p<0.001$

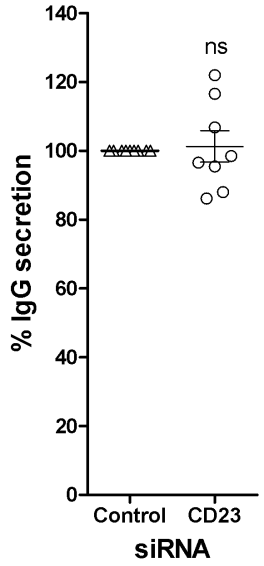

Figure 4.11. CD23 siRNA has no effect on IgG secretion by day 12.

Total B cells were transfected with either control siRNA (Δ) or CD23 siRNA (○) by electroporation and cultured for 12 days in the presence of IL-4 (200IU/ml) and anti-CD40 (1µg/ml). Supernatants were analysed for sIgG content by ELISA on day 12, relative to control siRNA-transfected cells (100%).

Error bars represent SEM and statistical analysis was performed using the Wilcoxon matched-pairs signed rank test (n=8, tonsil numbers 1, 8, 11, 13, 14, 17, 19 & 21).

It is important to note that no significant reduction in IgE secretion was observed until after day 7 (Figure 4.10). From day 7 onwards, following transfection with CD23 siRNA, mCD23 levels had returned to those of control siRNA-transfected cells (Figure 4.6). Thus any CD23-mediated differences in IgE secretion between days 7 and 12 can be attributed to sCD23, rather than mCD23.

Although the average reduction in IgE secretion by day 12 from CD23 siRNA-transfected cells was 47%, this included a range of IgE inhibition levels from 22% to 76% (Figure 4.10). The extent to which sIgE levels were inhibited was not related to the amount of IgE the cells secreted (data not shown). Given the correlation between sCD23 production and IgE secretion shown in Figure 4.8, the level of sIgE inhibition from the six donors in Figure 4.10 was plotted against the level of sCD23 inhibition from Figure 4.7. Figure 4.12 shows that there was a strong positive correlation (r=0.94) between the level of sIgE inhibition and the inhibition of sCD23 production (p=0.017, n=6).

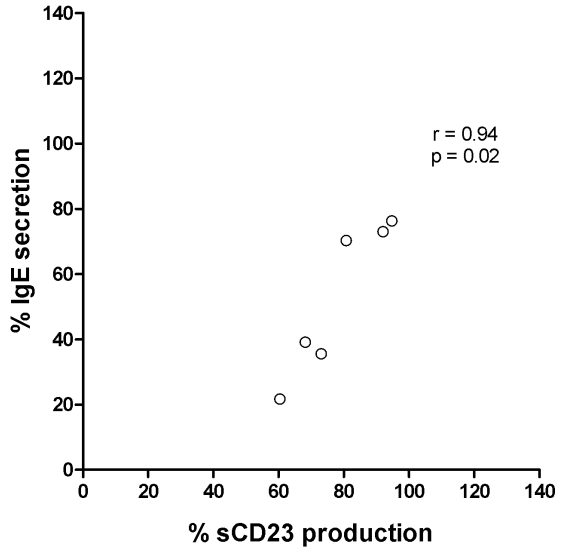

Figure 4.12. The extent of sIgE inhibition correlates with the extent of sCD23 inhibition.

Total B cells were transfected with CD23 siRNA by electroporation and cultured for 12 days in the presence of IL-4 (200IU/ml) and anti-CD40 (1µg/ml). Day 12 sCD23 ELISA data from Figure 4.7 was plotted against day 12 sIgE ELISA data from Figure 4.10.

Correlation analysis was performed using Spearman's rank correlation coefficient (r=0.94) (n=6, tonsil numbers 11, 15, 17, 19, 21 & 22).

4.4.2. CD23 siRNA has no effect on IgE and IgG expression

Having now shown that reducing sCD23 production in human B cells with CD23 siRNA can consequently reduce IgE secretion, more investigation was required as to the exact mechanism by which this may occur. To establish whether the reduction in IgE was specific to the secreted form of IgE, membrane and intracellular expression of IgE and IgG was analysed by flow cytometry. Human B cells were transfected with either control siRNA or CD23 siRNA and cultured for up to 12 days with IL-4 and anti-CD40. Cell samples were taken on days 7 and 12 for analysis of the percentage of IgE^+ and IgG^+ cells and the MFI of these cell populations (as described in Section 2.5.1).

Figure 4.13A shows the increase in IgE expression between days and 7 and 12 and the development of an IgE^{hi} population by day 12 (also previously shown in Figure 3.6). The IgE expression pattern between cells transfected with control siRNA, compared to CD23 siRNA, was very similar. Figure 4.13B and Figure 4.13C show there was no significant difference between the percentage of IgE^+ cells (or MFI) following transfection with control siRNA, compared to CD23 siRNA (n=6).

This was also the case for IgG expression, shown in Figure 4.14. Figure 4.14A shows how the expression of IgG decreased over time, due to switching to other isotypes. The IgG expression pattern between cells transfected with control siRNA, compared to CD23 siRNA, was very similar. Figure 4.14B and Figure 4.14C show there was no significant difference between the percentage of IgG^+ cells (or MFI) of cells following transfection with control siRNA, compared to CD23 siRNA (n=6).

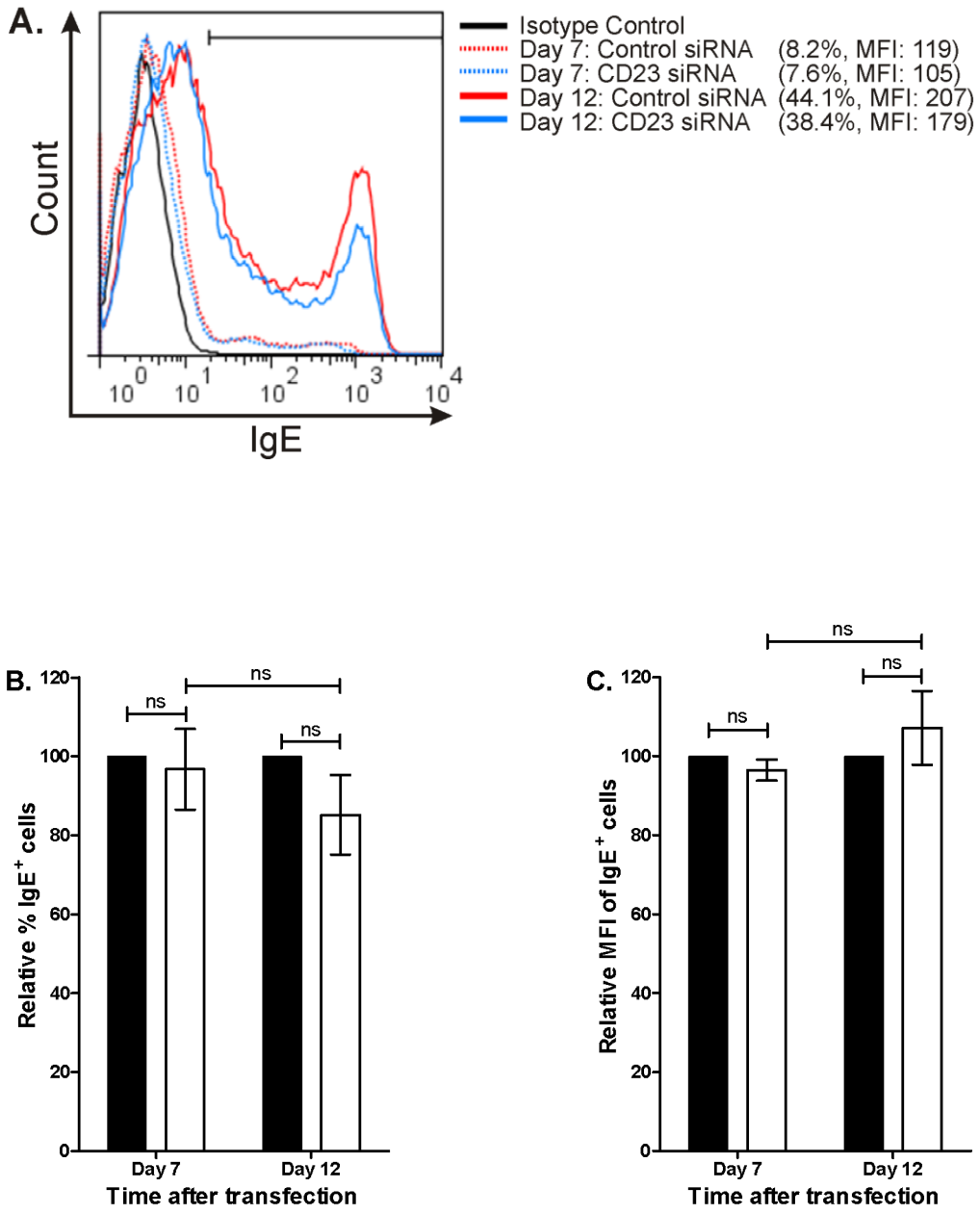

Figure 4.13. CD23 siRNA does not alter the % or MFI of IgE$^+$ cells.

Total B cells were transfected with either control siRNA (black) or CD23 siRNA (white) by electroporation and cultured for up to 12 days in the presence of IL-4 (200IU/ml) and anti-CD40 (1µg/ml). The expression of membrane and intracellular IgE was analysed on days 7 and 12 by flow cytometry. **(A)** An example of IgE expression levels on day 7 (dotted line) and day 12 (solid line) for cells transfected with either control siRNA (red) or CD23 siRNA (blue). The % of IgE$^+$ cells and MFI are indicated on the legend. Data shown from 1 (tonsil number 21) of 6 donors. Pooled data from multiple donors is shown for **(B)** the % of live IgE$^+$ cells and **(B)** the MFI of live IgE$^+$ cells, relative to control siRNA-transfected cells at each timepoint (100%). Error bars represent SEM and statistical analysis was performed using ANOVA with Bonferroni correction (n=6, tonsil numbers 11, 15, 17, 19, 21 & 22).

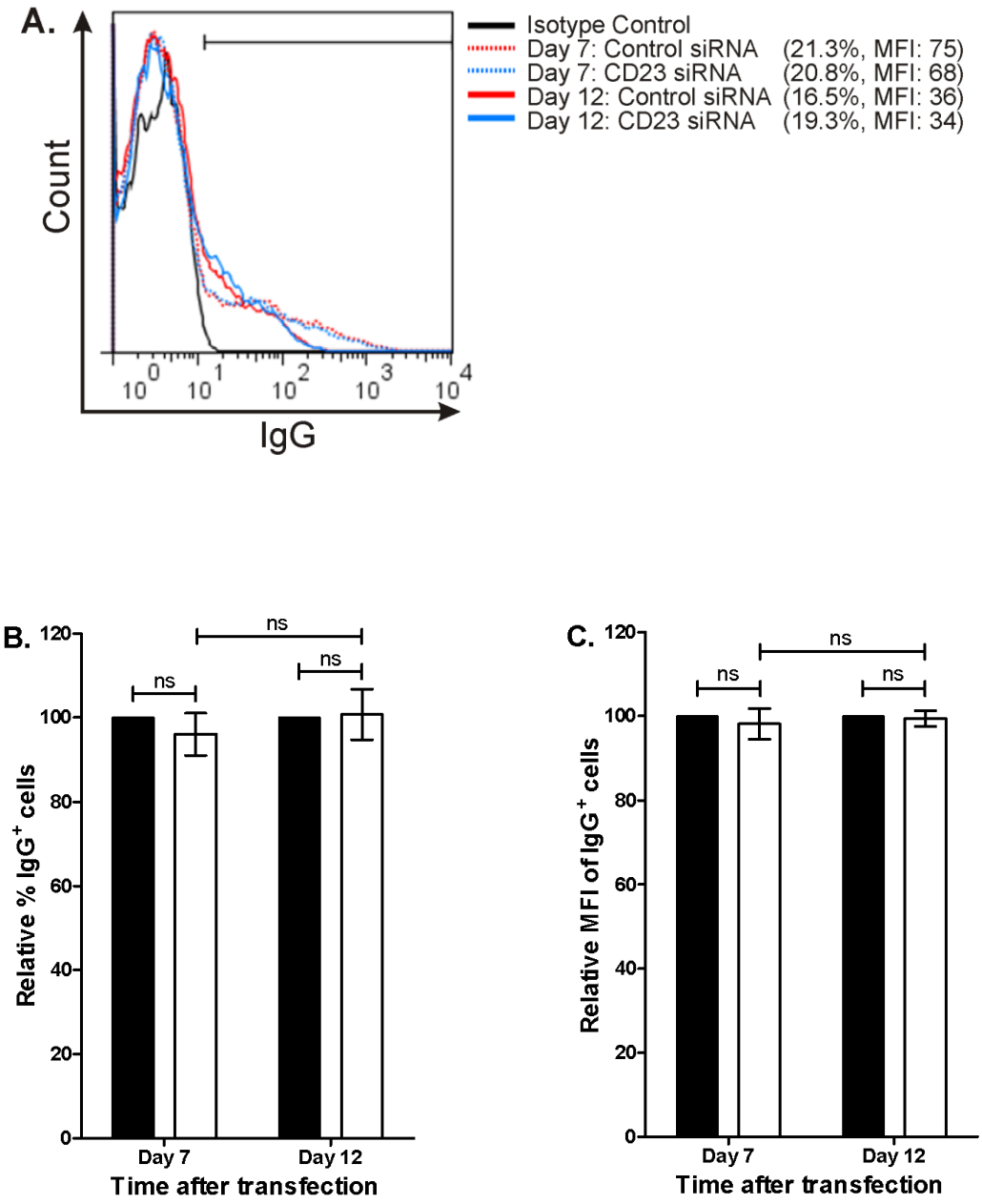

Figure 4.14. CD23 siRNA does not alter the % or MFI of IgG$^+$ cells.

Total B cells were transfected with either control siRNA (black) or CD23 siRNA (white) by electroporation and cultured for up to 12 days in the presence of IL-4 (200IU/ml) and anti-CD40 (1µg/ml). The expression of membrane and intracellular IgG was analysed on days 7 and 12 by flow cytometry. **(A)** An example of IgG expression levels on day 7 (dotted line) and day 12 (solid line) for cells transfected with either control siRNA (red) or CD23 siRNA (blue). The % of IgG$^+$ cells and MFI are indicated on the legend. Data shown from 1 (tonsil number 21) of 6 donors. Pooled data from multiple donors is shown for **(B)** the % of live IgG$^+$ cells and **(B)** the MFI of live IgG$^+$ cells, relative to control siRNA-transfected cells at each timepoint (100%). Error bars represent SEM and statistical analysis was performed using ANOVA with Bonferroni correction (n=6, tonsil numbers 11, 15, 17, 19, 21 & 22).

4.5. Mechanism of action of CD23 siRNA

The CD23 siRNA-mediated reduction in IgE secretion shown in Figure 4.10 can be attributed to the reduction in sCD23 production shown in Figure 4.7. To confirm this, further experiments were required to ensure that CD23 siRNA did not affect other pathways which could also explain the reduction in sCD23 and sIgE.

4.5.1. CD23 siRNA does not reduce ADAM10 expression

The metalloprotease ADAM10 is responsible for the initial cleavage of mCD23 from the cell surface to produce a 37kDa fragment of sCD23 (Weskamp, Ford *et al.*, 2006). A reduction in the expression level of ADAM10 could therefore lead to decreased mCD23 cleavage and sCD23 production. To ensure the surface expression levels of ADAM10 were the same in cells transfected with either control siRNA or CD23 siRNA, cell samples were taken at 24 hours, 48 hours, 5 days, 7 days and 12 days after transfection for flow cytometric analysis (as described in Section 2.5.1). Figure 4.15 shows there was no significant difference in the percentage of $ADAM10^{+}$ cells following transfection with either control siRNA or CD23 siRNA (n=3), revealing that the loss of ADAM10 was not responsible for the decrease in sCD23 levels.

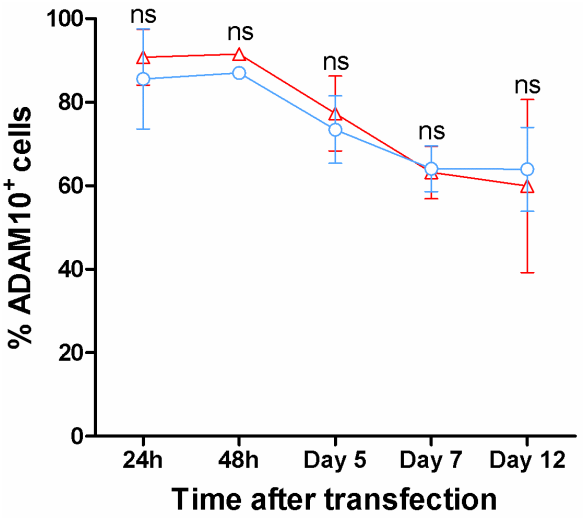

Figure 4.15. ADAM10 expression levels are the same on cells transfected with control siRNA or CD23 siRNA.

Total B cells were transfected with either control siRNA (Δ) or CD23 siRNA (○) by electroporation and cultured for up to 12 days in the presence of IL-4 (200IU/ml) and anti-CD40 (1µg/ml). The expression of ADAM10 was analysed at the times indicated by flow cytometry.

Error bars represent SEM and statistical analysis was performed using ANOVA with Bonferroni correction (n=3, tonsil numbers 12-14).

4.5.1. CD23 siRNA does not decrease εGLT levels

To shed light on the stage of IgE synthesis that is affected by CD23 siRNA, the effect on the level of ε germline transcripts (εGLTs) was investigated. The transcription of germline transcripts is essential for CSR and is the first step in the commitment of B cells to the synthesis of IgG, IgA and IgE (Bacharier, Jabara *et al.*, 1998; Gould, Beavil *et al.*, 2000).

To ensure the reduction seen in IgE synthesis following CD23 siRNA transfection (Figure 4.12) was due to reduced sCD23 levels and not a reduction in CSR to IgE, the levels of εGLTs were quantified by qPCR (as described in Section 2.8). Cells were harvested immediately following transfection with either control siRNA or CD23 siRNA (0 hours) and at 5 hours, 18 hours, 24 hours, 48 hours and 5 days following

transfection. Figure 4.16 shows the increase in εGLT levels over the period of 5 days in both control siRNA- and CD23 siRNA-transfected cells. No significant differences in εGLT levels were detected at either 24 or 48 hours following transfection. This indicates that CD23 siRNA does not reduce the induction of class switching to IgE.

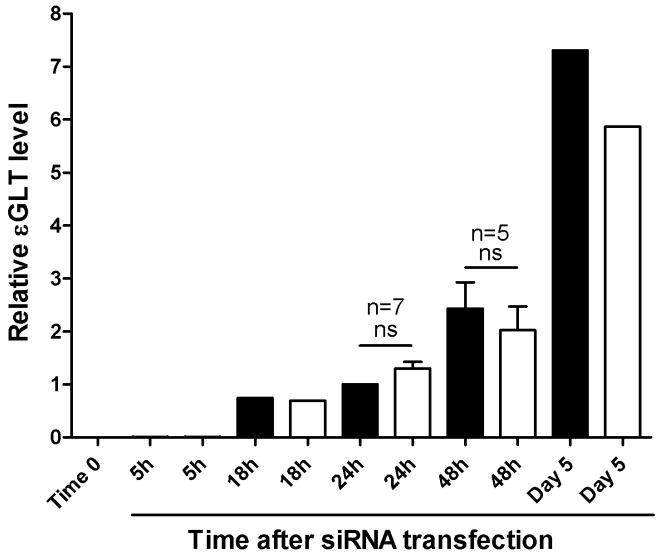

Figure 4.16. CD23 siRNA does not reduce εGLT levels.

Total B cells were transfected with either control siRNA (black) or CD23 siRNA (white) by electroporation and cultured for up to 5 days in the presence of IL-4 (200IU/ml) and anti-CD40 (1μg/ml). Cell samples were harvested at the times indicated and qPCR was performed to quantify RNA levels for εGLT. Expression levels were calculated by ΔΔCt analysis, normalised against the endogenous reference gene β2-microglobulin and expressed relative to control siRNA-transfected cells at 24 hours.

Error bars represent SEM and statistical analysis was performed using ANOVA with Bonferroni correction (n=1, unless indicated otherwise. Max n=7, tonsil numbers 4, 12-14, 17, 19 & 21).

4.6. CD23 siRNA-mediated effects on B cell cytokine secretion

Although it is well known that B cells can produce cytokines, less is known about whether B cells can differentiate into effector subsets that secrete polarized arrays

of cytokines. 'Effector' B cells have been divided into three groups determined by their cytokine profile: B effector 1 (Be1) cells; B effector 2 (Be2) cells; and regulatory B cells. Be1 cells secrete IFNγ, IL-6 and IL-12 in response to priming by T cells, in combination with antigen and/or TLR stimulation, in the presence of Th1-type cytokines (e.g. IFNγ) (Harris, Goodrich *et al.,* 2005; Harris, Haynes *et al.,* 2000). Be2 cells secrete IL-2, IL-4 and IL-13, in response to priming by T cells in combination with antigen, in the presence of Th2-type cytokines (e.g. IL-4). Both Be1 and Be2 cells secrete IL-5, IL-6, IL-10 and TNF (Harris, Goodrich *et al.*, 2005; Harris, Haynes *et al.*, 2000). Regulatory B cells have been shown to secrete high levels of IL-10 (B10 cells) in response to a combined stimulation of antigen, CD40L and TLR ligands (Bouaziz, Yanaba *et al.,* 2008; Fillatreau, Gray *et al.,* 2008; Mauri and Ehrenstein 2008; Yanaba, Bouaziz *et al.,* 2009).

Since the human B cells in the experiments described in this thesis are cultured with IL-4, it was hypothesised that it may be possible to detect the presence of Be2-type cytokines in the supernatants, despite the lack of T cells. A comparison could then be made between control siRNA- and CD23 siRNA-transfected cells to investigate whether a knockdown of CD23 has any impact on B cell cytokine secretion.

Human B cells were transfected with either control siRNA or CD23 siRNA and cultured for 12 days in the presence of IL-4 and anti-CD40. A custom-made MILLIPLEX® MAP Human Cytokine Assay was used to simultaneously quantify the supernatant levels of IFNγ (Be1 cytokine), IL-2 (Be2 cytokine), IL-13 (Be2 cytokine), IL-10 (both Be1 and Be2 cytokine) and IL-6 (both Be1 and Be2 cytokine) on day 12 (as described in Section 2.7). Figure 4.17A shows the standard curves generated for each individual cytokine and Figure 4.17B shows that the control samples of known cytokine concentrations, provided as part of the kit, all fell within the expected ranges.

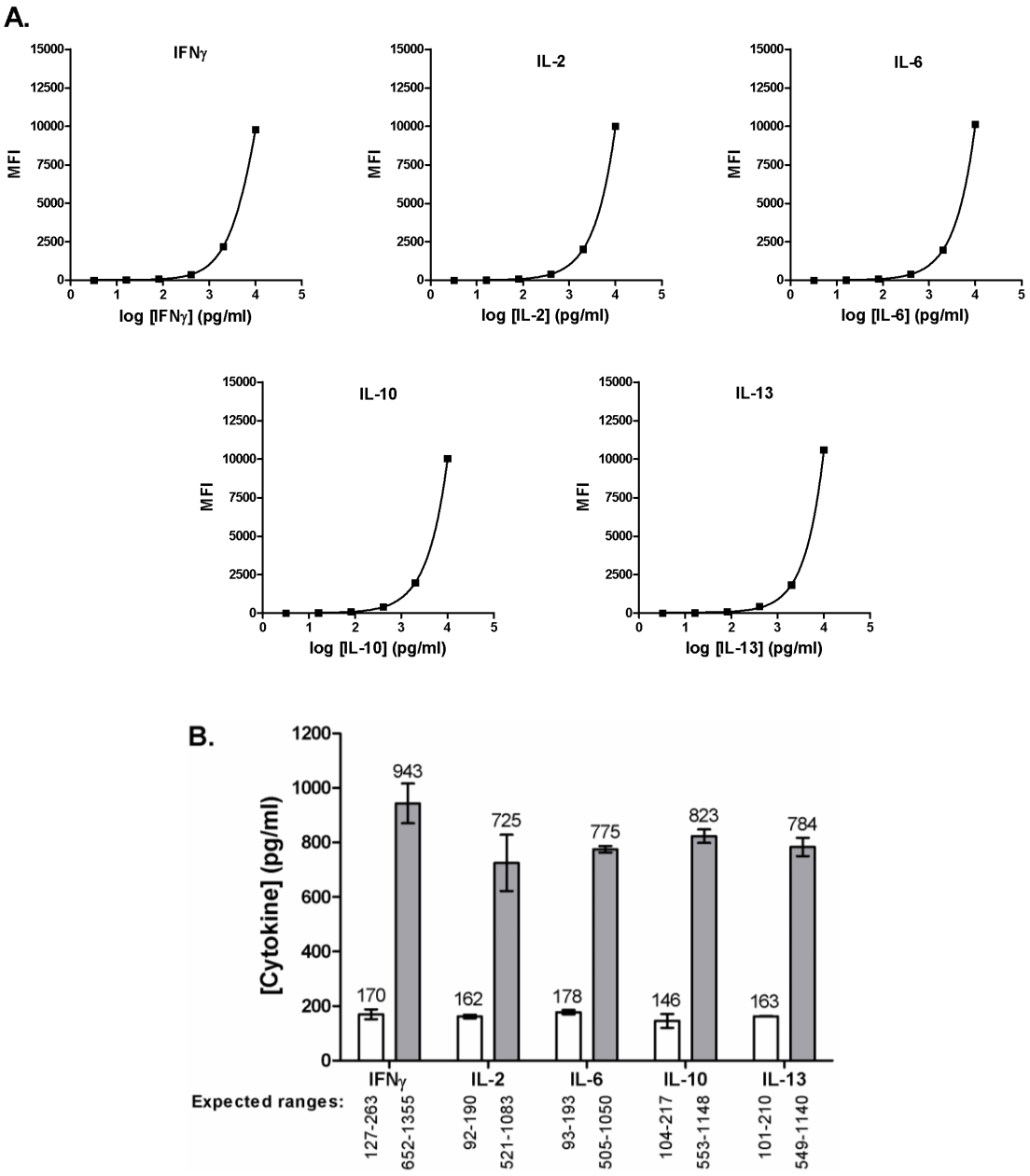

Figure 4.17. Assay optimisation for multiplex cytokine analysis.

(A) Using the MILLIPLEX® MAP Human Cytokine Assay, standard curves were generated for the simultaneous quantification of IFNγ, IL-2, IL-6, IL-10 and IL-13 (10,000pg/ml-3.2pg/ml). **(B)** Low concentration (white) and high concentration (grey) control samples, of known concentrations, were analysed for the simultaneous quantification of IFNγ, IL-2, IL-6, IL-10 and IL-13. Calculated pg/ml values are indicated above each bar and the expected ranges indicated below each bar. Error bars represent SEM of individual duplicates.

4.6.1. IFNγ

Since IFNγ is a Be1 cytokine no detection was expected. Figure 4.18 shows that this was indeed the case in ten out of eleven donors. However, a small amount of IFNγ (4.6pg/ml) was detected in the supernatant of CD23 siRNA-transfected cells from one donor.

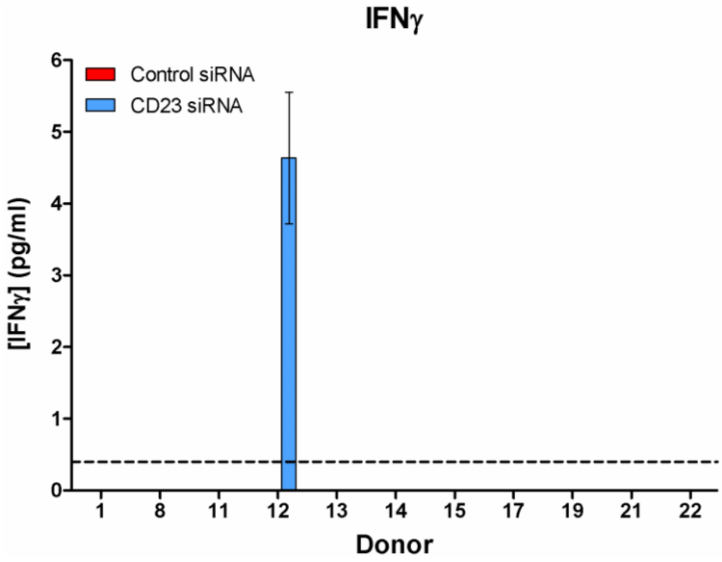

Figure 4.18. IFNγ could not be detected in B cell supernatants by day 12

Total B cells were transfected with either control siRNA (red) or CD23 siRNA (blue) by electroporation and cultured for 12 days in the presence of IL-4 (200IU/ml) and anti-CD40 (1µg/ml). Cell supernatants were harvested on day 12 and the levels of IFNγ were quantified using a MILLIPLEX® MAP Human Cytokine Assay. The minimum detection level is indicated by the dashed line.

Error bars represent SEM of individual duplicates (n=11, tonsil numbers as indicated).

4.6.1. IL-2 and IL-13

The detection of the cytokines IL-2 and IL-13 is shown in Figure 4.19. Only very low levels of IL-2 could be detected. IL-13 was detected in the supernatants from two donors. B cells from donor 4 produced 16pg/ml of IL-13 from control siRNA-

transfected cells and this increased to 50pg/ml from CD23 siRNA-transfected cells. B cells from donor 7 secreted a small amount of IL-13.

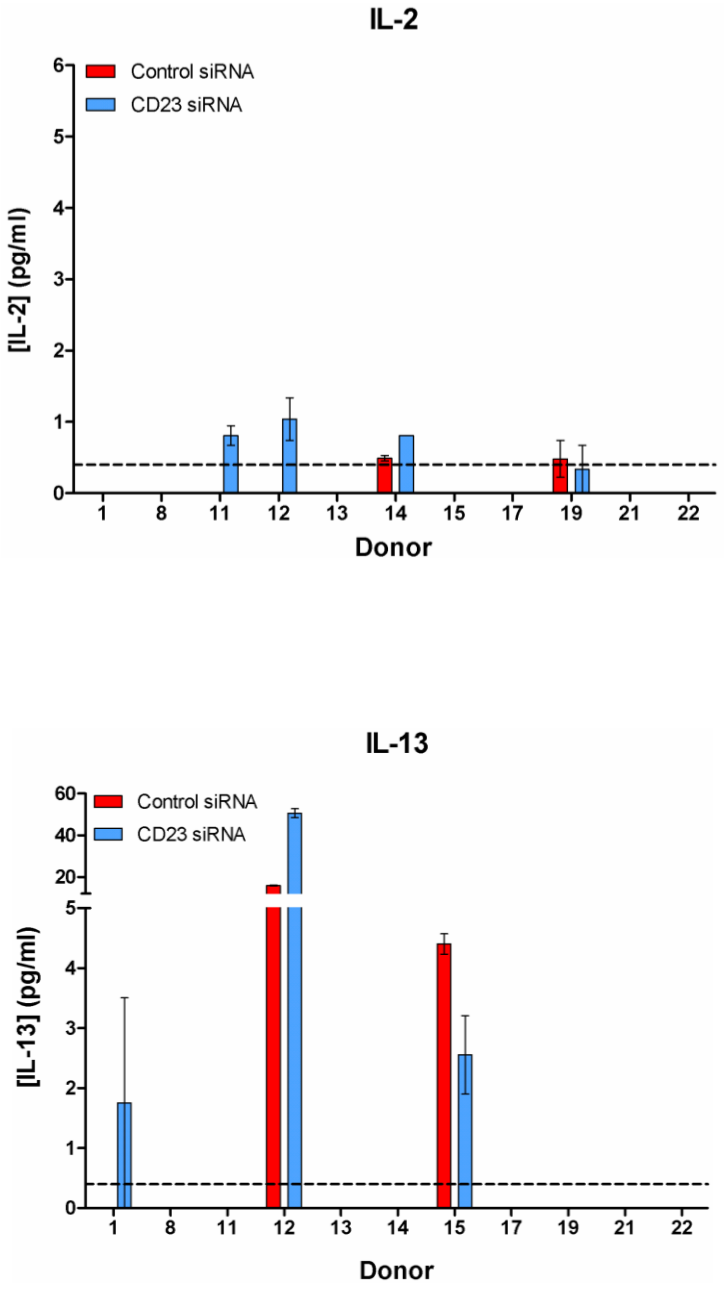

Figure 4.19. IL-2 and IL-13 could be detected in B cell supernatants by day 12

Total B cells were transfected with either control siRNA (red) or CD23 siRNA (blue) by electroporation and cultured for 12 days in the presence of IL-4 (200IU/ml) and anti-CD40 (1µg/ml). Cell supernatants were harvested on day 12 and the levels of IL-2 and IL-13 were quantified using a MILLIPLEX® MAP Human Cytokine Assay. The minimum detection level is indicated by the dashed line.

Error bars represent SEM of individual duplicates (n=11, tonsil numbers as indicated).

4.6.2. IL-10

The detection of the cytokine IL-10 is shown in Figure 4.20. Figure 4.20A shows the raw data for the detection of IL-10 in pg/ml for all eleven donors. It is clear to see that there was a wide range in the levels of IL-10 secretion, from 2 – 98pg/ml. Figure 4.20B presents this data as relative IL-10 secretion, normalised to IL-10 levels from cells transfected with control siRNA in each donor. IL-10 secretion from CD23 siRNA-transfected cells, compared to control siRNA-transfected cells, was elevated in five donors. Other donors showed either no difference between the two siRNA transfections or a slight decrease in IL-10 secretion from CD23 siRNA-transfected cells. Figure 4.20C summarises the data from all donors and shows the average increase in IL-10 secretion from CD23 siRNA-transfected cells, compared to control siRNA-transfected cells, was non-significant ($p=0.123$, $n=11$).

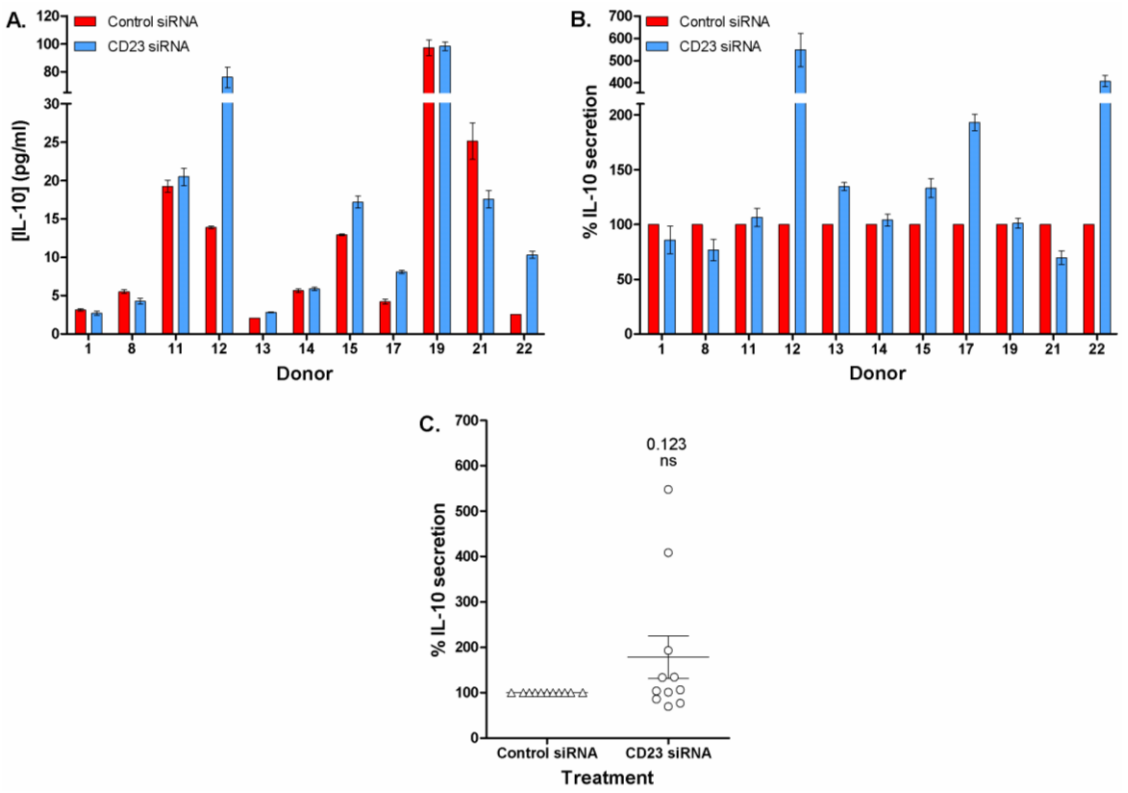

Figure 4.20. Depending on the donor, CD23 siRNA either increased or decreased IL-10 secretion.

Total B cells were transfected with either control siRNA (red) or CD23 siRNA (blue) by electroporation and cultured for 12 days in the presence of IL-4 (200IU/ml) and anti-CD40 (1µg/ml). Cell supernatants were harvested on day 12 and the levels of IL-10 were quantified using a MILLIPLEX® MAP Human Cytokine Assay. Data is displayed from individual donors as **(A)** the concentration of IL-10 in pg/ml and **(B)** the % of IL-10 secretion relative to cells transfected with control siRNA (100%). Error bars represent SEM of individual duplicates (n=11). **(C)** Pooled data from multiple donors for the % of IL-10 secretion relative to cells transfected with control siRNA (100%). Error bars represent SEM and statistical analysis was performed using the Wilcoxon matched-pairs signed rank test (n=11, tonsil numbers as indicated).

4.6.1. IL-6

The detection of the cytokine IL-6 is shown in Figure 4.21. Figure 4.21A shows the raw data for the detection of IL-6 in pg/ml for all eleven donors. IL-6 secretion levels varied widely between donors from 60 – 5600pg/ml. Of the eleven donors, cells from three donors secreted very high levels of IL-6 above 2500pg/ml. Figure 4.21B presents this data as relative IL-6 secretion, normalised to IL-6 levels from cells transfected with control siRNA in each donor. IL-6 secretion from CD23 siRNA-transfected cells, compared to control siRNA-transfected cells, was elevated in seven donors. Other donors showed no difference in IL-6 secretion between control siRNA- and CD23 siRNA-transfected cells. Figure 4.21C shows the average increase in IL-6 secretion from CD23 siRNA-transfected cells, compared to control siRNA-transfected cells, was statistically significant ($p=0.042$, $n=11$). These results suggest a mechanism by which IL-6 secretion is enhanced as a result of siRNA-induced CD23 knockdown. This will be discussed further in the chapter summary (Section 4.7).

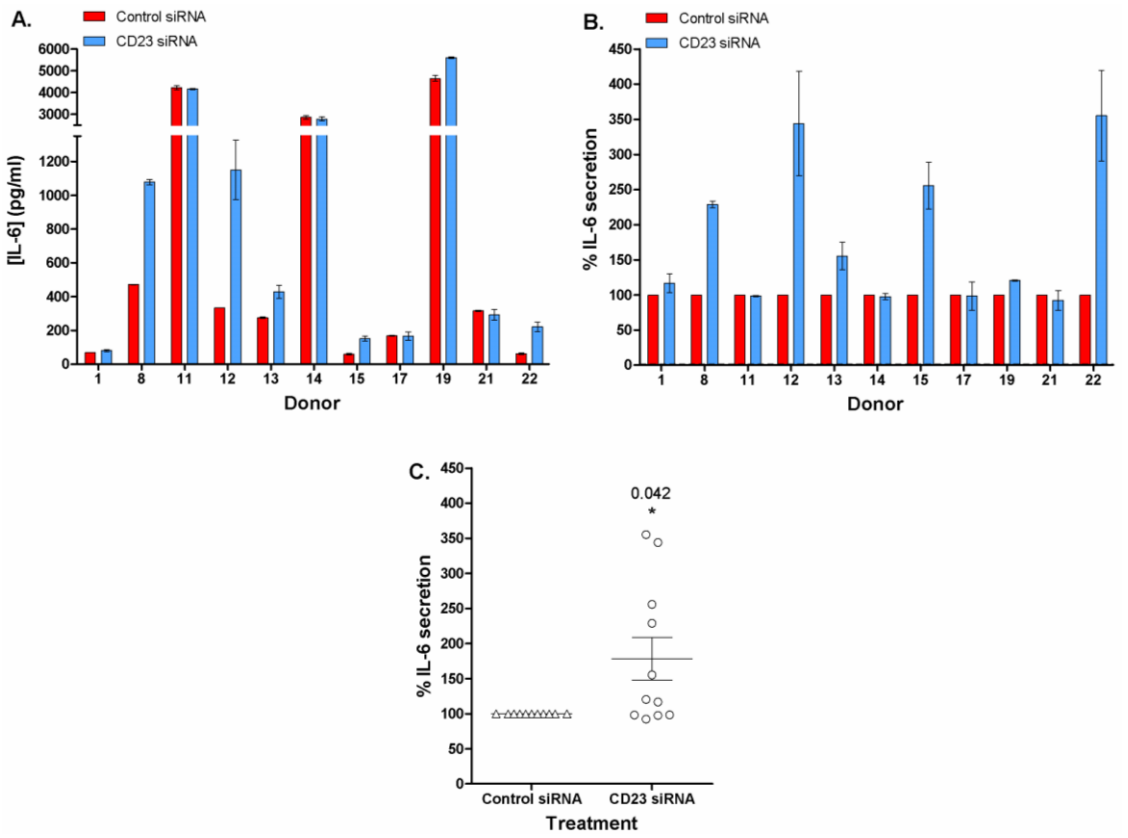

Figure 4.21. IL-6 secretion was significantly higher from cells transfected with CD23 siRNA compared to control siRNA.

Total B cells were transfected with either control siRNA (red) or CD23 siRNA (blue) by electroporation and cultured for 12 days in the presence of IL-4 (200IU/ml) and anti-CD40 (1µg/ml). Cell supernatants were harvested on day 12 and the levels of IL-6 were quantified using a MILLIPLEX® MAP Human Cytokine Assay. Data is displayed from individual donors as **(A)** the concentration of IL-6 in pg/ml and **(B)** the % of IL-6 secretion relative to cells transfected with control siRNA (100%). Error bars represent SEM of individual duplicates (n=11). **(C)** Pooled data from multiple donors for the % of IL-6 secretion relative to cells transfected with control siRNA (100%). Error bars represent SEM and statistical analysis was performed using the Wilcoxon matched-pairs signed rank test (n=11, tonsil numbers as indicated). * $p<0.05$

4.6.2. The relationship between IL-6, IL-10 and IgE secretion

IgE secretion from human B cells, induced by the combination of IL-4 and anti-CD40 stimulation, has been previously shown to be preceded by a strong activation of NF-κB and an increase in IL-6 secretion (Jeppson, Patel *et al.*, 1998). It was of interest to see if the wide range of IL-6 secretion levels shown in Figure 4.21 correlated with

levels of IgE secretion. Figure 4.22A shows there was no correlation between IL-6 and IgE secretion from control siRNA-transfected human B cells following 12 days in culture with IL-4 and anti-CD40.

Since Figure 3.4 showed the addition of recombinant human IL-10 could increase IgE secretion from human B cells *in vitro*, it was of interest to see if endogenous B cell-secreted IL-10 would have the same effect. Figure 4.22B shows there was no correlation between IL-10 secretion and IgE secretion from control siRNA-transfected human B cells following 12 days in culture with IL-4 and anti-CD40.

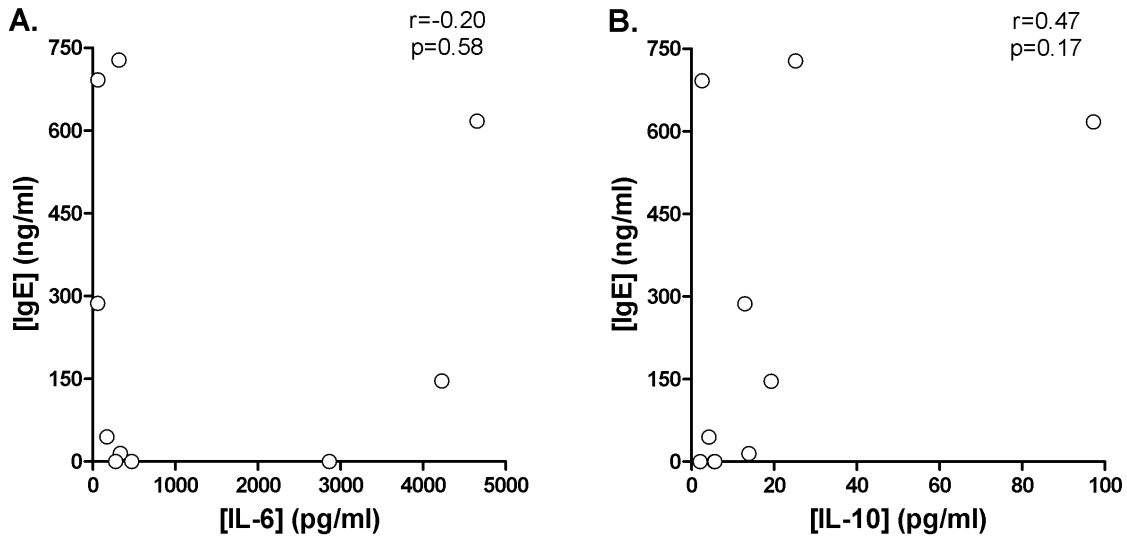

Figure 4.22. No correlation was shown between IL-6, or IL-10, and IgE secretion.

Total B cells were transfected with control siRNA by electroporation and cultured for 12 days in the presence of IL-4 (200IU/ml) and anti-CD40 (1µg/ml). **(A)** IL-6 secretion and **(B)** IL-10 secretion were quantified using a MILLIPLEX® MAP Human Cytokine Assay on day 12. IgE secretion was analysed by ELISA on day 12.

Correlation analysis was performed using Spearman's rank correlation coefficient (r values indicated on graphs) (n=10, tonsil numbers 8, 11-15, 17, 19, 21 & 22).

4.7. Summary

This chapter described a series of experiments using siRNA in human B cells to study the effects of CD23 knockdown on IgE synthesis with the overall aim of dissecting the roles of different forms of CD23 in the regulation of IgE.

No work has ever been published on the use of CD23 siRNA so the protocol required extensive optimisation. After selecting the appropriate concentration of siRNA to be used, human B cells were successfully transfected by electroporation (Figure 4.1). As the process of electroporation was found to reduce cell viability (Figure 4.3), cells transfected with a scrambled control siRNA were used for comparison in all future experiments.

qPCR analysis following transfection with CD23 siRNA showed a specific and significant reduction in CD23 mRNA levels with the optimum knockdown at 18-24 hours following transfection (Figure 4.5). This transient reduction in CD23 mRNA levels reduced the frequency and MFI of $mCD23^+$ cells until day 7 following transfection. However, by day 12, mCD23 expression had recovered to that of control siRNA-transfected cells (Figure 4.6). As introduced in Section 1.5.3, sCD23 is produced by ADAM10-mediated cleavage of mCD23. By day 12, but not at the earlier timepoints of days 5 or 7, CD23 siRNA-transfected cells showed significantly reduced sCD23 production (Figure 4.7). Supporting the correlation shown between sCD23 and sIgE in Figure 4.8, reduced sCD23 levels on day 12 were associated with reduced IgE secretion at the same timepoint (Figure 4.10 and Figure 4.12). As mCD23 expression had returned to normal from days 7-12 following transfection with CD23 siRNA, any CD23-mediated differences in IgE secretion between days 7 and 12 can be attributed to sCD23. This reduction in IgE was shown to be specific to the secreted form of IgE,

isotype-specific and not due to a reduction in the levels of CSR to IgE or ADAM10 expression (Figure 4.11 - Figure 4.16).

Multiplex cytokine analysis of supernatants from control siRNA- and CD23 siRNA-transfected cells revealed a significantly higher level of IL-6 secretion from CD23 siRNA-transfected cells (Figure 4.21). However, the range in the levels of IL-6 secretion did not correlate with IgE secretion (Figure 4.22). More in depth experiments are required to establish whether B cell-secreted IL-6 plays a role in regulating IgE secretion (discussed in Section 4.7.1). Multiplex cytokine analysis also detected the secretion of IL-10 from human B cells, although there appeared to be no consistent pattern of whether IL-10 secretion was increased or decreased following transfection with CD23 siRNA, compared to control siRNA (Figure 4.20). IFNγ (Figure 4.18) and high levels of IL-13 (Figure 4.19) and IL-10 (Figure 4.20) were detected in the supernatant from tonsil number 12 (non-allergic donor), particularly from CD23 siRNA-transfected cells. This mixed cytokine profile cannot be correlated with sIgE levels as no sIgE was detected by day 12, which may be interesting in itself. However, no IFNγ and only low levels of IL-13 and IL-10 were detected in the supernatants from the other tonsils which also secreted no IgE by day 12 (tonsil numbers 1, 8, 13 & 14).

In summary, these experiments utilised CD23 siRNA for the first time to show that a reduction in sCD23 is sufficient to reduce the secretion of IgE from primary human B cells *in vitro* (Cooper, Hobson et al., 2012). The relationship between sCD23 and sIgE shown in Figure 4.8, may reflect the avidity of sCD23 in the tri-molecular complexes with mIgE and mCD21 at the surface of the fluid B cell membrane. An investigation into the role of mCD21 in sCD23-mediated regulation of IgE will be covered in Chapter 6.

4.7.1. Further experiments

To truly show that reduced sCD23 production is sufficient to cause a reduction in IgE secretion it would be interesting to transfect cells with CD23 siRNA and then add sCD23 back in, in the form of recombinant CD23 or sCD23-containing supernatants, to see if the IgE secretion can be restored.

Experiments are currently underway to investigate the downstream cellular effects by which CD23 controls the synthesis of IgE. qPCR could be utilised to measure a selection of B cell signalling molecules, transcription factors and survival factors in cells transfected with control siRNA compared to CD23 siRNA. Another interesting experiment would be to optimise the knockdown of CD21 using siRNA (this was attempted but no knockdown was observed) and to see whether reduced mCD21 levels would also lead to reduced IgE secretion due to disruption of the mIgE-sCD23-mCD21 cross-linking network.

It would be interesting to continue the experiments investigating B cell cytokine secretion and how this is altered upon transfection with CD23 siRNA. As a very large panel of cytokines and chemokines are available to create custom multiplex cytokine assays, it would be useful to screen supernatants from control siRNA and CD23 siRNA-transfected cells for levels of many more cytokines. If a particular cytokine was found to be consistently down-regulated following CD23 siRNA transfection, this would give an indication of the signalling pathways through which sCD23 increases IgE secretion from human B cells.

Chapter 5. Inhibition of ADAM10 with GI254023X

5.1. Introduction

Since CD23 siRNA transfection reduced sCD23 through the early reduction of mCD23 expression (Chapter 4), a different approach was taken that would aim to reduce sCD23 levels through preventing mCD23 shedding, thus maintaining mCD23 levels. The ADAM10-specific small molecule inhibitor, GI254023X, was utilised to achieve this.

5.2. The ADAM10 inhibitor, GI254023X, does not affect cell viability

It was first necessary to ascertain whether addition of GI254023X into the B cell cultures would have any effect on cell viability. Human tonsil B cells were cultured for 5 days with IL-4 and anti-CD40 before addition of the ADAM10 inhibitor (1μM-15μM) as described in Section 2.4.1. Figure 5.1 shows cell viability on days 6, 7 and 12, relative to cells cultured with no inhibitor present at each timepoint. The viability of cells, cultured with no inhibitor present, was 29 ± 4% on day 6, 22 ± 5% on day 7 and 13 ± 4% on day 12 (n=6). Figure 5.1 clearly shows that the presence of the inhibitor did not cause a significant increase or decrease in cell viability at any timepoint in the culture period.

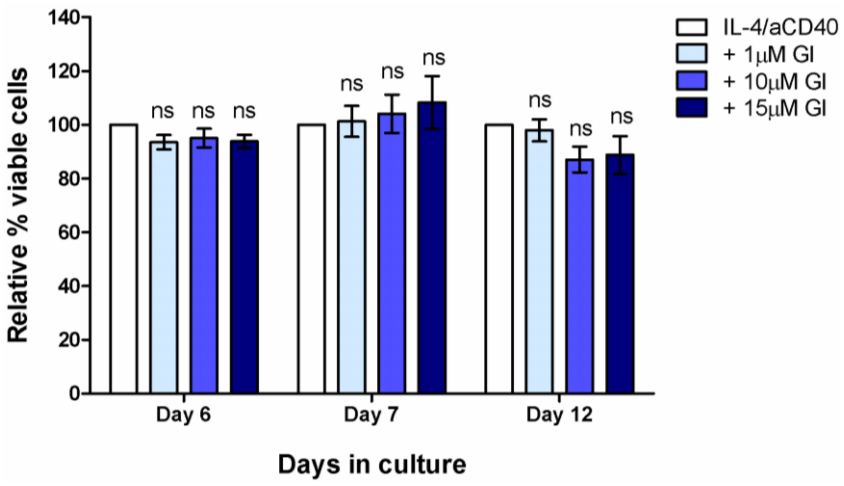

Figure 5.1. The ADAM10 inhibitor, GI254023X, does not affect cell viability.

Total B cells were cultured for up to 12 days in the presence of IL-4 (200IU/ml) and anti-CD40 (1μg/ml). GI254023X (1μM-15μM) was added on day 5 and the % of viable cells was analysed on days 6, 7 and 12 by flow cytometry, with live cell gating determined by forward versus side scatter. Cell viability is displayed as the % of viable cells, relative to cells cultured with no inhibitor at each timepoint (100%).

Error bars represent SEM and statistical analysis was performed using ANOVA with Bonferroni correction (n=6, tonsil numbers 20, 22-25 & 31).

5.3. ADAM10 inhibition with GI254023X increases mCD23 expression

To assess the ability of GI254023X to inhibit the ADAM10-mediated cleavage of mCD23, flow cytometry was utilised to quantitate the expression levels of mCD23 (as described in Section 2.5.1). Human tonsil B cells were cultured for up to 12 days with IL-4 and anti-CD40 with addition of GI254023X (0.25μM-15μM) on day 5. Cell samples were taken on days 6, 7 and 12, stained for mCD23 expression and analysed by flow cytometry. Figure 5.2A shows an example of mCD23 expression levels on the surface of cells cultured with no GI254023X present or with the addition of GI254023X (15μM). In this example, the addition of GI254023X led to an increase in the percentage and MFI of $mCD23^{+}$ cells, most evident at the latest timepoint of day 12.

Figure 5.2B and Figure 5.2C show pooled mCD23 expression data from multiple donors on day 12 with addition of a concentration range of GI254023X on day 5. This data is expressed relative to mCD23 expression on cells cultured with no GI254023X present. Figure 5.2B shows a small increase in the percentage of $mCD23^+$ cells with increasing concentrations of GI254023X but this did not reach statistical significance. However, Figure 5.2C shows a significant dose-dependent accumulation ($p<0.0001$) of mCD23 on the surface of $CD23^+$ cells as measured by the MFI. With the addition of the highest concentration of GI254023X (15μM), the MFI of $mCD23^+$ cells increased by an average of 53 ± 13% ($p=0.0009$, $n=6$).

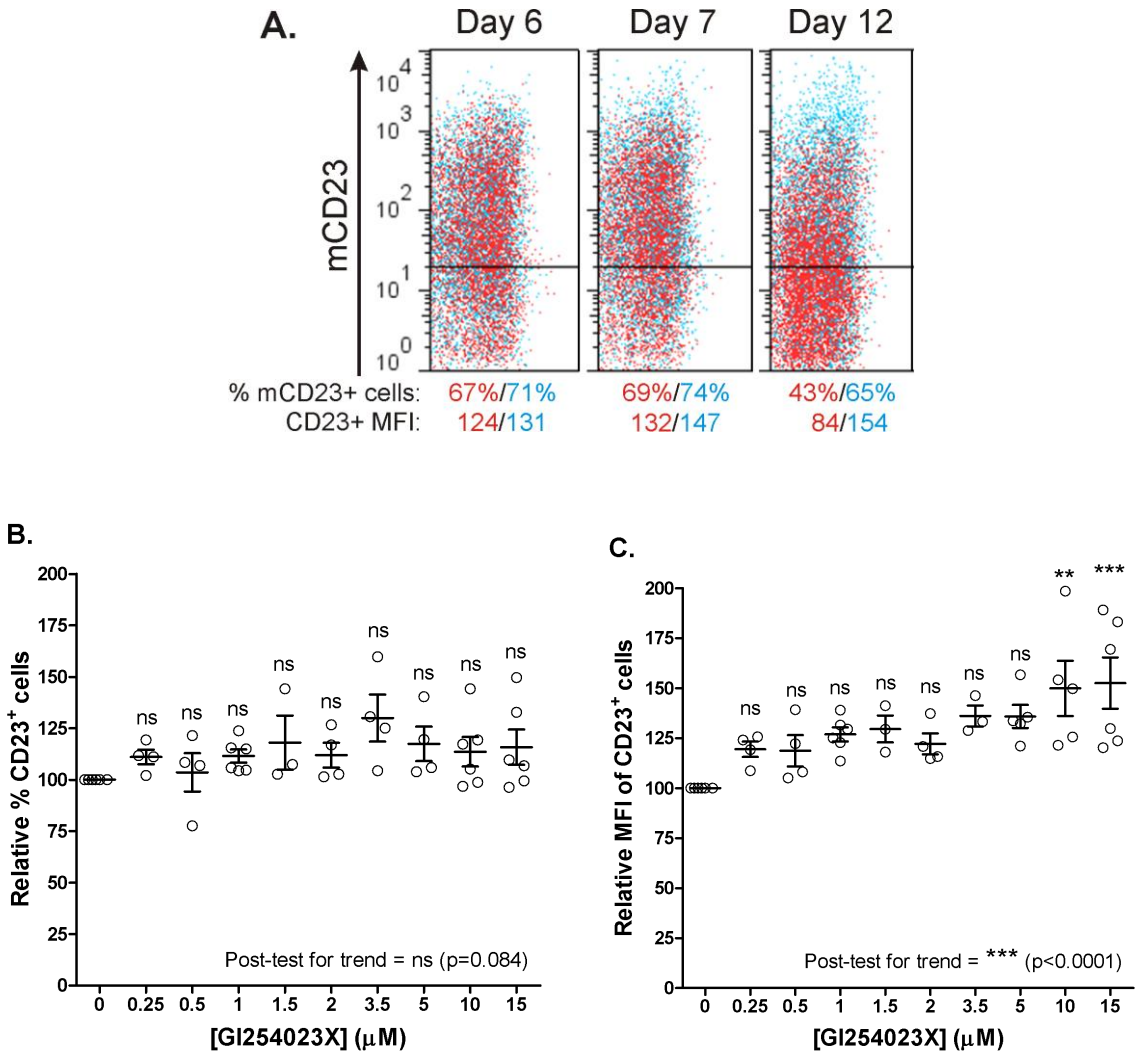

Figure 5.2. GI254023X increases the level of mCD23 expression on mCD23$^+$ cells.

Total B cells were cultured for 12 days in the presence of IL-4 (200IU/ml) and anti-CD40 (1µg/ml). GI254023X (0.25µM-15µM) was added on day 5 and the expression of mCD23 was analysed by flow cytometry on days 6, 7 and 12. **(A)** Overlay of mCD23 expression on cells cultured with GI254023X (15µM) (blue) or with no inhibitor (red). % of mCD23$^+$ cells and mCD23$^+$ MFI are indicated below each dot plot. Data shown from 1 (tonsil number 22) of 6 donors. Pooled multiple donor data for cells cultured with GI254023X (0.25µM-15µM), relative to cells cultured with no inhibitor (100%), is shown for **(B)** % of mCD23$^+$ cells and **(C)** CD23$^+$ MFI. Error bars represent SEM and statistical analysis was performed using ANOVA with Bonferroni correction (n=6, tonsil numbers 20, 22-25 & 31). ** p<0.01, *** p<0.001

5.4. ADAM10 inhibition with GI254023X reduces sCD23 production in a time-dependent manner

Since Figure 5.2 showed the accumulation of mCD23 through the use of an ADAM10 inhibitor it was expected that this would also be accompanied by a reduction in the levels of sCD23 in the supernatant. In the same experiments as described in the previous section, supernatant samples were taken on day 12 for analysis of sCD23 content by ELISA (as described in Section 2.6.3). Figure 5.3 shows a dose-dependent inhibition of sCD23 production when GI254023X was added on day 5. The addition of 10μM GI254023X resulted in a 28.3 ± 9.9% reduction in sCD23 production ($p=0.048$, $n=6$). Due to a larger error bar for the 15μM GI254023X data point, the observed reduction in sCD23 production (26.4 ± 11.3%) did not reach statistical significance ($p=0.06$, $n=6$) (Figure 5.3).

To assess the mechanism of action of GI254023X in more detail, a comparison was made between the levels of sCD23 inhibition when the inhibitor was added on days 5, 8 or 10. The level of sCD23 inhibition was analysed on day 12 and is shown in Figure 5.3. When the inhibitor was added progressively later in the incubation period the level of sCD23 inhibition decreased accordingly, resulting in higher levels of sCD23 detected in the supernatant. This was due to the shorter time period in which GI254023X was able to inhibit mCD23 shedding. Despite this, even the addition of GI254023X (15μM) as late as day 10 was still able to cause a small reduction in sCD23 production (10%, $n=1$) when analysed 2 days later on day 12. Taking the mean values, there was a significant dose-dependent trend in the reduction of sCD23 with increasing concentrations of ADAM10 inhibitor ($p=0.012$).

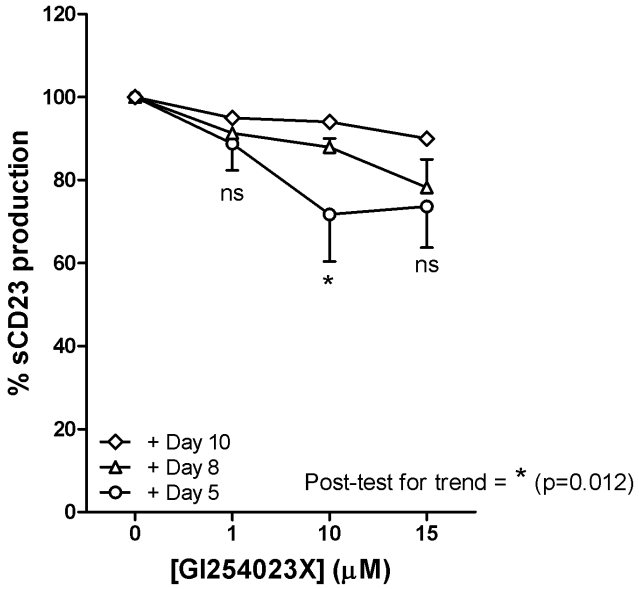

Figure 5.3. GI254023X decreases sCD23 production and the level of inhibition is dependent on the day of addition.

Total B cells were cultured for 12 days in the presence of IL-4 (200IU/ml) and anti-CD40 (1μg/ml). GI254023X (1μM-15μM) was added on either day 5 (○), 8 (Δ) or 10 (◊) and the production of sCD23 was analysed by ELISA on day 12, relative to cells cultured with no inhibitor (100%).

Error bars represent SEM and are shown downwards for day 5 data and upwards for day 8 data (no error bars for day 12 data). Statistical analysis was performed using ANOVA with Bonferroni correction (n=6, tonsil numbers 20, 22-25 & 31). * $p<0.05$

5.5. ADAM10 inhibition with GI254023X reduces IgE secretion in a time-dependent manner

In the same experiments as described in the previous section, supernatant samples were taken on day 12 for analysis of sIgE content by ELISA (as described in Section 2.6.1). Figure 5.4 shows a dose-dependent inhibition of IgE secretion when the inhibitor was added on day 5. The addition of both 10μM and 15μM GI254023X resulted in a significant decrease in sIgE levels. The maximum inhibition of IgE secretion (64.9 ± 7.2%) was observed in cells cultured with 10μM GI254023X ($p=0.007$, n=6).

To assess the mechanism of action of GI254023X in more detail, as discussed in the previous section for sCD23 inhibition, a comparison was made between the levels of sIgE inhibition when the inhibitor was added on days 5, 8 or 10. The level of sIgE inhibition was analysed on day 12 and is shown in Figure 5.4. When the inhibitor was added progressively later in the incubation period the level of sIgE inhibition decreased accordingly, resulting in higher levels of sIgE detected in the supernatant. Despite this, even the addition of GI254023X (15μM) as late as day 10 was still able to cause a large reduction (44%, n=1) in sCD23 production when analysed 2 days later on day 12. This complements the pattern of sCD23 inhibition when GI254023X was added progressively later in the incubation period (Figure 5.3). Taking the mean values, there was a significant dose-dependent trend in the reduction of sIgE with increasing concentrations of ADAM10 inhibitor ($p=0.0002$).

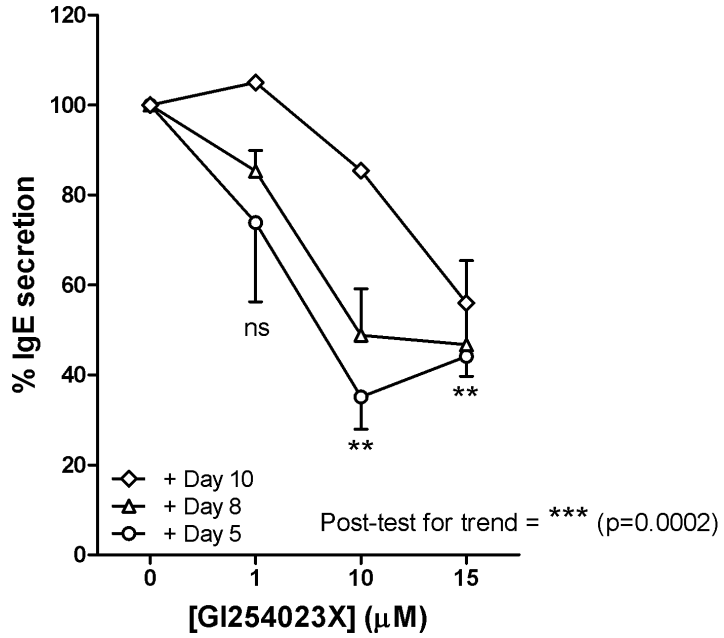

Figure 5.4. GI254023X decreases IgE secretion and the level of inhibition is dependent on the day of addition.

Total B cells were cultured for 12 days in the presence of IL-4 (200IU/ml) and anti-CD40 (1μg/ml). GI254023X (1μM-15μM) was added on either day 5 (○), 8 (Δ) or 10 (◊) and the secretion of IgE was analysed by ELISA on day 12, relative to cells cultured with no inhibitor (100%).

Error bars represent SEM and are shown downwards for day 5 data and upwards for day 8 data (no error bars for day 12 data). Statistical analysis was performed using ANOVA with Bonferroni correction (n=6, tonsil numbers 20, 22-25 & 31). ** $p<0.01$

5.5.1. ADAM10 inhibition with GI254023X has no effect on IgG secretion

To assess whether the reduction in IgE secretion was isotype-specific, the effect of GI254023X addition on IgG secretion was analysed. In the same supernatant samples used for the analysis of sCD23 and sIgE content, day 12 sIgG levels were quantified by ELISA (as described in Section 2.6.2). Figure 5.5 shows that the addition of 1μM, 10μM or 15μM GI254023X on day 5 did not significantly reduce the levels of sIgG by day 12 (n=6).

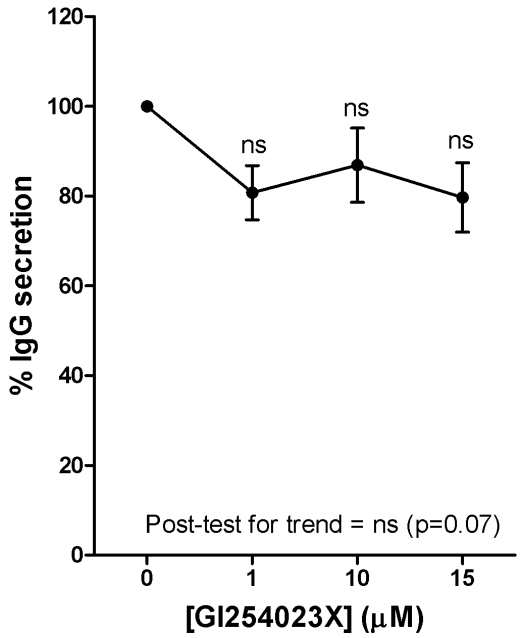

Figure 5.5. GI254023X has no significant effect on IgG secretion.

Total B cells were cultured for 12 days in the presence of IL-4 (200IU/ml) and anti-CD40 (1µg/ml). GI254023X (1µM-15µM) was added on day 5 and the secretion of IgG was analysed by ELISA on day 12, relative to cells cultured with no inhibitor (100%).

Error bars represent SEM and statistical analysis was performed using ANOVA with Bonferroni correction (n=6, tonsil numbers 20, 22-25 & 31).

5.5.2. ADAM10 inhibition with GI254023X has no significant effect on IgE or IgG expression levels

Having now shown that reducing sCD23 production in human B cells, through the addition of an ADAM10 inhibitor, can consequently reduce IgE secretion, it was necessary to check whether this reduction was specific to the secreted form of IgE. To investigate this, cells were cultured in the presence of GI254023X (added on day 5) and the membrane and intracellular expression of IgE and IgG was analysed by flow cytometry on day 12 (as described in Section 2.5.1).

Figure 5.6A and Figure 5.6B show very similar expression patterns for IgE and IgG, on days 7 and 12, between cells cultured only with IL-4 and anti-CD40 or with the addition of GI254023X (15µM) on day 5. Figure 5.6C shows there appeared to be a

slight reduction in the MFI of IgE^+ cells on day 12, although this was not statistically significant (p=0.12 for 15µM GI254023X, n=6). Figure 5.6D shows there was no reduction in the expression levels of IgG with the addition of GI254023X (n=6).

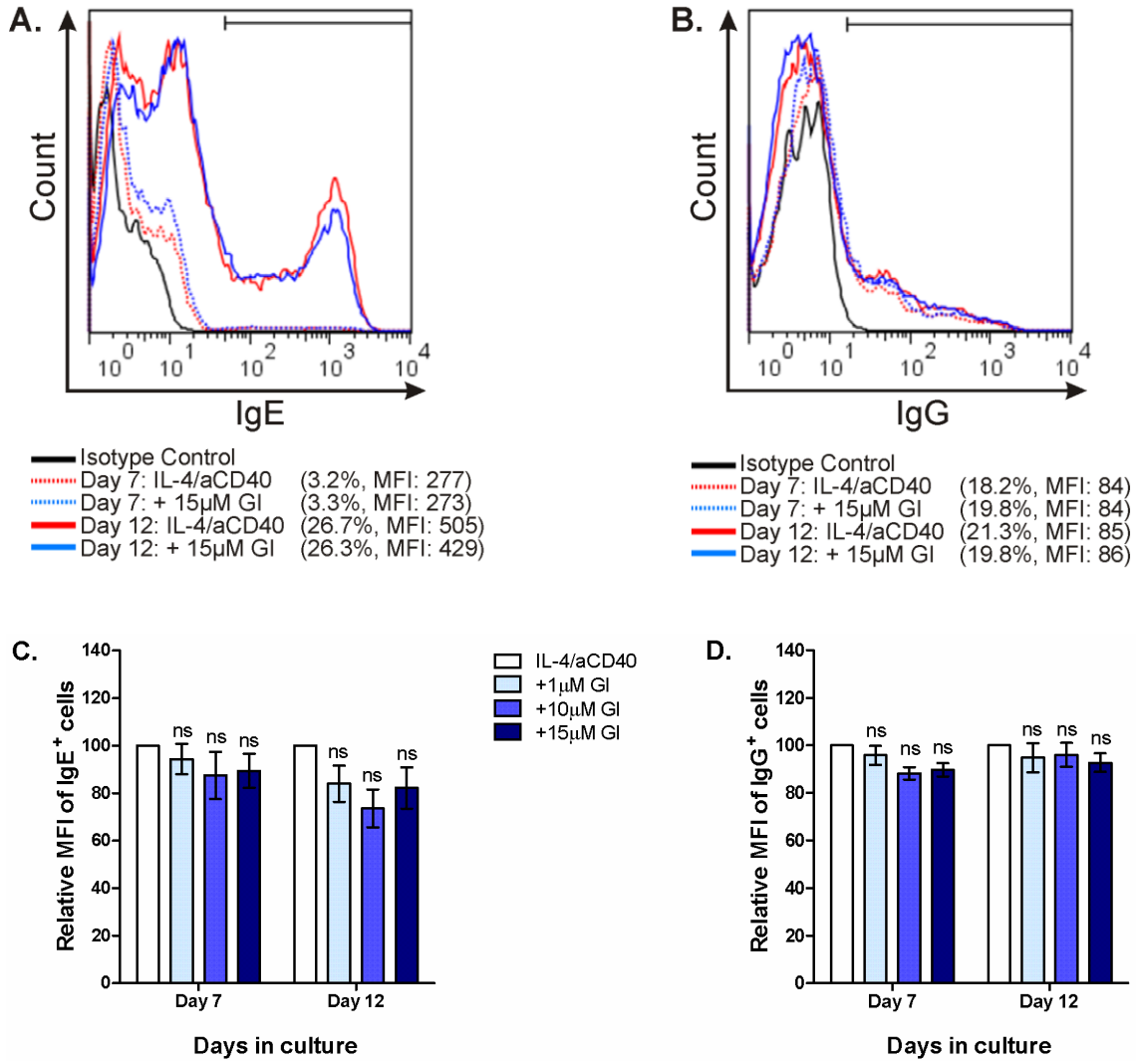

Figure 5.6. GI254023X has no significant effect on IgE or IgG expression levels.

Total B cells were cultured for 12 days in the presence of IL-4 (200IU/ml) and anti-CD40 (1µg/ml) and GI254023X (1µM, 10µM or 15µM) was added on day 5. The expression of membrane and intracellular IgE and IgG was analysed on days 7 and 12 by flow cytometry. An example of **(A)** IgE and **(B)** IgG expression levels on day 7 (dotted line) and day 12 (solid line) for cells cultured with either IL-4/aCD40 only (red) or with the addition of GI254023X (15µM) (blue). The % of IgE^+ cells and MFI are indicated on the legend. Data shown from 1 (tonsil number 25) of 6 donors. Pooled data from multiple donors is shown for the MFI of **(C)** live IgE^+ cells and **(D)** live IgG^+ cells, relative to cells cultured with no inhibitor at each timepoint (100%). Error bars represent SEM and statistical analysis was performed using ANOVA with Bonferroni correction (n=6, tonsil numbers 20, 22-25 & 31).

5.6. Summary

Previously, Chapter 4 concluded that a reduction in sCD23 alone was sufficient to reduce IgE secretion from human B cells. In this present chapter, an alternative approach was taken to see if the same outcome could be achieved. Whilst the experiments in Chapter 4 decreased sCD23 through a reduction in mCD23 (via siRNA), this present chapter described experiments which decreased sCD23 through maintaining mCD23 on the cell surface through inhibition of ADAM10 with a specific small molecule inhibitor (GI254023X). It has previously been shown that inhibition of ADAM10 *in vivo* (Gibb, El Shikh *et al.,* 2010; Sturgill, Mathews *et al.,* 2011) and the addition of GI254023X to human tonsil B cells (Weskamp, Ford *et al.,* 2006) results in decreased sCD23 production. However, subsequent effects on IgE were not analysed in these studies.

The results in this chapter showed how the addition of GI254023X to primary human B cells led to a significant dose-dependent increase in the MFI of $mCD23^{+}$ cells indicating the inhibitor was preventing the ADAM10-mediated cleavage of mCD23 (Figure 5.2). In support of this, addition of the inhibitor was shown to reduce sCD23 levels in the supernatant, the extent of which decreased when the inhibitor was added progressively later in the incubation period (Figure 5.3). This pattern of sCD23 reduction was paralleled in the level of sIgE reduction with a maximum inhibition of 65% (by day 12) following addition of GI254023X (10μM) on day 5 of the culture period (Figure 5.4). Adding GI254023X progressively later in the culture period and yet still observing a reduction in IgE secretion demonstrated that the inhibitor was regulating the secretion of IgE by a post-switch mechanism. There was no timepoint at which there appeared to be a committed pathway that could no longer be inhibited by

addition of GI243023X. The GI254023X-mediated inhibition of IgE was shown to be isotype-specific and to only affect the secreted form of IgE (Figure 5.5 and Figure 5.6).

In summary, prevention of mCD23 shedding through addition of an ADAM10-specific inhibitor led to a concentration-dependent decrease in sCD23 and sIgE. Since mCD23 was not cleaved but was actually elevated in these experiments, the observed inhibition of IgE synthesis firmly points to sCD23-mediated positive regulation. As in previous work with alternative matrix metalloprotease inhibitors and IL-4-stimulated human peripheral blood lymphocytes (Mayer, Bolognese *et al.,* 2000), we conclude that sCD23 is required to maintain IgE synthesis in human B cells (Cooper, Hobson *et al.,* 2012). A recent pre-clinical trial in mice showed intranasal administration of selective ADAM10 inhibitors led to reduced eosinophilia in the bronchoalveolar lavage fluid and reduced AHR (Mathews, Ford *et al.,* 2011). The work in this chapter provides further evidence to support ADAM10 and sCD23 as potential therapeutic targets in the treatment of asthma and allergic disease.

5.6.1. Further experiments

It would be worthwhile confirming the results shown in this chapter by transfecting human B cells with siRNA targeted against ADAM10. If the same results were achieved as with GI254023X then this would confirm the specificity of GI254023X for ADAM10 and provide further evidence for the role of sCD23 in the up-regulation of IgE synthesis from human B cells.

Chapter 6. Addition of recombinant CD23 and the role of mCD21

6.1. Introduction

McCloskey *et al* previously showed that addition of oligomeric sCD23 (lzCD23), above a certain threshold concentration, up-regulates IgE production from human tonsillar B cells. In contrast, monomeric derCD23 was shown to down-regulate IgE production (McCloskey, Hunt *et al.,* 2007). The IgE-potentiating ability of the more stable triCD23 (produced as described in Section 2.4.2) will be explored in this chapter. Although not a naturally occurring fragment, triCD23 has been specifically designed to mimic the trimeric state of endogenous sCD23 when it is first cleaved off the membrane in allergic tissues (Figure 1.3).

6.2. Assay Optimisation

First it was necessary to conduct preliminary tests to ensure the recombinant triCD23 protein contained no endotoxin and did not interfere with the detection of sIgE by ELISA.

6.2.1. triCD23 does not contain endotoxin

To address the first concern, the PyroGene™ Recombinant Factor C Assay for endotoxin detection was utilised (as described in Section 2.9). Figure 6.1 shows the endotoxin concentrations calculated in samples of a positive control, IL-4 and triCD23. IL-4 and triCD23 did not contain any endotoxin.

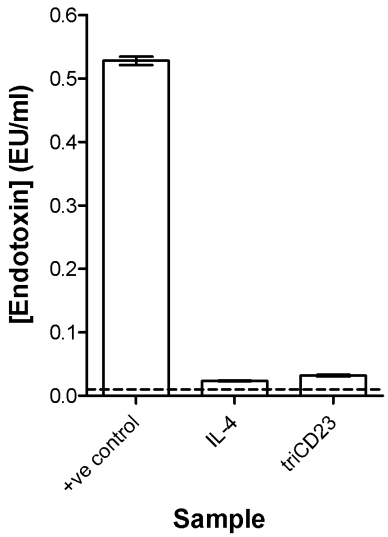

Figure 6.1. triCD23 does not contain any endotoxin.

The Pyrogene™ Recombinant Factor C (rFC) Endpoint Fluorescent Assay was used according to the manufacturer's instructions. 100µl of the positive control, IL-4 and triCD23 were added in triplicate to the 96-well plate and incubated at 37ºC for 10 minutes. rFC enzyme solution, assay buffer and fluorogenic substrate were mixed at a ratio of 1:4:5 and 100µl was added per well. The fluorescence at time zero and 1 hour was analysed at 380nm and endotoxin concentration (EU/ml) was calculated from the standard curve.

Error bars represent SEM of individual triplicates (n=1).

6.2.2. triCD23 does not interfere with the detection of sIgE by ELISA

To address the second concern, human serum IgE was diluted to 100ng/ml in Cell Culture Media and triCD23 was titrated in doubling dilutions from 1185nM (100,000ng/ml) into the diluted IgE. 100ng/ml of IgE alone was included as a control. After 10 days incubation at 37ºC sIgE content in the supernatants was analysed by ELISA. Figure 6.2 shows that the presence of triCD23 did not interfere with the detection of IgE by ELISA.

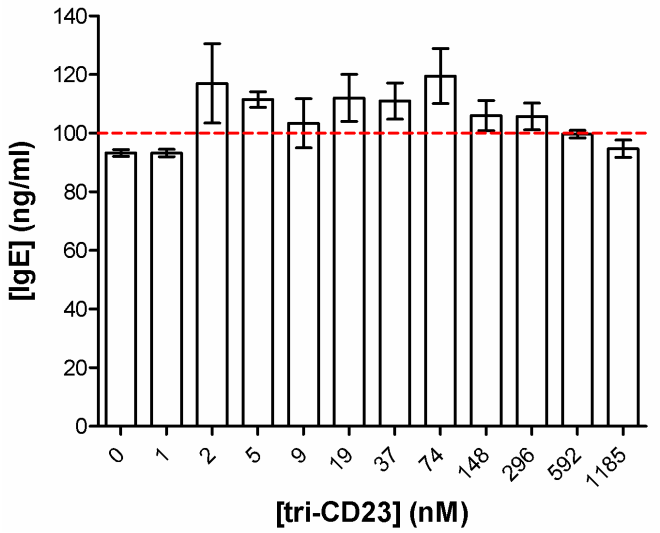

Figure 6.2. triCD23 does not interfere with the detection of sIgE by ELISA.

triCD23 was titrated in doubling dilutions from 1185nM (100,000ng/ml) and added to 100ng/ml IgE WHO standard (red line). IgE at 100ng/ml was used as a control (labelled as 0ng/ml triCD23). Levels of IgE were analysed 10 days later by ELISA.

Error bars represent SEM of individual triplicates (n=1).

6.3. Addition of recombinant CD23 proteins

6.3.1. triCD23 has no effect on cell viability

Following the completion of the preliminary tests the effects of adding recombinant CD23 proteins into the human B cell cultures were investigated. Human tonsillar B cells were isolated as described in Section 2.2 and recombinant CD23 proteins were produced and cultured with the human B cells as described in Section 2.4.2. Initially it was important to determine whether triCD23 and derCD23 would have any detrimental effects on B cell viability. To test this, cells were cultured for up to 12 days with IL-4 and anti-CD40 alone plus the addition of triCD23 (1µM) or derCD23 (3µM) on day 0. Cell viability was analysed on days 7 and 12 by flow cytometry with live cell gating determined by forward versus side scatter. Figure 6.3 shows that

although cell viability decreased over time there was no additional reduction in the viability of cells cultured with triCD23 or derCD23, compared to cells cultured with IL-4 and anti-CD40 alone (n=6).

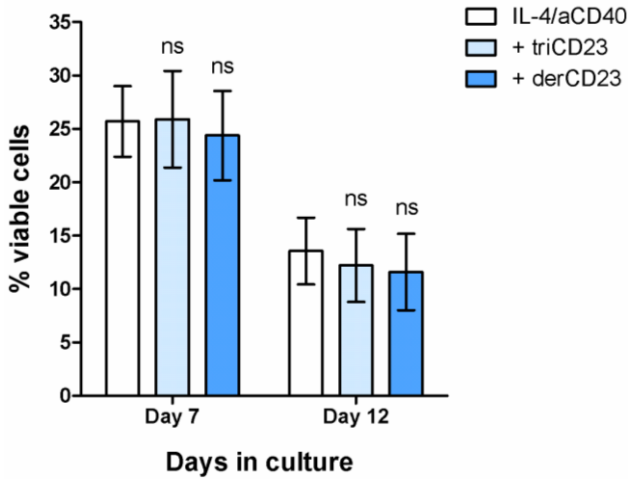

Figure 6.3. Addition of triCD23 or derCD23 does not significantly affect cell viability.

Total B cells were cultured for up to 12 days in the presence of IL-4 (200IU/ml) and anti-CD40 (1µg/ml) alone or with the addition of triCD23 (1µM) or derCD23 (3µM) on day 0. The % of viable cells was analysed on days 7 and 12 by flow cytometry with live cell gating determined by forward versus side scatter.

Error bars represent SEM and statistical analysis was performed using ANOVA with Bonferroni correction (n=6, tonsil numbers 18, 19, 25 & 30-32).

6.3.2. triCD23 up-regulates IgE secretion

Since it was now confirmed that addition of triCD23 or derCD23 into the human B cell cultures did not reduce cell viability, the effect on IgE and IgG secretion could next be investigated. In order to do this, isolated human B cells were cultured for 12 days with a concentration range of triCD23 or derCD23. Concentrations were selected to be lower than, equal to and above the calculated K_D value for trimeric CD23 binding to IgE (10^{-7}M) (Hibbert, Teriete *et al.*, 2005; McCloskey, Hunt *et al.*, 2007) and used at

a weight ratio of 1:3 (triCD23:derCD23) to maintain the same number of mIgE/mCD21 binding sites in each condition (Table 6.1).

	1 x	**10 x**	**50 x**	**85 x**	**100 x**
triCD23	11.8nM (1000ng/ml)	118nM (10,000ng/ml)	590nM (50,000ng/ml)	1.0µM (85,000ng/ml)	-
derCD23	35.4nM (572ng/ml)	354nM (5719ng/ml)	1.8µM (28,595ng/ml)	3.0µM (48,465ng/ml)	3.5µM (57,189ng/ml)

Table 6.1. Concentrations used of triCD23 and derCD23.

Concentrations were selected to be lower than, equal to and above the calculated K_D value for trimeric CD23 binding to IgE (10^{-7}M) and used at a weight ratio of 1:3 (triCD23:derCD23) to maintain the same number of mIgE/mCD21 binding sites in each condition. Concentrations highlighted in red were selected as the routine concentrations of triCD23 and derCD23 to be used in subsequent experiments.

Supernatants were analysed by ELISA for sIgE content on day 12 and the results are shown in Figure 6.4. The addition of triCD23 resulted in a concentration-dependent increase in the secretion of IgE. In contrast, addition of derCD23 resulted in a concentration-dependent decrease in the secretion of IgE. This experiment was repeated in six donors for 1µM triCD23 and 3µM derCD23 ('85 x' on Figure 6.4). At these concentrations IgE secretion increased 200.0 ± 27.2% in cells cultured with triCD23 (1µM) compared to cells cultured with IL-4 and anti-CD40 alone (p=0.008, n=6). IgE secretion from cells cultured with derCD23 (3µM) reduced by 42.2 ± 5.7% compared to IL-4 and anti-CD40 alone (p=0.04, n=6) (Figure 6.4). These results confirm findings from previous studies using recombinant trimeric CD23 proteins (Bowles, Jaeger *et al.*, 2011; McCloskey, Hunt *et al.*, 2007). However, triCD23 was around twice as effective at increasing IgE synthesis compared to the 'trimeric' CD23 proteins used in previous studies (lzCD23 or exCD23).

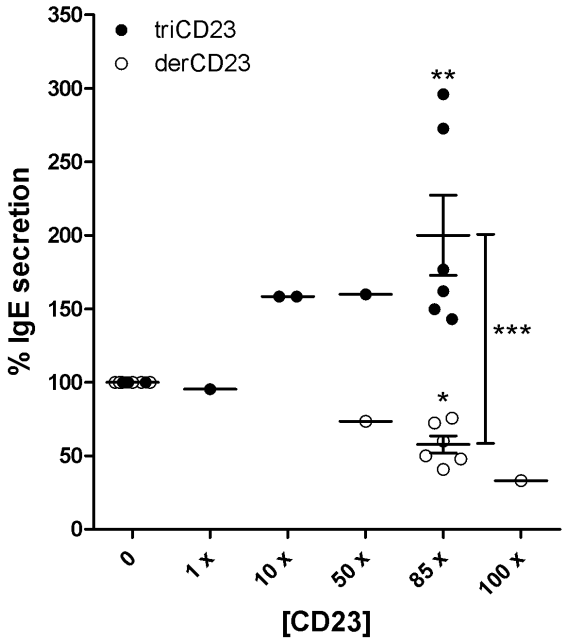

Figure 6.4. triCD23 increases and derCD23 decreases IgE secretion.

Total B cells were cultured for 12 days in the presence of IL-4 (200IU/ml) and anti-CD40 (1µg/ml) alone or with the addition of triCD23 (●) or derCD23 (○) as described in Table 6.1. IgE secretion was analysed by ELISA on day 12, relative to cells cultured with IL-4/anti-CD40 alone (100%).

Error bars represent SEM and statistical analysis was performed using ANOVA with Bonferroni correction (n=6, tonsil numbers 18, 19, 25 & 30-32). * $p<0.05$, ** $p<0.01$, *** $p<0.001$

6.3.1. triCD23 has no effect on IgG secretion

IgG secretion was analysed by ELISA to establish whether the increase in IgE secretion was isotype-specific. In the same supernatants used in Figure 6.4, Figure 6.5 shows IgG secretion levels from cells cultured for 12 days with triCD23 (1µM) or derCD23 (3µM). No significant difference was seen in the levels of IgG secretion, compared to cells cultured with IL-4 and anti-CD40 alone, with addition of triCD23 or derCD23.

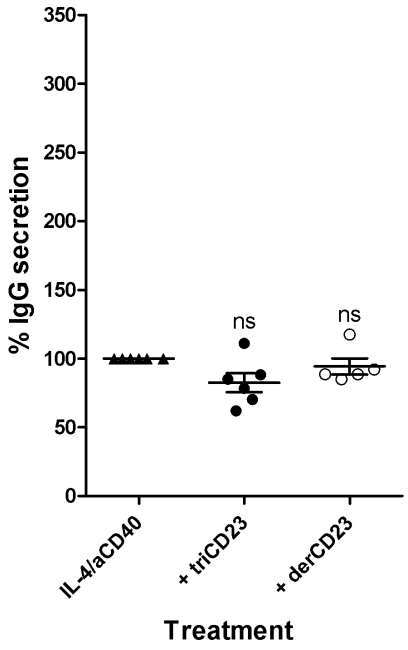

Figure 6.5. Addition of triCD23 or derCD23 has no significant effect on IgG secretion.

Total B cells were cultured for 12 days in the presence of IL-4 (200IU/ml) and anti-CD40 (1µg/ml) alone or with the addition of triCD23 (1µM) (●) or derCD23 (3µM) (○). IgG secretion was analysed by ELISA on day 12, relative to cells cultured with IL-4/anti-CD40 alone (100%).

Error bars represent SEM and statistical analysis was performed using ANOVA with Bonferroni correction (n=6, tonsil numbers 18, 19, 25 & 30-32).

6.3.2. triCD23 has no effect on IgE or IgG expression

To investigate whether the triCD23-mediated increase in IgE was specific to the secreted form of IgE, flow cytometry was utilised to quantify the expression levels of intracellular and membrane IgE (as described in Section 2.5.1). Human B cells were isolated and cultured for 12 days with IL-4 and anti-CD40 alone plus the addition of triCD23 (1µM) or derCD23 (3µM). Figure 6.6 shows the addition of neither triCD23 or derCD23 significantly altered the expression levels (as measured by MFI) of IgE or IgG. The increase in IgE secretion shown in Figure 6.4 was therefore not accompanied by an increase in the expression levels of IgE.

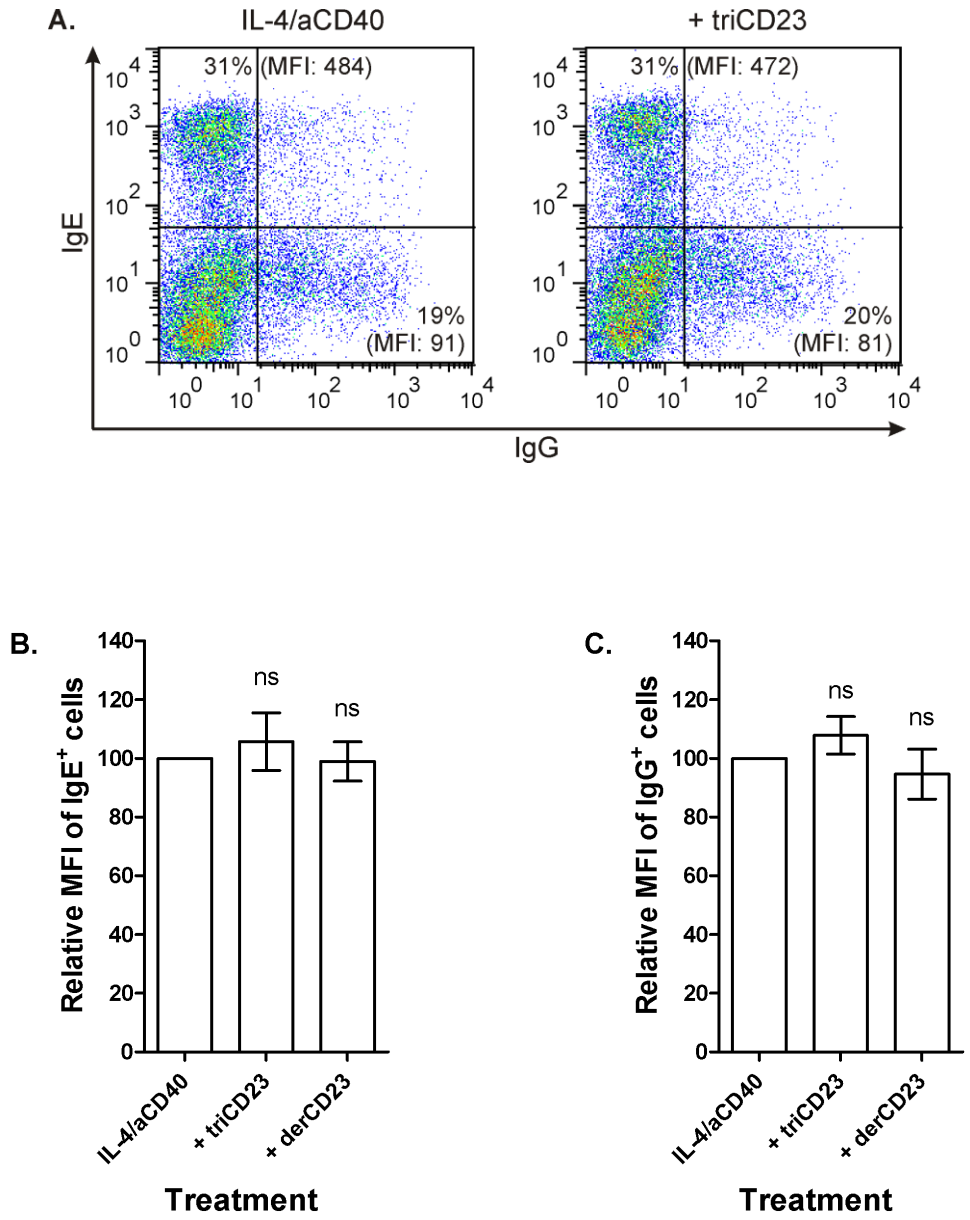

Figure 6.6. Addition of triCD23 or derCD23 has no significant effect on IgE or IgG expression levels.

Total B cells were cultured for 12 days in the presence of IL-4 (200IU/ml) and anti-CD40 (1µg/ml) alone or with the addition of triCD23 (1µM) or derCD23 (3µM). The expression of membrane and intracellular IgE and IgG was analysed on day 12 by flow cytometry. **(A)** An example of IgE expression levels on day 12 for cells transfected with IL-4/anti-CD40 alone or with the addition of triCD23. The % of IgE^+ and IgG^+ cells and MFI are indicated on the plots. Data shown from 1 (tonsil number 25) of 6 donors. Pooled data from multiple donors is shown for **(B)** the MFI of live IgE^+ cells **(B)** the MFI of live IgG^+ cells, relative to cells cultured with IL-4/anti-CD40 alone (100%). Error bars represent SEM and statistical analysis was performed using ANOVA with Bonferroni correction (n=6, tonsil numbers 18, 19, 25 & 30-32).

6.3.1. triCD23 can rescue GI254023X-mediated inhibition of IgE secretion

In Chapter 5, the ADAM10-specific small molecule inhibitor GI254023X was shown to decrease sCD23 production and IgE secretion from human B cells. The following experiment investigates the ability of triCD23 to rescue the GI254023X-mediated reduction of sCD23 and sIgE. Cells were cultured for 12 days with IL-4 and anti-CD40 alone plus the addition of triCD23 (1µM), GI254023X (5µM) or triCD23 & GI254023X on day 0. As previously shown in Figure 6.4, the addition of triCD23 led to an up-regulation of IgE secretion (Figure 6.7). When cells were cultured with GI254023X a large reduction in IgE secretion occurred (Figure 6.7), previously shown to be due to a reduction in sCD23 production (Figure 5.3 and Figure 5.4). When cells were cultured with a combination of the ADAM10 inhibitor and triCD23, a partial relief from GI254023X-mediated IgE suppression was observed (2.3-fold increase, n=2) (Figure 6.7). This result confirms the positive regulation of IgE synthesis by sCD23.

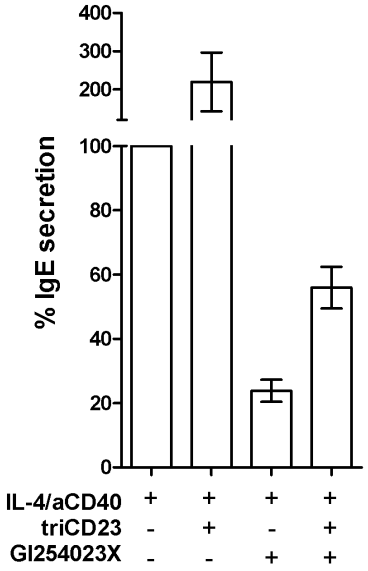

Figure 6.7. triCD23 rescues GI254023X-mediated inhibition of IgE secretion.

Total B cells were cultured for 12 days in the presence of IL-4 (200IU/ml) and anti-CD40 (1µg/ml) alone or with the addition of triCD23 (1µM), GI254023X (5µM) or triCD23 & GI254023X. IgE secretion was analysed by ELISA on day 12, relative to cells cultured with IL-4/anti-CD40 alone (100%).

Error bars represent SEM (n=2, tonsil numbers 25 & 31).

6.4. The mechanism of action of triCD23

Having identified a role for sCD23 in the positive regulation of IgE synthesis, the possible mechanisms involved were investigated further.

6.4.1. triCD23-mediated redistribution of mCD21 and mIgE

In 2005, structural studies showed the CD23-binding sites of IgE and CD21 to be in distinct locations on the lectin 'head' domain (Hibbert, Teriete *et al.,* 2005). With this in mind, confocal microscopy was utilised to assess whether triCD23 was capable of simultaneously binding to IgE and CD21, co-localising these molecules on the cell surface, to induce the up-regulation of sIgE (Gould, Beavil *et al.,* 1997).

Human tonsillar B cells were cultured with IL-4 and anti-CD40 for 8 days; the optimum timepoint for the dual expression of mIgE and mCD21 (Figure 6.8). Dead cells were removed and the remaining cells stimulated for 30 minutes with media alone, derCD23 (3µM) or triCD23 (1µM). When analysing these cells by confocal microscopy, as described in Section 2.10, only a small proportion of $mIgE^{+}mCD21^{+}$ cells could be detected on each slide. For the images shown in the following sections, only these double positive cells were imaged to analyse the ability of triCD23 to co-ligate both mIgE and mCD21.

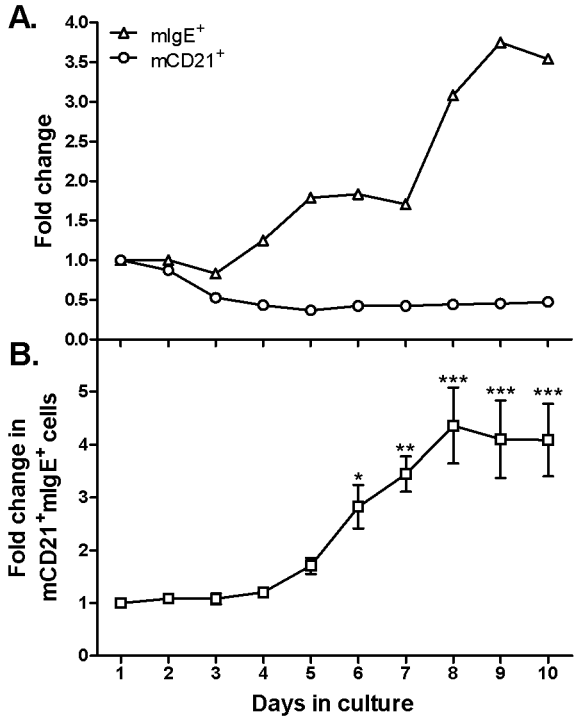

Figure 6.8. Differentiation of human B cells into mCD21$^+$mIgE$^+$ cells.

Human tonsillar B cells were cultured for up to 10 days with IL-4 (200IU/ml) and anti-CD40 (1µg/ml). mCD21 and mIgE expression were analysed by flow cytometry and the fold change plotted for the % of **(A)** mCD21$^+$ (○) or mIgE$^+$ (Δ) cells (data shown from 1 of 5 donors) and **(B)** mCD21$^+$mIgE$^+$ cells (□), relative to Day 1. Error bars represent SEM and statistical analysis was performed using ANOVA with Bonferroni correction (n=5). * $p<0.05$, ** $p<0.01$, *** $p<0.001$

Experimental work conducted by Dr M Jutton.

Figure 6.9A and Figure 6.9B show the even and uniform distribution of both mCD21 and mIgE on the surface of B cells incubated with either media alone or monomeric derCD23, respectively. The merged images in the bottom panels of Figure 6.9A and Figure 6.9B show no yellow regions of mCD21 and mIgE co-localisation. Figure 6.9C shows the redistribution and co-localisation of mCD21 and mIgE following incubation with triCD23. Several distinct microclusters formed and particularly strong capping of mCD21 and mIgE is indicated on the merged image in the bottom panel of Figure 6.9C.

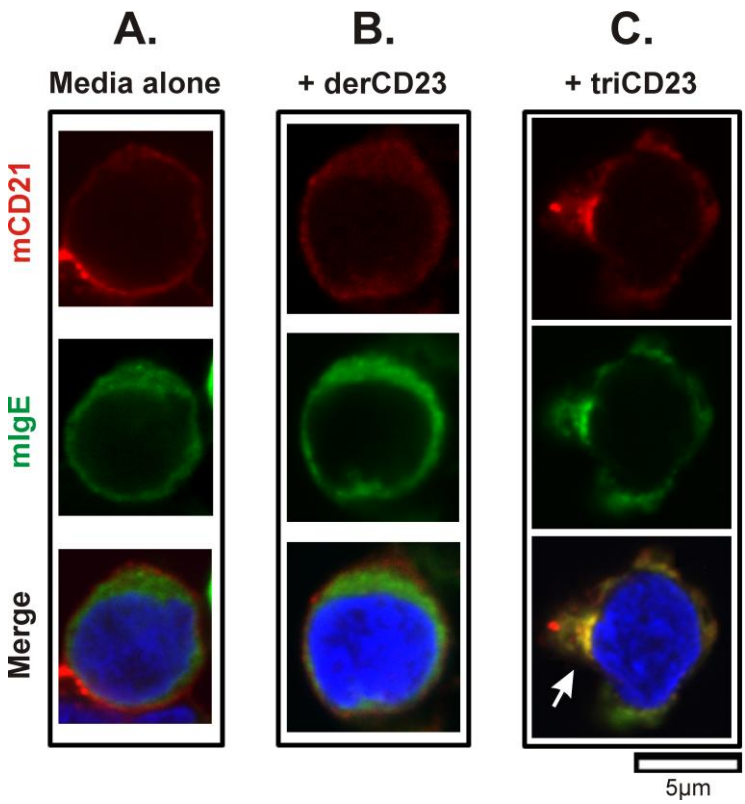

Figure 6.9. triCD23 co-localises mCD21 and mIgE on the surface of human B cells.

Human tonsillar B cells were cultured for 8 days with IL-4 (200IU/ml) and anti-CD40 (1µg/ml) and stimulated for 30 minutes with media alone, derCD23 (3µM/48µg/ml) or triCD23 (1µM/84µg/ml). Following fixation, cells were stained for mCD21 (red), mIgE (green) and the nucleus (blue) and visualised by confocal microscopy. Images show a single field of view with the third row showing a three-colour overlay. The white arrow indicates strong capping of mIgE with mCD21.

Data shown from 1 donor (tonsil number 18), representative of 3 (tonsil numbers 18, 25 & 32).

6.5. The role of mCD21 in sCD23-mediated regulation of IgE

The role of mCD21 as a binding partner to sCD23 in the up-regulation of IgE synthesis was further investigated through the use of an anti-CD21 mAb which binds to SCRs 3-4 on CD21. Antibodies against human CD21 have been shown to up-regulate or down-regulate IgE synthesis, in anti-CD40-stimulated tonsil B cells, in an epitope-dependent manner (Aubry, Pochon *et al.*, 1992; Henchoz, Gauchat *et al.*, 1994).

6.5.1. Anti-CD21 mAb reduces IgE secretion

Human B cells were cultured with IL-4 and anti-CD40 plus the addition of increasing concentrations of an anti-CD21 mAb (HB-5 clone) (as described in Section 2.4.3). Figure 6.10 shows the addition of the anti-CD21 mAb resulted in a dose-dependent decrease in IgE secretion. When cells were cultured with a combination of anti-CD21 mAb (10µg/ml) and triCD23 (1µM), the IgE-enhancing effects of triCD23 were blocked.

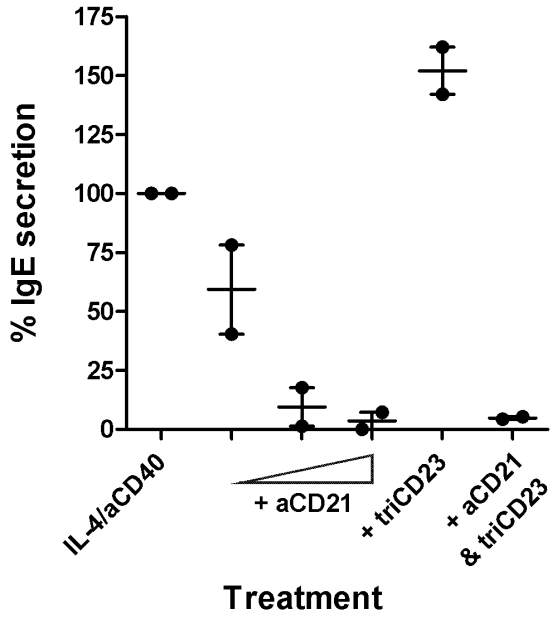

Figure 6.10. Anti-CD21 mAb reduces IgE secretion and blocks the IgE-enhancing effects of triCD23.

Human tonsillar B cells were cultured for 12 days with IL-4 (200IU/ml) and anti-CD40 (1µg/ml) alone, + anti-CD21 mAb (0.1, 1 or 10µg/ml), + triCD23 (1µM) or + aCD21 mAb (10µg/ml) & triCD23. IgE secretion was analysed by ELISA on day 12, relative to cells cultured with IL-4/anti-CD40 alone (100%).

Error bars represent SEM (n=2, tonsil numbers 31 & 32).

6.5.2. Anti-CD21 mAb reduces sCD23 production

Figure 5.2 and Figure 5.4, in Chapter 5, showed the addition of an ADAM10 inhibitor increased mCD23 expression levels through prevention of mCD23 cleavage, subsequently reducing sCD23 production and IgE secretion. Since addition of the anti-CD21 mAb reduced IgE secretion, the effect on sCD23 production and mCD23 expression were subsequently analysed.

Figure 6.11A shows sCD23 ELISA analysis on the same supernatants used in Figure 6.10. Addition of the anti-CD21 mAb reduced sCD23 production in a concentration-dependent manner. Figure 6.11B shows flow cytometric analysis of mCD23 and mCD21 expression on B cells following 12 days in culture with IL-4 and anti-CD40 alone plus the addition of increasing concentrations of anti-CD21 mAb. $mCD21^+$ cells (~10%) could be detected following stimulation with IL-4 and anti-CD40 alone (left panel, Figure 6.11B). In cells cultured with the anti-CD21 mAb present, no mCD21 expression could be detected as the fluorescent anti-CD21 detection antibody could no longer bind to mCD21. This proves that the anti-CD21 mAb was definitely binding to mCD21.

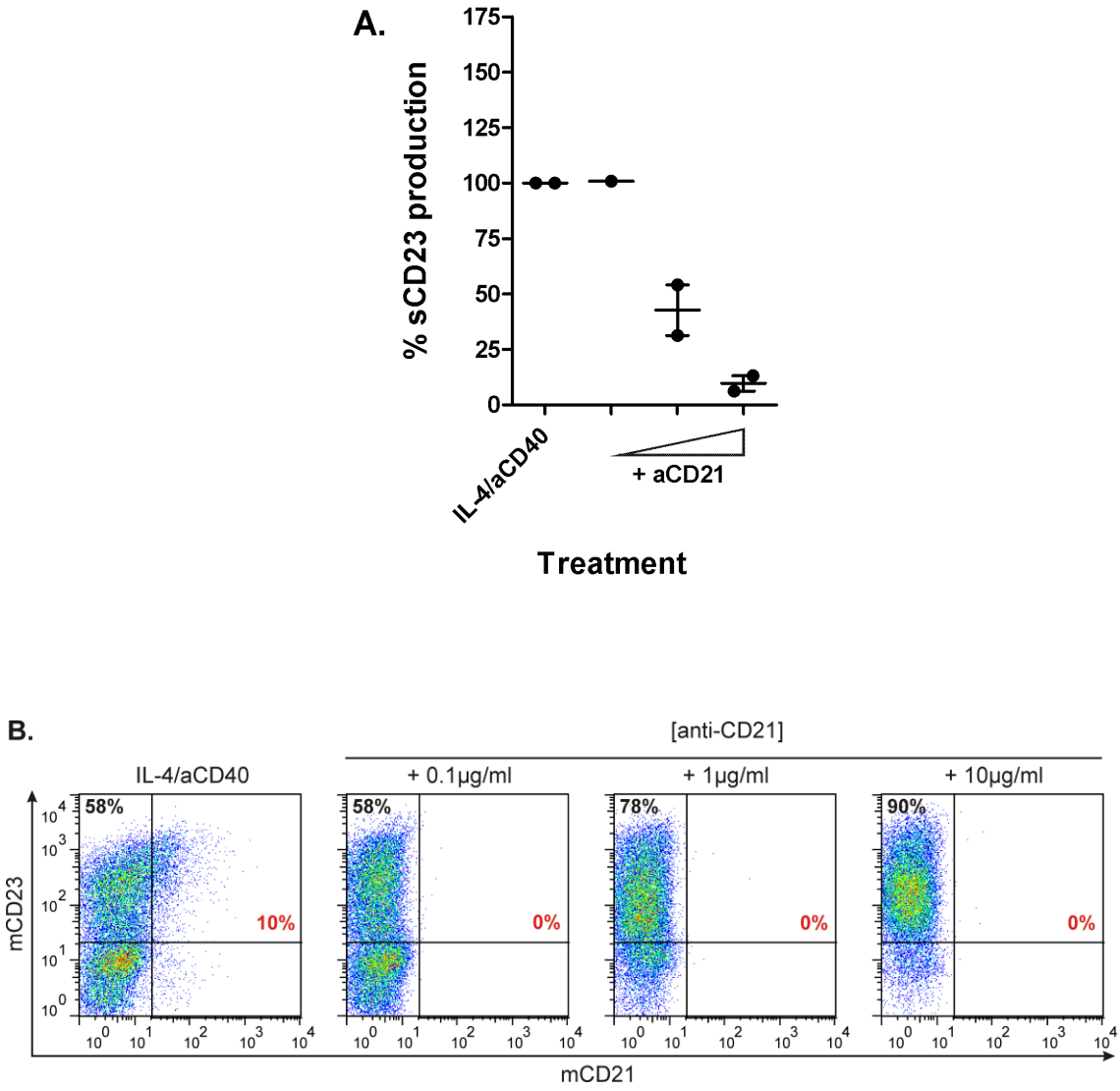

Figure 6.11. Anti-CD21 mAb reduces sCD23 production.

Total B cells were cultured for 12 days with IL-4 (200IU/ml) and anti-CD40 (1µg/ml) alone or with the addition of anti-CD21 mAb (0.1, 1 or 10µg/ml). **(A)** sCD23 production was analysed by ELISA on day 12, relative to cells cultured with IL-4/anti-CD40 alone (100%). Error bars represent SEM (n=2, tonsil numbers 31 & 32). **(B)** The expression of mCD23 and mCD21 was analysed on day 12 by flow cytometry. The % of $mCD23^+$ cells (black) and $mCD21^+$ cells (red) are indicated on each dot plot. Data shown from 1 (tonsil number 31) of 2 donors.

6.5.3. Anti-CD21 mAb reduces the triCD23-mediated clustering of mCD21

Given that the anti-CD21 mAb had been shown to bind to mCD21 and prevent the triCD23-mediated up-regulation of IgE synthesis, confocal microscopy was utilised to visualise this process (as described in Section 2.10). Human B cells were cultured for 8 days and stimulated for 30 minutes with either media alone, derCD23 (3μM), triCD23 (1μM), anti-CD21 mAb (10μg/ml) or a 15 minute pre-treatment with anti-CD21 mAb, followed by triCD23. Figure 6.12A and Figure 6.12B show the uniform distribution of mCD21 on the surface of B cells stimulated with media alone or derCD23, respectively. As previously shown in Figure 6.9, with cells from a different donor, stimulation with triCD23 resulted in the formation of distinct microclusters of mCD21 (Figure 6.12C). A similar pattern of mCD21 expression was observed when cells were stimulated with the anti-CD21 mAb (Figure 6.12D). This was presumably due to the ability of the anti-CD21 mAb to bind two molecules of mCD21 and, therefore, induce clustering. Figure 6.12E shows an example of mCD21 expression on a cell which was pre-treated with the anti-CD21 mAb before stimulation with triCD23. The distinct triCD23-mediated redistribution of mCD21 shown in Figure 6.12C is far less pronounced due to the pre-treatment with the anti-CD21 mAb (Figure 6.12E).

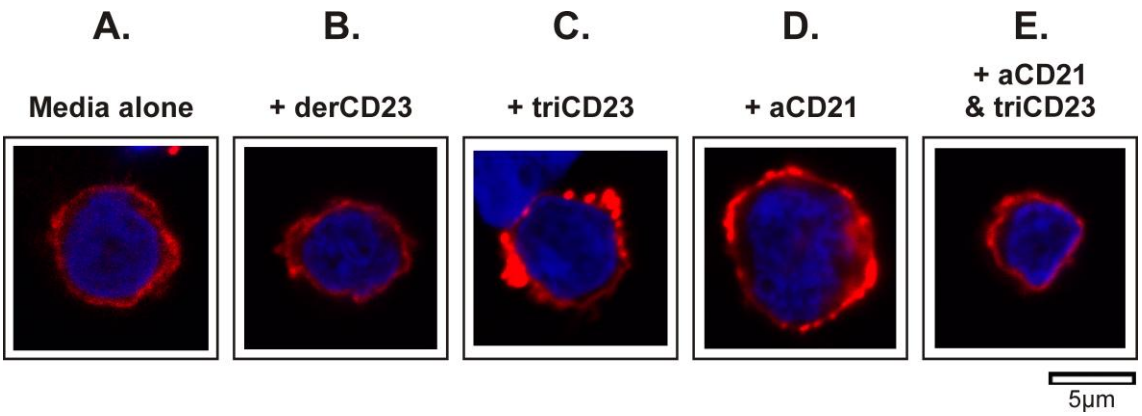

Figure 6.12. Pre-treatment with anti-CD21 mAb reduces triCD23-mediated clustering of mCD21.

Human tonsillar B cells were cultured for 8 days with IL-4 (200IU/ml) and anti-CD40 (1µg/ml) and stimulated for 30 minutes with **(A)** media alone, **(B)** derCD23 (3µM/48µg/ml), **(C)** triCD23 (1µM/84µg/ml), **(D)** anti-CD21 mAb (10µg/ml) or **(E)** anti-CD21 mAb & triCD23. Following fixation, cells were stained for mCD21 (red) and the nucleus (blue) and visualised by confocal microscopy. Images show a single field of view with a two-colour overlay.

n=1 (tonsil number 32).

6.6. Summary

The experiments in this present chapter set out to confirm the findings from previous studies (Bowles, Jaeger *et al.*, 2011; Mayer, Bolognese *et al.*, 2000; McCloskey, Hunt *et al.*, 2007) that the addition of recombinant trimeric sCD23 to primary human B cells can enhance IgE synthesis. For the purpose of these experiments, triCD23 was specifically designed to mimic the trimeric state of endogenous sCD23 when it is first cleaved off the membrane in allergic tissues.

After initial assay optimisation to confirm that the triCD23 preparation did not contain any endotoxin, interfere with sIgE detection by ELISA or reduce B cell viability (Figure 6.1 - Figure 6.3), the effects on IgE were analysed. Addition of triCD23 was shown to increase IgE secretion in a concentration-dependent manner with no effect on IgG secretion. triCD23 was shown to specifically increase the soluble form of IgE (Figure 6.6), confirming previous observations by other groups (Batista, Efremov *et al.*, 1995; Karnowski, Achatz-Straussberger *et al.*, 2006; Saxon, Kurbe-Leamer *et al.*, 1991). As a control, monomeric derCD23 was shown to reduce IgE secretion (Figure 6.4). These results indicate that only a *trimeric* complex of CD23 is capable of up-regulating IgE secretion, hypothesised to be through post-CSR dual-binding to both mIgE and mCD21 (Gould and Sutton 2008; Hibbert, Teriete *et al.*, 2005).

For the first time, experiments in this chapter showed that addition of recombinant trimeric CD23 can rescue GI254023X-mediated inhibition of sIgE, confirming the positive regulation of IgE synthesis by sCD23 (Figure 6.7). However, the level of IgE synthesis was not fully restored to that of cells cultured only with triCD23. This might be explained by off-target effects of the ADAM10 inhibitor, investigation of which would require further studies.

Confocal microscopy was utilised to visualise the expression patterns of mIgE and mCD21 in order to investigate the mechanism by which triCD23 is capable of up-regulating IgE secretion. Stimulation with triCD23 caused a redistribution of mIgE and mCD21 from a uniform pattern into distinct clusters (Figure 6.9 and Figure 6.12). The observed capping revealed that there seems to be no topological constraints to prevent a trimeric CD23 molecule from co-ligating mIgE and mCD21 and forming the predicted multi-molecular network on the cell surface (Hibbert, Teriete *et al.*, 2005). In cells where triCD23 binding to mCD21 was blocked with the addition of an anti-CD21 mAb, triCD23 was no longer able to increase IgE secretion (Figure 6.10). The cell surface clusters of mCD21, which formed following stimulation with triCD23 alone, could no longer be detected (Figure 6.12).

In summary, this chapter has provided further evidence for the positive regulation of IgE secretion by sCD23 in human B cells (Cooper, Hobson *et al.*, 2012). Unlike Chapters 4 and 5, which investigated the *inhibition* of sCD23, the results in this present chapter showed that an *increase* in sCD23 can lead to an *increase* in IgE secretion. The recombinant trimeric sCD23, triCD23, was shown to be biologically active and able to restore IgE secretion from cells in which sCD23 and sIgE had been reduced due to the addition of an ADAM10 inhibitor. Confocal microscopy provided visual evidence for the proposed mechanism by which sCD23 must bind to both mIgE and mCD21 to create ‘signalling rafts’, ultimately culminating in the up-regulation of IgE.

6.6.1. Further experiments

Throughout this chapter it was assumed, from Surface Plasmon Resonance (SPR) assays completed by other members of the laboratory, that triCD23 could bind to

mIgE. However, it would be useful to have a directly fluorescently-labelled triCD23 protein to definitively show binding to mIgE on the surface of human B cells by flow cytometry and confocal microscopy. The collection of confocal microscopy data in this chapter could be improved upon by isolating IgE^+ cells before stimulation with triCD23 and staining for mIgE and mCD21. This would vastly increase the density of $mIgE^+mCD21^+$ cells on each slide allowing for quantification of cells showing capping of mIgE and mCD21 and for statistical analysis to be performed. Visualising the binding of triCD23 to mIgE and CD21, inserted into artificial lipid bilayers, by Total Internal Reflection Fluorescence (TIRF) microscopy is currently underway in the laboratory.

The mechanism by which triCD23 is capable of increasing IgE secretion from human B cells requires further investigation. This includes measuring the effects on cell proliferation, division, apoptosis, differentiation and signalling pathways. It would also be interesting to investigate the effects of triCD23 on IgE mRNA, circle transcripts and GLTs by qPCR. Adding triCD23 progressively later in the 12 day incubation period may provide a greater understanding of when, and by what exact mechanism, triCD23 is targeting the cells to increase IgE synthesis. Work is currently underway in the laboratory to address these issues.

It would be interesting to cross-link an anti-IgE antibody and an anti-CD21 antibody to mimic the binding capabilities of trimeric sCD23. The antibody complex could be added to primary human B cells in an attempt to up-regulate the secretion of IgE.

Chapter 7. Overall Summary & General Discussion

This final chapter includes a general discussion on the importance of the results presented in this thesis and their contribution to the field of asthma and allergy research.

7.1. CD23-mediated regulation of IgE synthesis

The cytokines IL-4 and IL-13 induce the CSR to all immunoglobulin isotypes downstream from Cμ in the heavy-chain locus on human chromosome 14. Since IL-4 is known to up-regulate CD23, the expression of CD23 and IgE are inextricably linked (Delespesse, Sarfati *et al.,* 1992). The role of CD23 in the regulation of IgE in the human system appears to be much more complex than in the mouse (Gould and Sutton 2008).

This thesis has described an investigation into the role of CD23 in the regulation of *in vitro* IgE synthesis from primary human B cells. The experiments aimed to shed light on a suggested mechanism by which sCD23 positively regulates IgE synthesis exclusively in human B cells (Hibbert, Teriete *et al.,* 2005; McCloskey, Hunt *et al.,* 2007). In analysing this mechanism it is necessary to consider that there are multiple forms of sCD23, several potential ligands and various complexes with different affinities and topological constraints associated with binding to their ligands in solution and particularly on cells.

sCD23 is released from cells by the action of the endogenous metalloprotease ADAM10 (Lemieux, Blumenkron *et al.,* 2007; Weskamp, Ford *et al.,* 2006) and accumulates in the supernatant of B cells following IL-4 and anti-CD40-stimulated CSR to IgE (Christie, Barton *et al.,* 1997; Mayer, Bolognese *et al.,* 2000; Saxon, Ke *et al.,*

1990). The experiments described in this thesis used CD23 siRNA and an ADAM10-specific inhibitor (GI254023X) to confirm that expression and cleavage of mCD23 to release sCD23 is required for the enhancement of IgE synthesis in primary human B cells (Cooper, Hobson *et al.*, 2012).

Short-term inhibition of CD23 mRNA with siRNA led to a significant reduction in the frequency and MFI of $CD23^+$ cells until day 7 following transfection. By day 12, but not at the earlier timepoints of days 5 or 7, CD23 siRNA-transfected cells showed significantly reduced sCD23 production. This correlated with reduced IgE secretion implicating sCD23 in the up-regulation of human IgE synthesis (Figure 4.6, Figure 4.7 and Figure 4.10).

To further investigate the role of sCD23, ADAM10 was inhibited using a small molecule inhibitor (GI254023X). It has previously been shown that inhibition of ADAM10 *in vivo* (Gibb, El Shikh *et al.*, 2010; Sturgill, Mathews *et al.*, 2011) and the addition of GI254023X to human tonsil B cells (Weskamp, Ford *et al.*, 2006) results in decreased sCD23 production. However, subsequent effects on IgE were not analysed in these studies. The experiments in this thesis showed the addition of GI254023X resulted in increased mCD23 expression levels, reduced sCD23 production and reduced IgE secretion. Inhibition of sCD23 production and IgE secretion could still be achieved even when GI254023X was added progressively later in the incubation period, albeit to lesser extents, indicating that the ADAM10 inhibitor was regulating secretion of IgE by a post-switch mechanism (Figure 5.3 and Figure 5.4). Since mCD23 was not cleaved but was actually elevated in these conditions, the observed inhibition of IgE synthesis firmly points to positive regulation mediated through sCD23.

When sIgE binds to mCD23 it blocks metalloprotease cleavage and the release of sCD23 (Conrad, Ford *et al.,* 2007). However, this was not a complication in the present system as the sIgE concentrations in the medium ($<10^{-10}$M) were well below the K_D of the IgE-mCD23 interaction. As in previous studies with alternative matrix metalloprotease inhibitors and IL-4-stimulated human peripheral blood lymphocytes (Mayer, Bolognese *et al.,* 2000) it can be concluded that sCD23 is required to maintain IgE synthesis in human B cells.

This thesis also confirms previous findings (Bowles, Jaeger *et al.,* 2011; Mayer, Bolognese *et al.,* 2000; McCloskey, Hunt *et al.,* 2007) that addition of recombinant trimeric sCD23 to primary human B cells enhances IgE synthesis (Figure 6.4). Beyond this it has now been shown that when B cells are incubated with GI254023X in the presence of triCD23, a relief from GI254023X-mediated IgE suppression occurs (Figure 6.7). This confirms the positive regulation of IgE synthesis by sCD23 (Cooper, Hobson *et al.,* 2012).

7.2. The role of mCD21

mIgE and mCD21 are the prime candidates for mediating the stimulatory effects of sCD23. mCD21 expression was shown to decline in the first few days of incubation with IL-4 and anti-CD40 and reached a plateau on day 5 (Figure 6.8). Loss of mCD21 is probably due to the shedding of soluble fragments (Fremeaux-Bacchi, Bernard *et al.,* 1996) and further shedding may be prevented by the binding of sCD23 to mCD21 and mIgE. Although the concentrations of endogenous sCD23 (Figure 4.8) were far lower than the K_D for the 1:1 interaction with mCD21 or mIgE ($K_D = 10^{-6}$ and 10^{-8}M, respectively) (Hibbert, Teriete *et al.,* 2005; McCloskey, Hunt *et al.,* 2007), the avidity

effect of binding of three sCD23 'heads' as a trimer to multiple mCD21 and/or mIgE molecules may dramatically enhance binding affinity at the cell surface. Prior binding of sCD23 to mIgE, the stronger ligand, may enable the recruitment of mCD21 into a tri-molecular complex. The CD23 binding site for the two N-terminal domains of CD21 lies in the C-terminal 'tail' and is sufficiently distant from the IgE binding site to allow the simultaneous binding of both ligands in solution (Hibbert, Teriete *et al.,* 2005). Indeed, the observed capping of mIgE and mCD21 on B cells stimulated with triCD23 (Figure 6.9 and Figure 6.12) revealed that there are no topological constraints to prevent a trimeric CD23 molecule from co-ligating mIgE and mCD21 and forming the predicted multi-molecular network on the cell surface (Hibbert, Teriete *et al.,* 2005). In cells where triCD23 binding to mCD21 was blocked with the addition of an anti-CD21 mAb, triCD23 was no longer able to increase IgE secretion (Figure 6.10). This confirms sCD23 binding to mCD21 as an essential component in the up-regulation of IgE secretion.

Figure 4.8 revealed that there was a remarkable relationship between the concentration of sCD23 and sIgE after incubation of human B cells with IL-4 and anti-CD40 for 12 days. There appeared to only be a slight increase in sIgE at low sCD23 concentrations up to 60ng/ml (1.6μM). However, above this threshold a steep rise in sIgE with increasing concentrations of sCD23 was observed. This co-operative relationship may reflect the avidity of sCD23 in the tri-molecular complexes with mIgE and mCD21 at the surface of the fluid B cell membrane.

7.3. The mechanism of action of sCD23

Earlier work has shown that the incubation of PBMCs with sCD23 stimulates 'ongoing' IgE synthesis rather than increasing CSR to IgE, which would require stimulation by IL-4 or IL-13 (Saxon, Ke *et al.*, 1990). In the system described in this thesis using IL-4 and anti-CD40 stimulation, no difference in the expression of εGLT, an early marker for CSR, between control siRNA- and CD23 siRNA-transfected cells was observed (Figure 4.16). Neither inhibition of sCD23 through CD23 siRNA transfection or ADAM10 inhibition, nor addition of recombinant triCD23, altered the percentage or MFI of IgE^+ or IgG^+ cells when measured by flow cytometry (Figure 4.13, Figure 4.14 and Figure 6.6).

Additional experiments with tonsil B cells have shown CSR to occur in the first few days of the incubations (Hobson *et al*., unpublished). However, recombinant sCD23 can still increase IgE synthesis when added as late as day 9 in the incubation period (Jutton *et al*., unpublished). Results presented in this thesis showed that the addition of an ADAM10 inhibitor terminates incremental IgE synthesis after CSR has occurred (Figure 5.4) (Mayer, Bolognese *et al.*, 2000). Taken together, these experiments indicate an isotype-specific role for sCD23 in promoting IgE synthesis through a post-switch mechanism.

Fearon and Carter showed that co-ligation of antigen-specific mIgM and the CD19-CD21-TAPA complex on naïve B cells by antigen, covalently linked to the C3d fragment of complement, stimulates B cell proliferation in the immune response (Fearon and Carter 1995). The effect of a blocking antibody against CD21 *in vivo* demonstrated the importance of this mechanism for a robust T cell-dependent immune response (Hebell, Ahearn *et al.*, 1991). This mechanism operates by synergistic

signalling through mIgM and mCD21 to augment the expression of the B cell survival factors Bcl-X_L and Bcl-2, respectively (Roberts and Snow 1999). CD23 expressed in a fibroblast cell line can mimic the activity of the antigen-C3d complexes in lowering the threshold of B cell proliferation by an anti-IgM (surrogate antigen) (Reljic, Cosentino *et al.,* 1997). However, it is not known whether mIgE can mimic mIgM in this mechanism. The cytoplasmic sequence of IgE, required for survival, differs from that of IgM (and other isotypes) (Achatz, Nitschke *et al.,* 1997) although mIgE is associated with the same signal transduction proteins (the α and β subunits) as other isotypes (Venkitaraman, Williams *et al.,* 1991). Evidently mIgE has some capacity for signalling, but nothing is known about the signal transduction pathways.

It is informative to consider the sequence of events after placing the B cells into culture with IL-4 and anti-CD40. At first, sCD23 can only bind to mCD21, which may elicit a proliferative response (Bohnsack and Cooper 1988). When IgE is expressed on the membrane, sCD23 appears to sequester the mIgE and mCD21 into raft-like structures (Figure 6.9 and Figure 6.12) (Hibbert, Teriete *et al.,* 2005). These resemble the fate of cross-linked IgM-CD19-CD21-TAPA complexes in complement-enhanced IgM BCR activation (Fearon and Carter 1995; Pierce 2002). Whether formation of a mIgE-sCD23-mCD21 complex leads to similar functional consequences remains to be fully investigated.

7.4. Overall Conclusion

In this thesis, two experimental approaches were taken to reduce sCD23 production in primary human B cells. Both techniques culminated in reduced sCD23 production and reduced IgE secretion, albeit through different actions on mCD23

(reduced expression or inhibition of cleavage). Each approach had its limitations, but they were different from each other, and the combined results conclusively demonstrate that sCD23 stimulates IgE synthesis in human B cells. This was supported by contrasting experiments where addition of sCD23 led to an increase in the secretion of IgE. Together, these data support the hypothesis shown in Figure 7.1 whereby trimeric sCD23 molecules can bind both mIgE and mCD21 to stimulate IgE synthesis (Cooper, Hobson *et al.*, 2012).

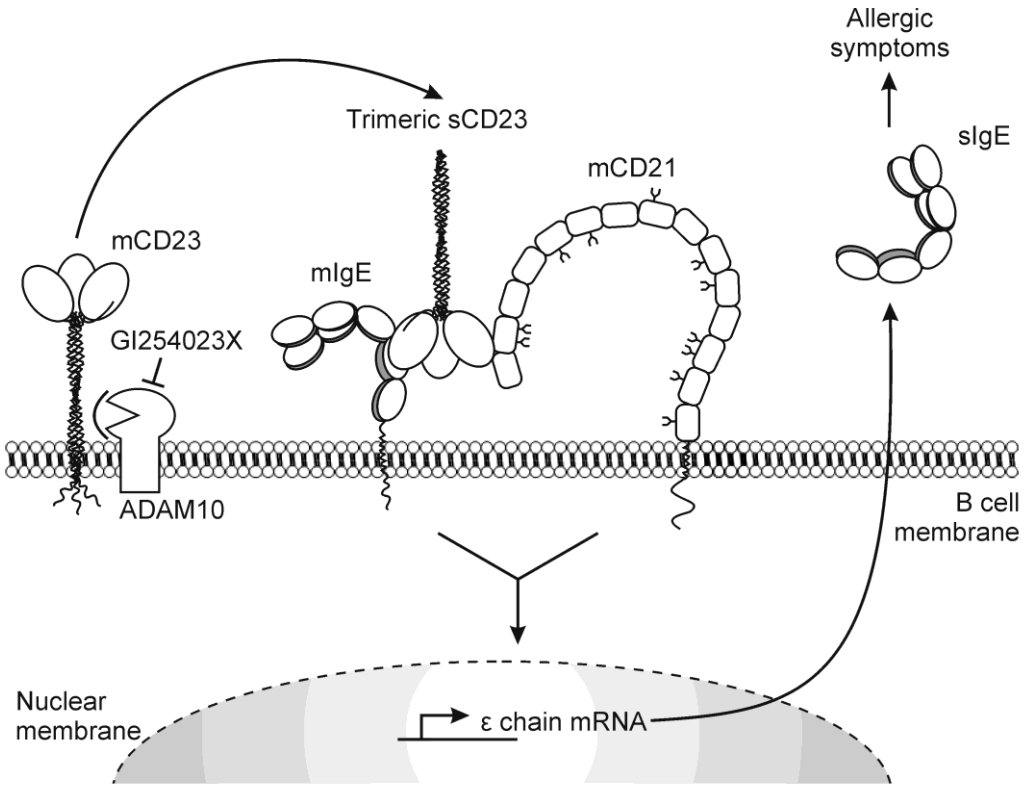

Figure 7.1. Proposed mechanism of IgE up-regulation by trimeric soluble CD23.

In this model, membrane CD23 (mCD23) is cleaved by ADAM10 to release trimeric soluble CD23 (sCD23), which co-ligates both membrane IgE (mIgE) and membrane CD21 (mCD21) on the surface of IgE-committed B cells to up-regulate IgE synthesis, triggering the onset of allergic symptoms.

From (Cooper, Hobson *et al.*, 2012).

The results in this thesis suggest that sCD23 may be an active partner, rather than an innocent bystander, in regulating IgE synthesis and, therefore, a promising therapeutic target for allergic disease. Two current strategies, the anti-CD23 mAb lumiliximab, which showed efficacy in lowering IgE levels in asthmatic patients (Rosenwasser, Busse *et al.,* 2003; Rosenwasser and Meng 2005) and metalloprotease inhibitors, already tested in mice (Mathews, Ford *et al.*, 2011), are aimed primarily at mCD23. The results described in this thesis, and those from others (Bowles, Jaeger *et al.*, 2011; Mayer, Bolognese *et al.*, 2000; McCloskey, Hunt *et al.*, 2007; Sarfati and Delespesse 1988; Saxon, Ke *et al.,* 1990), should encourage the rational design of inhibitors of sCD23 binding to its ligands for the treatment of asthma and allergic disease.

Appendix

Tonsil number	Date of consent	Allergic condition	Medication
1	21/01/2009	(Could not ask)	
2	19/03/2009	(Could not ask)	
3	23/04/2009	(Could not ask)	
4	19/05/2009		
5	11/06/2009		
6	11/06/2009		
7	22/07/2009		
8	04/08/2009		
9	16/09/2009		
10	20/10/2009		
11	10/11/2009	Eczema	
12	09/12/2009		
13	03/02/2010		
14	04/03/2010		
15	28/04/2010		
16	02/06/2010	Asthma	Very occasional steroid inhaler (bi-annual)
17	06/07/2010		
18	21/07/2010	Allergic rhinitis	Methylphenidate for ADHD
19	07/09/2010	Antibiotic allergy	
20	27/10/2010		
21	02/11/2010	Antibiotic allergy	
22	09/12/2010		
23	12/01/2011	Allergic rhinitis, eczema, nut & egg allergy	Cetirizine
24	26/01/2011		
25	02/03/2011		
26	30/03/2011		
27	11/05/2011		
28	17/05/2011		
29	17/05/2011		
30	18/10/2011		
31	10/11/2011		
32	07/12/2011		

Appendix 1. Information on tonsil donors used in experiments.

Information on the tonsil donors used in each experiment, the date of consent and any allergic conditions or medication which the patient was taking (n=32). Tonsil numbers used in each experiment are identified in figure legends.

References

Aberle, N., Gagro, A., Rabatic, S., Reiner-Banovac, Z. and Dekaris, D. (1997). "Expression of CD23 antigen and its ligands in children with intrinsic and extrinsic asthma." Allergy **52**(12): 1238-1242.

Achatz, G., Nitschke, L. and Lamers, M. C. (1997). "Effect of transmembrane and cytoplasmic domains of IgE on the IgE response." Science **276**(5311): 409-411.

Akdis, C. A., Blesken, T., Akdis, M., Wuthrich, B. and Blaser, K. (1998). "Role of interleukin 10 in specific immunotherapy." J Clin Invest **102**(1): 98-106.

Ala-Kapee, M., Nevanlinna, H., Mali, M., Jalkanen, M. and Schroder, J. (1990). "Localization of gene for human syndecan, an integral membrane proteoglycan and a matrix receptor, to chromosome 2." Somat Cell Mol Genet **16**(5): 501-505.

Asthma-UK (2011). Asthma UK's 2010-2011 Impact Report.

Aubry, J. P., Dugas, N., Lecoanet-Henchoz, S., Ouaaz, F., Zhao, H., Delfraissy, J. F., Graber, P., Kolb, J. P., Dugas, B. and Bonnefoy, J. Y. (1997). "The 25-kDa soluble CD23 activates type III constitutive nitric oxide-synthase activity via CD11b and CD11c expressed by human monocytes." J Immunol **159**(2): 614-622.

Aubry, J. P., Pochon, S., Gauchat, J. F., Nueda-Marin, A., Holers, V. M., Graber, P., Siegfried, C. and Bonnefoy, J. Y. (1994). "CD23 interacts with a new functional extracytoplasmic domain involving N-linked oligosaccharides on CD21." J Immunol **152**(12): 5806-5813.

Aubry, J. P., Pochon, S., Graber, P., Jansen, K. U. and Bonnefoy, J. Y. (1992). "CD21 is a ligand for CD23 and regulates IgE production." Nature **358**(6386): 505-507.

Avery, D. T., Ma, C. S., Bryant, V. L., Santner-Nanan, B., Nanan, R., Wong, M., Fulcher, D. A., Cook, M. C. and Tangye, S. G. (2008). "STAT3 is required for IL-21-induced secretion of IgE from human naive B cells." Blood **112**(5): 1784-1793.

Bacharier, L. B., Jabara, H. and Geha, R. S. (1998). "Molecular mechanisms of immunoglobulin E regulation." Int Arch Allergy Immunol **115**(4): 257-269.

Bajorath, J. and Aruffo, A. (1996). "Structure-based modeling of the ligand binding domain of the human cell surface receptor CD23 and comparison of two independently derived molecular models." Protein Sci **5**(2): 240-247.

Batista, F. D., Efremov, D. G., Tkach, T. and Burrone, O. R. (1995). "Characterization of the human immunoglobulin epsilon mRNAs and their polyadenylation sites." Nucleic Acids Res **23**(23): 4805-4811.

Beavil, A. J., Edmeades, R. L., Gould, H. J. and Sutton, B. J. (1992). "Alpha-helical coiled-coil stalks in the low-affinity receptor for IgE (Fc epsilon RII/CD23) and related C-type lectins." Proc Natl Acad Sci U S A **89**(2): 753-757.

Beavil, R. L., Graber, P., Aubonney, N., Bonnefoy, J. Y. and Gould, H. J. (1995). "CD23/Fc epsilon RII and its soluble fragments can form oligomers on the cell surface and in solution." Immunology **84**(2): 202-206.

Belleau, J. T., Gandhi, R. K., McPherson, H. M. and Lew, D. B. (2005). "Research upregulation of CD23 (FcepsilonRII) expression in human airway smooth muscle cells (huASMC) in response to IL-4, GM-CSF, and IL-4/GM-CSF." Clin Mol Allergy **3**: 6.

Bettler, B., Maier, R., Ruegg, D. and Hofstetter, H. (1989). "Binding site for IgE of the human lymphocyte low-affinity Fc epsilon receptor (Fc epsilon RII/CD23) is confined to the domain homologous with animal lectins." Proc Natl Acad Sci U S A **86**(18): 7118-7122.

Bohnsack, J. F. and Cooper, N. R. (1988). "CR2 ligands modulate human B cell activation." J Immunol **141**(8): 2569-2576.

Bouaziz, J. D., Yanaba, K. and Tedder, T. F. (2008). "Regulatory B cells as inhibitors of immune responses and inflammation." Immunol Rev **224**: 201-214.

Bowles, S. L., Jaeger, C., Ferrara, C., Fingeroth, J., Van De Venter, M. and Oosthuizen, V. (2011). "Comparative binding of soluble fragments (derCD23, sCD23, and exCD23) of recombinant human CD23 to CD21 (SCR 1-2) and native IgE, and their effect on IgE regulation." Cell Immunol **271**(2): 371-378.

Byrd, J. C., Kipps, T. J., Flinn, I. W., Castro, J., Lin, T. S., Wierda, W., Heerema, N., Woodworth, J., Hughes, S., Tangri, S., Harris, S., Wynne, D., Molina, A., Leigh, B. and O'Brien, S. (2010). "Phase 1/2 study of lumiliximab combined with fludarabine, cyclophosphamide, and rituximab in patients with relapsed or refractory chronic lymphocytic leukemia." Blood **115**(3): 489-495.

Carlsson, F., Hjelm, F., Conrad, D. H. and Heyman, B. (2007). "IgE enhances specific antibody and T-cell responses in mice overexpressing CD23." Scand J Immunol **66**(2-3): 261-270.

Caven, T. H., Shelburne, A., Sato, J., Chan-Li, Y., Becker, S. and Conrad, D. H. (2005). "IL-21 dependent IgE production in human and mouse in vitro culture systems is cell density and cell division dependent and is augmented by IL-10." Cell Immunol **238**(2): 123-134.

Caven, T. H., Sturgill, J. L. and Conrad, D. H. (2007). "BCR ligation antagonizes the IL-21 enhancement of anti-CD40/IL-4 plasma cell differentiation and IgE production found in low density human B cell cultures." Cell Immunol **247**(1): 49-58.

Cherukuri, A., Cheng, P. C. and Pierce, S. K. (2001). "The role of the CD19/CD21 complex in B cell processing and presentation of complement-tagged antigens." J Immunol **167**(1): 163-172.

Cho, S. W., Kilmon, M. A., Studer, E. J., van der Putten, H. and Conrad, D. H. (1997). "B cell activation and Ig, especially IgE, production is inhibited by high CD23 levels in vivo and in vitro." Cell Immunol **180**(1): 36-46.

Christie, G., Barton, A., Bolognese, B., Buckle, D. R., Cook, R. M., Hansbury, M. J., Harper, G. P., Marshall, L. A., McCord, M. E., Moulder, K., Murdock, P. R., Seal, S. M., Spackman, V. M., Weston, B. J. and Mayer, R. J. (1997). "IgE secretion is attenuated by an inhibitor of proteolytic processing of CD23 (Fc epsilonRII)." Eur J Immunol **27**(12): 3228-3235.

Conrad, D. H. (1990). "Fc epsilon RII/CD23: the low affinity receptor for IgE." Annu Rev Immunol **8**: 623-645.

Conrad, D. H., Ford, J. W., Sturgill, J. L. and Gibb, D. R. (2007). "CD23: an overlooked regulator of allergic disease." Curr Allergy Asthma Rep **7**(5): 331-337.

Cooper, A. M., Hobson, P. S., Jutton, M. R., Kao, M. W., Drung, B., Schmidt, B., Fear, D. J., Beavil, A. J., McDonnell, J. M., Sutton, B. J. and Gould, H. J. (2012). "Soluble CD23 Controls IgE Synthesis and Homeostasis in Human B Cells." J Immunol **188**(7).

Delespesse, G., Sarfati, M., Wu, C. Y., Fournier, S. and Letellier, M. (1992). "The low-affinity receptor for IgE." Immunol Rev **125**: 77-97.

Delespesse, G., Suter, U., Mossalayi, D., Bettler, B., Sarfati, M., Hofstetter, H., Kilcherr, E., Debre, P. and Dalloul, A. (1991). "Expression, structure, and function of the CD23 antigen." Adv Immunol **49**: 149-191.

Dempsey, P. W., Allison, M. E., Akkaraju, S., Goodnow, C. C. and Fearon, D. T. (1996). "C3d of complement as a molecular adjuvant: bridging innate and acquired immunity." Science **271**(5247): 348-350.

Dempsey, P. W. and Fearon, D. T. (1996). "Complement: instructing the acquired immune system through the CD21/CD19 complex." Res Immunol **147**(2): 71-75; discussion 119-120.

Di Lorenzo, G., Drago, A., Pellitteri, M. E., Candore, G., Colombo, A., Potestio, M., Di Salvo, A., Mansueto, S. and Caruso, C. (1999). "Serum levels of soluble CD23 in patients with asthma or rhinitis monosensitive to Parietaria. Its relation to total serum IgE levels and eosinophil cationic protein during and out of the pollen season." Allergy Asthma Proc **20**(2): 119-125.

Dierks, S. E., Bartlett, W. C., Edmeades, R. L., Gould, H. J., Rao, M. and Conrad, D. H. (1993). "The oligomeric nature of the murine Fc epsilon RII/CD23. Implications for function." J Immunol **150**(6): 2372-2382.

Dijkstra, A., Postma, D. S., Noordhoek, J. A., Lodewijk, M. E., Kauffman, H. F., ten Hacken, N. H. and Timens, W. (2009). "Expression of ADAMs ("a disintegrin and metalloprotease") in the human lung." Virchows Arch **454**(4): 441-449.

Durham, S. R., Smurthwaite, L. and Gould, H. J. (2000). "Local IgE production." Am J Rhinol **14**(5): 305-307.

Edry, E. and Melamed, D. (2004). "Receptor editing in positive and negative selection of B lymphopoiesis." J Immunol **173**(7): 4265-4271.

Ewart, M. A., Ozanne, B. W. and Cushley, W. (2002). "The CD23a and CD23b proximal promoters display different sensitivities to exogenous stimuli in B lymphocytes." Genes Immun **3**(3): 158-164.

Fearon, D. T. and Carter, R. H. (1995). "The CD19/CR2/TAPA-1 complex of B lymphocytes: linking natural to acquired immunity." Annu Rev Immunol **13**: 127-149.

Fillatreau, S., Gray, D. and Anderton, S. M. (2008). "Not always the bad guys: B cells as regulators of autoimmune pathology." Nat Rev Immunol **8**(5): 391-397.

Fiset, P. O., Cameron, L. and Hamid, Q. (2005). "Local isotype switching to IgE in airway mucosa." J Allergy Clin Immunol **116**(1): 233-236.

Fremeaux-Bacchi, V., Bernard, I., Maillet, F., Mani, J. C., Fontaine, M., Bonnefoy, J. Y., Kazatchkine, M. D. and Fischer, E. (1996). "Human lymphocytes shed a soluble form of CD21 (the C3dg/Epstein-Barr virus receptor, CR2) that binds iC3b and CD23." Eur J Immunol **26**(7): 1497-1503.

Getahun, A., Hjelm, F. and Heyman, B. (2005). "IgE enhances antibody and T cell responses in vivo via CD23+ B cells." J Immunol **175**(3): 1473-1482.

Gibb, D. R., El Shikh, M., Kang, D. J., Rowe, W. J., El Sayed, R., Cichy, J., Yagita, H., Tew, J. G., Dempsey, P. J., Crawford, H. C. and Conrad, D. H. (2010). "ADAM10 is essential for Notch2-dependent marginal zone B cell development and CD23 cleavage in vivo." J Exp Med **207**(3): 623-635.

Gilbert, H. E., Asokan, R., Holers, V. M. and Perkins, S. J. (2006). "The 15 SCR flexible extracellular domains of human complement receptor type 2 can mediate multiple ligand and antigen interactions." J Mol Biol **362**(5): 1132-1147.

Gough, L., Schulz, O., Sewell, H. F. and Shakib, F. (1999). "The cysteine protease activity of the major dust mite allergen Der p 1 selectively enhances the immunoglobulin E antibody response." J Exp Med **190**(12): 1897-1902.

Gould, H., Sutton, B., Edmeades, R. and Beavil, A. (1991). "CD23/Fc epsilon RII: C-type lectin membrane protein with a split personality?" Monogr Allergy **29**: 28-49.

Gould, H. J., Beavil, R. L., Reljic, R., Shi, J., Ma, C., Sutton, B. and Ghirlando, R. (1997). IgE Homeostasis: is CD23 the safety switch? . In IgE Regulation: Molecular Mechanisms. D. Vercelli. London, John Wiley & Sons Ltd**:** 37-59.

Gould, H. J., Beavil, R. L. and Vercelli, D. (2000). "IgE isotype determination: epsilon-germline gene transcription, DNA recombination and B-cell differentiation." Br Med Bull **56**(4): 908-924.

Gould, H. J. and Sutton, B. J. (2008). "IgE in allergy and asthma today." Nat Rev Immunol **8**(3): 205-217.

Gould, H. J., Sutton, B. J., Beavil, A. J., Beavil, R. L., McCloskey, N., Coker, H. A., Fear, D. and Smurthwaite, L. (2003). "The biology of IGE and the basis of allergic disease." Annu Rev Immunol **21**: 579-628.

Gould, H. J., Takhar, P., Harries, H. E., Durham, S. R. and Corrigan, C. J. (2006). "Germinal-centre reactions in allergic inflammation." Trends Immunol **27**(10): 446-452.

Harris, D. P., Goodrich, S., Gerth, A. J., Peng, S. L. and Lund, F. E. (2005). "Regulation of IFN-gamma production by B effector 1 cells: essential roles for T-bet and the IFN-gamma receptor." J Immunol **174**(11): 6781-6790.

Harris, D. P., Goodrich, S., Mohrs, K., Mohrs, M. and Lund, F. E. (2005). "Cutting edge: the development of IL-4-producing B cells (B effector 2 cells) is controlled by IL-4, IL-4 receptor alpha, and Th2 cells." J Immunol **175**(11): 7103-7107.

Harris, D. P., Haynes, L., Sayles, P. C., Duso, D. K., Eaton, S. M., Lepak, N. M., Johnson, L. L., Swain, S. L. and Lund, F. E. (2000). "Reciprocal regulation of polarized cytokine production by effector B and T cells." Nat Immunol **1**(6): 475-482.

Hasbold, J., Lyons, A. B., Kehry, M. R. and Hodgkin, P. D. (1998). "Cell division number regulates IgG1 and IgE switching of B cells following stimulation by CD40 ligand and IL-4." Eur J Immunol **28**(3): 1040-1051.

Hebell, T., Ahearn, J. M. and Fearon, D. T. (1991). "Suppression of the immune response by a soluble complement receptor of B lymphocytes." Science **254**(5028): 102-105.

Henchoz, S., Gauchat, J. F., Aubry, J. P., Graber, P., Pochon, S. and Bonnefoy, J. Y. (1994). "Stimulation of human IgE production by a subset of anti-CD21 monoclonal antibodies: requirement of a co-signal to modulate epsilon transcripts." Immunology **81**(2): 285-290.

Hermann, P., Armant, M., Brown, E., Rubio, M., Ishihara, H., Ulrich, D., Caspary, R. G., Lindberg, F. P., Armitage, R., Maliszewski, C., Delespesse, G. and Sarfati, M. (1999). "The vitronectin receptor and its associated CD47 molecule mediates proinflammatory cytokine synthesis in human monocytes by interaction with soluble CD23." J Cell Biol **144**(4): 767-775.

Hibbert, R. G., Teriete, P., Grundy, G. J., Beavil, R. L., Reljic, R., Holers, V. M., Hannan, J. P., Sutton, B. J., Gould, H. J. and McDonnell, J. M. (2005). "The structure of human CD23 and its interactions with IgE and CD21." J Exp Med **202**(6): 751-760.

Hodgkin, P. D., Lee, J. H. and Lyons, A. B. (1996). "B cell differentiation and isotype switching is related to division cycle number." J Exp Med **184**(1): 277-281.

Hoettecke, N., Ludwig, A., Foro, S. and Schmidt, B. (2010). "Improved synthesis of ADAM10 inhibitor GI254023X." Neurodegener Dis **7**(4): 232-238.

Holdom, M. D., Davies, A. M., Nettleship, J. E., Bagby, S. C., Dhaliwal, B., Girardi, E., Hunt, J., Gould, H. J., Beavil, A. J., McDonnell, J. M., Owens, R. J. and Sutton, B. J. (2011). "Conformational changes in IgE contribute to its uniquely slow dissociation rate from receptor FcvarepsilonRI." Nat Struct Mol Biol **18**(5): 571-576.

Holgate, S., Bousquet, J., Wenzel, S., Fox, H., Liu, J. and Castellsague, J. (2001). "Efficacy of omalizumab, an anti-immunoglobulin E antibody, in patients with allergic asthma at high risk of serious asthma-related morbidity and mortality." Curr Med Res Opin **17**(4): 233-240.

Iciek, L. A., Delphin, S. A. and Stavnezer, J. (1997). "CD40 cross-linking induces Ig epsilon germline transcripts in B cells via activation of NF-kappaB: synergy with IL-4 induction." J Immunol **158**(10): 4769-4779.

Jabara, H. H., Fu, S. M., Geha, R. S. and Vercelli, D. (1990). "CD40 and IgE: synergism between anti-CD40 monoclonal antibody and interleukin 4 in the induction of IgE synthesis by highly purified human B cells." J Exp Med **172**(6): 1861-1864.

Jabara, H. H. and Geha, R. S. (2005). "Jun N-terminal kinase is essential for CD40-mediated IgE class switching in B cells." J Allergy Clin Immunol **115**(4): 856-863.

Jeppson, J. D., Patel, H. R., Sakata, N., Domenico, J., Terada, N. and Gelfand, E. W. (1998). "Requirement for dual signals by anti-CD40 and IL-4 for the induction of nuclear factor-kappa B, IL-6, and IgE in human B lymphocytes." J Immunol **161**(4): 1738-1742.

Kaminski, D. A. and Stavnezer, J. (2004). "Antibody class switching: uncoupling S region accessibility from transcription." Trends Genet **20**(8): 337-340.

Karagiannis, S. N., Warrack, J. K., Jennings, K. H., Murdock, P. R., Christie, G., Moulder, K., Sutton, B. J. and Gould, H. J. (2001). "Endocytosis and recycling of the complex between CD23 and HLA-DR in human B cells." Immunology **103**(3): 319-331.

Karnowski, A., Achatz-Straussberger, G., Klockenbusch, C., Achatz, G. and Lamers, M. C. (2006). "Inefficient processing of mRNA for the membrane form of IgE is a genetic mechanism to limit recruitment of IgE-secreting cells." Eur J Immunol **36**(7): 1917-1925.

Kijimoto-Ochiai, S. (2002). "CD23 (the low-affinity IgE receptor) as a C-type lectin: a multidomain and multifunctional molecule." Cell Mol Life Sci **59**(4): 648-664.

Kitayama, D., Sakamoto, A., Arima, M., Hatano, M., Miyazaki, M. and Tokuhisa, T. (2008). "A role for Bcl6 in sequential class switch recombination to IgE in B cells stimulated with IL-4 and IL-21." Molecular Immunology **45**(5): 1337-1345.

KleinJan, A., Vinke, J. G., Severijnen, L. W. and Fokkens, W. J. (2000). "Local production and detection of (specific) IgE in nasal B-cells and plasma cells of allergic rhinitis patients." Eur Respir J **15**(3): 491-497.

Kobayashi, N., Nagumo, H. and Agematsu, K. (2002). "IL-10 enhances B-cell IgE synthesis by promoting differentiation into plasma cells, a process that is inhibited by CD27/CD70 interaction." Clin Exp Immunol **129**(3): 446-452.

Kobayashi, S., Haruo, N., Sugane, K., Ochs, H. D. and Agematsu, K. (2009). "Interleukin-21 stimulates B-cell immunoglobulin E synthesis in human beings concomitantly with activation-induced cytidine deaminase expression and differentiation into plasma cells." Hum Immunol **70**(1): 35-40.

Lamers, M. C. and Yu, P. (1995). "Regulation of IgE synthesis. Lessons from the study of IgE transgenic and CD23-deficient mice." Immunol Rev **148**: 71-95.

Lecoanet-Henchoz, S., Gauchat, J. F., Aubry, J. P., Graber, P., Life, P., Paul-Eugene, N., Ferrua, B., Corbi, A. L., Dugas, B., Plater-Zyberk, C. and et al. (1995). "CD23 regulates monocyte activation through a novel interaction with the adhesion molecules CD11b-CD18 and CD11c-CD18." Immunity **3**(1): 119-125.

Lee, B. W., Simmons, C. F., Jr., Wileman, T. and Geha, R. S. (1989). "Intracellular cleavage of newly synthesized low affinity Fc epsilon receptor (Fc epsilon R2) provides a second pathway for the generation of the 28-kDa soluble Fc epsilon R2 fragment." J Immunol **142**(5): 1614-1620.

Lemieux, G. A., Blumenkron, F., Yeung, N., Zhou, P., Williams, J., Grammer, A. C., Petrovich, R., Lipsky, P. E., Moss, M. L. and Werb, Z. (2007). "The low affinity IgE receptor (CD23) is cleaved by the metalloproteinase ADAM10." J Biol Chem **282**(20): 14836-14844.

Letellier, M., Sarfati, M. and Delespesse, G. (1989). "Mechanisms of formation of IgE-binding factors (soluble CD23)--I. Fc epsilon R II bearing B cells generate IgE-binding factors of different molecular weights." Mol Immunol **26**(12): 1105-1112.

Linehan, L. A., Warren, W. D., Thompson, P. A., Grusby, M. J. and Berton, M. T. (1998). "STAT6 is required for IL-4-induced germline Ig gene transcription and switch recombination." J Immunol **161**(1): 302-310.

Liu, Y. J., Cairns, J. A., Holder, M. J., Abbot, S. D., Jansen, K. U., Bonnefoy, J. Y., Gordon, J. and MacLennan, I. C. (1991). "Recombinant 25-kDa CD23 and interleukin 1 alpha promote the survival of germinal center B cells: evidence for bifurcation in the development of centrocytes rescued from apoptosis." Eur J Immunol **21**(5): 1107-1114.

Lorenzo, G. D., Mansueto, P., Melluso, M., Morici, G., Cigna, D., Candore, G. and Caruso, C. (1996). "Serum levels of total IgE and soluble CD23 in bronchial asthma." Mediators Inflamm **5**(1): 43-46.

MacGlashan, D., Jr., McKenzie-White, J., Chichester, K., Bochner, B. S., Davis, F. M., Schroeder, J. T. and Lichtenstein, L. M. (1998). "In vitro regulation of FcepsilonRIalpha expression on human basophils by IgE antibody." Blood **91**(5): 1633-1643.

MacGlashan, D. W., Jr., Bochner, B. S., Adelman, D. C., Jardieu, P. M., Togias, A., McKenzie-White, J., Sterbinsky, S. A., Hamilton, R. G. and Lichtenstein, L. M. (1997). "Down-regulation of Fc(epsilon)RI expression on human basophils during in vivo treatment of atopic patients with anti-IgE antibody." J Immunol **158**(3): 1438-1445.

Mali, M., Jaakkola, P., Arvilommi, A. M. and Jalkanen, M. (1990). "Sequence of human syndecan indicates a novel gene family of integral membrane proteoglycans." J Biol Chem **265**(12): 6884-6889.

Mathews, J., Gibb, D., Chen, B. H., Sherle, P. and Conrad, D. (2010). "CD23 sheddase a disintegrin and metallo-proteinase 10 (ADAM10) is also required for CD23 sorting into B cell derived exosomes." J Biol Chem.

Mathews, J. A., Ford, J., Norton, S., Kang, D., Dellinger, A., Gibb, D. R., Ford, A. Q., Massay, H., Kepley, C. L., Scherle, P., Keegan, A. D. and Conrad, D. H. (2011). "A potential new target for asthma therapy: A Disintegrin and Metalloprotease 10 (ADAM10) involvement in murine experimental asthma." Allergy **66**(9): 1193-1200.

Mauri, C. and Ehrenstein, M. R. (2008). "The 'short' history of regulatory B cells." Trends Immunol **29**(1): 34-40.

Mayer, R. J., Bolognese, B. J., Al-Mahdi, N., Cook, R. M., Flamberg, P. L., Hansbury, M. J., Khandekar, S., Appelbaum, E., Faller, A. and Marshall, L. A. (2000). "Inhibition of CD23 processing correlates with inhibition of IL-4-stimulated IgE production in human PBL and hu-PBL-reconstituted SCID mice." Clin Exp Allergy **30**(5): 719-727.

McCloskey, N., Hunt, J., Beavil, R. L., Jutton, M. R., Grundy, G. J., Girardi, E., Fabiane, S. M., Fear, D. J., Conrad, D. H., Sutton, B. J. and Gould, H. J. (2007). "Soluble CD23 monomers inhibit and oligomers stimulate IGE synthesis in human B cells." J Biol Chem **282**(33): 24083-24091.

Melewicz, F. M., Plummer, J. M. and Spiegelberg, H. L. (1982). "Comparison of the Fc receptors for IgE on human lymphocytes and monocytes." J Immunol **129**(2): 563-569.

Meuleman, N., Stamatopoulos, B., Dejeneffe, M., El Housni, H., Lagneaux, L. and Bron, D. (2008). "Doubling time of soluble CD23: a powerful prognostic factor for newly diagnosed and untreated stage A chronic lymphocytic leukemia patients." Leukemia **22**(10): 1882-1890.

Milovanovic, M., Heine, G., Zuberbier, T. and Worm, M. (2009). "Allergen extract-induced interleukin-10 in human memory B cells inhibits immunoglobulin E production." Clin Exp Allergy **39**(5): 671-678.

Moffatt, M. F., Gut, I. G., Demenais, F., Strachan, D. P., Bouzigon, E., Heath, S., von Mutius, E., Farrall, M., Lathrop, M. and Cookson, W. O. (2010). "A large-scale, consortium-based genomewide association study of asthma." N Engl J Med **363**(13): 1211-1221.

Moffatt, M. F., Kabesch, M., Liang, L., Dixon, A. L., Strachan, D., Heath, S., Depner, M., von Berg, A., Bufe, A., Rietschel, E., Heinzmann, A., Simma, B., Frischer, T., Willis-Owen, S. A., Wong, K. C., Illig, T., Vogelberg, C., Weiland, S. K., von Mutius, E., Abecasis, G. R., Farrall, M., Gut, I. G., Lathrop, G. M. and Cookson, W. O. (2007). "Genetic variants regulating ORMDL3 expression contribute to the risk of childhood asthma." Nature **448**(7152): 470-473.

Mudde, G. C., Bheekha, R. and Bruijnzeel-Koomen, C. A. (1995). "Consequences of IgE/CD23-mediated antigen presentation in allergy." Immunol Today **16**(8): 380-383.

Nakamura, T., Kloetzer, W. S., Brams, P., Hariharan, K., Chamat, S., Cao, X., LaBarre, M. J., Chinn, P. C., Morena, R. A., Shestowsky, W. S., Li, Y. P., Chen, A. and Reff, M. E. (2000). "In vitro IgE inhibition in B cells by anti-CD23 monoclonal antibodies is functionally dependent on the immunoglobulin Fc domain." Int J Immunopharmacol **22**(2): 131-141.

Parrish-Novak, J., Dillon, S. R., Nelson, A., Hammond, A., Sprecher, C., Gross, J. A., Johnston, J., Madden, K., Xu, W., West, J., Schrader, S., Burkhead, S., Heipel, M., Brandt, C., Kuijper, J. L., Kramer, J., Conklin, D., Presnell, S. R., Berry, J., Shiota, F., Bort, S., Hambly, K., Mudri, S., Clegg, C., Moore, M., Grant, F. J., Lofton-Day, C., Gilbert, T., Rayond, F., Ching, A., Yao, L., Smith, D., Webster, P., Whitmore, T., Maurer, M., Kaushansky, K., Holly, R. D. and Foster, D. (2000). "Interleukin 21 and its receptor are involved in NK cell expansion and regulation of lymphocyte function." Nature **408**(6808): 57-63.

Pene, J., Guglielmi, L., Gauchat, J. F., Harrer, N., Woisetschlager, M., Boulay, V., Fabre, J. M., Demoly, P. and Yssel, H. (2006). "IFN-gamma-mediated inhibition of human IgE synthesis by IL-21 is associated with a polymorphism in the IL-21R gene." J Immunol **177**(8): 5006-5013.

Pierce, S. K. (2002). "Lipid rafts and B-cell activation." Nat Rev Immunol **2**(2): 96-105.

Platzer, B., Ruiter, F., van der Mee, J. and Fiebiger, E. (2011). "Soluble IgE receptors--elements of the IgE network." Immunol Lett **141**(1): 36-44.

Punnonen, J., de Waal Malefyt, R., van Vlasselaer, P., Gauchat, J. F. and de Vries, J. E. (1993). "IL-10 and viral IL-10 prevent IL-4-induced IgE synthesis by inhibiting the accessory cell function of monocytes." J Immunol **151**(3): 1280-1289.

Reinisch, W., Willheim, M., Hilgarth, M., Gasche, C., Mader, R., Szepfalusi, S., Steger, G., Berger, R., Lechner, K., Boltz-Nitulescu, G. and et al. (1994). "Soluble CD23 reliably reflects disease activity in B-cell chronic lymphocytic leukemia." J Clin Oncol **12**(10): 2146-2152.

Reljic, R., Cosentino, G. and Gould, H. J. (1997). "Function of CD23 in the response of human B cells to antigen." Eur J Immunol **27**(2): 572-575.

Richens, J., Fairclough, L., Ghaemmaghami, A. M., Mahdavi, J., Shakib, F. and Sewell, H. F. (2007). "The detection of ADAM8 protein on cells of the human immune system and the demonstration of its expression on peripheral blood B cells, dendritic cells and monocyte subsets." Immunobiology **212**(1): 29-38.

Roberts, T. and Snow, E. C. (1999). "Cutting edge: recruitment of the CD19/CD21 coreceptor to B cell antigen receptor is required for antigen-mediated expression of Bcl-2 by resting and cycling hen egg lysozyme transgenic B cells." J Immunol **162**(8): 4377-4380.

Rogala, B. and Rymarczyk, B. (1999). "Soluble CD23 in allergic diseases." Arch Immunol Ther Exp (Warsz) **47**(4): 251-255.

Rosenwasser, L. J., Busse, W. W., Lizambri, R. G., Olejnik, T. A. and Totoritis, M. C. (2003). "Allergic asthma and an anti-CD23 mAb (IDEC-152): results of a phase I, single-dose, dose-escalating clinical trial." J Allergy Clin Immunol **112**(3): 563-570.

Rosenwasser, L. J. and Meng, J. (2005). "Anti-CD23." Clin Rev Allergy Immunol **29**(1): 61-72.

Rousset, F., Peyrol, S., Garcia, E., Vezzio, N., Andujar, M., Grimaud, J. A. and Banchereau, J. (1995). "Long-term cultured CD40-activated B lymphocytes differentiate into plasma cells in response to IL-10 but not IL-4." Int Immunol **7**(8): 1243-1253.

Sarfati, M., Bettler, B., Letellier, M., Fournier, S., Rubio-Trujillo, M., Hofstetter, H. and Delespesse, G. (1992). "Native and recombinant soluble CD23 fragments with IgE suppressive activity." Immunology **76**(4): 662-667.

Sarfati, M., Bron, D., Lagneaux, L., Fonteyn, C., Frost, H. and Delespesse, G. (1988). "Elevation of IgE-binding factors in serum of patients with B cell-derived chronic lymphocytic leukemia." Blood **71**(1): 94-98.

Sarfati, M., Chevret, S., Chastang, C., Biron, G., Stryckmans, P., Delespesse, G., Binet, J. L., Merle-Beral, H. and Bron, D. (1996). "Prognostic importance of serum soluble CD23 level in chronic lymphocytic leukemia." Blood **88**(11): 4259-4264.

Sarfati, M. and Delespesse, G. (1988). "Possible role of human lymphocyte receptor for IgE (CD23) or its soluble fragments in the in vitro synthesis of human IgE." J Immunol **141**(7): 2195-2199.

Sarfati, M., Nakajima, T., Frost, H., Kilccherr, E. and Delespesse, G. (1987). "Purification and partial biochemical characterization of IgE-binding factors secreted by a human B lymphoblastoid cell line." Immunology **60**(4): 539-545.

Saxon, A., Ke, Z., Bahati, L. and Stevens, R. H. (1990). "Soluble CD23 containing B cell supernatants induce IgE from peripheral blood B-lymphocytes and costimulate with interleukin-4 in induction of IgE." J Allergy Clin Immunol **86**(3 Pt 1): 333-344.

Saxon, A., Kurbe-Leamer, M., Behle, K., Max, E. E. and Zhang, K. (1991). "Inhibition of human IgE production via Fc epsilon R-II stimulation results from a decrease in the mRNA for secreted but not membrane epsilon H chains." J Immunol **147**(11): 4000-4006.

Schulz, O., Sutton, B. J., Beavil, R. L., Shi, J., Sewell, H. F., Gould, H. J., Laing, P. and Shakib, F. (1997). "Cleavage of the low-affinity receptor for human IgE (CD23) by a mite cysteine protease: nature of the cleaved fragment in relation to the structure and function of CD23." Eur J Immunol **27**(3): 584-588.

Schwarzmeier, J. D., Shehata, M., Hilgarth, M., Marschitz, I., Louda, N., Hubmann, R. and Greil, R. (2002). "The role of soluble CD23 in distinguishing stable and progressive forms of B-chronic lymphocytic leukemia." Leuk Lymphoma **43**(3): 549-554.

Sherr, E., Macy, E., Kimata, H., Gilly, M. and Saxon, A. (1989). "Binding the low affinity Fc epsilon R on B cells suppresses ongoing human IgE synthesis." J Immunol **142**(2): 481-489.

Shi, J., Ghirlando, R., Beavil, R. L., Beavil, A. J., Keown, M. B., Young, R. J., Owens, R. J., Sutton, B. J. and Gould, H. J. (1997). "Interaction of the low-affinity receptor CD23/Fc epsilonRII lectin domain with the Fc epsilon3-4 fragment of human immunoglobulin E." Biochemistry **36**(8): 2112-2122.

Soilleux, E. J., Barten, R. and Trowsdale, J. (2000). "DC-SIGN; a related gene, DC-SIGNR; and CD23 form a cluster on 19p13." J Immunol **165**(6): 2937-2942.

Spiegelberg, H. L. (1991). "Fc epsilon R2/CD23: its discovery and possible functions." Monogr Allergy **29**: 1-8.

Sturgill, J. L., Mathews, J., Scherle, P. and Conrad, D. H. (2011). "Glutamate signaling through the kainate receptor enhances human immunoglobulin production." J Neuroimmunol.

Takhar, P., Corrigan, C. J., Smurthwaite, L., O'Connor, B. J., Durham, S. R., Lee, T. H. and Gould, H. J. (2007). "Class switch recombination to IgE in the bronchial mucosa of atopic and nonatopic patients with asthma." J Allergy Clin Immunol **119**(1): 213-218.

Takhar, P., Smurthwaite, L., Coker, H. A., Fear, D. J., Banfield, G. K., Carr, V. A., Durham, S. R. and Gould, H. J. (2005). "Allergen drives class switching to IgE in the nasal mucosa in allergic rhinitis." J Immunol **174**(8): 5024-5032.

Tangye, S. G., Avery, D. T. and Hodgkin, P. D. (2003). "A division-linked mechanism for the rapid generation of Ig-secreting cells from human memory B cells." J Immunol **170**(1): 261-269.

Tangye, S. G., Ferguson, A., Avery, D. T., Ma, C. S. and Hodgkin, P. D. (2002). "Isotype switching by human B cells is division-associated and regulated by cytokines." J Immunol **169**(8): 4298-4306.

Tanigaki, K. and Honjo, T. (2007). "Regulation of lymphocyte development by Notch signaling." Nat Immunol **8**(5): 451-456.

Texido, G., Eibel, H., Le Gros, G. and van der Putten, H. (1994). "Transgene CD23 expression on lymphoid cells modulates IgE and IgG1 responses." J Immunol **153**(7): 3028-3042.

Thomas, M., Calamito, M., Srivastava, B., Maillard, I., Pear, W. S. and Allman, D. (2007). "Notch activity synergizes with B-cell-receptor and CD40 signaling to enhance B-cell activation." Blood **109**(8): 3342-3350.

Umland, S. P., Garlisi, C. G., Shah, H., Wan, Y., Zou, J., Devito, K. E., Huang, W. M., Gustafson, E. L. and Ralston, R. (2003). "Human ADAM33 messenger RNA expression profile and post-transcriptional regulation." Am J Respir Cell Mol Biol **29**(5): 571-582.

van Zaanen, H. C., Vet, R. J., de Jong, C. M., von dem Borne, A. E. and van Oers, M. H. (1995). "A simple and sensitive method for determining plasma cell isotype and monoclonality in bone marrow using flowcytometry." Br J Haematol **91**(1): 55-59.

Venkitaraman, A. R., Williams, G. T., Dariavach, P. and Neuberger, M. S. (1991). "The B-cell antigen receptor of the five immunoglobulin classes." Nature **352**(6338): 777-781.

Waldmann, T. A., Iio, A., Ogawa, M., McIntyre, O. R. and Strober, W. (1976). "The metabolism of IgE. Studies in normal individuals and in a patient with IgE myeloma." J Immunol **117**(4): 1139-1144.

Wan, T., Beavil, R. L., Fabiane, S. M., Beavil, A. J., Sohi, M. K., Keown, M., Young, R. J., Henry, A. J., Owens, R. J., Gould, H. J. and Sutton, B. J. (2002). "The crystal structure of IgE Fc reveals an asymmetrically bent conformation." Nat Immunol **3**(7): 681-686.

Weis, W. I., Drickamer, K. and Hendrickson, W. A. (1992). "Structure of a C-type mannose-binding protein complexed with an oligosaccharide." Nature **360**(6400): 127-134.

Weskamp, G., Ford, J. W., Sturgill, J., Martin, S., Docherty, A. J., Swendeman, S., Broadway, N., Hartmann, D., Saftig, P., Umland, S., Sehara-Fujisawa, A., Black, R. A., Ludwig, A., Becherer, J. D., Conrad, D. H. and Blobel, C. P. (2006). "ADAM10 is a principal 'sheddase' of the low-affinity immunoglobulin E receptor CD23." Nat Immunol **7**(12): 1293-1298.

Wilhelm, D., Klouche, M., Gorg, S. and Kirchner, H. (1994). "Expression of sCD23 in atopic and nonatopic blood donors: correlation with age, total serum IgE, and allergic symptoms." Allergy **49**(7): 521-525.

Williams, C. M. and Galli, S. J. (2000). "The diverse potential effector and immunoregulatory roles of mast cells in allergic disease." J Allergy Clin Immunol **105**(5): 847-859.

Wills-Karp, M. (1999). "Immunologic basis of antigen-induced airway hyperresponsiveness." Annu Rev Immunol **17**: 255-281.

Wood, N., Bourque, K., Donaldson, D. D., Collins, M., Vercelli, D., Goldman, S. J. and Kasaian, M. T. (2004). "IL-21 effects on human IgE production in response to IL-4 or IL-13." Cellular Immunology **231**(1-2): 133-145.

Wurzburg, B. A., Tarchevskaya, S. S. and Jardetzky, T. S. (2006). "Structural changes in the lectin domain of CD23, the low-affinity IgE receptor, upon calcium binding." Structure **14**(6): 1049-1058.

Yanaba, K., Bouaziz, J. D., Matsushita, T., Tsubata, T. and Tedder, T. F. (2009). "The development and function of regulatory B cells expressing IL-10 (B10 cells) requires antigen receptor diversity and TLR signals." J Immunol **182**(12): 7459-7472.

Yanagihara, Y., Sarfati, M., Marsh, D., Nutman, T. and Delespesse, G. (1990). "Serum levels of IgE-binding factor (soluble CD23) in diseases associated with elevated IgE." Clin Exp Allergy **20**(4): 395-401.

Ying, S., Humbert, M., Meng, Q., Pfister, R., Menz, G., Gould, H. J., Kay, A. B. and Durham, S. R. (2001). "Local expression of epsilon germline gene transcripts and RNA for the epsilon heavy chain of IgE in the bronchial mucosa in atopic and nonatopic asthma." J Allergy Clin Immunol **107**(4): 686-692.

Yokota, A., Kikutani, H., Tanaka, T., Sato, R., Barsumian, E. L., Suemura, M. and Kishimoto, T. (1988). "Two species of human Fc epsilon receptor II (Fc epsilon RII/CD23): tissue-specific and IL-4-specific regulation of gene expression." Cell **55**(4): 611-618.

Yu, K., Chedin, F., Hsieh, C. L., Wilson, T. E. and Lieber, M. R. (2003). "R-loops at immunoglobulin class switch regions in the chromosomes of stimulated B cells." Nat Immunol **4**(5): 442-451.

Yu, P., Kosco-Vilbois, M., Richards, M., Kohler, G. and Lamers, M. C. (1994). "Negative feedback regulation of IgE synthesis by murine CD23." Nature **369**(6483): 753-756.

Publications

1. **Cooper, A. M**., Hobson, P. S., Jutton, M. R., Kao, M. W., Drung, B., Schmidt, B., Fear, D. J., Beavil, A. J., McDonnell, J. M., Sutton, B. J. and Gould, H. J. (2012). "Soluble CD23 Controls IgE Synthesis and Homeostasis in Human B Cells." J Immunol **188**(7).

2. Borthakur, S., Hibbert, R. G., Pang, M. O. Y., Yahya, N., Bax, H. J., Kao, M. W., **Cooper, A. M**., Beavil, A. J., Sutton, B. J., Gould, H. J. and McDonnell, J. M. (2012). "Mapping of the CD23 binding site on IgE and allosteric control of the IgE-FcεRI interaction." J Biol Chem doi: 10.1074/jbc.C112.397059.

3. Dayal, S., Nedbal, J., Hobson, P., **Cooper, A. M**., Gould, H. J., Gellert, M., Felsenfeld, G. and Fear, D. J. (2011). "High Resolution Analysis of the Chromatin Landscape of the IgE Switch Region in Human B Cells." PLoS One **6**(9): e24571.

Published March 5, 2012, doi:10.4049/jimmunol.1102689

Soluble CD23 Controls IgE Synthesis and Homeostasis in Human B Cells

Alison M. Cooper,*,† Philip S. Hobson,*,† Mark R. Jutton,†,1 Michael W. Kao,*,† Binia Drung,‡ Boris Schmidt,‡ David J. Fear,*,§ Andrew J. Beavil,*,† James M. McDonnell,*,† Brian J. Sutton,*,† and Hannah J. Gould*,†

CD23, the low-affinity receptor for IgE, exists in membrane and soluble forms. Soluble CD23 (sCD23) fragments are released from membrane (m)CD23 by the endogenous metalloprotease a disintegrin and metalloprotease 10. When purified tonsil B cells are incubated with IL-4 and anti-CD40 to induce class switching to IgE in vitro, mCD23 is upregulated, and sCD23 accumulates in the medium prior to IgE synthesis. We have uncoupled the effects of mCD23 cleavage and accumulation of sCD23 on IgE synthesis in this system. We show that small interfering RNA inhibition of CD23 synthesis or inhibition of mCD23 cleavage by an a disintegrin and metalloprotease 10 inhibitor, GI254023X, suppresses IL-4 and anti-CD40–stimulated IgE synthesis. Addition of a recombinant trimeric sCD23 enhances IgE synthesis in this system. This occurs even when endogenous mCD23 is protected from cleavage by GI254023X, indicating that IgE synthesis is positively controlled by sCD23. We show that recombinant trimeric sCD23 binds to cells coexpressing mIgE and mCD21 and caps these proteins on the B cell membrane. Upregulation of IgE by sCD23 occurs after class-switch recombination, and its effects are isotype-specific. These results suggest that mIgE and mCD21 cooperate in the sCD23-mediated positive regulation of IgE synthesis on cells committed to IgE synthesis. Feedback regulation may occur when the concentration of secreted IgE becomes great enough to allow binding to mCD23, thus preventing further release of sCD23. We interpret these results with the aid of a model for the upregulation of IgE by sCD23. ***The Journal of Immunology*****, 2012, 188: 000–000.**

CD23 is the low-affinity receptor for IgE on B cells. It is initially expressed as a 45-kDa type II membrane protein (membrane [m]CD23) containing a lectin head domain, harboring the IgE binding site, and a C-terminal tail in the extracellular sequence (1, 2). CD23 is assembled into a trimer (3), the predominant form in the B cell membrane, by way of an α-helical coiled-coil stalk that links the three lectin head and tail domains to their transmembrane and cytoplasmic sequences (4). CD23 is expressed in two forms, CD23a and CD23b, resulting from alternative transcription initiation sites and differing only by six or seven amino acids in the intracellular N-terminal cytoplasmic sequence (5). CD23a is expressed on Ag-activated B cells, whereas CD23b expression is upregulated by IL-4 in allergic inflammation and is associated with elevated serum IgE (6–8). The anti-CD23 mAb lumiliximab downregulates IgE synthesis by human B cells in vitro (9) and reduced human serum IgE levels in a phase I clinical trial in patients with mild to moderate persistent allergic asthma (10, 11). This provides proof of principle that mCD23 is a valid target for therapy. Understanding the regulation of CD23 has the potential to inspire a more cost-effective interventional strategy.

It has long been known that CD23 negatively regulates the synthesis of IgE (12, 13). The most compelling evidence comes from CD23 knockout mice, which exhibit greatly increased levels of Ag-specific IgE after immunization (12, 13). IgE synthesis is also inhibited in human B cells by anti-CD23 Abs (9, 14, 15) or Ag–IgE complexes that bind to mCD23 (16). Neither free IgE nor Ab Fab fragments have this inhibitory activity, suggesting that cross-linking of mCD23 is required for the inhibition (15). These observations suggest that mCD23 may act in a negative-feedback mechanism on IgE synthesis.

mCD23 can be cleaved in the stalk region by the endogenous a disintegrin and metalloprotease 10 (ADAM10) to release a 37-kDa soluble fragment (soluble [s]CD23) both in vitro (17, 18) and in vivo (18–20). After the initial cleavage by ADAM10, sCD23 is susceptible to further cleavage by other proteases into fragments of various sizes (33, 29, 25, and 16 kDa), eliminating additional parts of the stalk and tail. These fragments lose the ability to independently form trimers but retain the ability to bind IgE, albeit at lower affinity (3). The 16-kDa fragment, termed derCD23, containing only the

*Medical Research Council and Asthma UK Centre in Allergic Mechanisms of Asthma, King's College London, Guy's Hospital, London SE1 9RT, United Kingdom; †Randall Division of Cell and Molecular Biophysics, King's College London, London SE1 1UL, United Kingdom; ‡Clemens Schöpf Institute of Chemistry and Biochemistry, Technical University of Darmstadt, Darmstadt 64289, Germany; and §Division of Asthma, Allergy and Lung Biology, King's College London, Guy's Hospital, London SE1 9RT, United Kingdom

[1]Current address: Sudler & Hennessey, Milan, Italy.

Received for publication September 16, 2011. Accepted for publication January 25, 2012.

This work was supported by Wellcome Trust Programme Grant 076343 and the U.K. Department of Health via the National Institute for Health Research Comprehensive Biomedical Research Centre award to Guy's and St. Thomas' National Health Service Foundation Trust in partnership with King's College London. The funders had no role in study design, data collection and analysis, decision to publish, or preparation of the manuscript. A.M.C. is a Medical Research Council (MRC) and Asthma UK-funded Ph.D. student as part of the MRC and Asthma UK Centre for Allergic Mechanisms of Asthma. M.R.J. was funded by a MRC Collaborative Award in Science and Engineering Ph.D. studentship with Novartis.

Address correspondence and reprint requests to Prof. Hannah J. Gould, Randall Division of Cell and Molecular Biophysics, King's College London, Room 3.6B, New Hunt's House, Guy's Campus, London SE1 1UL, U.K. E-mail address: hannah.gould@kcl.ac.uk

The online version of this article contains supplemental material.

Abbreviations used in this article: ADAM10, a disintegrin and metalloprotease 10; CSR, class-switch recombination; Ct, threshold cycle; derCD23, 16-kDa fragment of soluble CD23 resulting from cleavage by group I allergen of *Dermatophagoides pteronyssinus*; εGLT, ε germline transcript; m, membrane; MFI, mean fluorescence intensity; qPCR, quantitative PCR; s, soluble; sIgE, secreted IgE; siRNA, small interfering RNA; triCD23, recombinant trimeric soluble CD23.

lectin domain and 10 aa of the tail, results from cleavage by the house dust mite allergen, group I allergen of *Dermatophagoides pteronyssinus* (21, 22). Whether sCD23, resulting from mCD23 cleavage, is involved in the positive regulation of IgE synthesis is not as clear as the negative regulation by mCD23. A number of studies have shown that sCD23 fragments either up- or downregulate IgE synthesis in human B cells (23, 24), depending on their size and ability to form trimers (9, 25, 26). The use of selective ADAM10 inhibitors is considered a potential therapy for asthma, based on a recent preclinical trial in mice (19). Thus, sCD23, as well as mCD23, may be promising targets for therapy.

Human CD23 binds not only to IgE, but also to CD21 (CR2) (24), CD11b (CR3), CD11c (CR4) (27), the vitronectin receptor ($\alpha_v\beta_3$) (28), and potentially other, as yet unidentified, proteins. However, IgE and CD21 are the only known ligands on mature B cells, with both binding sites distinct from each other and from the interface between the head domains in the CD23 trimer (29). Prior to the discovery of CD21 as the counterreceptor for CD23 on B cells (24, 30), CD21 was already well characterized as the receptor for the C3d fragments of complement that play an important role in the complement cascade and adaptive immunity (31, 32). In human CD23, the binding site for CD21 resides in the C-terminal tail (29). This tail is not present in murine CD23 (33), which may explain why sCD23 expressed in transgenic mice does not upregulate IgE during immunization, leaving only downregulation through mCD23 (13, 34, 35). sCD21, shed from cell membranes, is thought to inhibit IgE synthesis in human B cells by binding to free trimeric sCD23, thereby preventing the binding to mCD21 (26, 36). Abs against human CD21 modify IgE synthesis in anti-CD40–stimulated tonsil B cells in an epitope-dependent manner (24, 37). Hence, mCD21 is implicated in mediating the effects of sCD23 on IgE synthesis.

Due to the multiple forms of CD23, multiple ligands, and various activities of the different complexes, the mechanisms involved in IgE regulation by CD23 are still poorly understood. In the current study, we have focused on the positive regulation of IgE synthesis. In 2000, Mayer et al. (23) showed that IL-4– and anti-CD40–stimulated IgE synthesis in human PBMCs can be reduced by the addition of metalloprotease inhibitors. It is uncertain whether this is a direct effect on the B cells or whether it is due to inhibition of mCD23 cleavage and, therefore, sCD23 production. If sCD23 acts on B cells, are the stimulatory signals mediated by mCD21 or an unidentified counterreceptor?

To gain further insight into this question, we have stimulated purified human tonsil B cells with IL-4 and anti-CD40 and used either small interfering RNA (siRNA) to inhibit CD23 synthesis or an ADAM10 inhibitor (GI254023X) (38) to prevent cleavage of mCD23, leading to a reduction in sCD23 levels through two different mechanisms. We have followed the loss of mCD23 from the B cell surface, the appearance of sCD23 in the medium, and the expression and secretion of IgE as a function of time for up to 12 d by flow cytometry and ELISA. We have added a recombinant trimeric sCD23 (triCD23) to the ADAM10-inhibited B cells to test its ability to compensate for the reduction of endogenous sCD23. Finally, we have followed the expression of mIgE and mCD21 during the incubation of tonsil B cells with IL-4 and anti-CD40 and examined the effects of triCD23 binding to these ligands by confocal microscopy.

Materials and Methods

Isolation of human tonsil B cells

Following informed written consent, with ethical approval from Guy's Research Ethics Committee, we obtained human tonsils from donors undergoing routine tonsillectomies. The allergic status of the donor was determined by verbal communication with the parents at the time of consent. Mononuclear cells were separated by density on a Ficoll gradient (GE Healthcare) and B cells isolated using 2-aminoethylisothiouronium bromide-treated SRBCs (TCS Biosciences). B cells were routinely >98% $CD20^+$ and <2% $CD3^+$, as determined by flow cytometry (9).

siRNA transfection

Total B cells were transfected with CD23 siGENOME SMARTpool siRNA (3 μg) (referred to as CD23 siRNA) or ON-TARGET*plus* Non-targeting siRNA Pool #1 (3 μg) (referred to as control siRNA; Thermo Scientific Dharmacon) using the Amaxa Human B cell Nucleofector kit and Nucleofector II Device (Lonza), according to the manufacturer's instructions. Transfection efficiency, 30 min after transfection, was determined to be 97% using a fluorescent nonfunctional siRNA (siGLO Red; Thermo Scientific Dharmacon). The efficiency of CD23 knockdown was quantified by quantitative PCR (qPCR).

Cell culture

B cells were cultured in 24-well plates (Nunc) at 0.5×10^6 cells/ml in RPMI 1640 with penicillin (100 IU/ml), streptomycin (100 μg/ml), glutamine (2 mM; Invitrogen), 10% FCS (Hyclone; Perbio Biosciences), transferrin (35 μg/ml), and insulin (5 μg/ml) (Sigma-Aldrich). Cells were activated with IL-4 (200 IU/ml; R&D Systems) and anti-CD40 Ab (1 μg/ml; G28.5; American Type Culture Collection) for up to 12 d. Mouse anti-human CD21 mAb (HB5; Santa Cruz Biotechnology) was added to cells at 0.1, 1, or 10 μg/ml. Epitope analysis has shown this clone to inhibit CD23 binding to CD21 (30). The ADAM10 inhibitor GI254023X was purified on a CombiFlash Rf (Teledyne ISCO) system (column: RediSep Rf, 4 g silica; flow rate: 18 ml/min; solvent: acetonitrile; t_R: 10 min). HPLC analysis at 220 nm confirmed a purity of ≥98% (38). Cells were grown for 5 d to allow the upregulation of mCD23 and class-switch recombination (CSR) to IgE before addition of the inhibitor (1–15 μM). Monomeric derCD23 (16145 Da) was made as previously described (29). lzCD23, made as previously described (9), was modified to produce the more stable trimer triCD23 (84414 Da), consisting of residues 131–321 of human CD23 prefixed by the trimerization motif $(IAAIESK)_4$ and expressed and refolded from inclusion bodies using the *Escherichia coli* vector pET151. This additionally provides N-terminal HIS_6 and V5 epitope tags and a TEV enzyme cleavage site that has been left uncleaved in the final product (M.W. Kao, J. Hunt, R.L. Beavil, M.N. Yahya, H.J. Gould, J.M. McDonnell, B.J. Sutton, and A.J. Beavil, manuscript in preparation). rCD23 proteins were dialyzed into PBS and sterile-filtered before addition to human B cell cultures. Concentrations were selected to be close to the calculated K_D value for trimeric CD23 binding to IgE (10^{-7} M) (9, 29) and used at a weight ratio of 1:3 (triCD23/derCD23) to maintain the same number of mIgE/mCD21 binding sites in each condition.

qPCR

Total RNA was isolated from cells using RNeasy Mini kits (Qiagen), primed with oligo(dT) and random hexamers, and reverse transcribed using Superscript II (Invitrogen). qPCR was performed using TaqMan MGB gene expression assays (see below) and TaqMan Universal PCR Master Mix on a 7900HT real-time PCR machine (Applied Biosystems). Gene expression was normalized to an endogenous reference gene (β_2-microglobulin) and quantified by ΔΔ threshold cycle (Ct) analysis (SDS 2.1 software): GAPDH, Hs02786624_g1; β_2-microglobulin, 4310886E; CD23, Hs00233627_m1; ε germline transcript (εGLT) forward, 5′-CTGTCCAGGAACCCGACAGA-3′, and reverse, 5′-TGCAGCAGCGGGTCAAG 3′ with MGB probe 6FAM-AG GCACCAAATG-MGB.

Flow cytometry

B cells were stained for mCD23 expression with mouse anti-human CD23-FITC (1:50; DakoCytomation) and membrane ADAM10 expression with mouse anti-human ADAM10-PE (1:50; R&D Systems) and incubated on ice in the dark for 45 min. For intracellular staining, cells were fixed with 4% paraformaldehyde (Electron Microscopy Sciences) in PBS for 15 min, washed, and resuspended in permeabilization buffer (PBS, 0.05% Triton X-100, and 0.5% saponin [Sigma-Aldrich]) for 15 min. Goat anti-human IgE-FITC (1:500; Vector Laboratories) and monoclonal mouse anti-human IgG-APC (1:50; Miltenyi Biotec) were added and incubated on ice in the dark for 45 min. Collection of flow cytometry data was conducted using an FACSCalibur (BD Biosciences), with gating on live cells determined by forward versus side scatter, and events were analyzed using FlowJo software (Tree Star).

Ig ELISA

Maxisorp plates (Nunc) were coated with polyclonal mouse anti-human IgE (1:7000; DakoCytomation) or polyclonal goat anti-human IgG (1:1000;

AbD Serotec) in pH 9.8 carbonate buffer (distilled water, 0.2 M $NaCO_3$, and 0.2 M $NaHCO_3$) overnight at 4˚C. Unbound sites were blocked with 2% milk powder in PBS + 0.05% Tween 20 (Sigma-Aldrich) for 1 h at room temperature. Supernatant samples were then added at appropriate dilutions and plates incubated overnight at 4˚C. Human serum IgE (from 800 ng/ml; NIBSC) or IgG (from 200 ng/ml; Sigma-Aldrich) were used to construct standard curves. Binding was detected by mouse anti-human IgE-HRP (1:1000; DakoCytomation) or goat anti-human IgG-HRP (1:1000; Sigma-Aldrich) in 1% milk powder in PBS + 0.05% Tween 20 for 2 h at 37˚C. The color reaction was developed with *o*-Phenylenediamine (Sigma-Aldrich) and analyzed at 492 nm using an automated plate reader (Titertek). Ig concentration was calculated from the standard curve using GraphPad Prism 5.03 software (GraphPad, San Diego, CA), with a minimum detectable concentration of ~2 ng/ml. IgE secretion (by day 12) ranged from 2–1255 ng/ml (mean 401 ± 71 ng/ml; $n = 26$). IgG secretion (by day 12) ranged from 113–2264 ng/ml (mean 365 ± 269 ng/ml; $n = 8$).

sCD23 ELISA

Human sCD23 EASIA ELISA kits (BioSource International) were used according to the manufacturer's instructions. Briefly, supernatants were added to microtiter plates precoated with a mixture of monoclonal anti-CD23 Abs, and anti-CD23–HRP was added for 2 h at room temperature. The color reaction was developed with tetramethylbenzidine and analyzed at 450 nm. The kit recognizes the 16-, 25-, 29-, and 37-kDa fragments of sCD23, with a minimum detectable concentration of ~200 pg/ml. sCD23 production (by day 12) ranged from 13–102 ng/ml (mean 58 ± 4 ng/ml; $n = 33$).

Confocal microscopy

Human tonsillar B cells were stimulated for 8 d with IL-4 and anti-CD40, harvested, and dead cells removed by density on a Ficoll gradient. A total of 3×10^5 cells was stimulated with media alone, derCD23 (3 μM/48 μg/ml), triCD23 (1 μM/84 μg/ml), or anti-CD21 (10 μg/ml) at 37˚C for 30 min. Cells were fixed with 4% paraformaldehyde, washed (with PBS + 0.05% Triton X-100), mounted onto poly-L-lysine–coated coverslips, and fixed again with 4% paraformaldehyde. Coverslip-mounted cells were stained with goat anti-human IgE-FITC (1:200; Vector Laboratories) and monoclonal mouse anti-CD21 (1:100; HB5 clone; Santa Cruz Biotechnology) for 1 h, washed, and secondary anti-mouse-Alexa 594 (1:500; Molecular Probes, Invitrogen) was added for 45 min. The nuclear stain Hoescht 33258 (1:20000; Molecular Probes, Invitrogen) was added for 10 min, cells were washed three times, and immunofluorescence visualized with an SP2 confocal microscope (Leica Microsystems).

Statistical analysis

Flow cytometry and ELISA data are shown relative to control-treated cells (either transfected with control siRNA or stimulated with IL-4 and anti-CD40 alone) to compensate for interdonor variation. Data from 7 out of 33 donors who failed to respond to IL-4 and anti-CD40, with undetectable levels of IgE expression and secretion by day 12, were excluded. Data are summarized as mean ± SEM. Statistical analysis was performed using ANOVA with Bonferroni correction, unless otherwise stated. A p value of < 0.05 was considered significant ($*p < 0.05$, $**p < 0.01$, $***p < 0.001$). Significance to control conditions is indicated above data, and significance between two conditions is shown between data. Correlation analysis was performed using Spearman's rank correlation coefficient.

Results

siRNA-induced inhibition of CD23 mRNA, mCD23, sCD23, and IgE secretion

Human tonsillar B cells were transfected with a pool of four siRNA duplexes, directed against CD23, and stimulated with IL-4 and anti-CD40 for up to 12 d. A significant inhibition of CD23 mRNA expression was observed following transfection with CD23 siRNA compared with control siRNA (Fig. 1A), but no effect was seen on the expression of a nontargeted gene, GAPDH (Fig. 1B). The maximum knockdown of CD23 (70.0 ± 0.1%) occurred between 18 and 24 h following transfection, after which CD23 mRNA levels began to recover to that of control siRNA-transfected cells.

Despite the short-term inhibition of CD23 mRNA shown in Fig. 1, mCD23 protein levels were reduced following transfection with CD23 siRNA. Fig. 2A shows a representative example of flow cytometric analysis of mCD23 levels from 18 h to 12 d following

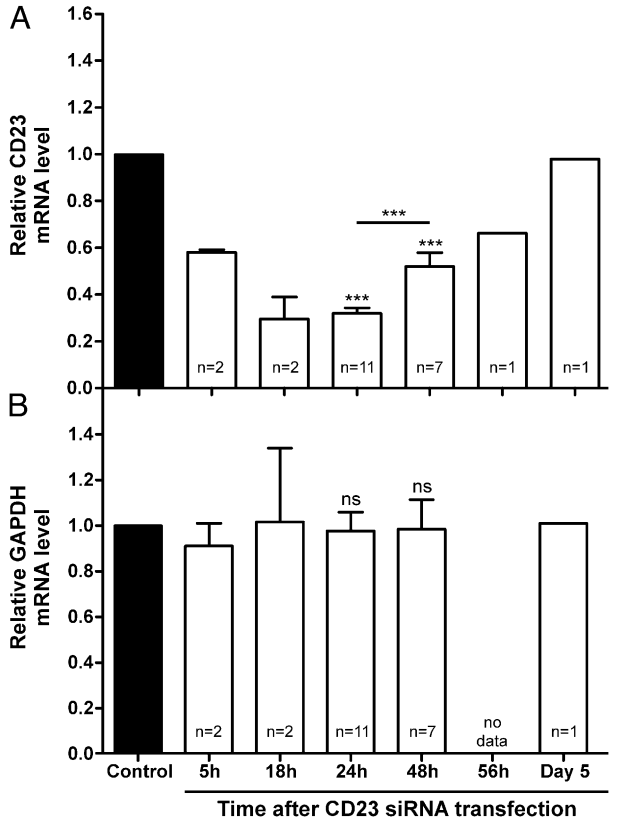

FIGURE 1. siRNA-induced inhibition of CD23 mRNA expression. Human tonsillar B cells were transfected with either control siRNA (black bars) or CD23 siRNA (white bars) and cultured for up to 5 d with IL-4 (200 IU/ml) and anti-CD40 (1 μg/ml). Cells were harvested at the times indicated, and qPCR was performed to quantify mRNA expression levels for CD23 (**A**) and GAPDH (**B**). Expression levels were calculated by ΔΔCt analysis, normalized against the endogenous reference gene β_2-microglobulin, and expressed relative to control siRNA-transfected cells at each timepoint ($n = 11$). $***p < 0.001$.

transfection with either control siRNA or CD23 siRNA. In control siRNA-transfected cells, mCD23 expression reached a peak on day 5 (88.4 ± 2.8%, $n = 8$). Fig. 2B shows that the percentage of $mCD23^+$ cells was reduced following transfection with CD23 siRNA, and this reduction remained statistically significant until day 7, although it was largely recovered by 48 h. The level of mCD23 expression on cells, as measured by the mean fluorescence intensity (MFI), was significantly lower on cells transfected with CD23 siRNA compared with control siRNA (Fig. 2C). This reduction also remained statistically significant until day 7, but the MFI was suppressed to a greater degree than the percentage of $mCD23^+$ cells and took longer to recover.

sCD23 is produced by cleavage of mCD23, initially by the membrane-bound metalloprotease ADAM10 (18). sCD23 was first detectable in the supernatant 4 d after transfection with either control siRNA or CD23 siRNA (data not shown). In accordance with the reduced mCD23 levels, sCD23 production decreased significantly following CD23 siRNA transfection (Fig. 3A). By day 12, sCD23 levels were, on average, 17.4% (± 5.7%) lower in supernatants from cells transfected with CD23 siRNA compared with control siRNA. No significant reduction was seen at the earlier time points of days 5 and 7. The expression level of ADAM10 was no different between control siRNA and CD23 siRNA-transfected cells at any time point during the culture (Supplemental Fig. 1), which reveals that the loss of ADAM10 was not responsible for the decrease in sCD23 levels.

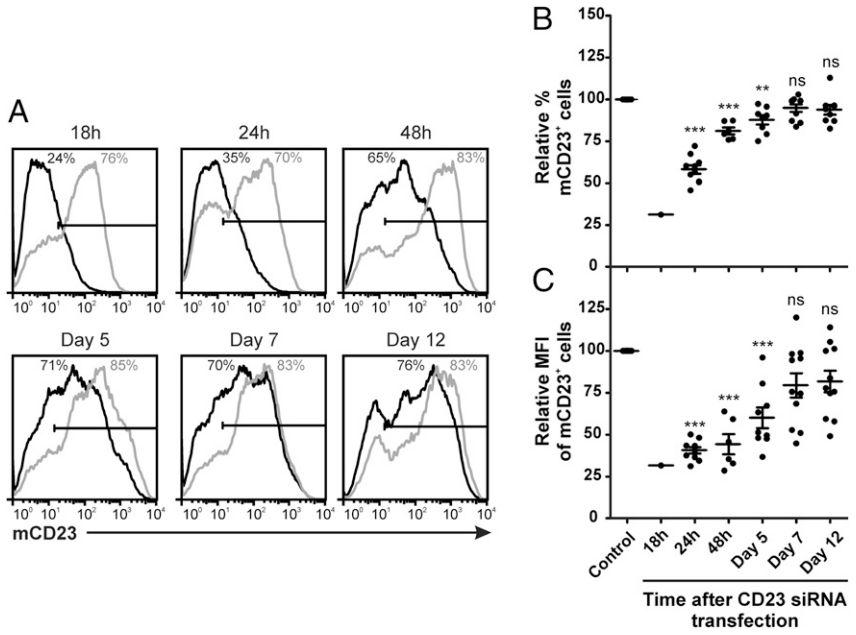

FIGURE 2. Reduced mCD23 expression following CD23 siRNA transfection. (**A**) Human tonsillar B cells were transfected with either control siRNA (gray line) or CD23 siRNA (black line) and cultured for up to 12 d with IL-4 (200 IU/ml) and anti-CD40 (1 μg/ml). mCD23 expression was analyzed by flow cytometry, and the percent of mCD23$^+$ cells (above isotype control as indicated by horizontal marker) is indicated on the histograms (n = 1, representative of 11). Multiple donor data, relative to control siRNA-transfected cells at each time point, are shown for percent mCD23$^+$ cells (**B**) and CD23$^+$ MFI (**C**), at 18 h to 12 d following transfection (n = 11). $^{**}p < 0.01$, $^{***}p < 0.001$.

Because transfection with CD23 siRNA successfully resulted in reduced sCD23 levels by day 12, we next investigated the association between reduced sCD23 production and IgE synthesis at this time point. Secreted IgE (sIgE) was first detectable in the supernatant 5 d after stimulation with IL-4 and anti-CD40 (data not shown). Fig. 3A also shows the relative levels of sIgE 5, 7, and 12 d after transfection with control siRNA or CD23 siRNA. Of the 10 donors analyzed for sCD23 production, 4 donors did not produce any detectable sIgE by day 12 and so were excluded from the analysis. CD23 siRNA-transfected cells secreted 47.4% (± 9.5%) less IgE than control siRNA-transfected cells (Fig. 3A). The extent to which sIgE levels were inhibited was not related to the amount of IgE the cells secreted. Fig. 3B correlates the level of inhibition of sCD23 production with the level of inhibition of IgE secretion. The positive correlation between sCD23 and sIgE is statistically significant (r = 0.94; p = 0.0167), as determined by

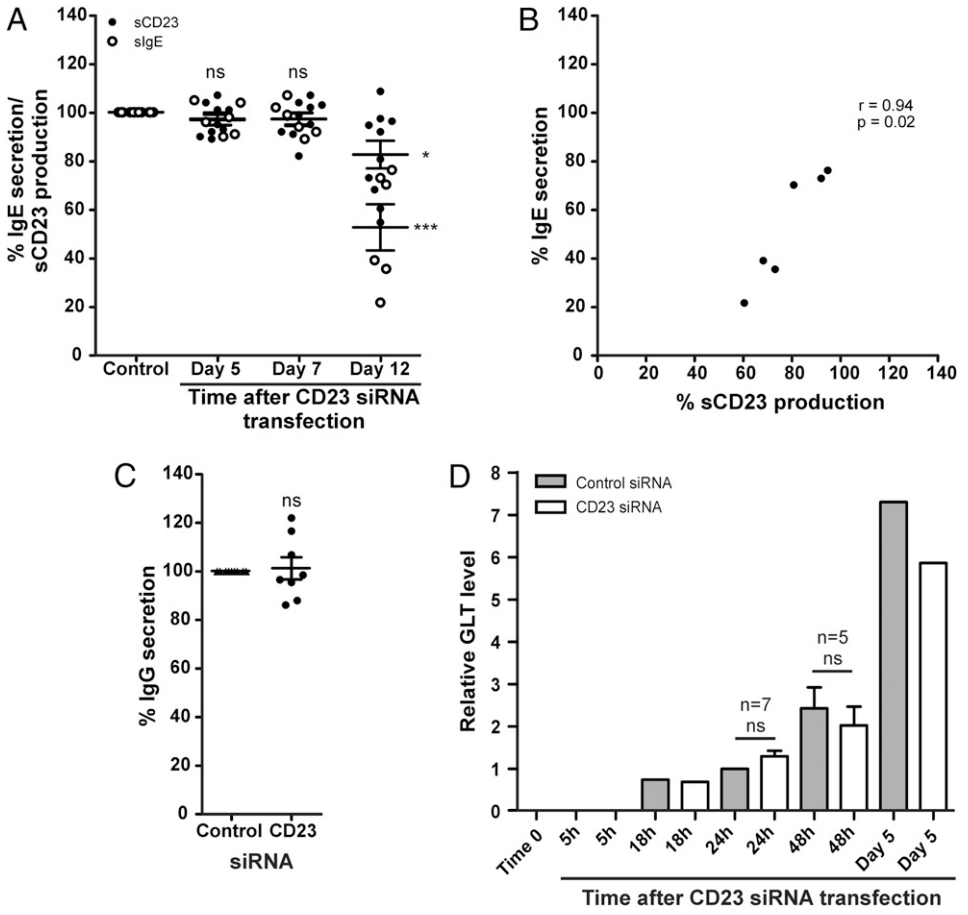

FIGURE 3. Inhibition of sCD23 production by CD23 siRNA correlates with reduced IgE secretion. Human tonsillar B cells were transfected with either control siRNA or CD23 siRNA and cultured for up to 12 d with IL-4 (200 IU/ml) and anti-CD40 (1 μg/ml). (**A**) Supernatants were harvested on days 5, 7, and 12, and the percent inhibition of sCD23 production (●) (n = 10) and IgE secretion (○) (n = 6) were analyzed by ELISA, relative to control siRNA-transfected cells. (**B**) Correlation between inhibition of IgE secretion and inhibition of sCD23 production on day 12 (n = 6). (**C**) Supernatants were harvested on day 12, and the percent inhibition of IgG secretion was analyzed by ELISA, relative to control siRNA-transfected cells (n = 8). (**D**) qPCR was performed to quantify RNA levels for εGLT up to 5 d following transfection with either control (gray bars) or CD23 siRNA (white bars). Expression levels were calculated by ΔΔCt analysis, normalized against the endogenous reference gene β_2-microglobulin, and expressed relative to control siRNA-transfected cells at 24 h (n = 1, unless indicated otherwise). $^{*}p < 0.05$, $^{***}p < 0.001$.

Spearman's rank correlation coefficient (n = 6). Importantly, CD23 siRNA transfection led to no significant changes in the levels of IgG secretion by day 12 (Fig. 3C). From day 7 onwards, following transfection with CD23 siRNA, mCD23 levels had returned to those of control siRNA-transfected cells (Fig. 2B, 2C). Thus, any CD23-mediated differences in IgE secretion between days 7 and 12 can be attributed to sCD23 rather than mCD23.

Fig. 3D shows qPCR analysis of εGLT, an early marker of CSR to IgE. No significant differences in εGLT levels were detected between control siRNA and CD23 siRNA-transfected cells at either 24 or 48 h following transfection, despite the inhibition of IgE secretion shown in Fig. 3A. Membrane and intracellular staining for IgE and IgG, analyzed by flow cytometry, showed no significant changes in the percentage of IgE^+ or IgG^+ cells between control siRNA and CD23 siRNA-transfected cells at days 7 or 12 (Supplemental Fig. 2). In addition, there were no differences in general cell viability (live cell gating determined by forward versus side scatter) or maturation (CD38 expression) between control siRNA and CD23 siRNA-transfected cells (data not shown).

ADAM10 inhibition with GI254023X reduces mCD23 shedding, sCD23 release, and IgE secretion

Because CD23 siRNA transfection reduced sCD23 through the early reduction of mCD23 expression, a different approach was taken that would reduce sCD23 levels through preventing mCD23 shedding, thus maintaining mCD23 levels. To achieve this, we used the ADAM10 inhibitor GI254023X. Human tonsillar B cells were stimulated with IL-4 and anti-CD40 for 5 d, after which GI254023X was added at 1–15 μM. The addition of GI254023X did not lead to a significant increase in the percentage of $CD23^+$ cells, although a significant dose-dependent accumulation of mCD23 on the surface of $CD23^+$ cells (as measured by MFI) was observed by day 12 (Fig. 4A). With the addition of 10 μM GI254023X, this was accompanied by a significant reduction in sCD23 production (28.3 ± 9.9%) (Fig. 4B) and a significant reduction in IgE secretion (64.9 ± 7.2%) (Fig. 4C), with no effect on IgG secretion (data not shown).

To assess the mechanism of action, GI254023X was added at days 8 or 10, in addition to day 5, and sCD23 and sIgE levels were determined at day 12. Fig. 4B and 4C show that when the inhibitor was added progressively later in the incubation period, the levels of both sCD23 and sIgE were higher, due to the shorter time period in which GI254023X could inhibit mCD23 shedding. However, inhibition of sCD23 production and IgE secretion could still be achieved even when GI254023X was added as late as day 10 in the incubation period. In further support of this association, Fig. 4D shows the relationship between sCD23 and sIgE levels, measured in the supernatant following 12 d stimulation with IL-4 and anti-CD40. The sCD23 concentrations are indicated in nanograms per milliliter, and also in micromoles, to facilitate comparison with the known K_D values of interaction with IgE and CD21 (see *Discussion*). The positive correlation between sCD23 and sIgE is statistically significant (r = 0.77; $p \leq 0.0001$), as determined by Spearman's rank correlation coefficient (n = 33). There appear to be two phases in the relationship, separated by a threshold concentration of sCD23 (60 ng/ml/1.6 μM), above which a steep rise in IgE secretion was observed.

Effect of exogenous sCD23 fragments on IgE secretion

We have previously shown that oligomeric sCD23 (lzCD23) above a certain threshold concentration upregulates, whereas monomeric sCD23 (derCD23) downregulates, IgE production from human tonsillar B cells (9). The IgE-potentiating ability of the more stable

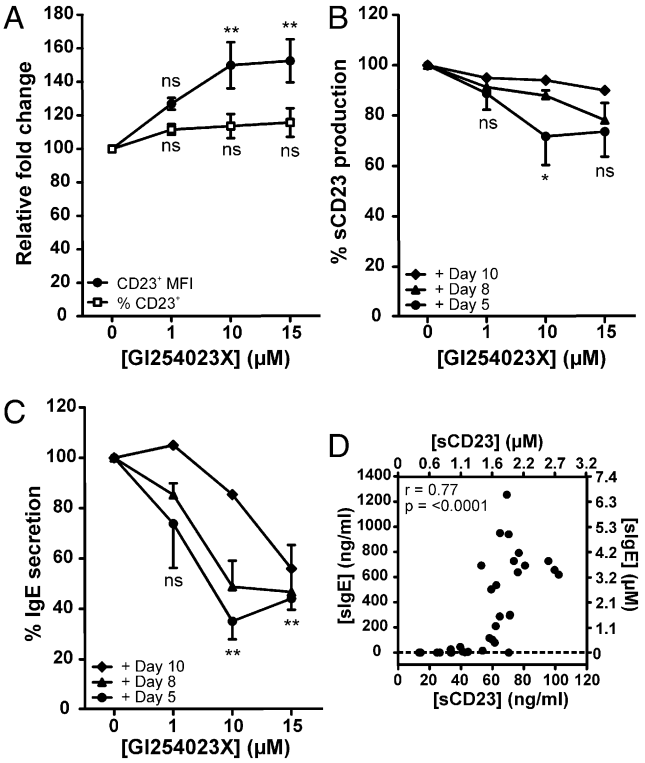

FIGURE 4. ADAM10 inhibition with GI254023X reduces mCD23 shedding, sCD23 release, and IgE secretion. Human tonsillar B cells were cultured for 12 d with IL-4 (200 IU/ml) and anti-CD40 (1 μg/ml) in the absence or presence of varying concentrations of GI254023X, added on day 5 unless otherwise stated. (**A**) mCD23 expression was analyzed by flow cytometry on day 12 and the fold change plotted for the percent of $mCD23^+$ cells (□) and $CD23^+$ MFI (●), relative to cells cultured with IL-4/anti-CD40 alone (n = 6). (**B**) GI254023X was added on days 5 (●) (n = 6), 8 (▲) (n = 2), or 10 (◆) (n = 1), and supernatants were analyzed on day 12 for sCD23 (B) production and IgE secretion (**C**), relative to cells cultured with IL-4/anti-CD40 alone. (**D**) Correlation between sCD23 and sIgE levels after 12 d (n = 33). Values are shown in nanograms per milliliter on the bottom x-axis and left y-axis and in micromoles on the top x-axis and right y-axis (1 μM 190-kDa sIgE = 190 ng/ml; 1 μM 37-kDa sCD23 = 37 ng/ml). $^*p < 0.05$, $^{**}p < 0.01$.

triCD23 was assessed by culturing B cells with IL-4, anti-CD40, and triCD23 (1 μM) (added at day 0) for 12 d. Although not a naturally occurring fragment, triCD23 has been specifically designed to mimic the trimeric state of endogenous sCD23 when it is first cleaved off the membrane in allergic tissues. Western blot analysis showed triCD23 did not degrade into smaller fragments during the 12 d in culture (data not shown). Analysis by ELISA on day 12 showed a 200.0% (± 27.2%) increase in IgE secretion from cells cultured with triCD23 compared with IL-4 and anti-CD40 alone, whereas cells cultured with monomeric derCD23 produced significantly less IgE (Fig. 5A). These effects were isotype specific, as IgG secretion remained unaffected, and flow cytometric analysis showed triCD23 had no effect on the percentage of IgE^+ cells (Supplemental Fig. 3), suggesting that triCD23 preferentially promotes expression of the secreted form of IgE.

The ability of triCD23 to rescue the inhibition of sCD23 production and IgE secretion caused by addition of the ADAM10 inhibitor (GI254023X) was then investigated. As shown in Fig. 5B, IgE secretion increased 2.3-fold when GI254023X (5 μM) was cocultured with triCD23 (1 μM) compared with GI254023X alone.

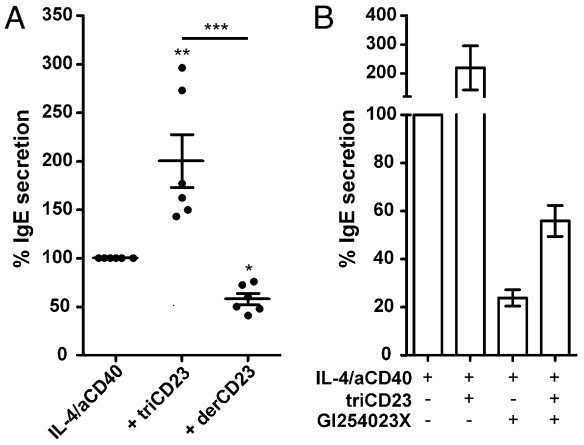

FIGURE 5. Effect of exogenous sCD23 fragments on IgE secretion. (**A**) Human tonsillar B cells were cultured for 12 d with IL-4 (200 IU/ml) and anti-CD40 (1 μg/ml) alone, + triCD23 (1 μM/84 μg/ml), or + derCD23 (3 μM/48 μg/ml). Supernatants were analyzed on day 12 for IgE secretion, relative to cells cultured with IL-4/anti-CD40 alone (n = 6). (**B**) Human tonsillar B cells were cultured for 12 d with IL-4/anti-CD40 alone, + triCD23 (1 μM), + GI254023X (5 μM), or + triCD23 and GI254023X. Supernatants were analyzed on day 12 for IgE secretion, relative to cells cultured with IL-4/anti-CD40 alone (n = 2). *$p < 0.05$, **$p < 0.01$, ***$p < 0.001$.

Trimeric sCD23 colocalizes mIgE and mCD21

Having established in this study that sCD23 was involved in the positive regulation of IgE, we next sought to identify the mechanism by which this may occur. Confocal microscopy was used to test the binding of triCD23 to mIgE and mCD21 and visualize the surface dynamics of these complexes. Human tonsillar B cells were cultured with IL-4 and anti-CD40 for 8 d to ensure sufficient time for the dual expression of mIgE and mCD21 (Supplemental Fig. 4) and then stimulated for 30 min in the presence of media alone, derCD23, or triCD23. The *left* and *middle panels* of Fig. 6A show the uniform distribution of mIgE and mCD21 on the surface of B cells incubated with either media alone or monomeric derCD23, respectively. *The right panel* of Fig. 6A shows the redistribution and colocalization of mIgE and mCD21, following incubation with triCD23. Several distinct microclusters formed, and particularly strong capping of mIgE and CD21 is indicated on the merged image in the *bottom right panel* of Fig. 6A.

To further investigate the role of mCD21 in the sCD23-mediated regulation of IgE synthesis, tonsil B cells were cultured with increasing concentrations of an anti-CD21 mAb (HB5 clone) for 12 d. Fig. 6B shows the addition of anti-CD21 resulted in a dose-dependent decrease in IgE secretion. This was accompanied by an increase in mCD23 expression and a decrease in sCD23 production (data not shown). When cells were cultured with a combination of anti-CD21 (10 μg/ml) and triCD23 (1 μM), the IgE-stimulating effects of triCD23 were blocked. Fig. 6C shows confocal microscopy analysis of mCD21 expression. Total B cells were cultured with IL-4 and anti-CD40 for 8 d and then stimulated for 30 min in the presence of anti-CD21, triCD23, or anti-CD21 and triCD23. Distinct microclusters of mCD21 formed on the surface of cells stimulated with either anti-CD21 or triCD23. In the cells pretreated with anti-CD21 before stimulation with triCD23, the distribution of mCD21 was more uniform. Together, these data support the hypothesis shown in Fig. 7, whereby trimeric sCD23 molecules can bind both mIgE and mCD21 to stimulate IgE synthesis.

Discussion

The cytokines IL-4 and IL-13 induce the CSR to all Ig isotypes downstream from Cμ in the H-chain locus on human chromosome 14, but can be replaced by other cytokines for switching to isotypes other than IgE. IL-4 upregulates CD23, so that the expression of CD23 and IgE are inextricably linked (25). The role of

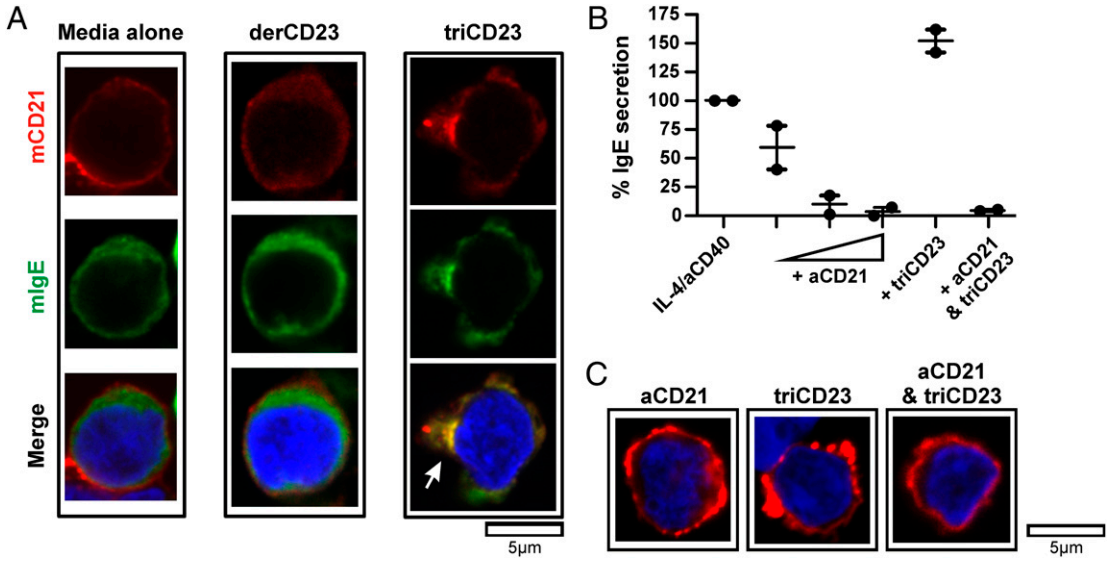

FIGURE 6. triCD23 colocalizes both mIgE and mCD21 to upregulate IgE secretion. (**A**) Human tonsillar B cells were cultured for 8 d with IL-4 (200 IU/ml) and anti-CD40 (1 μg/ml) and stimulated for 30 min with media alone, derCD23 (3 μM/48 μg/ml), or triCD23 (1 μM/84 μg/ml). Cells were stained with mouse anti-CD21, plus secondary anti-mouse-Alexa 594 (red), anti-IgE-FITC (green), and the nuclear stain Hoescht (blue). Cells were visualized by confocal microscopy and images show a single field of view, with the *bottom panel* showing a three-color overlay. The white arrow indicates strong capping of mIgE with mCD21 (n = 1, representative of 3). Scale bar, 5 μm. (**B**) Human tonsillar B cells were cultured for 12 d with IL-4/anti-CD40 alone, + anti-CD21 (0.1, 1, or 10 μg/ml), + triCD23 (1 μM), or + anti-CD21 (aCD21; 10 μg/ml) and triCD23. IgE secretion was analyzed by ELISA on day 12, relative to cells cultured with IL-4/anti-CD40 alone (n = 2). (**C**) Cells were cultured as described in (A) and stimulated with anti-CD21 (10 μg/ml), triCD23 (1 μM), or anti-CD21 and triCD23. Cells were stained for mCD21 (red) and the nucleus (blue), as previously described for (A), and visualized by confocal microscopy (n = 1). Scale bar, 5 μm.

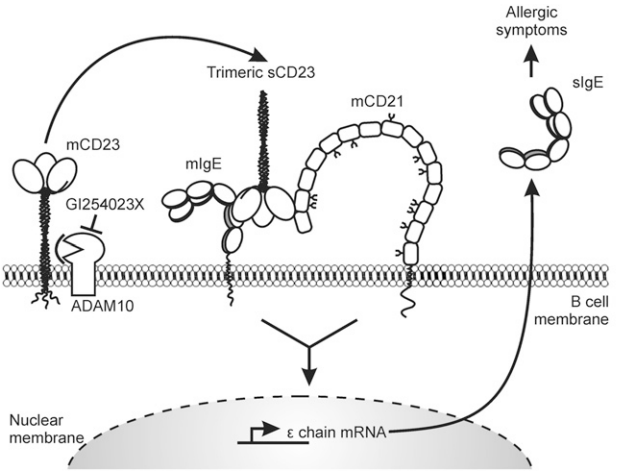

FIGURE 7. Proposed mechanism of IgE upregulation by trimeric sCD23. In this model, mCD23 is cleaved by ADAM10 to release trimeric sCD23, which coligates both mIgE and mCD21 on the surface of IgE-committed B cells to upregulate IgE synthesis, triggering the onset of allergic symptoms.

CD23 in the regulation of IgE in the human system appears to be more complex than in the mouse (2).

Negative regulation of IgE synthesis through mCD23 occurs in murine B cells in vivo (13, 39) and in human B cells in vitro (15). In human B cells, this requires the cross-linking of mCD23 (e.g., by Abs or Ag–IgE complexes). In the current study, we focused on a suggested mechanism by which sCD23 positively regulates IgE synthesis exclusively in human B cells (9, 29). In analyzing this mechanism, it is necessary to consider that there are multiple forms of sCD23, several potential ligands, and various complexes with different affinities and topological constraints associated with binding to their ligands in solution and particularly on cells.

sCD23 is released from cells by the action of an endogenous metalloprotease, identified as ADAM10 (17, 18), and accumulates in the supernatant of B cells following IL-4– and anti-CD40–stimulated CSR to IgE (23, 40, 41). In this study, we have used CD23 siRNA and an ADAM10 inhibitor (GI254023X) to confirm that mCD23 expression and cleavage to release sCD23 is required for the enhancement of IgE synthesis in primary human B cells.

Short-term inhibition of CD23 mRNA with siRNA led to a significant reduction in the frequency and MFI of $CD23^+$ cells until day 7 following transfection. By day 12, but not at the earlier time points of days 5 and 7, CD23 siRNA-transfected cells showed significantly reduced sCD23 production, which correlated with reduced IgE secretion, implicating sCD23 in the upregulation of human IgE synthesis (Figs. 1–3).

To further investigate the role of sCD23, ADAM10 was inhibited using GI254023X. It has been previously been shown that inhibition of ADAM10 in vivo (20, 42), and the addition of GI254023X to human tonsil B cells (18), results in decreased sCD23 production. However, subsequent effects on IgE were not analyzed. In this study, addition of GI254023X resulted in increased mCD23 expression, reduced sCD23 production, and reduced IgE secretion. Inhibition of sCD23 production and IgE secretion could still achieved when GI254023X was added progressively later in the incubation period, albeit to lesser extents, indicating that the ADAM10 inhibitor is regulating secretion of IgE by a postswitch event (Fig. 4). Because mCD23 is not cleaved, but is actually elevated in these conditions, the observed inhibition of IgE synthesis firmly points to positive regulation mediated through sCD23. Derepression of negative signaling through mCD23 does not appear to play a major role. When sIgE binds to mCD23, it blocks metalloprotease cleavage and the release of sCD23 (16). However, this is not a complication in the present system, as the sIgE concentrations in the medium ($<10^{-10}$ M) are well below the K_D of the IgE–mCD23 interaction. As in previous work with alternative matrix metalloprotease inhibitors and IL-4–stimulated human PBLs (23), we conclude that sCD23 is required to maintain IgE synthesis in human B cells.

We confirmed the findings from previous studies (9, 23, 26) that addition of recombinant trimeric sCD23 (triCD23) to primary human B cells enhances IgE synthesis (Fig. 5A). We now also show that when B cells are incubated with GI254023X in the presence of triCD23, a relief from GI254023X-mediated IgE suppression is observed (Fig. 5B), confirming the positive regulation of IgE synthesis by sCD23. However, the level of IgE synthesis was not fully restored to that of cells cultured only with triCD23. This might be explained by off-target effects of the ADAM10 inhibitor. Further studies are required to investigate this possibility.

mIgE and mCD21 are the prime candidates for mediating the stimulatory effects of sCD23. We show in this study that mCD21 expression declines in the first few days of incubation with IL-4 and anti-CD40 and reaches a plateau on day 5 (Supplemental Fig. 4). Loss of mCD21 is probably due to the shedding of soluble fragments (43), and further shedding may be prevented by the binding of sCD23 to mCD21 and mIgE. Although the concentrations of endogenous sCD23 (Fig. 4D) are far lower than the K_D for the 1:1 interaction with mCD21 or mIgE ($K_D = 10^{-6}$ and 10^{-8} M, respectively) (9, 29), the avidity effect of binding of three sCD23 heads as a trimer to multiple mCD21 and/or mIgE molecules may dramatically enhance binding affinity at the cell surface. Prior binding of sCD23 to mIgE, the stronger ligand, may enable the recruitment of mCD21 into a trimolecular complex. The CD23 binding site for the two N-terminal domains of CD21 lies in the C-terminal tail and is sufficiently distant from the IgE binding site to allow the simultaneous binding of both ligands in solution (29). Indeed, the observed capping of mIgE and mCD21 on B cells stimulated with triCD23 (Fig. 6A) reveals that there are likewise no topological constraints to prevent a trimeric CD23 molecule from coligating mIgE and mCD21 and forming the predicted multimolecular network on the cell surface (29). In cells in which CD23 binding to mCD21 is blocked with the addition of an anti-CD21 mAb, triCD23 is no longer able to increase IgE secretion (Fig. 6B).

Fig. 4D reveals that there is a remarkable relationship between the concentration of sCD23 and sIgE after incubation of tonsil B cells with IL-4 and anti-CD40. There appears to only be a slight increase in sIgE at low sCD23 concentrations, up to 60 ng/ml (1.6 μM) (concentrations calculated for the 37-kDa fragment). However, above this threshold, we observed a steep rise in sIgE with increasing concentrations of sCD23. The relationship shown in Fig. 4D may reflect the avidity of sCD23 in the trimolecular complexes with mIgE and mCD21 at the surface of the fluid B cell membrane, as this curve exhibits cooperativity.

Earlier work has shown that the incubation of PBMCs with sCD23 stimulates ongoing IgE synthesis, rather than increasing CSR to IgE, which would require stimulation by IL-4 (or IL-13) (41). In our system, with IL-4 and anti-CD40 stimulation, we observed no difference in the expression of εGLT, an early marker for CSR, in CD23 siRNA- compared with control siRNA-transfected cells (Fig. 3D). Neither inhibition of sCD23 through siRNA transfection nor addition of recombinant triCD23 altered the proportion of IgE^+ or IgG^+ cells when measured by flow cytometry (Supplemental Figs. 2, 3B). Additional experiments

with tonsil B cells have shown CSR to occur in the first few days of the incubations (P.S. Hobson, unpublished observations). However, recombinant sCD23 can still increase IgE synthesis when added as late as day 9 in the incubations (M.R. Jutton, unpublished observations). It has also been shown that the addition of a metalloprotease inhibitor terminates incremental IgE synthesis after CSR has occurred (Fig. 4C) (23). Taken together, these experiments indicate an isotype-specific role for sCD23 in promoting IgE synthesis through a postswitch mechanism.

Fearon and Carter (31) showed that coligation of Ag-specific IgM and the CD19–CD21–TAPA complex on naive B cells by Ag, covalently linked to the C3d fragment of complement, stimulates B cell proliferation in the immune response. The effect of a blocking Ab against CD21 in vivo demonstrated the importance of this mechanism for a robust T cell-dependent immune response (44). The mechanism operates by synergistic signaling through IgM and CD21 to augment the expression of the B cell survival factors Bcl-X_L and Bcl-2, respectively (45). CD23 expressed in a fibroblast cell line can mimic the activity of the Ag–C3d complexes in lowering the threshold of B cell proliferation by an anti-IgM (surrogate Ag) (46). However, it is not known whether mIgE can mimic mIgM in this mechanism. The cytoplasmic sequence of IgE, required for survival, differs from that of IgM (and other isotypes) (47), although mIgE is associated with the same signal transduction proteins (the α and β subunits) as other isotypes (48). Evidently, mIgE has some capacity for signaling, but nothing is known about the signal transduction pathways.

It is informative to consider the sequence of events after placing the B cells into culture with IL-4 and anti-CD40. At first, sCD23 can only bind to mCD21, which may elicit a proliferative response (49). When IgE is expressed on the membrane, sCD23 appears to sequester the mIgE and mCD21 in raftlike structures (Fig. 6A) (29), which resemble the fate of cross-linked IgM–CD19–CD21–TAPA complexes in complement-enhanced IgM BCR activation (31, 50). Whether formation of an mIgE–sCD23–mCD21 complex would lead to similar functional consequences remains to be investigated.

In this study, two experimental approaches were taken to reduce sCD23 production in primary human B cells. Both techniques culminated in reduced sCD23 production and reduced IgE secretion, albeit through different actions on mCD23 (reduced expression or inhibition of cleavage). Each approach has its limitations, but they are different from each other, and the combined results conclusively demonstrate that sCD23 stimulates IgE synthesis in human B cells.

Our results suggest that sCD23 may be an active partner, rather than an innocent bystander, in regulating IgE synthesis and therefore a promising therapeutic target for allergic disease. Two current strategies, the anti-CD23 mAb lumiliximab, which showed efficacy in lowering IgE levels in asthmatic patients (10, 11), and metalloprotease inhibitors, already tested in mice (19), are aimed primarily at mCD23. Our results, and those from others (9, 23, 26, 41, 51), should encourage the rational design of inhibitors of sCD23 binding to its ligands for the treatment of allergy and asthma.

Acknowledgments

We thank the staff at the Evelina Children's Hospital and Guy's and St. Thomas' National Health Service Foundation Trust for help with the collection of tonsils. We also thank R.L. Beavil and C. Wu of the Medical Research Council and Asthma UK Protein Production Facility for providing the anti-CD40 mAb and the design of triCD23.

Disclosures

The authors have no financial conflicts of interest.

References

1. Spiegelberg, H. L. 1991. Fc epsilon R2/CD23: its discovery and possible functions. *Monogr. Allergy* 29: 1–8.
2. Gould, H. J., and B. J. Sutton. 2008. IgE in allergy and asthma today. *Nat. Rev. Immunol.* 8: 205–217.
3. Beavil, R. L., P. Graber, N. Aubonney, J. Y. Bonnefoy, and H. J. Gould. 1995. CD23/Fc epsilon RII and its soluble fragments can form oligomers on the cell surface and in solution. *Immunology* 84: 202–206.
4. Beavil, A. J., R. L. Edmeades, H. J. Gould, and B. J. Sutton. 1992. Alpha-helical coiled-coil stalks in the low-affinity receptor for IgE (Fc epsilon RII/CD23) and related C-type lectins. *Proc. Natl. Acad. Sci. USA* 89: 753–757.
5. Yokota, A., H. Kikutani, T. Tanaka, R. Sato, E. L. Barsumian, M. Suemura, and T. Kishimoto. 1988. Two species of human Fc epsilon receptor II (Fc epsilon RII/CD23): tissue-specific and IL-4-specific regulation of gene expression. *Cell* 55: 611–618.
6. Lorenzo, G. D., P. Mansueto, M. Melluso, G. Morici, D. Cigna, G. Candore, and C. Caruso. 1996. Serum levels of total IgE and soluble CD23 in bronchial asthma. *Mediators Inflamm.* 5: 43–46.
7. Di Lorenzo, G., A. Drago, M. E. Pellitteri, G. Candore, A. Colombo, M. Potestio, A. Di Salvo, S. Mansueto, and C. Caruso. 1999. Serum levels of soluble CD23 in patients with asthma or rhinitis monosensitive to Parietaria. Its relation to total serum IgE levels and eosinophil cationic protein during and out of the pollen season. *Allergy Asthma Proc.* 20: 119–125.
8. Yanagihara, Y., M. Sarfati, D. Marsh, T. Nutman, and G. Delespesse. 1990. Serum levels of IgE-binding factor (soluble CD23) in diseases associated with elevated IgE. *Clin. Exp. Allergy* 20: 395–401.
9. McCloskey, N., J. Hunt, R. L. Beavil, M. R. Jutton, G. J. Grundy, E. Girardi, S. M. Fabiane, D. J. Fear, D. H. Conrad, B. J. Sutton, and H. J. Gould. 2007. Soluble CD23 monomers inhibit and oligomers stimulate IGE synthesis in human B cells. *J. Biol. Chem.* 282: 24083–24091.
10. Rosenwasser, L. J., W. W. Busse, R. G. Lizambri, T. A. Olejnik, and M. C. Totoritis. 2003. Allergic asthma and an anti-CD23 mAb (IDEC-152): results of a phase I, single-dose, dose-escalating clinical trial. *J. Allergy Clin. Immunol.* 112: 563–570.
11. Rosenwasser, L. J., and J. Meng. 2005. Anti-CD23. *Clin. Rev. Allergy Immunol.* 29: 61–72.
12. Cho, S. W., M. A. Kilmon, E. J. Studer, H. van der Putten, and D. H. Conrad. 1997. B cell activation and Ig, especially IgE, production is inhibited by high CD23 levels in vivo and in vitro. *Cell. Immunol.* 180: 36–46.
13. Yu, P., M. Kosco-Vilbois, M. Richards, G. Köhler, and M. C. Lamers. 1994. Negative feedback regulation of IgE synthesis by murine CD23. *Nature* 369: 753–756.
14. Nakamura, T., W. S. Kloetzer, P. Brams, K. Hariharan, S. Chamat, X. Cao, M. J. LaBarre, P. C. Chinn, R. A. Morena, W. S. Shestowsky, et al. 2000. In vitro IgE inhibition in B cells by anti-CD23 monoclonal antibodies is functionally dependent on the immunoglobulin Fc domain. *Int. J. Immunopharmacol.* 22: 131–141.
15. Sherr, E., E. Macy, H. Kimata, M. Gilly, and A. Saxon. 1989. Binding the low affinity Fc epsilon R on B cells suppresses ongoing human IgE synthesis. *J. Immunol.* 142: 481–489.
16. Conrad, D. H., J. W. Ford, J. L. Sturgill, and D. R. Gibb. 2007. CD23: an overlooked regulator of allergic disease. *Curr. Allergy Asthma Rep.* 7: 331–337.
17. Lemieux, G. A., F. Blumenkron, N. Yeung, P. Zhou, J. Williams, A. C. Grammer, R. Petrovich, P. E. Lipsky, M. L. Moss, and Z. Werb. 2007. The low affinity IgE receptor (CD23) is cleaved by the metalloproteinase ADAM10. *J. Biol. Chem.* 282: 14836–14844.
18. Weskamp, G., J. W. Ford, J. Sturgill, S. Martin, A. J. Docherty, S. Swendeman, N. Broadway, D. Hartmann, P. Saftig, S. Umland, et al. 2006. ADAM10 is a principal 'sheddase' of the low-affinity immunoglobulin E receptor CD23. *Nat. Immunol.* 7: 1293–1298.
19. Mathews, J. A., J. Ford, S. Norton, D. Kang, A. Dellinger, D. R. Gibb, A. Q. Ford, H. Massay, C. L. Kepley, P. Scherle, et al. 2011. A potential new target for asthma therapy: a disintegrin and metalloprotease 10 (ADAM10) involvement in murine experimental asthma. *Allergy* 66: 1193–1200.
20. Gibb, D. R., M. El Shikh, D. J. Kang, W. J. Rowe, R. El Sayed, J. Cichy, H. Yagita, J. G. Tew, P. J. Dempsey, H. C. Crawford, and D. H. Conrad. 2010. ADAM10 is essential for Notch2-dependent marginal zone B cell development and CD23 cleavage in vivo. *J. Exp. Med.* 207: 623–635.
21. Gough, L., O. Schulz, H. F. Sewell, and F. Shakib. 1999. The cysteine protease activity of the major dust mite allergen Der p 1 selectively enhances the immunoglobulin E antibody response. *J. Exp. Med.* 190: 1897–1902.
22. Schulz, O., B. J. Sutton, R. L. Beavil, J. Shi, H. F. Sewell, H. J. Gould, P. Laing, and F. Shakib. 1997. Cleavage of the low-affinity receptor for human IgE (CD23) by a mite cysteine protease: nature of the cleaved fragment in relation to the structure and function of CD23. *Eur. J. Immunol.* 27: 584–588.
23. Mayer, R. J., B. J. Bolognese, N. Al-Mahdi, R. M. Cook, P. L. Flamberg, M. J. Hansbury, S. Khandekar, E. Appelbaum, A. Faller, and L. A. Marshall. 2000. Inhibition of CD23 processing correlates with inhibition of IL-4-stimulated IgE production in human PBL and hu-PBL-reconstituted SCID mice. *Clin. Exp. Allergy* 30: 719–727.
24. Aubry, J. P., S. Pochon, P. Graber, K. U. Jansen, and J. Y. Bonnefoy. 1992. CD21 is a ligand for CD23 and regulates IgE production. *Nature* 358: 505–507.
25. Delespesse, G., M. Sarfati, C. Y. Wu, S. Fournier, and M. Letellier. 1992. The low-affinity receptor for IgE. *Immunol. Rev.* 125: 77–97.
26. Bowles, S. L., C. Jaeger, C. Ferrara, J. Fingeroth, M. Van De Venter, and V. Oosthuizen. 2011. Comparative binding of soluble fragments (derCD23,

sCD23, and exCD23) of recombinant human CD23 to CD21 (SCR 1-2) and native IgE, and their effect on IgE regulation. *Cell. Immunol.* 271: 371–378.
27. Bajorath, J., and A. Aruffo. 1996. Structure-based modeling of the ligand binding domain of the human cell surface receptor CD23 and comparison of two independently derived molecular models. *Protein Sci.* 5: 240–247.
28. Hermann, P., M. Armant, E. Brown, M. Rubio, H. Ishihara, D. Ulrich, R. G. Caspary, F. P. Lindberg, R. Armitage, C. Maliszewski, et al. 1999. The vitronectin receptor and its associated CD47 molecule mediates proinflammatory cytokine synthesis in human monocytes by interaction with soluble CD23. *J. Cell Biol.* 144: 767–775.
29. Hibbert, R. G., P. Teriete, G. J. Grundy, R. L. Beavil, R. Reljic, V. M. Holers, J. P. Hannan, B. J. Sutton, H. J. Gould, and J. M. McDonnell. 2005. The structure of human CD23 and its interactions with IgE and CD21. *J. Exp. Med.* 202: 751–760.
30. Aubry, J. P., S. Pochon, J. F. Gauchat, A. Nueda-Marin, V. M. Holers, P. Graber, C. Siegfried, and J. Y. Bonnefoy. 1994. CD23 interacts with a new functional extracytoplasmic domain involving N-linked oligosaccharides on CD21. *J. Immunol.* 152: 5806–5813.
31. Fearon, D. T., and R. H. Carter. 1995. The CD19/CR2/TAPA-1 complex of B lymphocytes: linking natural to acquired immunity. *Annu. Rev. Immunol.* 13: 127–149.
32. Cherukuri, A., P. C. Cheng, and S. K. Pierce. 2001. The role of the CD19/CD21 complex in B cell processing and presentation of complement-tagged antigens. *J. Immunol.* 167: 163–172.
33. Dierks, S. E., W. C. Bartlett, R. L. Edmeades, H. J. Gould, M. Rao, and D. H. Conrad. 1993. The oligomeric nature of the murine Fc epsilon RII/CD23. Implications for function. *J. Immunol.* 150: 2372–2382.
34. Texido, G., H. Eibel, G. Le Gros, and H. van der Putten. 1994. Transgene CD23 expression on lymphoid cells modulates IgE and IgG1 responses. *J. Immunol.* 153: 3028–3042.
35. Lamers, M. C., and P. Yu. 1995. Regulation of IgE synthesis. Lessons from the study of IgE transgenic and CD23-deficient mice. *Immunol. Rev.* 148: 71–95.
36. Frémeaux-Bacchi, V., E. Fischer, S. Lecoanet-Henchoz, J. C. Mani, J. Y. Bonnefoy, and M. D. Kazatchkine. 1998. Soluble CD21 (sCD21) forms biologically active complexes with CD23: sCD21 is present in normal plasma as a complex with trimeric CD23 and inhibits soluble CD23-induced IgE synthesis by B cells. *Int. Immunol.* 10: 1459–1466.
37. Henchoz, S., J. F. Gauchat, J. P. Aubry, P. Graber, S. Pochon, and J. Y. Bonnefoy. 1994. Stimulation of human IgE production by a subset of anti-CD21 monoclonal antibodies: requirement of a co-signal to modulate epsilon transcripts. *Immunology* 81: 285–290.
38. Hoettecke, N., A. Ludwig, S. Foro, and B. Schmidt. 2010. Improved synthesis of ADAM10 inhibitor GI254023X. *Neurodegener. Dis.* 7: 232–238.
39. Cheng, L. E., Z. E. Wang, and R. M. Locksley. 2010. Murine B cells regulate serum IgE levels in a CD23-dependent manner. *J. Immunol.* 185: 5040–5047.
40. Christie, G., A. Barton, B. Bolognese, D. R. Buckle, R. M. Cook, M. J. Hansbury, G. P. Harper, L. A. Marshall, M. E. McCord, K. Moulder, et al. 1997. IgE secretion is attenuated by an inhibitor of proteolytic processing of CD23 (Fc epsilonRII). *Eur. J. Immunol.* 27: 3228–3235.
41. Saxon, A., Z. Ke, L. Bahati, and R. H. Stevens. 1990. Soluble CD23 containing B cell supernatants induce IgE from peripheral blood B-lymphocytes and co-stimulate with interleukin-4 in induction of IgE. *J. Allergy Clin. Immunol.* 86: 333–344.
42. Sturgill, J. L., J. Mathews, P. Scherle, and D. H. Conrad. 2011. Glutamate signaling through the kainate receptor enhances human immunoglobulin production. *J. Neuroimmunol.* 233: 80–89.
43. Frémeaux-Bacchi, V., I. Bernard, F. Maillet, J. C. Mani, M. Fontaine, J. Y. Bonnefoy, M. D. Kazatchkine, and E. Fischer. 1996. Human lymphocytes shed a soluble form of CD21 (the C3dg/Epstein-Barr virus receptor, CR2) that binds iC3b and CD23. *Eur. J. Immunol.* 26: 1497–1503.
44. Hebell, T., J. M. Ahearn, and D. T. Fearon. 1991. Suppression of the immune response by a soluble complement receptor of B lymphocytes. *Science* 254: 102–105.
45. Roberts, T., and E. C. Snow. 1999. Cutting edge: recruitment of the CD19/CD21 coreceptor to B cell antigen receptor is required for antigen-mediated expression of Bcl-2 by resting and cycling hen egg lysozyme transgenic B cells. *J. Immunol.* 162: 4377–4380.
46. Reljić, R., G. Cosentino, and H. J. Gould. 1997. Function of CD23 in the response of human B cells to antigen. *Eur. J. Immunol.* 27: 572–575.
47. Achatz, G., L. Nitschke, and M. C. Lamers. 1997. Effect of transmembrane and cytoplasmic domains of IgE on the IgE response. *Science* 276: 409–411.
48. Venkitaraman, A. R., G. T. Williams, P. Dariavach, and M. S. Neuberger. 1991. The B-cell antigen receptor of the five immunoglobulin classes. *Nature* 352: 777–781.
49. Bohnsack, J. F., and N. R. Cooper. 1988. CR2 ligands modulate human B cell activation. *J. Immunol.* 141: 2569–2576.
50. Pierce, S. K. 2002. Lipid rafts and B-cell activation. *Nat. Rev. Immunol.* 2: 96–105.
51. Sarfati, M., and G. Delespesse. 1988. Possible role of human lymphocyte receptor for IgE (CD23) or its soluble fragments in the in vitro synthesis of human IgE. *J. Immunol.* 141: 2195–2199.

JBC Papers in Press. Published on July 19, 2012 as Manuscript C112.397059
The latest version is at http://www.jbc.org/cgi/doi/10.1074/jbc.C112.397059

Mapping of the CD23 binding site on IgE and allosteric control of the IgE-FcεRI interaction

Susmita Borthakur[1,*], Richard G. Hibbert[2,‡], Marie O.Y. Pang[1], Norhakim Yahya[1], Heather J. Bax[1], Michael W. Kao[1], Alison M. Cooper[1], Andrew J. Beavil[1], Brian J. Sutton[1], Hannah J. Gould[1], and James M. McDonnell[1]

[1]From the Randall Division of Cell and Molecular Biophysics, King's College London, Guy's Campus, London, SE1 1UL, United Kingdom; MRC & Asthma UK Centre in Allergic Mechanisms of Asthma, London, United Kingdom. [2]Department of Biochemistry, Oxford University, Oxford, OX1 3QU, United Kingdom

Current address: [*]Department of Physiology and Biophysics, Case Western Reserve University, Cleveland, OH 44106, USA. [‡]Division of Biochemistry and Center for Biomedical Genetics, Netherlands Cancer Institute, Plesmanlaan 121, 1066 CX Amsterdam, The Netherlands

Running Title: *The CD23 binding site on IgE and IgE allostery*

To whom correspondence should be addressed: James M. McDonnell, Tel. +44 207 848 6970, Fax: +44 207 848 6435, Email: james.mcdonnell@kcl.ac.uk

Keywords: Allergy, allostery, antibody, CD23, Immunoglobulin E

CAPSULE

Background: Immunoglobulin E (IgE) has two cellular receptors, FcεRI and CD23, that mediate distinct functional effects.

Results: We have identified the CD23 binding site on IgE and show that FcεRI and CD23 allosterically compete for binding.

Conclusion: A mechanism of communication exists within the IgE molecule to prevent simultaneous engagement with the two receptors.

Significance: Competition between IgE's receptors explains ligand cross-regulation.

SUMMARY

IgE, the antibody that mediates allergic responses, acts as part of a self-regulating protein network. Its unique effector functions are controlled through interactions of its Fc region with two cellular receptors, FcεRI on mast cells and basophils and CD23 on B cells. IgE cross-linked by allergen triggers mast cell activation via FcεRI, while IgE-CD23 interactions control IgE expression levels. We have determined the CD23 binding site on IgE, using a combination of NMR chemical shift mapping and site-directed mutagenesis. We show that the CD23 and FcεRI interaction sites are at opposite ends of the Cε3 domain of IgE, but that receptor binding is mutually inhibitory, mediated by an allosteric mechanism. This prevents CD23-mediated cross-linking of IgE bound to FcεRI on mast cells and resulting antigen-independent anaphylaxis. The mutually inhibitory nature of receptor binding provides a degree of autonomy for the individual activities mediated by IgE-FcεRI and IgE-CD23 interactions.

Immunoglobulin E (IgE) is the antibody isotype responsible for mediating allergic reactions. It functions through interactions with its two receptors, FcεRI and CD23 (also known as FcεRII). The binding of IgE to FcεRI is essential for type I hypersensitivity, while the interaction between CD23 and IgE is crucial for IgE-mediated facilitated allergen binding, processing and presentation (1). Through interactions with membrane IgE,

soluble CD23 fragments can up- or down-regulate synthesis of IgE, depending on the oligomerization state of CD23 (2). IgE expression can also be controlled by a negative feedback mechanism through an interaction of IgE-allergen complexes with membrane-bound CD23 on IgE^+ B cells (3). Since CD23 both positively and negatively regulates IgE expression, a critical role for CD23 in IgE homeostasis has been proposed.

High-resolution structures have been determined for Fc fragments of IgE (4,5), the extracellular region of FcεRIα (6), the C-type lectin domain of CD23 (7,8), and complexes of IgE-Fc-FcεRIα (4,9). The structures of the complex explain the 1:1 stoichiometry observed for the IgE-Fc-FcεRIα interaction; one FcεRIα molecule engages two IgE Cε3 domains simultaneously near the Cε2-Cε3 domain interface. In contrast, the stoichiometry of binding CD23 to IgE is 2:1 (10), with a biphasic affinity, trimeric CD23 apparently binding with an affinity an order of magnitude higher than monomeric CD23 (11).

The structure of IgE is noteworthy for a marked bend between the second and third constant domains of the Fc region. It has been suggested that this bend imparts conformational constraints on the Fab arms, which might favor cross-linking of mast cell-bound IgE by allergens with specific disposition of epitopes (12). The IgE Fc region shows an intriguing mixture of structural rigidity and conformational flexibility, with the aforementioned rigid bend between the Cε2 and Cε3 domains (5) and an unusual degree of intrinsic structural lability within the Cε3 domain (13). Conformational flexibility around the Cε3-Cε4 interface has been noted previously (14); motions around an axis at this interface control whether both Cε3 domains are in a correct orientation to bind simultaneously to the FcεRIα receptor. If only one Cε3 domain binds to FcεRIα then the affinity is about 10,000-fold weaker than when both Cε3 domains are engaged (15).

In this study we define the CD23 binding site on the Cε3 domain of IgE using NMR spectroscopy and site-directed mutagenesis. We show that the CD23 and FcεRI binding sites occur on opposite ends of the Cε3 domain of IgE. We demonstrate that allosteric inhibition prohibits simultaneous binding of these two receptors, and that this mechanism prevents engagement and cross-linking of IgE bound to mast cells by soluble CD23.

EXPERIMENTAL PROCEDURES

Protein expression and purification. Recombinant human IgE-Fc (comprised of domains Cε2-Cε4) (5), the αγ-fusion protein (the FcεRIα extracellular region fused to an IgG4 Fc) (10), soluble FcεRIα (13), derCD23 (7) and the Cε3 domain (13) were each produced and purified as described previously. MAb 7.12 was produced from a B cell hybridoma (16). Primers for site-directed mutagenesis were obtained from Sigma-Genosys (Sigma Lifescience), and mutagenesis was performed using the QuikChange II Kit (Stratagene). Mutant constructs were expressed and purified using the same methods as the wildtype proteins.

NMR spectroscopy. NMR spectroscopy was performed on protein samples in a buffer containing 25mM Tris, 125 mM NaCl, 4mM $CaCl_2$, pH 6.8, at protein concentrations between 120 and 900 μM. Data were collected at 25°C on Bruker spectrometers equipped with CryoProbes operating at 500 and 700 MHz. For chemical shift perturbation experiments, unlabelled derCD23 ligands were concentrated to 2mM and then titrated in small aliquots to samples of 200μM ^{15}N-labelled Cε3 until saturation was seen. The

NMR chemical shifts of the urea denatured and native state Cε3 domain are available from the BioMagResBank database under accession numbers 18482 and 18483.

Surface plasmon resonance. All experiments were performed on a Biacore T100 instrument (GE Healthcare), essentially as described previously (7,9). All measurements were done independently at least twice, using standard double reference subtraction methods for data analysis (17). Specific binding surfaces were prepared using standard amine coupling methods for derCD23 and the αγ-fusion protein, whereas IgE-Fc was biotinylated and captured on a streptavidin surface. Coupling densities were kept low (<100 RU) to minimize potential avidity effects. Ligands in HBS (10mM HEPES, pH 7.4, 150mM NaCl, 4mM $CaCl_2$, 0.005% surfactant p20) were injected at 25 μl/min with a 1-min association phase followed by a 15-min dissociation phase. For the sandwich binding experiments, approximately 90RU of IgE-Fc was captured on an αγ-fusion protein surface during a 1-min injection of a 10nM IgE-Fc sample; after a 3-min stabilization period, 0-100μM derCD23 was injected for 1-min followed by a 15-min dissociation phase.

FRET assay. Inhibition assays were performed by competing 1μM terbium-chelate labelled derCD23 and 0-20μM Alexa 647-labelled IgE-Fc with a range of concentrations of unlabelled αγ-fusion protein. Protein mixtures were prepared in Lanthascreen buffer (Invitrogen) in triplicate, in 384-well plates (Greiner Bio-One), and equilibrated overnight at room temperature. FRET measurements were made on an Artemis plate reader (Berthold Technologies). TR-FRET ratios were calculated for each well as the emission of acceptor at 665nm divided by the emission of donor at 620nm and then multiplied by 10,000. Apparent K_D and B_{max} values were derived from non-linear curve fitting of inhibition titrations.

Mast cell degranulation assay. The human mast cell line LAD-2 (NIH) was primed by addition of 2.5nM IgE (NIBSC) or a buffer-only control for one hour, before addition of cross-linking reagents. Polyclonal rabbit anti-human IgE (Dako) was added at 20nM and soluble CD23 constructs at 0.1, 1 and 10μM, and incubated for 1 hour at 37°C. Supernatants were harvested and tested for β-hexosaminidase release, as described previously (18). Controls included cells treated with wash buffer plus 1% Triton-X for total release, with buffer-only to measure background release, typically about 10% of total release, with 2.5nM IgE-only, and with 10μM CD23-only. The level of degranulation measured for Triton-X treated cells was defined as 100% release and all samples were compared to that.

B cell activation assays. Human tonsillar B cells were activated with IL-4 (200IU/ml) (R&D Systems), anti-CD40 antibody (1μg/ml) (G28.5; ATCC), and either 1μM derCD23 or 1μM triCD23, as described previously (19).

RESULTS

In an earlier study, we identified the IgE binding site on CD23 using NMR chemical shift perturbation studies (7). Here we performed the reciprocal NMR binding experiment, mapping the interaction site of CD23 onto the Cε3 domain from IgE. Using an approach described by Schulman *et al.* (20), we assigned the backbone resonances of the molten globule Cε3 domain by first performing resonance assignments of Cε3 denatured in 6M urea and then, through gradual titration of buffer conditions, tracking those resonances to the native state Cε3 domain. Next, we titrated unlabelled monomeric CD23 protein (derCD23) against an ^{15}N-labelled Cε3 sample and used the assigned NMR spectra to identify residues

that were affected by addition of ligand. Similar to what was observed on derCD23 in the reciprocal titration (7), a small number of Cε3 residues showed peak shifting and line broadening during the derCD23 titration (Fig. 1A), consistent with an interaction showing intermediate and fast/intermediate exchange kinetics. When mapped onto the surface of the protein, the identified residues from three discontinuous sequences (amino acids 405-407, 409-411 and 413 from the E-F helix, amino acids 377-380 from the C-D loop, and residue 436 from the C-terminal region) form a contiguous surface representing the binding site on Cε3 for CD23 (Figure 1B). A plot of change in peak intensity versus residue number can be seen in Figure S1.

This region is at the end of the Cε3 domain, near to the interface with Cε4, in contrast to the interaction site for FcεRI, which is at the other end of Cε3 near the interface with Cε2 (4,9) (Fig. 1B). Among other immunoglobulin-receptor interactions, sites analogous to the Cε3-Cε4 interface are utilized in the interactions of FcαRI with IgA (21), CHIR-AB1 with IgY (22), and FcRn, protein A and protein G with IgG (23-25). A comparison of the CD23 binding surface on IgE with the analogous IgA and IgG binding surfaces shows areas of overlap but a nonconserved interaction motif, in contrast to the striking conservation of interaction surfaces for IgE-FcεRIα and IgG-FcγR complexes (4).

The identification of this CD23 interaction site on IgE provides a structural explanation for the experimentally observed 2:1 (CD23:IgE) stoichiometry (10), as the dimeric IgE-Fc can bind to two separate CD23 lectin head domains. The two CD23 interactions were shown to have slightly different binding affinities and thermodynamic characteristics (10), as was also observed for the FcαRI-IgA interaction (21). The two binding affinities imply an asymmetry of the two CD23 binding sites, which may possibly be allosterically induced. CD23's capacity for inducing a conformational change in IgE is discussed further below.

Following the NMR mapping of interaction epitopes for both proteins, we used site-directed mutagenesis to validate the interaction site in the context of the full IgE-Fc construct and to define the energetic contributions of individual residues. Ten mutants from derCD23 and eleven mutants from IgE-Fc (domains Cε2-4) were produced, purified and characterized; their binding affinities were measured using an SPR assay (7). Table 1 summarizes the results of the site-directed mutagenesis studies. Mutations on both proteins that affect binding are entirely consistent with the NMR-defined interaction sites. Charged residues have the largest energetic effect on binding. CD23 mutations D227A, E257A, R224A and R188A all show a change in binding free energy (ΔΔG) of about +6 kJ mol^{-1} (Table 1). Uncharged residues also contribute to the binding energy; a prominently exposed tyrosine residue (Y189) in the center of CD23's IgE binding site makes a substantial contribution to binding energy. The CD23 binding surface on IgE is also predominantly electrostatic, with residues D409, E412, R376 and K380 showing the largest effects on CD23 binding energetics. Because the NMR data indicated a site on Cε3 very near to the Cε4 interface (Fig. 1B) and because binding sites from several other immunoglobulin-receptor interactions involve sites analogous to the Cε3-Cε4 interface (21-23), we also made a pair of mutations in the F-G loop of the Cε4 domain, close to the CD23 binding site in Cε3. However, neither Q535A nor Q538A appear to affect CD23 binding, leading

us to believe that CD23's binding surface on IgE is largely restricted to residues from Cε3.

Earlier studies indicated that soluble CD23 can compete with FcεRI binding, and this was attributed to steric competition for an overlapping binding site within the Cε3 domain (26,27). However, our data show that the CD23 and FcεRI binding sites are spatially distinct and suggest that the mechanism of mutual inhibition must be allosteric in nature. We performed a set of competitive binding assays to confirm this experimentally. Firstly, using an SPR assay, we showed that derCD23 can bind to IgE-Fc immobilized to an SPR chip but cannot bind to IgE-Fc captured by immobilized FcεRIα (Fig. 2A,B); a positive control, a Fab fragment of the anti-IgE antibody 7.12 (16), directed against the Cε2 domain, did bind to FcεRIα-captured IgE-Fc (data not shown). Secondly, we showed that IgE-Fc can bind to immobilized derCD23, but an IgE-Fc-sFcεRIα complex cannot bind to derCD23 (Fig. 2C,D). These data indicate that CD23 and FcεRI interactions with IgE are mutually inhibitory. Finally, we also tested the ability of the receptors to compete for binding to IgE in a solution TR-FRET experiment (28). This assay can be performed under equilibrium binding conditions, allowing a different set of mechanistic properties to be tested than in the kinetic SPR experiments. Under equilibrium conditions, different inhibition patterns are observed for competitive and allosteric inhibitors. A competitive inhibitor affects the apparent binding affinity, with inhibitor I reducing the apparent affinity by a ratio of $(1+[I]/K_I)$; whereas an allosteric inhibitor affects the apparent B_{max} of the interaction without changing the apparent K_D (29). Soluble FcεRIα inhibits the IgE-Fc-derCD23 interaction (Fig. 2E) and derCD23 inhibits the IgE-Fc-FcεRIα interaction (Fig. 2F), and both inhibitors result in a decrease of apparent interaction B_{max} values without affecting the apparent K_D of the interactions. These experiments confirm mutual inhibition by the two IgE receptors and offer experimental evidence that an allosteric mechanism is involved.

Given the location of the CD23 binding site, the most obvious mechanism for allostery is a conformational change around the interface between the Cε3 and Cε4 domains. Crystal structures of IgE-Fc and IgE-Fc-FcεRIα complexes indicate that the Cε3 domains can exist in "open" and "closed" states, with only an open state being capable of binding FcεRI (4,9,14). A detailed study of the open and closed states concluded that it is the motions around the Cε3 A-B helix, sitting at the Cε3-Cε4 interface, that control the orientation of the two Cε3 domains (14). Indeed, Wurzburg *et al.* suggested that the Cε3-Cε4 domain interface might serve as a drug target for allosteric inhibitors of FcεRI binding. It appears that nature has already utilized this approach to modulate FcεRI binding of IgE by CD23.

Soluble trimeric CD23 has been shown to bind to and cross-link membrane IgE on B cells, resulting in B cell activation (19). However, it is essential that trimeric CD23 not cross-link IgE bound to FcεRI on the surface of mast cells. If this were to occur then high levels of CD23 would result in mast cell activation in the absence of allergens. Our data from binding experiments (Fig. 2B) predict that soluble CD23 cannot directly cross-link IgE bound to FcεRI on mast cells. We tested this prediction in a mast cell degranulation assay using the $FcεRI^+$ LAD-2 human mast cell line. In this assay, cells are first primed by adding IgE, followed by addition of potential cross-linking reagents and measurement of release of the mast cell granule-associated enzyme β-

hexosaminidase. An anti-IgE antibody results in FcεRI-mediated activation of the mast cell and robust β-hexosaminidase release, but the addition of either the monomeric derCD23 or a trimeric CD23 construct (triCD23) fails to induce mast cell degranulation (Fig. 3A). In contrast, trimeric CD23 effectively cross-links IgE on B cells, resulting in activation of these cells and increased production of soluble IgE (19) (Fig. 3B).

DISCUSSION

Immunoglobulins have evolved two separate sites for binding to receptors. One site is near the hinge region in IgG and at the Cε2-Cε3 interface in IgE, while the other is at the interface of the C-terminal domain and the penultimate domain: the Cε3-Cε4 interface in IgE. A mechanism of communication has evolved within the IgE molecule between these two distant sites to prevent simultaneous engagement of CD23 and FcεRI. This may be a unique property of IgE; it is known, for example, that IgG binding of either FcRn or protein A at the Cγ2-Cγ3 interface does not affect binding of FcγRIIa at the hinge region (30). Since IgE and CD23 both exist in membrane bound and soluble forms, and soluble FcεRIα has also recently been shown to exist at functionally relevant concentrations (31), there is considerable potential for receptor cross-regulation. Mutually exclusive receptor binding assures independent functions for IgE-FcεRI and IgE-CD23 interactions.

IgE is a clinically important drug target. An anti-IgE antibody (omalizumab) is an effective therapy, currently used in the treatment of moderate to severe asthma that is not controlled by corticosteroids. Omalizumab binds to the Cε3 domain of IgE and competitively inhibits FcεRI binding, although its *in vivo* activity relies on more than just inhibition of this interaction (32). Results presented here demonstrate that IgE is amenable to allosteric inhibition, an approach that may have significant advantages over competitive inhibition (33), and lay the foundation for the development of allosteric modulators of IgE-receptor interactions.

REFERENCES

1. Gould, H. J., Sutton, B. J., Beavil, A. J., Beavil, R. L., McCloskey, N., Coker, H. A., Fear, D., and Smurthwaite, L. (2003) *Annu Rev Immunol* **21**, 579-628
2. Aubry, J. P., Pochon, S., Graber, P., Jansen, K. U., and Bonnefoy, J. Y. (1992) *Nature* **358**, 505-507
3. Luo, H. Y., Hofstetter, H., Banchereau, J., and Delespesse, G. (1991) *J Immunol* **146**, 2122-2129
4. Garman, S. C., Wurzburg, B. A., Tarchevskaya, S. S., Kinet, J. P., and Jardetzky, T. S. (2000) *Nature* **406**, 259-266
5. Wan, T., Beavil, R. L., Fabiane, S. M., Beavil, A. J., Sohi, M. K., Keown, M., Young, R. J., Henry, A. J., Owens, R. J., Gould, H. J., and Sutton, B. J. (2002) *Nat Immunol* **3**, 681-686
6. Garman, S. C., Kinet, J. P., and Jardetzky, T. S. (1998) *Cell* **95**, 951-961
7. Hibbert, R. G., Teriete, P., Grundy, G. J., Beavil, R. L., Reljic, R., Holers, V. M., Hannan, J. P., Sutton, B. J., Gould, H. J., and McDonnell, J. M. (2005) *J Exp Med* **202**, 751-760
8. Wurzburg, B. A., Tarchevskaya, S. S., and Jardetzky, T. S. (2006) *Structure* **14**, 1049-1058
9. Holdom, M. D., Davies, A. M., Nettleship, J. E., Bagby, S. C., Dhaliwal, B., Girardi, E., Hunt, J., Gould, H. J., Beavil, A. J., McDonnell, J. M., Owens, R. J., and Sutton, B. J. (2011) *Nat Struct Mol Biol* **18**, 571-576
10. Shi, J., Ghirlando, R., Beavil, R. L., Beavil, A. J., Keown, M. B., Young, R. J., Owens, R. J., Sutton, B. J., and Gould, H. J. (1997) *Biochemistry* **36**, 2112-2122
11. Dierks, S. E., Bartlett, W. C., Edmeades, R. L., Gould, H. J., Rao, M., and Conrad, D. H. (1993) *J Immunol* **150**, 2372-2382
12. Hunt, J., Keeble, A. H., Dale, R. E., Corbett, M. K., Beavil, R. L., Levitt, J., Swann, M. J., Suhling, K., Ameer-Beg, S., Sutton, B. J., and Beavil, A. J. (2012) *J Biol Chem* **287**, 17459-17470
13. Price, N. E., Price, N. C., Kelly, S. M., and McDonnell, J. M. (2005) *J Biol Chem* **280**, 2324-2330
14. Wurzburg, B. A., Garman, S. C., and Jardetzky, T. S. (2000) *Immunity* **13**, 375-385
15. Hunt, J., Beavil, R. L., Calvert, R. A., Gould, H. J., Sutton, B. J., and Beavil, A. J. (2005) *J Biol Chem* **280**, 16808-16814
16. Kanowith-Klein, S., Hofman, F., and Saxon, A. (1988) *Clin Immunol Immunopathol* **48**, 214-224
17. Myszka, D. G. (1999) *J Mol Recognit* **12**, 279-284
18. Hammond, G., and Koffer, A. (2006) Secretion Assays. in *Cell Biology* (Celis, J. E. ed.), Third Ed., Elsevier, Amsterdam.
19. Cooper, A. M., Hobson, P. S., Jutton, M. R., Kao, M. W., Drung, B., Schmidt, B., Fear, D. J., Beavil, A. J., McDonnell, J. M., Sutton, B. J., and Gould, H. J. (2012) *J Immunol* **188**, 3199-3207
20. Schulman, B. A., Kim, P. S., Dobson, C. M., and Redfield, C. (1997) *Nat Struct Biol* **4**, 630-634
21. Herr, A. B., White, C. L., Milburn, C., Wu, C., and Bjorkman, P. J. (2003) *J Mol Biol* **327**, 645-657
22. Taylor, A. I., Sutton, B. J., and Calvert, R. A. (2010) *Dev Comp Immunol* **34**, 97-101
23. Martin, W. L., West, A. P., Jr., Gan, L., and Bjorkman, P. J. (2001) *Mol Cell* **7**, 867-877
24. Deisenhofer, J. (1981) *Biochemistry* **20**, 2361-2370

25. Sauer-Eriksson, A. E., Kleywegt, G. J., Uhlen, M., and Jones, T. A. (1995) *Structure* **3**, 265-278
26. Suemura, M., Kikutani, H., Sugiyama, K., Uchibayashi, N., Aitani, M., Kuritani, T., Barsumian, E. L., Yamatodani, A., and Kishimoto, T. (1991) *Allergy Proc* **12**, 133-137
27. Kelly, A. E., Chen, B. H., Woodward, E. C., and Conrad, D. H. (1998) *J Immunol* **161**, 6696-6704
28. Selvin, P. R. (2002) *Annu Rev Biophys Biomol Struct* **31**, 275-302
29. Fersht, A. (1999) *Structure and Mechanism in Protein Science.*, W.H. Freeman, New York
30. Wines, B. D., Powell, M. S., Parren, P. W., Barnes, N., and Hogarth, P. M. (2000) *J Immunol* **164**, 5313-5318
31. Dehlink, E., Platzer, B., Baker, A. H., Larosa, J., Pardo, M., Dwyer, P., Yen, E. H., Szepfalusi, Z., Nurko, S., and Fiebiger, E. (2011) *PLoS One* **6**, e19098
32. Babu, K. S., Arshad, S. H., and Holgate, S. T. (2001) *Allergy* **56**, 1121-1128
33. Schon, A., Lam, S. Y., and Freire, E. (2011) *Future Med Chem* **3**, 1129-1137

Acknowledgements: We thank Dr. Rebecca Beavil (King's College London) for the gift of mAb 7.12 and Dr. Malcom Begg (GlaxoSmithKline, Stevenage, UK) for assistance with LAD-2 cell culture. Research was supported by grants from the Wellcome Trust and the Medical Research Council.

FIGURE LEGENDS

Figure 1. NMR mapping of the CD23 and IgE interaction surfaces. (A) Increasing amounts of unlabelled derCD23 were added to a 200μM sample of ^{15}N-labelled Cε3; five spectra of the titration are overlaid (red, zero derCD23; magenta, 50μM; blue, 100μM; cyan, 150μM; green, 200 μM). Insets show magnified views of the indicated regions. (B) The NMR-derived derCD23 interaction site on Cε3 was mapped onto the structure of IgE-Fc (1F6A [6]) and shown as surface representation. For comparison, the residues of IgE that interact with FcεRI are indicated in green. (C) The IgE interaction surface on CD23 was defined previously [7] and shown here as a surface representation. The interacting surfaces of IgE and CD23 are coloured according to electrostatic potential and coded such that regions with a potential <−4 k_BT are red, whereas those >4 k_BT are blue (k_B, Boltzmann constant; T, absolute temperature).

Figure 2. Competition binding experiments between derCD23 and sFcεRIα for IgE-Fc. The binding of derCD23 was tested against (A) IgE-Fc immobilized on a sensor surface and (B) IgE-Fc captured on an FcεRIα-immobilized surface; the start of the derCD23 injection is indicated with an arrow. DerCD23 binding to immobilized IgE-Fc with a K_D of 2.3μM; no measureable binding was observed for derCD23 to IgE-Fc complexed to FcεRIα. (C) The binding of IgE-Fc to immobilized derCD23 was compared with (D) the binding of a complex of IgE-Fc/sFcεRIα to the same surface; the start of the injection of the complex is indicated with an arrow. IgE-Fc binds to derCD23 with a K_D of 2.4μM, but the IgE-Fc/sFcεRIα complex does not bind to derCD23. All SPR binding experiments were performed using identical two-fold serial dilutions of ligands, from 40μM to 78nM. (E) Binding between terbium-labelled derCD23

and Alexa 647-labelled IgE-Fc was measured in a solution TR-FRET assay in the presence of increasing concentrations of unlabelled αγ-fusion protein as inhibitor; zero (black), 0.5nM (red), 2.5nM (blue) and 5nM (green). (F) Binding between terbium-labelled αγ-fusion protein and Alexa 647-labelled IgE-Fc was measured with increasing concentrations of unlabelled derCD23 as inhibitor; zero (black), 25μM (red), 50μM (blue) and 185μM (green).

Figure 3. Soluble CD23 does not cross-link IgE bound to FcεRI on mast cells. The ability of soluble CD23 to engage IgE on B cells and mast cells was tested. (A) After preincubation of IgE, the addition of anti-IgE antibody results in activation of the FcεRIα$^+$ LAD-2 mast cell line, as measured by release of β-hexosaminidase. Neither monomeric derCD23 nor trimeric triCD23 is able to cross-link IgE and activate mast cells in this assay. (B) In contrast, triCD23 effectively cross-links mIgE on the surface of IgE$^+$ human tonsillar B cells, resulting in activation of these cells and increased secretion of IgE. B cell cultures were activated with IL-4 and anti-CD40, and soluble CD23 was added at 1μM; supernatants were harvested 12 days after activation, tested for IgE levels and compared with levels for cells treated with IL-4/anti-CD40 alone (*=$p<0.05$; **=$p<0.01$). The regulatory activities of soluble CD23 on IgE$^+$ B cells are described in detail in (19).

Table 1. Effects of mutations on the IgE-CD23 interaction

IgE-Fc mutation	K_D (μM)	ΔΔG (kJ mol^{-1})	derCD23 mutation	K_D (μM)	ΔΔG (kJ mol^{-1})
wildtype	2.3	-	wildtype	2.3	-
D409A	26.3	+6.0	D227A	30.9	+6.4
E412A	24.2	+5.8	E257A	26.7	+6.1
R376A	19.7	+5.3	R224A	26.2	+6.0
K380A	13.3	+4.3	R188A	25.0	+5.9
K435A	5.0	+1.9	Y189A	15.6	+4.7
K352A	3.8	+1.2	K276A	10.9	+3.9
R351A	2.6	+0.3	L226A	6.6	+2.6
D347A	2.5	+0.2	D236A	5.8	+2.3
P439A	2.5	+0.2	D192A	4.3	+1.6
Q535A	2.5	+0.2	E265A	2.5	+0.2
Q538A	2.4	+0.1			

FIGURE 1

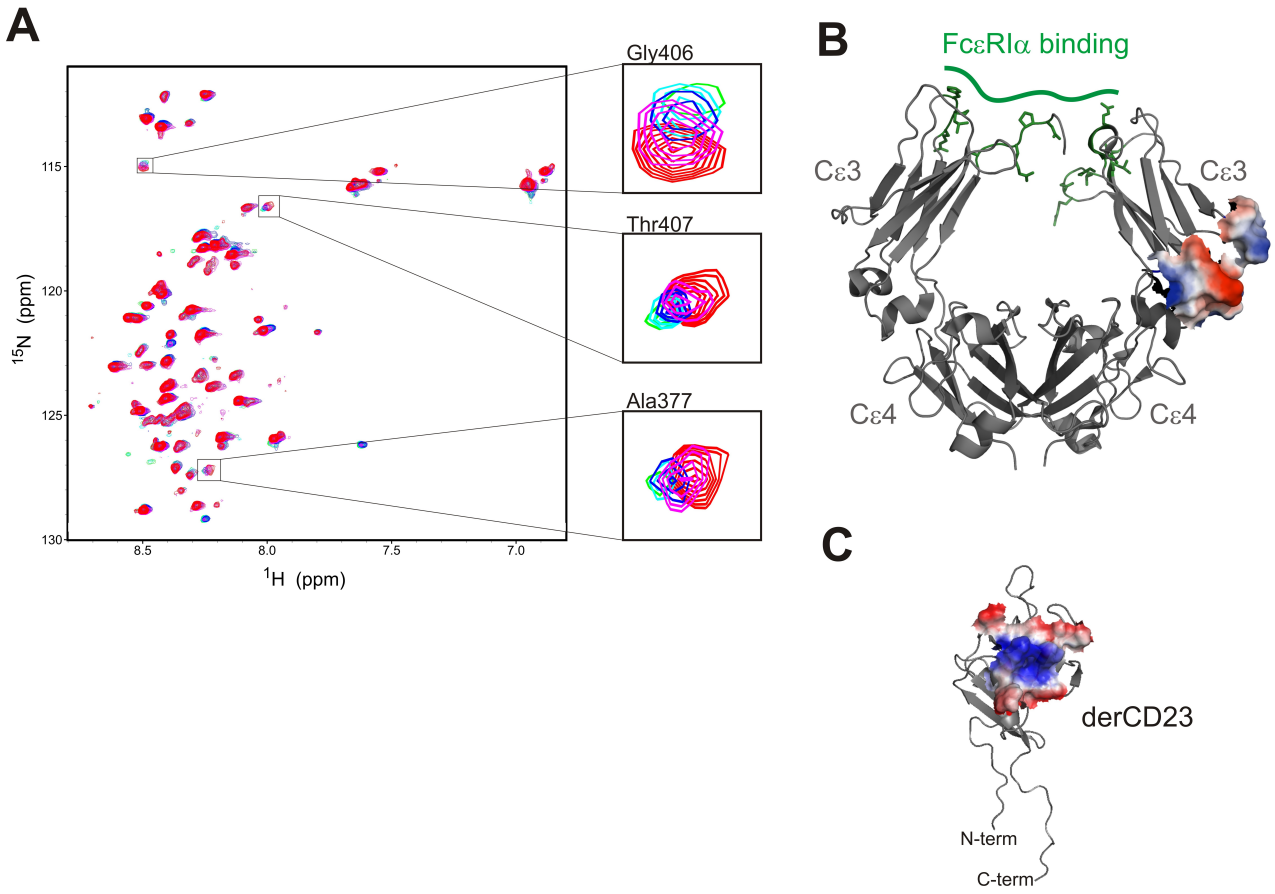

FIGURE 2

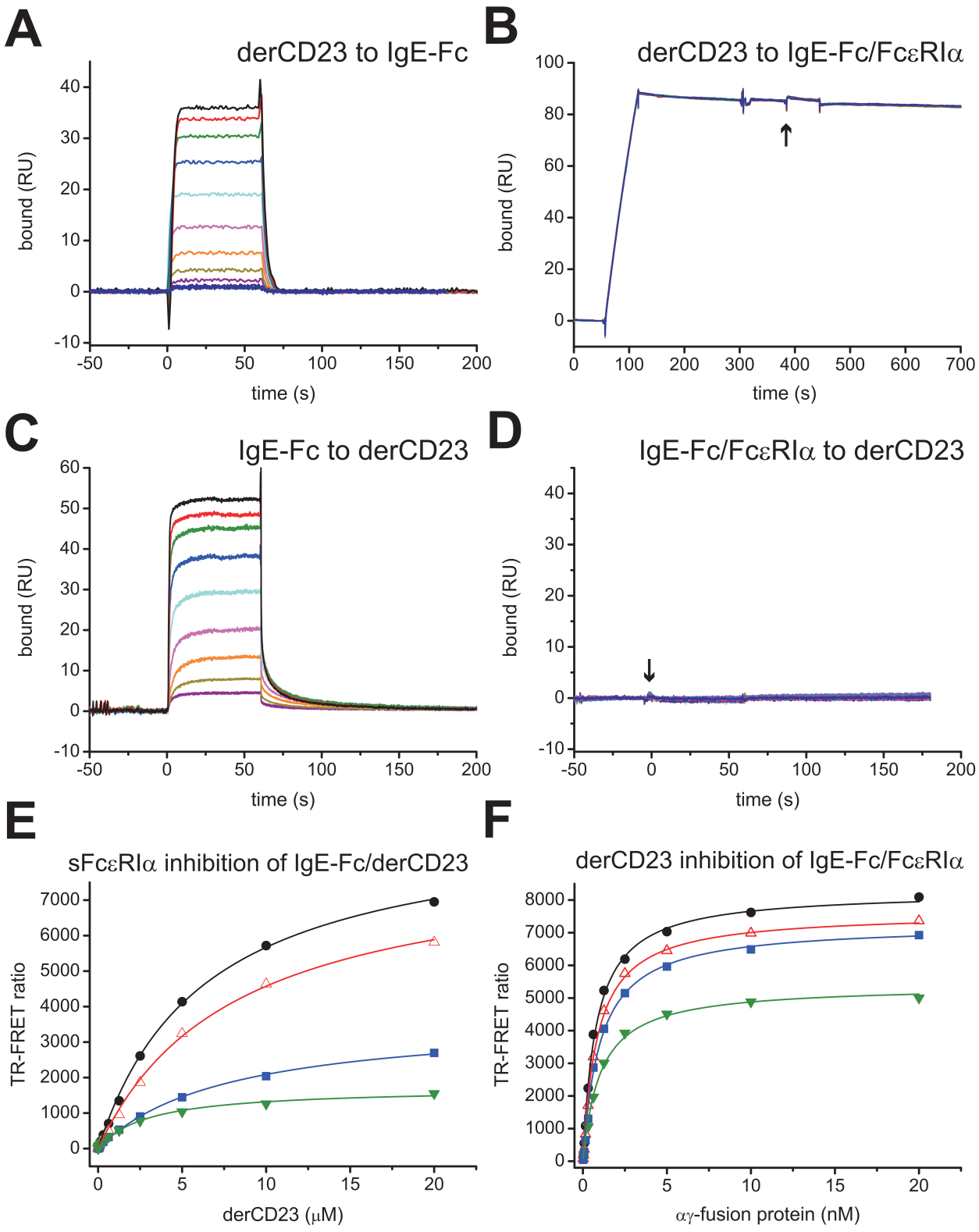

FIGURE 3

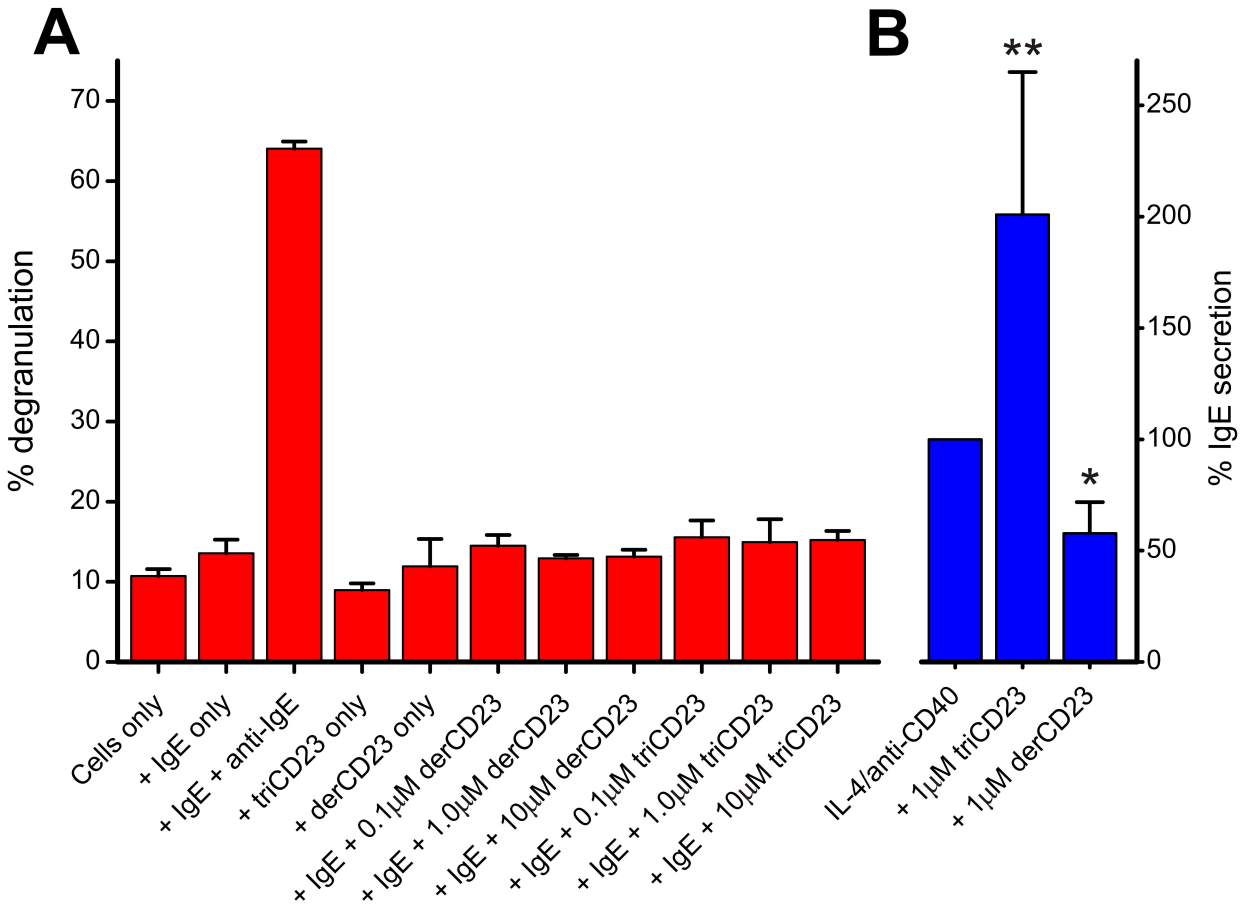

OPEN ACCESS Freely available online

PLoS one

High Resolution Analysis of the Chromatin Landscape of the IgE Switch Region in Human B Cells

Sandeep Dayal[1], Jakub Nedbal[2,3,4], Philip Hobson[2,3,4], Alison M. Cooper[2,3,4], Hannah J. Gould[2,3,4], Martin Gellert[1], Gary Felsenfeld[1]*, David J. Fear[2,3]*

1 Laboratory of Molecular Biology, National Institute of Diabetes and Digestive and Kidney Diseases, National Institutes of Health, Bethesda, Maryland, United States of America, **2** Division of Asthma, Allergy and Lung Biology, King's College London, London, United Kingdom, **3** Medical Research Council and Asthma UK Centre in Allergic Mechanisms of Asthma, King's College London, London, United Kingdom, **4** Randall Division of Cell and Molecular Biophysics, King's College London, London, United Kingdom

Abstract

Antibodies are assembled by a highly orchestrated series of recombination events during B cell development. One of these events, class switch recombination, is required to produce the IgG, IgE and IgA antibody isotypes characteristic of a secondary immune response. The action of the enzyme activation induced cytidine deaminase is now known to be essential for the initiation of this recombination event. Previous studies have demonstrated that the immunoglobulin switch regions acquire distinct histone modifications prior to recombination. We now present a high resolution analysis of these histone modifications across the IgE switch region prior to the initiation of class switch recombination in primary human B cells and the human CL-01 B cell line. These data show that upon stimulation with IL-4 and an anti-CD40 antibody that mimics T cell help, the nucleosomes of the switch regions are highly modified on histone H3, accumulating acetylation marks and tri-methylation of lysine 4. Distinct peaks of modified histones are found across the switch region, most notably at the 5′ splice donor site of the germline (I) exon, which also accumulates AID. These data suggest that acetylation and K4 tri-methylation of histone H3 may represent marks of recombinationally active chromatin and further implicates splicing in the regulation of AID action.

Citation: Dayal S, Nedbal J, Hobson P, Cooper AM, Gould HJ, et al. (2011) High Resolution Analysis of the Chromatin Landscape of the IgE Switch Region in Human B Cells. PLoS ONE 6(9): e24571. doi:10.1371/journal.pone.0024571

Editor: Brian P. Chadwick, Florida State University, United States of America

Received June 29, 2011; **Accepted** August 12, 2011; **Published** September 20, 2011

Funding: D.F. is a Research Councils U.K. funded Fellow and has been further supported by Asthma U.K. funded core support for the MRC & Asthma U.K. Centre for Allergic Mechanisms of Asthma. This work has been supported by a Biotechnology and Biological Sciences Research Council grant BB/H019634/1, and the Intramural Research Program of the National Institute of Diabetes and Digestive and Kidney Diseases, National Institutes of Health, USA. The authors further acknowledge financial support from the UK Department of Health via the National Institute for Health Research (NIHR) Comprehensive Biomedical Research Centre award to Guy's & St Thomas' NHS Foundation Trust in partnership with King's College London. The funders had no role in study design, data collection and analysis, decision to publish, or preparation of the manuscript.

Competing Interests: The authors have declared that no competing interests exist.

* E-mail: david.fear@kcl.ac.uk (DJF); garyf@intra.niddk.nih.gov (GF)

Introduction

Antibodies, which are essential components of vertebrate adaptive immunity, are produced as a result of complex genome rearrangements and mutation events in the B cell receptor loci. In developing B lymphocytes, V(D)J recombination at immunoglobulin heavy and light chain loci results in a diverse repertoire of antigen binding specificities necessary for the recognition of a spectrum of foreign antigens. During the immune response, somatic hypermutation (SHM) and affinity maturation refine these specificities through the introduction of mutations into the variable regions while class switch recombination (CSR) exchanges the constant regions of the immunoglobulin heavy chains (IgH) to produce the different antibody isotypes, or classes. The germline IgH locus consists of a linear array of constant region (C_H) genes spanning over one hundred kilobases, with Cμ, which encodes IgM, proximal to the rearranged V(D)J gene segments [1]. With the exception of Cδ, each downstream C_H gene contains an individual promoter, short intervening (I) exon and a 2–10 kb switch (S) region followed by coding region exons [2]. During CSR, DNA double strand breaks (DSBs) are generated in the donor (initially Sμ) and downstream target switch regions [3,4]. These switch regions then recombine to place the target C_H immediately downstream of the assembled V(D)J gene segments, allowing the expression of a new immunoglobulin isotype whilst maintaining antigen specificity [5].

In the past few decades some of the key components and mechanistic steps of CSR have been elucidated. The enzyme activation induced cytidine deaminase (AID) has been shown to play a central role in both SHM and CSR [6–8]. Extracellular cytokine signals initiate CSR by activating transcription of donor and target C_H genes (germline transcription, GLT) [9] and upon further signalling by CD40-ligand, or one of its analogs [10,11], recombination ensues. AID deaminates deoxycytidines within IgH switch regions, converting them to deoxyuridines [12–14]. If there are two close-lying events on opposite strands, the resulting U:G mismatches initiate a cascade of activities that ultimately result in the formation of DNA DSBs in the donor and target switch regions [15,16]. DNA repair mechanisms resolve these DSBs, ligating the donor and target switch regions, moving the target C_H exons adjacent to the expressed V(D)J gene segments [17].

Chromatin structure is known to play an important role in most, if not all, vertebrate processes that require direct access to DNA, such as transcription, replication and recombination. In many cases, distinct post-translational modifications in the N-terminal histone tails correlate strongly with "active" or "silent" transcriptional states. For example, acetylation of histones H3 and H4 marks regions of transcriptionally active chromatin, whereas tri-methylation of histone H3 at lysine 27 is associated with transcriptionally silent loci [18]. Local chromatin accessibility is changed by alterations in nucleosome positioning through ATP-dependent remodelling activities or through the recruitment of histone modification enzymes such as histone acetyl transferases (HATs) or histone methyl transferases (HMTs) [19].

Several lines of evidence have suggested that switch region chromatin structure plays a key role in promoting a permissive environment required for AID attack. Hyperacetylation of histones H3 and H4 and tri-methylation of histone H3 on lysine 4 (K4) and lysine 9 (K9) have previously been shown to be associated with activated switch regions in both mice and humans [20–25]. However, the present work is the first to examine chromatin structure over a human switch region at high resolution.

We have focused on the histone modifications that occur prior to CSR to IgE in human B cells. IgE is the antibody class that mediates the allergic response and its regulation is therefore of considerable interest. In particular, we have investigated the changes in chromatin structure that occur under conditions that induce ε germline gene transcription; an event that precedes, and is necessary for, CSR to IgE [26–28]. Purified B cells from different individuals undergo class switching at low and variable frequencies and show considerable variation in chromatin changes associated with this process [23]. This variability has previously made these events difficult to analyse in the human system. Here we have taken advantage of the availability of both cultured cells from a human B cell line (CL-01) and purified tonsil B cells from several donors. Although the CL-01 cell line was initially reported to undergo CSR to IgG, IgA and IgE following cytokine and CD40 stimulation [27,29] several laboratories, including our own, have found that this line now appears to have lost this ability (E. Max personal communication). While this would be a limitation for the analysis of the combined steps of immunoglobulin class switching (germline gene transcription, DNA recombination and B cell differentiation into immunoglobulin-secreting plasma cells), it reduces complexity to the single, essential, initial step of germline gene transcription: an event that occurs in the CL-01 cells and takes place in all primary human B cells, rather than a minor population [28]. This combination of sample materials allows us to robustly identify key chromatin remodelling events that occur at the Ig locus upon stimulation of εgermline transcription (εGLT) in the human system.

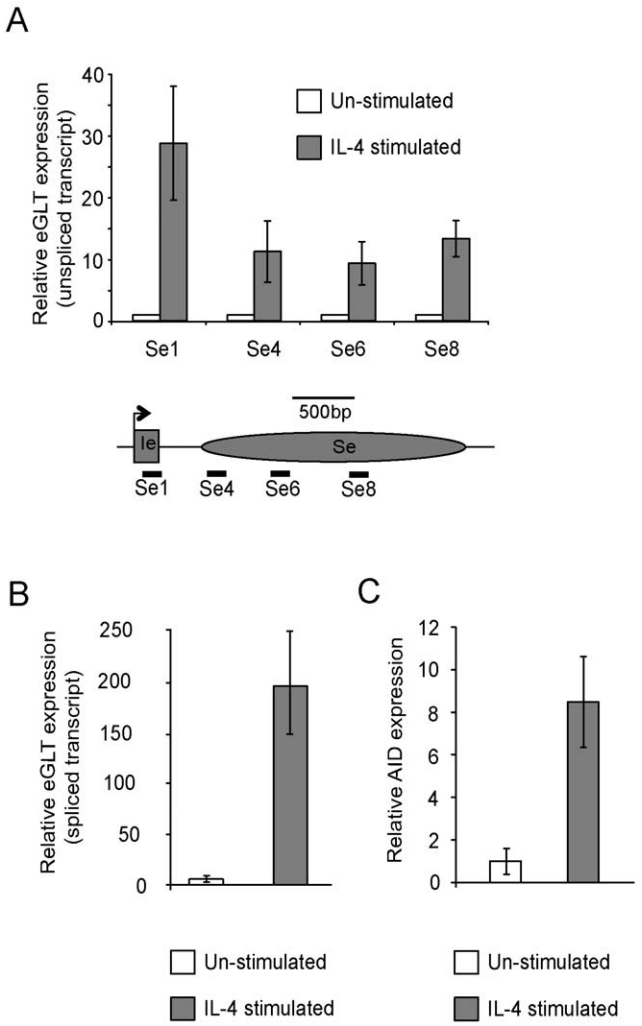

Figure 1. Analysis of ε germline gene transcripts and AID expression in CL-01 cells. Steady state transcript levels were quantified by qRT-PCR using HPRT as an endogenous control. All results are represented as changes relative to unstimulated CL-01 cells. The mean result from 3 separate experiments is shown. Error bars display standard deviation. Induction of (A) primary (un-spliced) ε germline gene transcripts, (B) mature (spliced) ε germline transcripts and (C) AID, in CL-01 cells following IL-4 stimulation for 72 hours. A schematic representation of the Ig ε locus is shown in panel A, with the elements approximately to scale, indicating the location of the primer/TaqMan probe sets used for the analysis of primary ε germline gene transcripts. Mature (spliced) ε germline transcripts were detected using a forward primer and TaqMan probe located in Iε and reverse primer in C_H ε exon 1 (not shown).
doi:10.1371/journal.pone.0024571.g001

Results

Effect of IL-4 stimulation on CL-01 cells

We began by using the CL-01 cell line to investigate the chromatin changes associated with the initiation of CSR to IgE in human B cells. These cells have been reported to initiate germline transcription of this region in response to IL-4 [27,29,34]. In order to investigate the human IgE switch region at high resolution, PCR primers were designed at unique sites spanning a region from Iε-Sε (Fig. S1). Four primers sets spanning Iε-Sε were used to quantify the expression level of primary (unspliced) ε germline transcripts (Fig. 1A). As expected, unstimulated cells expressed low levels of εGLT. Consistent with changes associated with the early stages of CSR, addition of IL-4 to the cultures for 72 hours resulted in a 10- to 30-fold increase in the primary transcript expression level. At this time point the change in the level of spliced εGLT was even greater, over 150 fold (Fig. 1B), while AID levels increased 8 fold (Fig. 1C), compared to the unstimulated cells.

Given the marked effect of IL-4 on transcription, we asked whether the addition of IL-4 also altered chromatin structure and acquisition of histone modifications over this region. The average nucleosome density (nucleosome occupancy) across Iε-Sε (Fig. 2) was determined, as previously described [31], to investigate the gross chromatin structure and thus general accessibility of the IgE

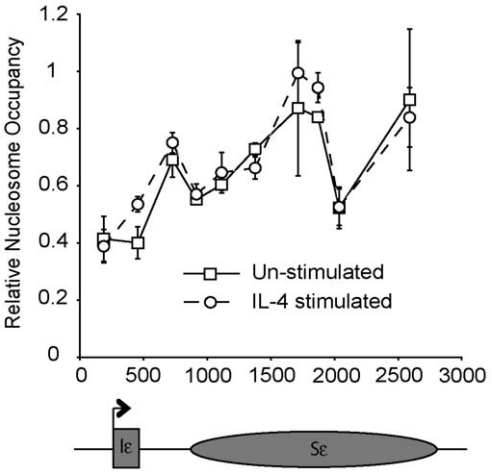

Figure 2. Nucleosome occupancy over Sε in CL-01 cells. Nucleosome occupancy over Sε was assessed in a mononucleosome chromatin fraction and compared to genomic DNA. The relative abundance of each primer location following ChIP was determined by qPCR. The mean result from 3 separate chromatin preparations is shown. Error bars display standard deviation. Data from un-stimulated cells is shown by squares and solid lines and stimulated cells by circles and dashed lines. A schematic representation of the Ig ε locus is shown, with the elements approximately to scale, indicating the position of each primer/TaqMan probe set plotted on the X axis.
doi:10.1371/journal.pone.0024571.g002

switch region. Although nucleosome occupancy did not change following IL-4 treatment, nucleosome density increased from Iε towards the 3′ end of Sε in both the stimulated and un-stimulated cells. The presence of the histone variant H2A.Z is known to correlate with transcriptionally accessible chromatin structures [35], thus the accumulation of this variant was also investigated. Consistent with the nucleosome occupancy data, no changes in H2A.Z levels were seen upon IL-4 stimulation (Fig. S2).

We next surveyed the switch region for a range of histone modifications commonly associated with gene activation or repression. Following IL-4 stimulation, there were significant increases in the diacetylation of lysines 9 and 14 on histone H3 (AcH3) and tri-methylation of histone H3 lysine 4 (H3K4me3, Fig. 3). Although both of these modifications were increased across the whole Iε-Sε region, they were particularly enriched near the DNA encoding the Iε exon 5′ splice donor site and were markedly less abundant 3′ of Iε and at the 5′ end of Sε. IL-4 stimulation resulted in no significant change in histone H4 acetylation (AcH4) or histone H3K4 di-methylation (H3K4me2, Fig. S3), although these modifications were enriched in the vicinity of the Iε splice donor in both conditions. Little or no change was observed upon stimulation in H3 tri-methylation at K9 (H3K9me3), K27 (H3K27me3) or K36 (H3K36me3) (Fig. S3). However H3K9me3 and H3K27me3 levels were slightly depleted relative to input (values$<$1), indicating that these characteristic marks of inactive chromatin modifications are under-represented in this region.

Effect of IL-4 and CD40 stimulation on CL-01 cells

Although IL-4 stimulation is sufficient to initiate εGLT expression (Figs. 1A and 1B), a "second signal" such as CD40 ligation, is required to initiate class switch recombination [10,36]. IL-4 stimulation of CL-01 cells results in greatly increased tri-methylation of lysine 4 and acetylation of histone H3 around Iε (Fig. 3). We wished to determine whether the addition of the

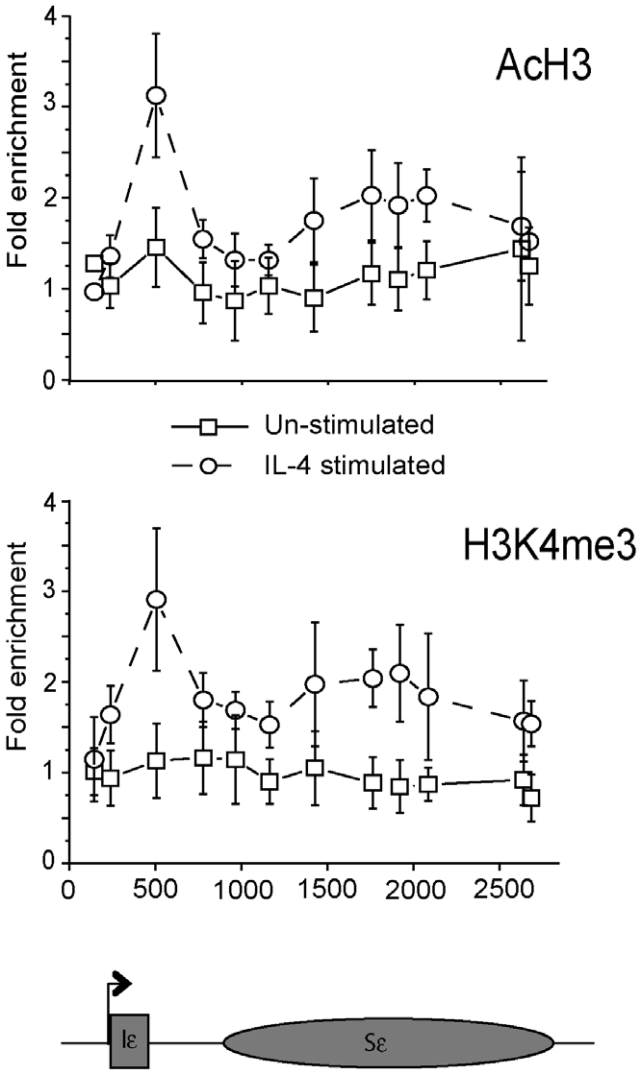

Figure 3. ChIP analysis of histone modifications at the Ig ε locus in CL-01 cells following IL-4 stimulation. Levels of di-acetylated (K9 and K14) histone H3 (top panel) and histone H3 tri-methylated at K4 (bottom panel) were assessed by ChIP using size-selected native chromatin to ensure high resolution. Analysis of histone modifications was carried out in CL-01 cells cultured for 72 hours with or without IL-4 stimulation. Mean results from 3 separate chromatin extractions are plotted as fold enrichments over an input control. Data from unstimulated cells is shown by squares and solid lines and stimulated cells by circles and dashed lines. Error bars show standard deviations. A schematic representation of the Ig ε locus is shown below the graphs, with the elements approximately to scale, indicating the position of each primer/TaqMan probe set plotted on the X axis.
doi:10.1371/journal.pone.0024571.g003

second signal altered the pattern of accumulation of these histone modifications over Sε. In addition to the increase in H3 acetylation and K4 tri-methylation (Fig. 3), previous studies had demonstrated increased tri-methylation of histone H3 lysine 9 at switch regions following stimulation of CSR [23] [25]; therefore these modifications were chosen for further analysis following culture of CL-01 cells with IL-4 and anti-CD40 antibody (Fig. S4).

No further changes in histone modifications were seen upon addition of anti-CD40 (and IL-4) to the cultures, compared to IL-4 alone. As for the IL-4 stimulated cells, AcH3 and H3K4me3 levels increased dramatically near the Iε exon 5′ splice site but

were increased to a lesser extent over the switch region; H3K9me3 did not change in response to either mode of stimulation (Fig. S4).

Effect of IL-4 and CD40 stimulation on primary human B cells

To gain greater insights into the changes in Sε chromatin structure associated with human class switch recombination, we extended our studies to total primary B cells purified from tonsils from five human donors (Fig. 4). Cells were stimulated with IL-4 and anti-CD40 for 48 hours, when the highest levels of germline transcripts were observed in these cells (data not shown). In primary human B cells, stimulation with IL-4 and anti-CD40 results in CSR to IgG and IgE [28,37,38]. In order to investigate whether histone modification occurs differentially at IgG versus IgE, histone H3 acetylation and K4 tri-methylation were also measured at the Iγ1 promoter and a unique site within the γ1 switch region. Extensive sequence similarity within the IgG subtypes prevented a high resolution analysis of this gene. For comparison, histone modifications were also investigated at two genes not expressed in B cells: *myf4* (a transcription factor involved in myocyte differentiation) and *NeuroD1* (a transcription factor involved in neurogenesis).

Although specific distribution patterns were variable in the primary B cells, histone H3 acetylation (AcH3) levels increased (up to 20-fold) in all samples over Iε and Sε following stimulation with IL-4 and anti-CD40 (Fig. 4). As was seen in the CL-01 cells, in samples 1, 4 and 5, a distinct peak of acetylation was seen at the Iε exon 5′ splice site; no such peak was seen in sample 2 or 3, although acetylation levels did increase significantly following stimulation. With the exception of the Iε primers in sample 3, acetylation levels tended to be low 5′ of I exons but were significantly higher across the switch regions. In all samples except sample 3, acetylation levels were higher at the γ1 primer sets than the corresponding ε region. By comparison, H3 acetylation was low at the non-B cell genes.

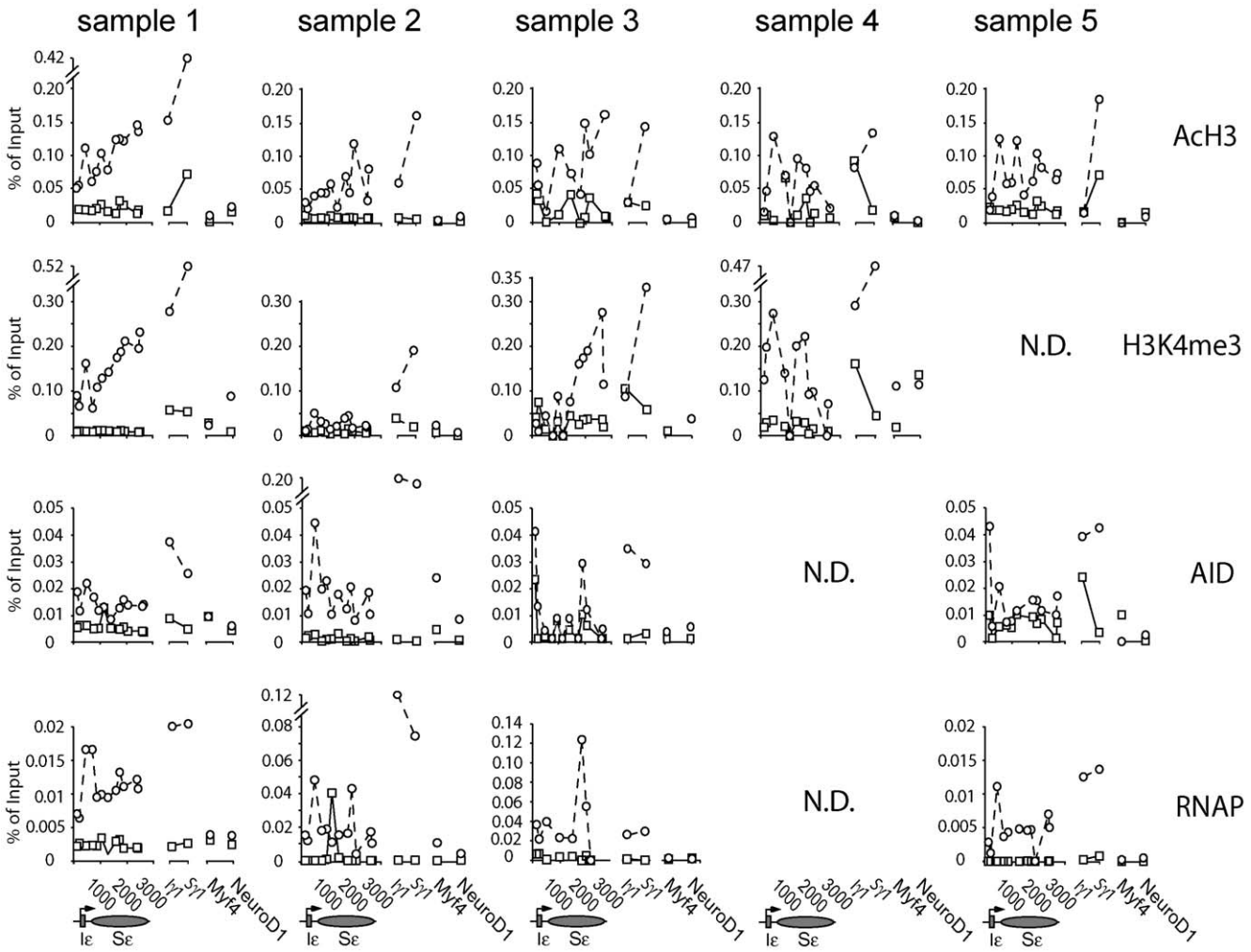

Figure 4. ChIP analysis of histone modifications at the Ig ε locus in primary human B cells. Levels of pan-acetylated histone H3, histone H3 tri-methylated at K4, RNA polymerase II (RNAP) and AID were assessed by ChIP using formaldehyde crosslinked chromatin from primary human B cells stimulated with IL-4 and anti-CD40 for 48 hours. Results from the individual donors for Sε primers sets are plotted alongside those for 5′Iγ1 and Sγ1 and two non-B cell expressed genes (*Myf4* and *NeuroD1*) for comparison. Data from unstimulated cells is shown by squares and solid lines and stimulated cells by circles and dashed lines. A schematic representation of the Ig ε locus is shown below the graphs, with the elements approximately to scale, indicating the position of each primer/TaqMan probe set. Additional (non-IgE) probes are also annotated on the X axis. N.D. – not determined.

doi:10.1371/journal.pone.0024571.g004

Histone H3 lysine 4 tri-methylation levels across the ε locus were also increased upon stimulation of primary human B cells, in the three out of four donors (1, 3 and 4) for whom data were available (Fig. 4), again in agreement with the CL-01 data (Fig. 3). As observed for H3 acetylation, levels of stimulation were variable in the different donors. In two donors (1 and 4, to a greater or lesser extent, respectively) a peak of H3K4 tri-methylation is see at the Iε exon 5′ splice site (Fig. 4). As was also observed for H3 acetylation, H3K4 tri-methylation was higher at the 3′ end of Sε than was seen in the CL-01 cells. Elevation of H3K4me3 levels was also observed at the γ1 locus and was as much as two-fold higher than at the ε locus. Compared to the switch regions, levels of H3K4 tri-methylation were reduced at *Myf4* and *NeuroD1* in stimulated B cells.

We also profiled AID and RNA polymerase II (RNAP) binding patterns in primary B cells. In four individual experiments, we detected increased but variable RNAP and AID occupancy across the ε and γ1 loci upon stimulation (Fig. 4). As was true of the histone modifications, a trend towards a peak of AID and RNAP was seen at the Iε exon 5′ splice site in samples 1, 2 and 5. Interestingly, sample 3 showed little AID accumulation despite displaying robust H3 acetylation, H3K4 tri-methylation and RNAP accumulation. In stimulated B cells AID and RNAP levels were higher at γ1 than ε, while levels were lower at *Myf4* and *NeuroD1*.

To further investigate the chromatin structure of the IgE switch region prior to CSR, CpG DNA methylation across Sε was analysed by bisulphite modification in primary human B cells isolated from 3 donors (Fig. S5). Levels of DNA methylation were not significantly changed following IL-4 and anti-CD40 stimulation of B cells. Further, CpG sites located just upstream of the I exon 5′ splice site (site 176) exhibited reduced levels of methylation compared to surrounding regions while the sites at the 3′ end of Sε (sites 2081–2313) had slightly reduced levels of methylation than the 5′ end. Two further sites, one within Iε (98) and one at the 5′ end of Sε (580), also displayed noticeably lower levels of methylation than their surrounding sites.

Discussion

In this study, we sought to identify changes in chromatin conformation within the human immunoglobulin heavy chain ε locus upon stimulation by treatments known to activate class switching to IgE. We initially took advantage of the CL-01 human B cell line to measure changes in histone modifications associated with the first stages of class switching in a highly reproducible system. These results were then used as reference points for the much more variable responses obtained with primary human B cells.

Measurements of nucleosome distribution across the ε switch region at high resolution (one primer/probe set every 220 bp on average) in CL-01 cells revealed that, although the density of nucleosomes (occupancy) generally increased towards the 3′ end of Sε this pattern of distribution was not affected by IL-4 stimulation (Fig. 2). Reduced nucleosome occupancy at transcription start sites is thought to be associated, in part, with increased levels of the histone variant H2A.Z [35]. However, we found that levels of H2A.Z were largely constant across Sε (Fig. S2), and not higher at the promoter, nor did they change significantly upon IL-4 stimulation.

The presence of nucleosomes in the switch region does not preclude AID attack; AID can readily deaminate deoxycytidine residues on transcriptionally active nucleosomal DNA *in vitro* [39]. However, the observed relative depletion of nucleosomes in the promoter region in unstimulated and IL-4 stimulated cells reveals that this region has increased accessibility to trans-acting factors (transcription factors, polymerase and AID) even before the activation of germline gene transcription. This conclusion is consistent with, and supports, our previous findings showing detectable levels of ε germline gene transcripts in resting B cells [28].

Cerutti and co-workers first made use of the CL-01 cell line to study human B cell activities, utilising CD40-ligand-expressing cells or an anti-CD40 mAb, to stimulate class switching to IgG and IgE. However, we have been unable to stimulate these cells to undergo class switching. This result confirms findings from other groups that, over time, these cells have lost their ability to undergo class switching. Despite their inability to undergo the later stages of recombination, we find that CL-01 cells nonetheless display characteristic remodelling of the chromatin at the IgE locus, including increases in histone H3 acetylation and tri-methylation of H3 at K4 (Fig. 3). The data demonstrate that these chromatin changes occur independently of recombination, a finding supported by the primary B cell data where chromatin changes in the bulk population are clearly visible despite a low frequency of cells switching to IgE.

That histone H3 acetylation and H3K4 tri-methylation was observed at the ε locus in both the CL-01 and primary B cells is not surprising; these chromatin marks generally correlate strongly with transcriptional activation [19], which is observed in every B cell upon IL-4 and CD40 stimulation [28]. Our current high resolution mapping of these histone modifications extends our previous findings [23] and is largely in agreement with several previous reports identifying changes in these histone modifications in response to CSR induction, although these were in all cases carried out at low resolution and in mice [20–22,24,25]. Tri-methylation of H3K4 is commonly detected proximal to transcription start sites in transcriptionally active genes [18,40]. However, because H3K4me3 has been detected in human Sε (Figs. 3 and 4) and murine Sγ1 [24], as well as recombining V_H genes [41,42], our data supports the hypothesis that H3K4me3 is also a mark of recombinationally active chromatin. Indeed, the V(D)J recombinase RAG2 contains an H3K4me3-binding PHD domain that is required for its proper function [43–45]. It is possible that a yet undiscovered PHD-containing cofactor is involved in the proper targeting of AID to H3K4me3-enriched activated switch regions.

We did not observe the significant changes in histone H4 acetylation or tri-methylation of histone H3 at lysine 9 within switch regions that had previously been reported in murine [21,22,25] and human B cells [23]. This demonstrates that analyses of histone modifications at single points over large loci can give misleading impressions of general levels of enrichments over these regions. Additionally, different constant regions could utilize different histone modifications to promote CSR. Previous studies have described switch recombination at γ loci, while we particularly noted H3K9me3 accumulation at Sμ and Sγ regions [23]. Our present high resolution analysis however has focused on Sε. Wang et al. [24] also observed induction of H3K36me3 just 3′ of murine Sγ1 in stimulated splenic B cells. We did not detect a corresponding increase in H3K36me3 levels at the 3′ end of Sε in CL-01 cells (Fig. S3). In addition to target identity and species-specific differences, the size of the respective switch regions could explain this difference. Because mouse Sγ1 is approximately 10 kb in size, the observed elevation in H3K36me3 could simply reflect its association with transcriptional elongation [18,46–48], not a specific feature of switch region chromatin. Sε is approximately 2 kb in length and thus may be too close to the transcription start site to accumulate detectable H3K36 tri-methylation marks.

The histone modifications associated with silent heterochromatin, tri-methylated H3K27 and K9, are already depleted at Sε before stimulation. Similarly, marks of active chromatin, H4 acetylation and H3K4me2 are elevated in this region before stimulation. None of these modifications are significantly affected by IL-4 stimulation, but provide an environment permissive for AID deposition and action. These results support a model in which the chromatin structure is "poised" within the switch regions prior to cytokine stimulation [28].

In our primary human B cell studies we observed quantitative differences in the enrichment of acetylated H3 and H3K4me3 between activated Sε and Sγ1 (Fig. 4). Broadly, the elevated levels of these histone modifications at Sγ1 compared to Sε correlated with greater RNAP occupancy and to a lesser extent AID distribution. While it would have been desirable to perform a high-resolution analysis of Sγ1, the high degree of sequence repetition at the IgG genes prevented this. Thus, we cannot discount the possibility that these differences do not reflect the "general" level of modification across the γ1 locus. However, at least in places, Sγ1 is more highly modified than anywhere within Sε. These findings suggest that transcriptional activity, and in turn AID accumulation, at the switch regions is likely to be facilitated by the extent of histone modification over the genes; this could explain the preferential switching to γ compared to ε C_H genes in response to IL-4 and CD40 signalling.

In both the CL-01 cells (Fig. 3) and primary human B cells (Fig. 4) the nucleosomes near the Iε exon 5′ splice site are extensively modified and this coincided with a localised reduction in DNA methylation and accumulation of RNAP and AID in human B cells. A growing body of literature reveals a link between chromatin structure and splicing [49]. Interestingly, Sims et al. [50] found that the H3K4me3-binding chromatin remodelling factor CHD1, which binds spliceosomal components, is required for efficient RNA splicing. These data may go some way toward explaining the interesting earlier findings that implicated the requirement for the GLT splice site for successful CSR [51] and supports the recent observation that AID associates with paused RNA polymerase through an interaction with the spliceosome factor spt5 [52]. It is possible that the altered chromatin structure over the splice site may not only recruit complexes that are essential for germline gene transcript processing, but also complexes responsible for the process of DNA cleavage and recombination.

The use of the CL-01 model system allowed us to obtain highly reproducible data for changes associated with IL-4/anti-CD40 stimulation, which included increased histone H3 acetylation and H3K4 tri-methylation. In the corresponding studies in primary B cells, the specific distribution patterns varied among donors, but comparison to the CL-01 data makes it clear that the overall trends in primary B cells are similar to those in CL-01 cells. In the five donors investigated, no correlation could be seen between the levels of histone modification at Sε at 48 hours and IgE secretion at 12 days. Cell death is significant in the long-term (12 day) cultures (Supplemental Table S1), yet this does not appear to be a limiting factor for IgE production. We suggest that while histone modification is necessary for CSR it is not sufficient, and other factors must be involved in determining the success of CSR in individual B cells.

Abnormal IgE production is associated with a range of pathologies, including asthma, allergic rhinitis, Hyper-IgE and Hyper-IgM Syndromes. The development of therapeutic approaches to controlling these disease states necessitates the elucidation of mechanisms underlying CSR to IgE in human systems. Our findings suggest that approaches that specifically target the chromatin structural state in the switch region could be employed, for example by manipulating the chromatin structure of Sε using methods that would not affect switching to other C_H genes [53].

Materials and Methods

Primary Human B Cell purification

Human B cells were isolated from tonsils collected from patients undergoing routine tonsillectomies at the Evelina Children's Hospital (Guy's and St. Thomas' NHS Foundation Trust - ethics approval from Guy's Research Ethics Committee). The patients were all aged between 2 and 14, had no history of asthma, any known allergies or long standing medical conditions (except tonsillitis) and were not taking any medications. The patients' parents or legal guardians gave informed written consent for participation in this study. Total B cells were isolated from the tonsil as previously described [30]. B cell purity was assessed by flow cytometry using fluorescently-labelled antibodies (DakoCytomation) and a FACSCalibur^{TM} flow cytometer (BD Biosciences). B cell populations were routinely >95% $CD19^+$, with <5% contaminating $CD3^+$ T cells. Generally, around 60% of these cells expressed IgM, with <2% IgG or IgE expressing cells (data not shown).

Cell culture

B cells were cultured in 24-well plates (Nunc) at 0.5×10^6 cells/mL in RPMI medium (Invitrogen Ltd.), supplemented with transferrin (35 μg/mL, Sigma-Aldrich Company Ltd.), insulin (5 μg/mL, Sigma-Aldrich Company Ltd.), penicillin (100 IU/mL), streptomycin (100 μg/mL), glutamine (2 mM) (all Invitrogen Ltd.) and 10% foetal bovine serum (FBS) (Hyclone, Perbio Biosciences Ltd.). Where indicated, media were supplemented with 1 μg/mL anti-CD40 antibody (G28.5, ATCC) and 200 IU/mL of recombinant human IL-4 (R&D Systems Ltd.). Unless specified in the text, cells were cultured for 48 hours prior to extraction of chromatin (see below) and for 12 days for analysis of IgE production. At the 48 hour time point cell viability is routinely 80–90%, as judged by trypan blue exclusion. Cell viability following 12 days in culture, as judged by flow cytometry, was more variable and is displayed for each donor in Supplemental Table S1.

CL-01 cells were cultured in RPMI 1640 medium with Glutamax (Invitrogen Ltd.) supplemented with 5% FBS (ATCC) and antibiotics. Where indicated, cells were cultured with 200 IU/mL of recombinant human IL-4 (R&D Systems Ltd.) and 1 μg/mL anti-CD40 monoclonal antibody (mAb) (G28.5, ATCC). To determine whether CSR had taken place after 7 days stimulation with IL-4 and anti-CD40, cells were stained for extracellular IgG or IgE and analysed by flow cytometry and the secretion of soluble IgE and IgG was investigated by ELISA [28]. No surface bound or secreted IgE or IgG was detected from the CL-01 cells following stimulation (data not shown). The CL-01 cells were also stimulated with IL-4 in combination with trimeric CD40-ligand [27], however CSR to IgG and IgE could not be detected (data not shown).

Detection of IgE

Secretion of IgE was analysed by ELISA as previously described [28]. Briefly, Maxisorp plates (Nalge Europe Ltd.) were coated with polyclonal mouse anti-human IgE (DakoCytomation) in sodium carbonate buffer (pH 9.8) overnight at 4°C. Unbound sites were blocked with 2% non-fat milk powder (Marvel) in PBS/0.05% Tween (Sigma-Aldrich Company Ltd.). Samples were

added and the plates were incubated for 16 hours at 4°C; NIP-IgE (JW8/5/13, ECACC, UK) was used to construct a standard curve. IgE was detected by mouse anti-human IgE conjugated to HRP (DakoCytomation) diluted 1/1000 in PBS/Tween 20 0.05%/1% non-fat milk powder for 4 hours at room temperature and revealed with OPD (Sigma-Aldrich Company Ltd.), with a minimum detection limit of 2 ng/mL. Surface IgE was detected by flow cytometry using a goat anti-human IgE antibody (Vector Laboratories Inc., Burlingame, USA). The percentage of IgE^+ cells and amount of IgE secreted for each sample are shown in Supplemental Table S1.

RNA extraction and quantitative RT-PCR (qRT-PCR)

Total RNA was extracted from 2×10^6 cells using the RNeasy RNA isolation kit (Qiagen). Genomic DNA contamination was removed from 10 μg of total RNA using the Turbo DNA-free Kit (Ambion). cDNA was generated using the SuperScript III First-Strand Synthesis SuperMix for qRT-PCR (Invitrogen Ltd.). qRT-PCR was performed using the ABI-7900HT machine and TaqMan Universal PCR Mastermix (Applied Biosystems). Relative transcript levels were determined by comparing Ct values from equivalent amounts of cDNA derived from untreated cells to those from other experimental samples, all normalized to the endogenous reference gene human HPRT (Applied Biosystems) (ΔΔCt analysis). Supplemental Table S2 and S3 list oligonucleotides used in qRT-PCR experiments.

Nucleosome Occupancy Analysis

Mono-, di- and tri-nucleosome fractions of native chromatin were prepared and DNA extracted as previously described [31]. Genomic DNA was isolated using the DNeasy Blood & Tissue Kit (Qiagen) and used as a reference for quantitative PCR (qPCR). DNA samples were quantified using the Quant-iT PicoGreen dsDNA reagent (Invitrogen Ltd.). 2 ng of DNA were subjected to qPCR using multiple primer/probe sets and qPCR was performed as described for qRT-PCR. Relative nucleosome abundance was calculated using the formula: $2^{\text{Ct(genomic)-Ct(nucleosomal)}}$.

Native *chromatin immunoprecipitation*

Native (non-formaldehyde-crosslinked) *chromatin immunoprecipitations* (ChIPs) were performed and analysed in the IL-4 stimulated CL-01 experiments as previously described [31]. Antibodies used in this study included: anti-acetyl H3 (Millipore, 06-599), anti-acetyl H4 (Millipore, 06-598), anti-H3K4me2 (Millipore, 07-030), anti-H3K4me3 (Millipore, CS200580), anti-H3K9me3 (Abcam, ab8898), anti-H3K27me3 (Millipore, 07-449), anti-H3K36me3 (Abcam, ab9050), anti-H2AZ (Millipore, 07-954), anti-RNA Polymerase II (Covance, 8WG16) and anti-AID (Abcam, ab5197).

Formaldehyde crosslinked *chromatin immunoprecipitation*

All ChIP experiments analyzing chromatin from cells cultured with IL-4 and anti-CD40 mAb stimulation (CL-01 and primary human B cells) were performed by formaldehyde crosslinking, MNase-treatment and sonication of chromatin. Briefly, 1×10^8 cells were fixed at 20°C for 4 minutes in 1% formaldehyde in 10 mL of culture medium. The cross-linking reaction was stopped by the addition of glycine to a final concentration of 125 mM. The cells were spun and the cell pellet resuspended in 1× PBS containing 125 mM glycine and incubated at 20°C for 5 minutes. Nuclei were isolated as detailed for primary human B cells [23] and CL-01 [31]. MNase digestion and chromatin extraction were performed as previously described [23]. Chromatin was sonicated to aid DNA fragmentation to a 100 bp–500 bp range. 10 μg of chromatin were diluted in 0.4 mL modified RIPA buffer (140 mM NaCl, 10 mM Tris pH 7.5, 1 mM EDTA, 0.5 mM EGTA, 1% Triton X-100, 0.01% SDS, 0.1% NaDeoxycholate) and incubated overnight at 4°C with 3–5 μg of the appropriate antibody and 25 μL of Protein G-magnetic beads (Active Motif) in the presence of protease inhibitor cocktail and 5 mM sodium butyrate (Sigma-Aldrich Company Ltd.). Beads were washed twice in IPWB1 (20 mM Tris pH 8.0, 50 mM NaCl, 2 mM EDTA, 1% Triton X-100, 0.1% SDS) and twice in IPWB2 (10 mM Tris pH 8.0, 150 mM NaCl, 1 mM EDTA, 1% NP-40, 250 mM LiCl, 1% Sodium Deoxycholate). Beads were resuspended in 100 μL of 10% Chelex 100 Resin (Bio-rad), boiled for 5 minutes, RNase-treated for 60 minutes at 37°C and proteinase K-treated for 30 minutes at 55°C. Samples were boiled for 10 minutes and DNA-containing supernatant was isolated for qPCR analysis. Equivalent volumes of isolated ChIP DNA and input DNA were subjected to qPCR. A standard curve was generated to convert the differences in Ct values to percent of input.

qPCR analysis of ChIP experiments

Following extraction and purification of DNA from ChIPs, qPCR was performed to determine enrichment of target sequences. All primers used bound uniquely to the genome. Sε and negative control primer sets were designed using Primer Express (Applied Biosystems) and checked for unique alignment to the genome by BLAST analysis. Because of the repetitive nature of the human IgG genes a novel primer design strategy was employed to identify unique primer/probe pairs. Briefly, the γ1 switch region sequence was incrementally divided into short overlapping oligonucleotides of 18 to 25 bp in length. Oligonucleotides having a GC content of 40 to 60% and containing no repeats of greater than 4 nucleotides were selected for further analysis. UNAfold analysis was performed to exclude oligonucleotides that could form homo-dimers at 45°C or with annealing temperatures outside of the desired range (59 to 63°). Oligonucleotides that bound uniquely to Sγ1 were identified using FASTA. Finally, suitable oligonucleotide pairs were identified that produced amplicons of less than 190 bp in length and had a difference in annealing temperatures of less than 2°C. Primer pairs were checked for unique alignment by BLAST and probes designed using the Universal ProbeLibrary Assay Design Centre (Roche Applied Science). The location of all the IgE and IgG primer sets (relative to the I exon) is shown in Supplemental Table S3, and displayed graphically (Fig. S1). qPCR analysis was carried out as described above. Sufficient DNA was recovered from the native CL-01 cell histone ChIPs to allow accurate quantification of recovered samples using the Quant-iT PicoGreen assay (Invitrogen Ltd.); fold enrichment values have therefore been displayed for these ChIPs in Figures 1, 3, S2 and S3. Insufficient DNA was recovered from crosslinked Polymerase and AID ChIPs to allow accurate quantification. For all crosslinked ChIPs, recovered DNA was quantified using a standard curve, generated from genomic DNA serial dilutions, and expressed as percent recovery compared to input.

Bisulphite modification analysis

Genomic DNA was extracted from 1×10^7 cells using a Wizard® genomic DNA extraction kit (Promega, Madison, USA). CpG methylation site mapping was performed by bisulphite modification (BSM) of DNA, adapted from Frommer et al. [32], followed by PCR amplification and sequencing. 10 μg of genomic DNA were digested with Kpn I (New England Biolabs UK Ltd.) and purified by phenol extraction, followed by ethanol precipitation.

DNA was denatured by treatment with 0.2 M NaOH at 37°C for 15 minutes. To this, was added 30 µl of 10 mM hydroquinone and 520 µl of 3 M sodium bisulphite pH 5 (both freshly prepared; Sigma-Aldrich Company Ltd.). Samples were incubated in the dark for 16 hours at 50°C prior to salt removal using the Wizard DNA clean-up system (Promega). DNA was desulphonated in a final concentration of 0.3 M NaOH at room temperature for 15 minutes, neutralised by adding 1 volume of 6 M ammonium acetate, precipitated with 3 volumes of ethanol and resuspended in 20 µL TE buffer.

Primers for the amplification of BSM DNA were designed using MethPrimer [33]. All PCR reactions were carried out on 2 µl of BSM DNA in a 50 µl reaction volume containing 1.5 mM $MgCl_2$ and Hotstart Platinum Taq (Invitrogen Ltd.). PCR-amplified products were cloned using the TOPO® cloning system (Invitrogen Ltd.) and individual colonies sequenced. 20 sequences were collected for each CpG site. The following primer pairs were used for the amplification of BSM modified DNA: E1F TTTGTTGATTGGGATTATTAAGTT A, E1R CAAACAACCTCTCCCTCACAACTAC; E2F TTTTTTTTGTATGGGGA TATAGGAA, E2R CCCAACTCAAACCTAACTCAACTAA; E3F AGTTGAATTA GGTTGATTTGGATTT, E3R AACCTACTCACTCCAACTTTTAACC; E4F TGG GTTGAGTTGAGTTAGGTTAAAT, E4R CCCCTTACAAACAACAAACTCTTA T.

Supporting Information

Table S1 IgE production and cell viability of B cell cultures. IgE production and cell viability of each primary human B cell culture was determined following 12 days stimulation with IL-4 and anti-CD40. Secreted IgE was determined by ELISA, the % of IgE^+ cells and cell viability were determined by flow cytometry. UD. – Undetected.
(DOCX)

Table S2 qRT PCR Assays. Details of the assays used for quantitative RT-PCR analyses are given; AID and HPRT were detected by proprietary assays from Applied Biosystems. εGLT assays were designed "in-house" and used MGB dual labelled probes (Applied Biosystems).
(DOCX)

Table S3 qPCR assays. Details of the assays used for quantitative PCR analysis of ChIPs and unspliced (primary) εGLT assays are given; Sε assays were designed "in-house" and used dual labelled probes, γ1, *NeuroD1* and *Myf4* assays were designed to use dual labelled Universal Probe Library probes (Roche). The approximate genomic location of each assay is given.
(PDF)

Figure S1 Location of qPCR primer sets across the IgE locus. The location of the IgE qPCR primer sets is displayed on a graphical represention (to scale) of the IgE locus.
(TIF)

Figure S2 ChIP analysis of H2A.Z deposition at the Ig ε locus in CL-01 cells. H2A.Z deposition over Sε was investigated in CL-01 by ChIP using size-selected native chromatin. Cells were harvested following 72 hours culture with or without IL-4. Mean results from 3 separate chromatin extractions are plotted as fold enrichments over an input control. Data from unstimulated cells is shown by open squares and solid lines, stimulated cells are open circles and dashed lines. Error bars show standard deviations. A schematic representation of the Ig ε locus, with the elements approximately to scale, is shown below the graph indicating the position of each primer/TaqMan probe set plotted on the X axis.
(TIF)

Figure S3 ChIP analysis of histone modifications at the Ig ε locus in CL-01 cells following IL-4 stimulation. Histone modification over Sε was investigated in CL-01 by ChIP using size-selected native chromatin. Cells were harvested following 72 hours culture with or without IL-4. Mean results from 3 separate chromatin extractions are plotted as fold enrichments over an input control. Data from unstimulated cells is shown by open squares and solid lines, stimulated cells are open circles and dashed lines. Error bars show standard deviations. A schematic representation of the Ig ε locus, with the elements approximately to scale, is shown below each graph indicating the position of each primer/TaqMan probe set plotted on the X axis. The following histone modifications are shown: AcH4, di-methyl H3K4, tri-methyl H3K36, tri-methyl H3K9 and tri-methyl H3K27.
(TIF)

Figure S4 ChIP analysis of histone modifications at the Ig ε locus in CL-01 cells following IL-4 and anti-CD40 stimulation. Histone modification over Sε was investigated in CL-01 by ChIP using size-selected native (non-crosslinked) chromatin. Cells were harvested following 72 hours culture with or without IL-4 and anti-CD40. Mean results from 3 separate chromatin extractions are plotted as fold enrichments over an input control. Data from unstimulated cells is shown by open squares and solid lines; stimulated cells are open circles and dashed lines. Error bars show standard deviations. A schematic representation of the Ig ε locus, with the elements approximately to scale, is shown below each graph indicating the position of each primer/TaqMan probe set plotted on the X axis.
(TIF)

Figure S5 Analysis of DNA CpG methylation over Sε and Sγ1. CpG methylation was analysed across Sε by bisulphite modification of DNA followed by sequencing. Genomic DNA was extracted from tonsil B cells isolated from three donors, 20 sequences were collected for each CpG site. The percentage of methylated deoxcytidines found across the three donors is plotted; error bars show the standard deviation in the data between the three donors. The location of the CpG site is shown on the x axis: Numbers refer to the distance (bp) from the Iε start site and the location is displayed on the graphical representation of the IgE locus below; long vertical lines show each CpGs analysed, short lines show the location of CpGs that could not be analysed (distance from Iε is given below the graphic). The locations of 5 sites that have especially low levels of methylation are emphasised.
(TIF)

Acknowledgments

We thank the staff at the Evelina Children's Hospital Guy's and St. Thomas' National Health Service Foundation Trust for their help with the collection of tonsils.

Author Contributions

Conceived and designed the experiments: SD HJG MG GF DJF. Performed the experiments: SD DF AMC PH. Analyzed the data: SD DJF. Contributed reagents/materials/analysis tools: JN AMC PH. Wrote the paper: SD HJG MG GF DJF.

References

1. Hofker MH, Walter MA, Cox DW (1989) Complete physical map of the human immunoglobulin heavy chain constant region gene complex. ProcNatlAcadSciUSA 86: 5567–5571.
2. Kataoka T, Miyata T, Honjo T (1981) Repetitive sequences in class-switch recombination regions of immunoglobulin heavy chain genes. Cell 23: 357–368.
3. Wuerffel RA, Du J, Thompson RJ, Kenter AL (1997) Ig Sgamma3 DNA-specifc double strand breaks are induced in mitogen-activated B cells and are implicated in switch recombination. JImmunol 159: 4139–4144.
4. Casellas R, Nussenzweig A, Wuerffel R, Pelanda R, Reichlin A, et al. (1998) Ku80 is required for immunoglobulin isotype switching. EMBO J 17: 2404–2411.
5. Chaudhuri J, Basu U, Zarrin A, Yan C, Franco S, et al. (2007) Evolution of the immunoglobulin heavy chain class switch recombination mechanism. AdvImmunol 94: 157–214.
6. Muramatsu M, Sankaranand VS, Anant S, Sugai M, Kinoshita K, et al. (1999) Specific expression of activation-induced cytidine deaminase (AID), a novel member of the RNA-editing deaminase family in germinal center B cells. JBiolChem 274: 18470–18476.
7. Muramatsu M, Kinoshita K, Fagarasan S, Yamada S, Shinkai Y, et al. (2000) Class switch recombination and hypermutation require activation-induced cytidine deaminase (AID), a potential RNA editing enzyme. Cell 102: 553–563.
8. Revy P, Muto T, Levy Y, Geissmann F, Plebani A, et al. (2000) Activation-induced cytidine deaminase (AID) deficiency causes the autosomal recessive form of the Hyper-IgM syndrome (HIGM2). Cell 102: 565–575.
9. Stavnezer-Nordgren J, Sirlin S (1986) Specificity of immunoglobulin heavy chain switch correlates with activity of germline heavy chain genes prior to switching. EMBO J 5: 95–102.
10. Gascan H, Gauchat JF, Aversa G, Van Vlasselaer P, de Vries JE (1991) Anti-CD40 monoclonal antibodies or CD4+ T cell clones and IL-4 induce IgG4 and IgE switching in purified human B cells via different signaling pathways. JImmunol 147: 8–13.
11. Castigli E, Wilson SA, Scott S, Dedeoglu F, Xu S, et al. (2005) TACI and BAFF-R mediate isotype switching in B cells. JExpMed 201: 35–39.
12. Jacobs H, Bross L (2001) Towards an understanding of somatic hypermutation. CurrOpinImmunol 13: 208–218.
13. Rada C, Williams GT, Nilsen H, Barnes DE, Lindahl T, et al. (2002) Immunoglobulin isotype switching is inhibited and somatic hypermutation perturbed in UNG-deficient mice. CurrBiol 12: 1748–1755.
14. Storb U, Stavnezer J (2002) Immunoglobulin genes: generating diversity with AID and UNG. CurrBiol 12: R725–R727.
15. Manis JP, Gu Y, Lansford R, Sonoda E, Ferrini R, et al. (1998) Ku70 is required for late B cell development and immunoglobulin heavy chain class switching. JExpMed 187: 2081–2089.
16. Tian M, Alt FW (2000) Transcription-induced cleavage of immunoglobulin switch regions by nucleotide excision repair nucleases in vitro. JBiolChem 275: 24163–24172.
17. Neuberger MS, Harris RS, Di Noia J, Petersen-Mahrt SK (2003) Immunity through DNA deamination. Trends BiochemSci 28: 305–312.
18. Barski A, Cuddapah S, Cui K, Roh TY, Schones DE, et al. (2007) High-resolution profiling of histone methylations in the human genome. Cell 129: 823–837.
19. Fischle W, Wang Y, Allis CD (2003) Histone and chromatin cross-talk. Curr Opin Cell Biol 15: 172–183.
20. Nambu Y, Sugai M, Gonda H, Lee CG, Katakai T, et al. (2003) Transcription-coupled events associating with immunoglobulin switch region chromatin. Science 302: 2137–2140.
21. Li Z, Luo Z, Scharff MD (2004) Differential regulation of histone acetylation and generation of mutations in switch regions is associated with Ig class switching. ProcNatlAcadSciUSA 101: 15428–15433.
22. Wang L, Whang N, Wuerffel R, Kenter AL (2006) AID-dependent histone acetylation is detected in immunoglobulin S regions. JExpMed 203: 215–226.
23. Chowdhury M, Forouhi O, Dayal S, McCloskey N, Gould HJ, et al. (2008) Analysis of intergenic transcription and histone modification across the human immunoglobulin heavy-chain locus. ProcNatlAcadSciUSA 105: 15872–15877.
24. Wang L, Wuerffel R, Feldman S, Khamlichi AA, Kenter AL (2009) S region sequence, RNA polymerase II, and histone modifications create chromatin accessibility during class switch recombination. JExpMed 206: 1817–1830.
25. Kuang FL, Luo Z, Scharff MD (2009) H3 trimethyl K9 and H3 acetyl K9 chromatin modifications are associated with class switch recombination. ProcNatlAcadSciUSA 106: 5288–5293.
26. Lundgren M, Persson U, Larsson P, Magnusson C, Smith CI, et al. (1989) Interleukin 4 induces synthesis of IgE and IgG4 in human B cells. EurJImmunol 19: 1311–1315.
27. Cerutti A, Zan H, Schaffer A, Bergsagel L, Harindranath N, et al. (1998) CD40 ligand and appropriate cytokines induce switching to IgG, IgA, and IgE and coordinated germinal center and plasmacytoid phenotypic differentiation in a human monoclonal IgM+IgD+ B cell line. JImmunol 160: 2145–2157.
28. Fear DJ, McCloskey N, O'Connor B, Felsenfeld G, Gould HJ (2004) Transcription of Ig germline genes in single human B cells and the role of cytokines in isotype determination. JImmunol 173: 4529–4538.
29. Zan H, Cerutti A, Dramitinos P, Schaffer A, Casali P (1998) CD40 engagement triggers switching to IgA1 and IgA2 in human B cells through induction of endogenous TGF-beta: evidence for TGF-beta but not IL-10-dependent direct S mu→S alpha and sequential S mu→S gamma, S gamma→S alpha DNA recombination. JImmunol 161: 5217–5225.
30. McCloskey N, Pound JD, Holder MJ, Williams JM, Roberts LM, et al. (1999) The extrafollicular-to-follicular transition of human B lymphocytes: induction of functional globotriaosylceramide (CD77) on high threshold occupancy of CD40. EurJImmunol 29: 3236–3244.
31. Litt MD, Simpson M, Recillas-Targa F, Prioleau MN, Felsenfeld G (2001) Transitions in histone acetylation reveal boundaries of three separately regulated neighboring loci. EMBO J 20: 2224–2235.
32. Frommer M, McDonald LE, Millar DS, Collis CM, Watt F, et al. (1992) A genomic sequencing protocol that yields a positive display of 5-methylcytosine residues in individual DNA strands. ProcNatlAcadSciUSA 89: 1827–1831.
33. Li LC, Dahiya R (2002) MethPrimer: designing primers for methylation PCRs. Bioinformatics 18: 1427–1431.
34. Cerutti A, Zan H, Schaffer A, Bergsagel L, Harindranath N, et al. (1998) CD40 ligand and appropriate cytokines induce switching to IgG, IgA, and IgE and coordinated germinal center and plasmacytoid phenotypic differentiation in a human monoclonal IgM+IgD+ B cell line. J Immunol 160: 2145–2157.
35. Weber CM, Henikoff JG, Henikoff S (2010) H2A.Z nucleosomes enriched over active genes are homotypic. Nat Struct Mol Biol 17: 1500–1507.
36. Gauchat JF, Gascan H, de Waal MR, de Vries JE (1992) Regulation of germline epsilon transcription and induction of epsilon switching in cloned EBV-transformed and malignant human B cell lines by cytokines and CD4+ T cells. JImmunol 148: 2291–2299.
37. Splawski JB, Fu SM, Lipsky PE (1993) Immunoregulatory role of CD40 in human B cell differentiation. JImmunol 150: 1276–1285.
38. Jumper MD, Splawski JB, Lipsky PE, Meek K (1994) Ligation of CD40 induces sterile transcripts of multiple Ig H chain isotypes in human B cells. JImmunol 152: 438–445.
39. Shen HM, Poirier MG, Allen MJ, North J, Lal R, et al. (2009) The activation-induced cytidine deaminase (AID) efficiently targets DNA in nucleosomes but only during transcription. JExpMed.
40. Schneider R, Bannister AJ, Myers FA, Thorne AW, Crane-Robinson C, et al. (2004) Histone H3 lysine 4 methylation patterns in higher eukaryotic genes. NatCell Biol 6: 73–77.
41. Goldmit M, Ji Y, Skok J, Roldan E, Jung S, et al. (2005) Epigenetic ontogeny of the Igk locus during B cell development. NatImmunol 6: 198–203.
42. Morshead KB, Ciccone DN, Taverna SD, Allis CD, Oettinger MA (2003) Antigen receptor loci poised for V(D)J rearrangement are broadly associated with BRG1 and flanked by peaks of histone H3 dimethylated at lysine 4. ProcNatlAcadSciUSA 100: 11577–11582.
43. Liu Y, Subrahmanyam R, Chakraborty T, Sen R, Desiderio S (2007) A plant homeodomain in RAG-2 that binds Hypermethylated lysine 4 of histone H3 is necessary for efficient antigen-receptor-gene rearrangement. Immunity 27: 561–571.
44. Matthews AG, Kuo AJ, Ramon-Maiques S, Han S, Champagne KS, et al. (2007) RAG2 PHD finger couples histone H3 lysine 4 trimethylation with V(D)J recombination. Nature 450: 1106–1110.
45. Ramon-Maiques S, Kuo AJ, Carney D, Matthews AG, Oettinger MA, et al. (2007) The plant homeodomain finger of RAG2 recognizes histone H3 methylated at both lysine-4 and arginine-2. Proc Natl Acad Sci U S A 104: 18993–18998.
46. Pokholok DK, Harbison CT, Levine S, Cole M, Hannett NM, et al. (2005) Genome-wide map of nucleosome acetylation and methylation in yeast. Cell 122: 517–527.
47. Kizer KO, Phatnani HP, Shibata Y, Hall H, Greenleaf AL, et al. (2005) A novel domain in Set2 mediates RNA polymerase II interaction and couples histone H3 K36 methylation with transcript elongation. Mol Cell Biol 25: 3305–3316.
48. Morris KV (2005) siRNA-mediated transcriptional gene silencing: the potential mechanism and a possible role in the histone code. Cell Mol Life Sci 62: 3057–3066.
49. Schwartz S, Ast G (2010) Chromatin density and splicing destiny: on the cross-talk between chromatin structure and splicing. Embo Journal 29: 1629–1636.
50. Sims RJ, 3rd, Millhouse S, Chen CF, Lewis BA, Erdjument-Bromage H, et al. (2007) Recognition of trimethylated histone H3 lysine 4 facilitates the recruitment of transcription postinitiation factors and pre-mRNA splicing. Mol Cell 28: 665–676.
51. Hein K, Lorenz MG, Siebenkotten G, Petry K, Christine R, et al. (1998) Processing of switch transcripts is required for targeting of antibody class switch recombination. JExpMed 188: 2369–2374.
52. Pavri R, Gazumyan A, Jankovic M, Di Virgilio M, Klein I, et al. (2010) Activation-induced cytidine deaminase targets DNA at sites of RNA polymerase II stalling by interaction with Spt5. Cell 143: 122–133.
53. Morris K (2005) siRNA-mediated transcriptional gene silencing: the potential mechanism and a possible role in the histone code. Cellular and Molecular Life Sciences 62: 3057–3066.